

Efficient resilience analysis and decision-making for complex engineering systems

Von der Fakultät für Bauingenieurwesen und Geodäsie
der Gottfried Wilhelm Leibniz Universität Hannover
zur Erlangung des Grades

**Doktor-Ingenieur
Dr.-Ing.**

genehmigte Dissertation
von

Julian Salomon, M. Sc.

2023

Referent: Prof. Dr.-Ing. Michael Beer
Korreferenten: Prof. Dr. Daniel Straub
Prof. Dr.-Ing. Monika Sester
Prof. Dr.-Ing. Michael Haist

Tag der Promotion: 19. Juli 2023

Eidesstattliche Versicherung

Hiermit versichere ich, die Regeln der geltenden Promotionsordnung zu kennen und eingehalten zu haben und mit einer Prüfung nach den Bestimmungen der Promotionsordnung einverstanden zu sein, die Dissertation selbst verfasst zu haben, keine Textabschnitte von Dritten oder eigener Prüfungsarbeiten ohne Kennzeichnung übernommen und alle von mir benutzten Hilfsmittel und Quellen in meiner Arbeit angegeben zu haben, Dritten weder unmittelbar noch mittelbar geldwerte Leistungen für Vermittlungstätigkeiten oder für die inhaltliche Ausarbeitung der Dissertation erbracht zu haben, die Dissertation noch nicht als Prüfungsarbeit für eine staatliche oder andere wissenschaftliche Prüfung oder die gleiche oder eine in wesentlichen Teilen ähnliche Arbeit bei einer anderen Hochschule als Dissertation eingereicht zu haben.

Hannover, 12. Juni 2023

.....
(Unterschrift)

Zusammenfassung

Moderne Gesellschaften sind weltweit zunehmend von der reibungslosen Funktionalität immer komplexer werdender Systeme, wie beispielsweise Infrastruktursysteme, digitale Systeme wie das Internet oder hochentwickelten Maschinen, abhängig. Sie bilden die Eckpfeiler unserer technologisch fortgeschrittenen Welt, und ihre Effizienz steht in direktem Zusammenhang mit unserem Wohlbefinden sowie dem Fortschritt der Gesellschaft. Diese wichtigen Systeme sind jedoch einer ständigen und breiten Palette von Bedrohungen natürlichen, technischen und anthropogenen Ursprungs ausgesetzt. Das Auftreten globaler Krisen wie die COVID-19-Pandemie und die anhaltende Bedrohung durch den Klimawandel haben die Anfälligkeit der weit verzweigten und voneinander abhängigen Systeme sowie die Unmöglichkeit einer Gefahrenvorhersage in voller Gänze eindrücklich verdeutlicht. Die Pandemie mit ihren weitreichenden und unerwarteten Auswirkungen hat gezeigt, wie ein externer Schock selbst die fortschrittlichsten Systeme zum Stillstand bringen kann, während der anhaltende Klimawandel immer wieder beispiellose Risiken für die Systemstabilität und -leistung hervorbringt. Diese globalen Krisen unterstreichen den Bedarf an Systemen, die nicht nur Störungen standhalten, sondern sich auch schnell und effizient von ihnen erholen können. Das Konzept der Resilienz und die damit verbundenen Entwicklungen umfassen diese Anforderungen: Analyse, Abwägung und Optimierung der Zuverlässigkeit, Robustheit, Redundanz, Anpassungsfähigkeit und Wiederherstellbarkeit von Systemen – sowohl aus technischer als auch aus wirtschaftlicher Sicht.

In dieser kumulativen Dissertation steht daher die Entwicklung umfassender und effizienter Instrumente für die Resilienz-basierte Analyse und Entscheidungsfindung von komplexen Systemen im Mittelpunkt. Das neu entwickelte Resilienz-Entscheidungsfindungsverfahren steht im Kern dieser Entwicklungen. Es basiert auf einem adaptierten systemischen Risikomaß, einer zeitabhängigen, probabilistischen Resilienzmetrik sowie einem Gittersuchalgorithmus und stellt eine bedeutende Innovation dar, da es Entscheidungsträgern ermöglicht, ein optimales Gleichgewicht zwischen verschiedenen Arten von Resilienz-steigernden Maßnahmen unter Berücksichtigung monetärer Aspekte zu identifizieren.

Zunehmend weisen Systemkomponenten eine erhebliche Eigenkomplexität auf, was dazu führt, dass sie selbst als Systeme modelliert werden müssen. Hieraus ergeben sich Systeme aus Systemen mit hoher Komplexität. Um diese Herausforderung zu adressieren, wird eine neue Methodik abgeleitet, indem das zuvor eingeführte Resilienzrahmenwerk auf multidimensionale Anwendungsfälle erweitert und synergetisch mit einem etablierten Konzept aus der Zuverlässigkeitstheorie, der Überlebenssignatur, zusammengeführt wird. Der neue Ansatz kombiniert die Vorteile beider ursprünglichen Komponenten: Einerseits ermöglicht er einen direkten Vergleich verschiedener Resilienz-steigernder Maßnahmen aus einem mehrdimensionalen Suchraum, der zu einem opti-

malen Kompromiss in Bezug auf die Systemresilienz führt. Andererseits ermöglicht er durch die Separationseigenschaft der Überlebenssignatur eine signifikante Reduktion des Rechenaufwands. Sobald eine Subsystemstruktur berechnet wurde – ein typischerweise rechenintensiver Prozess – kann jede Charakterisierung des probabilistischen Ausfallverhaltens von Komponenten validiert werden, ohne dass die Struktur erneut berechnet werden muss.

In der Realität sind Messungen, Expertenwissen sowie weitere Informationsquellen mit vielfältigen Unsicherheiten belastet. Hierfür wird eine effiziente Methode vorgeschlagen, die auf der Kombination von Überlebenssignatur, unscharfer Wahrscheinlichkeitstheorie und nicht-intrusiver stochastischer Simulation (NISS) basiert. Dadurch entsteht ein effizienter Ansatz zur Quantifizierung der Zuverlässigkeit komplexer Systeme unter Berücksichtigung des gesamten Unsicherheitsspektrums. Der neue Ansatz, der die vorteilhaften Eigenschaften seiner ursprünglichen Komponenten synergetisch zusammenführt, erreicht eine bedeutende Verringerung des Rechenaufwands aufgrund der Separationseigenschaft der Überlebenssignatur. Er erzielt zudem eine drastische Reduzierung der Stichprobengröße aufgrund der adaptierten NISS-Methode: Es wird nur eine einzige stochastische Simulation benötigt, um Unsicherheiten zu berücksichtigen. Die neue Methodik stellt nicht nur eine Neuerung auf dem Gebiet der Zuverlässigkeitsanalyse dar, sondern kann auch in das Resilienzrahmenwerk integriert werden.

Für eine Resilienzanalyse von real existierenden Systemen ist die Berücksichtigung kontinuierlicher Komponentenfunktionalität unerlässlich. Diese wird in einer weiteren Neuentwicklung adressiert. Durch die Einführung der kontinuierlichen Überlebensfunktion und dem Konzept der Diagonal Approximated Signature als entsprechendes Ersatzmodell kann das bestehende Resilienzrahmenwerk sinnvoll erweitert werden, ohne seine grundlegenden Vorteile zu beeinträchtigen.

Im Kontext der Regeneration komplexer Investitionsgüter wird ein umfassendes Analyserahmenwerk vorgestellt, um die Übertragbarkeit und Anwendbarkeit aller entwickelten Methoden auf komplexe Systeme jeglicher Art zu demonstrieren. Das Rahmenwerk integriert die zuvor entwickelten Methoden der Resilienz-, Zuverlässigkeits- und Unsicherheitsanalyse. Es bietet Entscheidungsträgern die Basis für die Identifikation resilienter Regenerationspfade in zweierlei Hinsicht: Zum einen im Sinne von Regenerationspfaden mit inhärenter Resilienz und zum anderen Regenerationspfade, die zu einer maximalen Systemresilienz unter Berücksichtigung technischer und monetärer Einflussgrößen des zu analysierenden komplexen Investitionsgutes führen.

Zusammenfassend bietet diese Dissertation innovative Beiträge zur effizienten Resilienzanalyse und Entscheidungsfindung für komplexe Ingenieursysteme. Sie präsentiert universell anwendbare Methoden und Rahmenwerke, die flexibel genug sind, um beliebige Systemtypen und Leistungsmaße zu berücksichtigen. Dies wird in zahlreichen Fallstudien von willkürlichen Flussnetzwerken, funktionalen Modellen von Axialkompressoren bis hin zu substrukturierten Infrastruktursystemen mit mehreren tausend Einzelkomponenten demonstriert.

Schlüsselwörter: Resilienz, Entscheidungsfindung, Unsicherheit, Komplexe Systeme, Zuverlässigkeit.

Abstract

Modern societies around the world are increasingly dependent on the smooth functionality of progressively more complex systems, such as infrastructure systems, digital systems like the internet, and sophisticated machinery. They form the cornerstones of our technologically advanced world and their efficiency is directly related to our well-being and the progress of society. However, these important systems are constantly exposed to a wide range of threats of natural, technological, and anthropogenic origin. The emergence of global crises such as the COVID-19 pandemic and the ongoing threat of climate change have starkly illustrated the vulnerability of these widely ramified and interdependent systems, as well as the impossibility of predicting threats entirely. The pandemic, with its widespread and unexpected impacts, demonstrated how an external shock can bring even the most advanced systems to a standstill, while the ongoing climate change continues to produce unprecedented risks to system stability and performance. These global crises underscore the need for systems that can not only withstand disruptions, but also, recover from them efficiently and rapidly. The concept of resilience and related developments encompass these requirements: analyzing, balancing, and optimizing the reliability, robustness, redundancy, adaptability, and recoverability of systems – from both technical and economic perspectives.

This cumulative dissertation, therefore, focuses on developing comprehensive and efficient tools for resilience-based analysis and decision-making of complex engineering systems. The newly developed resilience decision-making procedure is at the core of these developments. It is based on an adapted systemic risk measure, a time-dependent probabilistic resilience metric, as well as a grid search algorithm, and represents a significant innovation as it enables decision-makers to identify an optimal balance between different types of resilience-enhancing measures, taking into account monetary aspects.

Increasingly, system components have significant inherent complexity, requiring them to be modeled as systems themselves. Thus, this leads to systems-of-systems with a high degree of complexity. To address this challenge, a novel methodology is derived by extending the previously introduced resilience framework to multidimensional use cases and synergistically merging it with an established concept from reliability theory, the survival signature. The new approach combines the advantages of both original components: a direct comparison of different resilience-enhancing measures from a multidimensional search space leading to an optimal trade-off in terms of system resilience, and a significant reduction in computational effort due to the separation property of the survival signature. It enables that once a subsystem structure has been computed – a typically computational expensive process – any characterization of the probabilistic failure behavior of components can be validated without having to recompute the structure.

In reality, measurements, expert knowledge, and other sources of information are loaded with multiple uncertainties. For this purpose, an efficient method based on the combination of survival signature, fuzzy probability theory, and non-intrusive stochastic simulation (NISS) is proposed. This results in an efficient approach to quantify the reliability of complex systems, taking into account the entire uncertainty spectrum. The new approach, which synergizes the advantageous properties of its original components, achieves a significant decrease in computational effort due to the separation property of the survival signature. In addition, it attains a dramatic reduction in sample size due to the adapted NISS method: only a single stochastic simulation is required to account for uncertainties. The novel methodology not only represents an innovation in the field of reliability analysis, but can also be integrated into the resilience framework.

For a resilience analysis of existing systems, the consideration of continuous component functionality is essential. This is addressed in a further novel development. By introducing the continuous survival function and the concept of the Diagonal Approximated Signature as a corresponding surrogate model, the existing resilience framework can be usefully extended without compromising its fundamental advantages.

In the context of the regeneration of complex capital goods, a comprehensive analytical framework is presented to demonstrate the transferability and applicability of all developed methods to complex systems of any type. The framework integrates the previously developed resilience, reliability, and uncertainty analysis methods. It provides decision-makers with the basis for identifying resilient regeneration paths in two ways: first, in terms of regeneration paths with inherent resilience, and second, regeneration paths that lead to maximum system resilience, taking into account technical and monetary factors affecting the complex capital good under analysis.

In summary, this dissertation offers innovative contributions to efficient resilience analysis and decision-making for complex engineering systems. It presents universally applicable methods and frameworks that are flexible enough to consider system types and performance measures of any kind. This is demonstrated in numerous case studies ranging from arbitrary flow networks, functional models of axial compressors to substructured infrastructure systems with several thousand individual components.

Keywords: Resilience, decision-making, uncertainty, complex systems, reliability.

Acknowledgments

I would like to extend my gratitude to my doctoral supervisor, Prof. Dr.-Ing. Michael Beer, for granting me the opportunity to delve into the world of academia. His willingness to engage in open dialogues, share valuable insights, and consistently provide support and encouragement has been crucial in my journey. I am grateful for his generosity and the firm belief he has shown in me.

I wish to express my thanks to the members of the dissertation defense committee: Prof. Dr. Daniel Straub, Prof. Dr.-Ing. Monika Sester, and Prof. Dr.-Ing. Michael Haist for kindly agreeing to serve on the committee.

My appreciation extends to my colleagues for the intellectually stimulating conversations, academic and beyond, and for the many shared moments of laughter and joy. I particularly thank Niklas R. Winnewisser for his constant and reliable support and the many hours of spirited discussions that have greatly facilitated my work.

Finally, my deepest gratitude is to my family, my friends and my wife. To my parents, Cornelia and Wolfgang, for guiding me to this point, for their unwavering support, their love, their steadfast belief in me, and for always being there. To my friends and family, for the wonderful moments that brighten life and provide perspective on what is truly valuable. And to my wife, Katharina, the love of my life, my anchor, my home, for your boundless support, love, and understanding. Your presence is my constant source of strength and inspiration.

*To my parents, Cornelia and Wolfgang,
and to my beloved wife, Katharina,
this work is dedicated,
in deep gratitude for their never-ending love and support.*

Contents

1	Introduction	1
1.1	Motivation	1
1.2	Resilience definition and origin	2
1.3	Resilience quantification	6
1.3.1	Fundamentals	6
1.3.2	Categorization	10
1.3.3	Deterministic resilience metrics	14
1.3.4	Probabilistic resilience metrics	15
1.4	System reliability	19
1.4.1	Assessment approaches and quantification	19
1.4.2	Concept of survival signature	20
1.5	Uncertainty	23
1.5.1	Definition and classification	24
1.5.2	Approaches to uncertainty incorporation and handling	25
1.5.3	Fuzzy probability	27
1.6	Decision-making and economic aspects	28
1.7	Aims and objectives	31
1.8	Original contributions	33
1.9	Structure of the thesis	36
2	Resilience decision-making for complex systems	37
2.1	Introduction	38
2.2	Theoretical fundamentals	40
2.2.1	Resilience quantification	40
2.2.2	Systemic risk measure	42
2.2.3	Adapted systemic risk measure	43
2.2.4	Grid search algorithm	44
2.3	Resilience decision-making	45
2.4	Multistage high-speed axial compressor	48
2.4.1	Model	49
2.4.2	Costs of endowment properties	50
2.4.3	Scenario	51

2.5	Berlin's <i>U-Bahn</i> and <i>S-Bahn</i> system	52
2.5.1	Model	53
2.5.2	Endowment property costs	55
2.5.3	Scenarios	56
2.6	Conclusion	58
3	Multidimensional resilience decision-making for complex and substructured systems	60
3.1	Introduction	61
3.2	Resilience decision-making	63
3.2.1	Resilience quantification	64
3.2.2	Adapted systemic risk measure	66
3.2.3	Grid search algorithm and the curse of dimensionality	67
3.3	Concept of survival signature	67
3.3.1	Structure function	68
3.3.2	Survival signature	68
3.3.3	Probability structure	68
3.3.4	Survival function	69
3.4	Proposed methodology	69
3.4.1	Definition of substructured systems	70
3.4.2	Extension of the adapted systemic risk measure	71
3.4.3	Augmentation of the resilience analysis	72
3.5	Multistage high-speed axial compressor	74
3.5.1	Model	74
3.5.2	Costs of endowment properties	76
3.5.3	Scenario	76
3.6	Complex system	78
3.6.1	Model	79
3.6.2	Costs of endowment properties	82
3.6.3	Scenario	82
3.7	<i>U-Bahn</i> and <i>S-Bahn</i> system of Berlin	85
3.7.1	Model	86
3.7.2	Costs of endowment properties	90
3.7.3	Scenario	91
3.8	Conclusion and outlook	96
4	Efficient reliability analysis of complex systems in consideration of imprecision	98
4.1	Introduction	99
4.2	Theoretical fundamentals	102
4.2.1	Survival signature	102

4.2.2	Uncertainty	104
4.2.3	Fuzzy probability	106
4.2.4	Non-intrusive imprecise stochastic simulation	107
4.3	Proposed methodology	108
4.3.1	LEMCS algorithm	109
4.3.2	GEMCS algorithm	110
4.3.3	Repeated p-box analysis for fuzzy probability approximation	111
4.3.4	Decision-making procedure	111
4.4	Multistage high-speed axial compressor	113
4.4.1	Model	113
4.4.2	Reliability analysis	114
4.5	Complex system	117
4.5.1	Model	117
4.5.2	Reliability analysis	117
4.5.3	Imprecision decision-making	122
4.6	Conclusion and outlook	124
5	The concept of diagonal approximated signature: new surrogate modeling approach for continuous-state systems in the context of resilience optimization	126
5.1	Introduction	127
5.2	Theoretical fundamentals	131
5.2.1	Structure function	131
5.2.2	Coherent system	132
5.2.3	Concept of binary-state survival signature	132
5.2.4	Concept of continuous-state survival signature	134
5.3	Proposed methodology	135
5.3.1	Continuous-state survival function	135
5.3.2	Surrogate model: the concept of diagonal approximated signature	137
5.4	Case studies	143
5.4.1	System structure functions	143
5.4.2	Stochastic modeling of the component degradation process	148
5.4.3	Numerical results	149
5.5	Discussion	166
5.5.1	Case studies	166
5.5.2	Comparison with related research	168
5.5.3	Contextualization in terms of resilience	170
5.6	Conclusions & outlook	171
6	Resilience-based decision criteria for optimal regeneration	173
6.1	Motivation	174

6.2	Scope of the paper	176
6.3	Functional modeling approach	178
6.3.1	Extraction of structure functions based on sensitivity analyses	178
6.3.2	Kucherenko indices	182
6.4	Resilience analysis	183
6.4.1	Resilience metric	183
6.4.2	Adapted systemic risk measure	185
6.4.3	Grid search algorithm	186
6.5	Constrained resilience analysis of an axial compressor	186
6.5.1	Resilience analysis setting	186
6.5.2	Costs of endowment properties	188
6.5.3	Scenario and numerical results in a two-dimensional setting	188
6.5.4	Scenario and numerical results in multiple dimensions	190
6.6	Reliability analysis	192
6.6.1	Repeated evaluation of the survival function	192
6.6.2	Concept of binary-state survival signature	193
6.6.3	Concept of multi-state survival signature	195
6.7	Uncertainty analysis	196
6.7.1	Imprecision and its implementation via fuzzy probability	197
6.7.2	Efficient simulation algorithm under consideration of imprecision	198
6.8	Conclusions	200
7	Conclusions and outlook	202
7.1	Conclusions	202
7.2	Outlook	204
8	List of publications	205
	Bibliography	207

1 Introduction

1.1 Motivation

In the modern era, societies across the globe increasingly rely on the seamless functioning of complex systems, including infrastructure networks, industrial plants, digital networks, cyber-physical systems, and sophisticated machinery. These systems serve as the backbone of our technologically advanced societies, and their efficiency is directly linked to societal well-being and progress. However, the reality is that these systems face continuous exposure to a wide array of threats from natural, technical, and anthropogenic sources, jeopardizing their functionality and must not be overlooked [1, 2]. With the continuously increasing complexity and interconnectedness of these systems, it is practically infeasible to predict, identify and prevent all potential adverse effects.

The emergence of global challenges, such as the COVID-19 pandemic and the persisting threat of climate change, has further emphasized the vulnerabilities of these systems. The pandemic, with its far-reaching and unexpected impacts has demonstrated how an external shock can bring even the most advanced systems to a standstill [3], while the ongoing climate change continually poses unprecedented threats to system stability and performance [1, 4]. These global crises underscore the need for robust systems that can not only withstand disruptions but also recover from them efficiently and rapidly.

The concept of resilience, along with its related developments, encompasses these requirements: analyzing, balancing and optimizing the reliability, robustness, redundancy, adaptability, and recoverability of systems – both from technical and economic perspectives [5–7]. Initially introduced in the fields of ecology [8] and psychology [9], the notion of resilience has made a significant transition into the engineering realm, mainly due to its relevance and application in system security [10–13]. It signifies a paradigm shift from a “fail-safe” strategy that focuses on preventing system failures to a “safe-to-fail” approach that (also) concentrates on efficient system recovery after inevitable and unpredictable failures [1, 14–16].

The quest for improved comprehension and application of resilience in engineering is an ongoing challenge, further accentuated by the rapid evolution, increased complexity, and interdependency of modern systems [17]. The concept of resilience continues to gain rapid popularity within different scientific communities and sectors, thereby constituting a dynamic and active research field [12]. In response to the COVID-19 pandemic, numerous publications have demanded an imperative increase in the resilience of key systems, such as the healthcare system [18], food

system [19], education system [20], global supply chains [21, 22], and many more. Consequently, it is indispensable to address this concept in a more nuanced manner. This includes the development of comprehensive definitions, considering its various facets and implications, and creating standardized methodologies for its quantification, assessment, application, and decision-making in the field of system engineering [6, 23, 24].

The aim of this dissertation is to contribute to the ongoing discourse on enhancing the resilience of complex engineering systems. It provides insights, broad strategies, and efficient decision-making approaches that are crucial for improving their overall resilience and effectiveness.

1.2 Resilience definition and origin

The concept of “resilience” has its roots in the Latin word “resilire”, meaning “to bounce back”, and is prevalent across various domains including ecology, economics, psychology, and sociology, as well as in the context of engineering systems, see, e.g., [25, 26]. This variability in the notion’s use across disciplinary boundaries inevitably leads to a multitude of different definitions that, while mostly overlapping at the core to some degree, often have entirely distinct nuances.

The interest in the concept of resilience as an empirically observable quantity emerged, according to Masten in [27], simultaneously, but independently, during the 1970s, in the disciplines of ecology, see [8], and psychology, see, e.g., [9, 28]. These studies, as well as a variety of others, have been substantially influenced by the basic insights of general systems theory provided by Bertalanffy in [29]. Masten, a highly respected, and influential figure in the field of psychology, specifically, on the study of resilience in child development, considers resilience to be a dynamic process that involves positive adaptation and successful recovery in the face of significant adversity or stress. Resilience is not viewed as a fixed trait, but rather as a complex interaction of multiple systems – including individual, family, and societal factors – that enhances an individual’s ability to recover from adverse experiences. Masten emphasizes that resilience arises from “ordinary magic”, i.e., it is a general phenomenon arising from normative human adaptive systems, rather than an exceptional, rare trait [30, 31]. In a more systemic context, Masten defines resilience cross-disciplinarily in [27] as: “[...] *the capacity of a dynamic system to adapt successfully to disturbances that threaten system function, viability, or development.*” and adds: “*The concept can be applied to systems of many kinds at many interacting levels, both living and nonliving, such as a microorganism, a child, a family, a security system, an economy, a forest, or the global climate.*” Other widely considered studies on the definition of resilience in the field of psychology are provided, e.g., in [32–35].

In the domain of economics, Martin provides a widely cited definition of resilience in [36] as: “[...] *the capacity of a [...] economy to reconfigure, that is adapt, its structure (firms, industries, technologies and institutions) so as to maintain an acceptable growth path in output, employment and wealth over time.*” Additional studies addressing the definition of resilience in an economic context are given, e.g., in [37–39]. In comparison, a definition in an urban context is proposed by Alberti et al. in [40] as: “[...] *resilience in cities – the degree to which cities tolerate*

alteration before reorganizing around a new set of structures and processes ([41]) – depends on the cities’ ability to simultaneously maintain ecosystem and human functions.” In [4], Meerow et al., meanwhile, critically examine the academic literature on urban resilience, provide a comprehensive overview, especially with a focus on the topic of climate change, and offer their own well-regarded definition: “*Urban resilience refers to the ability of an urban system – and all its constituent socio-ecological and socio-technical networks across temporal and spatial scales – to maintain or rapidly return to desired functions in the face of a disturbance, to adapt to change, and to quickly transform systems that limit current or future adaptive capacity.*” Note that the definitions and disciplines related to resilience discussed in this section are not comprehensive and only provide a partial representation. Comprehensive overviews on the origins, prevalence, and definitions of the concept of resilience and discussion on its application across disciplines is provided in studies such as [26] by Martin-Breen & Anderies, [42] by Bhamra et al, and [43] by Francis & Bekera.

Resilience science is an exceedingly dynamic, emerging and interdisciplinary field of research, naturally resulting in a variety of approaches, definitions, interpretations, and discussions being published. This interdisciplinary perspective on the concept of resilience is addressed in [44]. In this highly referenced work, Southwick et al. focus on the concept of resilience in terms of definitional problems across disciplines. On the one hand, the authors emphasize a context-dependent understanding of resilience, endorsing a variety of definitions tailored to distinct situations. On the other hand, they underscore the necessity for a broad, comprehensive interpretation, achievable through interdisciplinary collaboration between numerous disciplines, such as engineering, ecology, biology, and social sciences. Thus, the authors advocate for a delicate balance between specialized and generalized conceptions of resilience. However, controversial definitional terms also exist within the same discipline. In the context of engineering systems Linkov & Palma-Oliveira, in [45], provide an analysis of different definitions of the concept of resilience with a focus on the distinction between risk and resilience. Furthermore, the resilience concept is addressed in terms of definitional issues by Mayunga in [46] in the domain of community resilience and by Manyena in [47] regarding the its distinction to the notion of vulnerability. Four properties that are inherent to a resilient system, valid for both physical and social systems are presented by Bruneau et al. in [48] as the “dimensions of resilience”. These four properties have received considerable attention in the literature and are commonly referred to as the four R’s, see, e.g., [49] and [50]:

- **Robustness:** Refers to the strength or the capability of elements, systems, and other units of investigation to endure a specific level of stress or demand without experiencing degradation or functional loss.
- **Redundancy:** Denotes the degree of existing elements, systems or other units of investigation that are substitutable and can meet the functional demands placed upon them in the event of a disruption, degradation, or loss of functionality.

- Resourcefulness: Represents the ability to recognize problems, prioritize tasks, and allocate resources in situations where elements, systems, or other units of analysis are threatened by disruption. Resourcefulness can further be defined as the capacity to utilize material (e.g., monetary, physical, technological, and informational) and human resources to address priorities and accomplish objectives.
- Rapidity: Refers to the ability to address priorities and achieve objectives in a time-sensitive manner in order to minimize losses and prevent future disruptions.

It shall be noted that these definitions, although consistently associated with the concept of resilience, are in some cases controversially defined in the literature. In minor terms, this means that only modest adjustments that slightly change the meaning appear in the definitions. For example, Tierney & Bruneau in [51] define robustness following the four R's, as “[...] *the ability of systems, system elements, and other units of analysis to withstand disaster forces without significant degradation or loss of performance.*” Compared to the original work, involving the same author, Bruneau, see [48], this definition includes only a slight adjustment, however, the usage of the term “significant” permits more interpretation of the notion robustness, in this case meaning, it allows for certain performance degradations of the system, compared to the original definition. A more significant deviation from the definition of robustness given in [48], is the description by Faturechi & Miller-Hooks. In their work [52], it is described as: “*Robustness measures the ability of a system to continue in operation and, thus, maintain some level of functionality, even when exposed to disruption.*” This definition is more similar to the adaptation by Tierney & Bruneau than that given by Bruneau et al. It should be noted, however, that although there are inconsistencies in the literature regarding the naming of dimensions and phenomena in the context of the concept of resilience, the description and attribution of these phenomena to this very resilience concept is quite consistent.

A primary definition that is arguably one of the most highly regarded references on resilience definition in the scientific literature is provided by Holling. In [8], Holling introduced the idea of system resilience in terms of ecological systems, defining it as “[...] *a measure of the persistence of systems and their ability to absorb change and disturbance and still maintain the same relationships between populations or state variables.*” Although for an entirely different discipline, this definition includes key features that are consistent, in whole or in part, across numerous definitions of resilience for engineering systems that have appeared subsequently, such as in the work of Fiksel [53], Little [54], Hollnagel et al. [55], Bruneau & Reinhorn [56], and Youn et al. [57].

Further work on the definition of resilience in an engineering context is provided for example by Park et al., who describe resilience in [58] as an “[...] *emergent property of what an engineering system does, rather than a static property the system has.*” In [59], Holling addresses the direct differences between the resilience of systems in engineering and the resilience of ecological systems. Woods explores and categorizes in [60] various technical definitions of system resilience in engineering complex adaptive systems. The author delineates resilience into four principal

concepts: 1. rebound from trauma and return to equilibrium, 2. synonymy with robustness, 3. the antithesis of brittleness, and 4. as adaptive network architectures that can sustain the ability to adapt to future surprises. These concepts serve as cornerstones for comprehending and applying resilience in engineering practice. In [61], the authors specifically address the definition and quantification approaches of resilience in transportation systems.

A comprehensive literature review on the definition of resilience in an engineering context is presented in [6] by Ayyub. Based on selected highly influential documents on the topic of resilience definition, such as those of the Presidential Policy Directive (PPD-21) [62], National Research Council [63], the ASCE Committee on Critical Infrastructure [64], or the Civil Contingencies Secretariat of the Cabinet Office, London, United Kingdom [65], Ayyub defines ten criteria a comprehensive definition of resilience has to meet. The focus here is on the scope of this definition's application to complex systems in a wide variety of engineering domains, such as buildings, infrastructure systems, networks, communities, and the like, and on the necessity of establishing a basis for resilience measurability, i.e., promising resilience metrics. The following ten criteria are provided by Ayyub:

1. Expanding on earlier conceptual definitions, specifically Presidential Policy Directives (PPDs) [62, 66].
2. Evaluation of initial and residual capacities or strengths before and after a disruptive event, i.e., robustness.
3. Addressing the capacity to prepare, plan, absorb, recover, or adapt effectively to adverse events [63].
4. Representing disturbances as stochastic processes with occurrence rates and demand intensity.
5. Allowing the consideration of diverse performance inputs based on respective failure modes for a variety of assets at risk, e.g., environment, socioeconomic structures, essential public services, human populations, physical infrastructure, and social networks and systems [67, 68].
6. Acknowledging system changes over time, including improvements, fragility, or aging.
7. Taking into account complete or partial recovery and associated recovery times.
8. Incorporating potential system performance enhancements post-recovery.
9. Relating to established concepts such as reliability and risk, building on pertinent reliability and risk metrics.
10. Facilitating the development of resilience metrics with significant units.

Addressing these criteria, Ayyub further provides in [6] a comprehensive definition of resilience in the context of complex systems that is highly respected in the literature and draws from the content of the PPD-21 on critical infrastructure security and resilience [62]: “*Resilience notionally means the ability to prepare for and adapt to changing conditions and withstand and recover rapidly from disruptions. Resilience includes the ability to withstand and recover from disturbances of the deliberate attack types, accidents, or naturally occurring threats or incidents. The resilience of a system’s function can be measured based on the persistence of a corresponding functional performance under uncertainty in the face of disturbances.*”. This definition serves as a robust foundation for quantifying resilience and demonstrates the concept’s relevance across diverse engineering fields while maintaining the core aspects originally introduced by Holling [8] and embracing the former definitions. In the further course of this dissertation, as well as in all included publications, the term resilience has been and is understood based on this definition provided by Ayyub.

1.3 Resilience quantification

An essential prerequisite for assessing resilience in the context of engineering systems is the availability of quantitative measures of resilience. Consequently, numerous methods have been developed over the past two decades, and many more are being published each year. Several authors provide comprehensive reviews of this very dynamic development of resilience metrics in systemic contexts [12, 23, 45, 69–74] and mathematical derivation and examination of measures in the context of resilience is provided, e.g., by Ayyub in [6]. In addition to quantitative assessment approaches for systemic resilience, it should be noted that qualitative approaches have also been published, as seen, e.g., in [12]. However, as this dissertation clearly focuses on systems in an engineering context, the emphasis is on resilience assessment methods that aim at resilience quantification, as a basis for the development of approaches to identify specific and meaningful resilience enhancement strategies.

1.3.1 Fundamentals

Bruneau et al. introduce in [48] the well-known concept of the resilience triangle, along with their widely respected resilience metric that is described in Sec. 1.3.3. Figure 1.1 illustrates the resilience triangle, which describes the loss area spanned from a system performance over time after a disruptive event at time t_0 and the subsequent recovery of the system back to the original performance level at time t_1 . In Fig. 1.1, point A represents the original system performance before a disruptive event occurred, point B the performance immediately after the performance-reducing disruptive event, and point D the recovered performance on the same level as the original pre-disturbance performance. Accordingly, a system is more resilient the smaller the area of its resilience triangle, i.e., the loss area. This concept is the basis for numerous quantification approaches to systemic resilience that have appeared since and is cited extensively

in the literature.

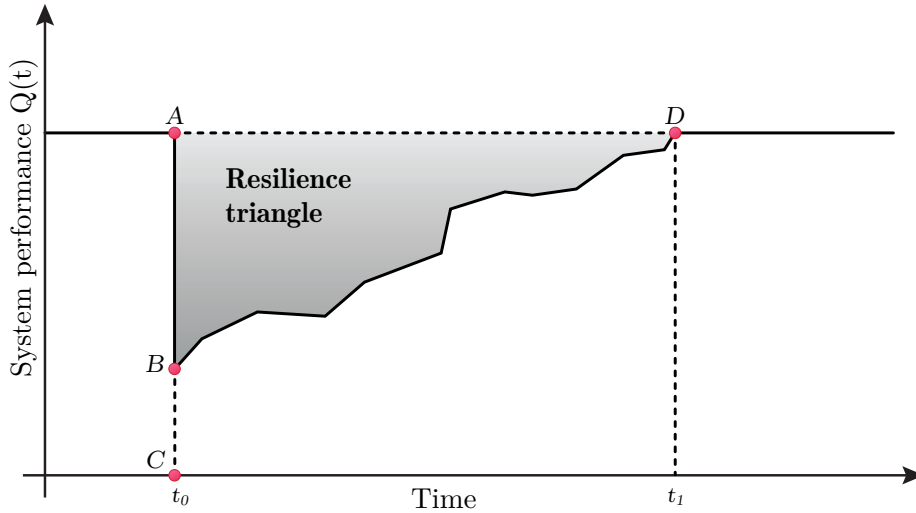


Figure 1.1: Resilience triangle; adapted from [48], [75] and [6].

Shinozuka et al. define in [75] two of the four resilience dimensions, robustness and rapidity, as quantifiable properties of a resilient system, according to the points marked in Fig. 1.1, as follows:

$$\text{Robustness} = B - C, \quad (1.1)$$

$$\text{Rapidity} = \frac{A - B}{t_1 - t_0}, \quad (1.2)$$

where robustness is given in percentage and rapidity as the average recovery rate in percentage per time. Note that Eq. 1.1 corresponds rather to the interpretation of the resilience dimension “robustness” according to the interpretation of Tierney & Bruneau in [51] than to the original one by Bruneau et al. in [48], see Sec. 1.2. These definitions and concepts, while not necessarily part of every resilience metric, have helped and continue to aid in understanding the research of quantifying system resilience. They are directly or indirectly incorporated into numerous quantification approaches in the literature.

In their work [76], Henry & Ramirez-Marquez present, in addition to a resilience metric, three system states and two system transitions that a system traverses during a characteristic performance cycle, i.e., when it is exposed to a disruptive event and subsequently recovers its operational capabilities. Fig. 1.2 illustrates these states and transitions that need to be taken into account by comprehensive measures for resilience quantification. The system passes through the following phases and transitions: (i) The original state, whose duration reflects the reliability of the system, is the initial phase. (ii) The transition of the system towards a disruptive state, triggered by the occurrence of a performance degrading disruptive event, is characterized by the robustness of the system that contributes to mitigate the performance degradation. This transition is also characterized by the vulnerability of the system, i.e., the inverse of robustness.

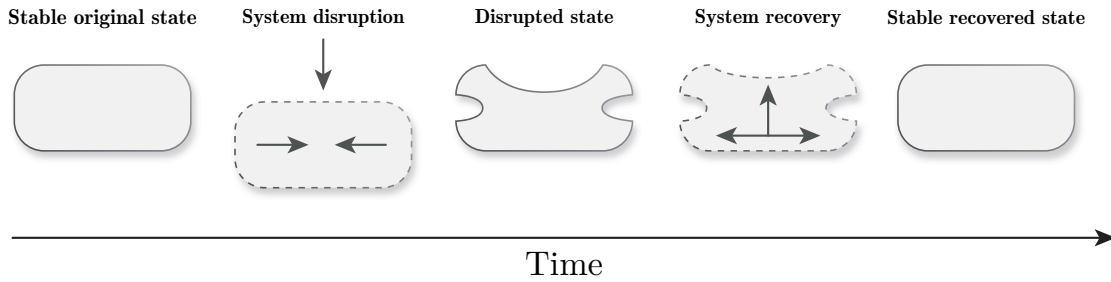


Figure 1.2: System state transitions for resilience quantification; adapted from [76].

(iii) The subsequent phase, the disruptive phase, is determined by its duration until recovery starts and consequently performance is (re)gained. (iv) The system recovery, i.e., the transition of the system to a new stable and recovered state. This transition is characterized by the rapidity and the quality of the recovery. (v) The new recovered stable state of the system.

Taking into account these phases and transitions, and according to works by, for example, Shinozuka et al. [75], Henry & Ramirez-Marquez [76], Baroud et al. [77], Pant et al. [78], Hosseini et al. [12] and several others, three important dimensions for resilience quantification, can be determined: 1. Reliability: the ability of a system to maintain a typical performance before the occurrence of a disruptive event. 2. Robustness: the ability of a system to mitigate the performance-degrading effects of a disruptive event and thus maintain a certain level of performance. Alternatively, this dimension is frequently defined by the opposite, i.e., vulnerability, represented by the loss of performance after the occurrence of a disruptive event. 3. Recoverability: the ability of a system to comprehensively and rapidly recover the performance of the system, whereby the new performance level can be identical to the original one, but can also be below or above it. A practical example of a post-recovery performance level above the original level might be if the recovery process is used to implement, for instance, hardware/software updates or other improvements to the system. These dimensions, essential for quantification and widely recognized in the literature, are shown in Fig. 1.3 in a typical systemic performance cycle.

It should be noted that similar to the research on a resilience definition, inconsistencies do exist regarding the notations related to the context of resilience quantification in the literature. However, these inconsistencies mainly pertain to the terminology of consistently applied phenomena. For example, Shinozuka et al. [75], Ayyub [6, 10], Faturechi & Miller-Hooks [52], Hosseini et al. [12], and many other authors use the notion of robustness as the quality of remaining performance after a performance-degrading disruptive event, see Eq. 1.1. On the other hand, Galaitsi et al. [79] for instance, use the term resistance for precisely this dimension of resilience quantification. In contrast, they refer to robustness as the dimension that is described by numerous authors, e.g., Madni & Jackson [80], Pant et al. [78], Hosseini et al. [12] and Gillespie-Marthaler et al. [81], as reliability in the context of resilience. However, it must be emphasized again that the underlying phenomena are characterized identically and are consistently assigned in the literature, i.e.,

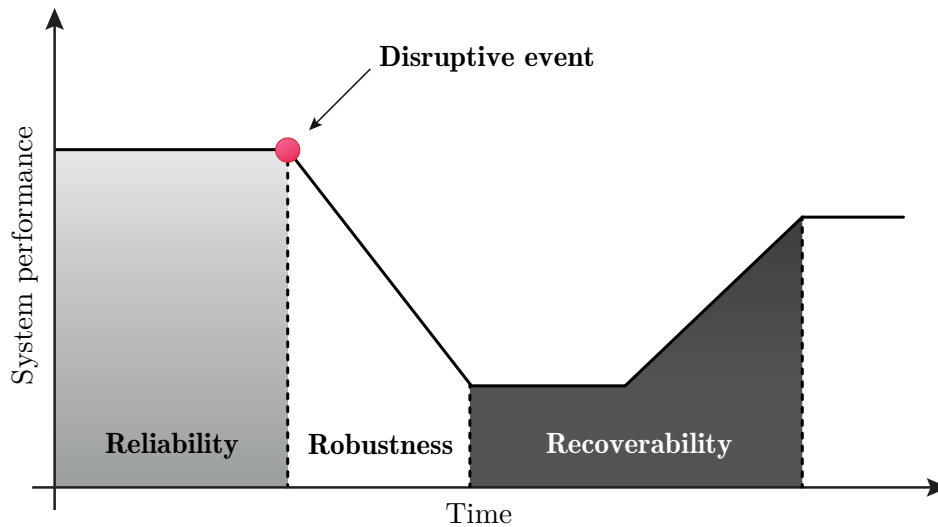


Figure 1.3: Resilience dimensions in the evolution of a system before and after the occurrence of a performance disruptive event: (i) reliability, (ii) robustness, vulnerability, (iii) recoverability; adapted from [76] and [78].

practically all sources agree that both exemplarily described properties are essential for the quantification of resilience. Therefore, these inconsistencies are almost exclusively limited to terminology.

Examples of highly regarded, comprehensive, and recent developments in the domain of resilience quantification are presented in the following. Bergström et al. emphasize in [23] the importance of resilience in contemporary literature, noting the critical connection between increasing system complexity and associated risks. Meanwhile, Sun et al. concentrate in [73] on infrastructure resilience, underscoring the close relationship between resilience and functionality, respectively performance measures. In [82], Moslehi & Reddy provide a performance-based resilience assessment methodology for engineered complex systems where resilience is quantified through loss of functionality and associated monetary costs incurred by the system stakeholders under different scenarios, covered in a consequence matrix and allowing for the evaluation of various resilience enhancement options. Cai et al. instead, provide in [83], a resilience metric predicated on system availability, incorporating the system's intrinsic structure and restoration resources as principal factors. They introduce a dynamic Bayesian network-based evaluation methodology, derived from the proposed resilience metric, allowing for prediction of the system resilience value and furnishing implementation guidance for system planning, design, operation, construction, and management. In [43], Francis & Bakera developed a high-regarded elaborate resilience analysis framework that encompasses system identification, resilience objective setting, vulnerability analysis, and stakeholder engagement. In addition, they propose an uncertainty-weighted resilience metric grounded on three resilience capacities: adaptive capacity, absorptive capacity, and recoverability. Singh et al. propose in [84] the resilience deficit index, an index for resilience quantification of buildings, that focuses on the loss of resilience, connecting the concept of the resilience triangle with monetary aspects. It is worth mentioning that Bruneau is among

the authors of this novel work, who, 20 years ago, together with his colleagues, developed the well-known Resilience Index in [48], the basis for this new approach, see Sec. 1.3.3. In [85] Didier et al. develop a quantitative measure to quantify the resilience of critical infrastructure called Resilience-Compositional Demand/Supply (Re-CoDeS). Their methodology considers both the ability of the civil infrastructure system to continue to provide its services or resource to the community and the corresponding demand for those services or resources within the community following a disaster event, i.e., a confrontation of supply, demand, and the consumption of the resource or service in question. It should be noted that these studies represent only a fraction of the published developments in recent years.

A major challenge in the assessment of systemic resilience is that, to date, no resilience metric has been developed that can be considered universal in the sense that it is applicable across different system types and independent of the type of stress [74]. With such a metric, analysts would be able to compare the resilience of a wide variety of systems and evaluate large, interconnected assemblies of systems in terms of their resilience. Since this has not yet been realized, some of the current review studies, such as those mentioned above, focus on categorizing diverse resilience assessment approaches, see Sec. 1.3.2, and classifying them in terms of their capacity, limitations, and areas of application.

1.3.2 Categorization

The range of sophisticated quantification approaches for systemic resilience has reached a high level in the literature. Nevertheless, variations in the definition of resilience persist, and consequently the frameworks used to assess resilience quantitatively or qualitatively are not very standardized and may not provide clear guidance to decision-makers, see, e.g., [43]. This, the dynamic nature of the research field, and the vast number of different resilience quantification approaches – major review studies such as those by Hosseini et al. [12] and Cheng et al. [74] have presented more than 60 and more than 80 highly regarded resilience metrics, respectively – makes it essential to develop appropriate categorization schemes. Not only can these schemes aid in identifying suitable resilience metrics for individual issues in practice, but the clarity and guidance provided by them may also assist in exploring and developing new resilience metrics and frameworks.

In [12], Hosseini et al. propose a highly regarded categorization scheme for resilience assessment methodologies. This scheme is shown in Fig. 1.4 and is bifurcated into two overarching categories: qualitative and quantitative approaches.

1. Qualitative approaches: These methods aim to evaluate the resilience of a system without the application of numerical descriptors. Instead, they rely on subjective analysis and human judgment. Within this category, two sub-categories can be identified:
 - A. Conceptual frameworks: These are grounded on best practices and heuristic methods that provide a structure for understanding resilience. They often serve as guides for the design and development of resilient systems.

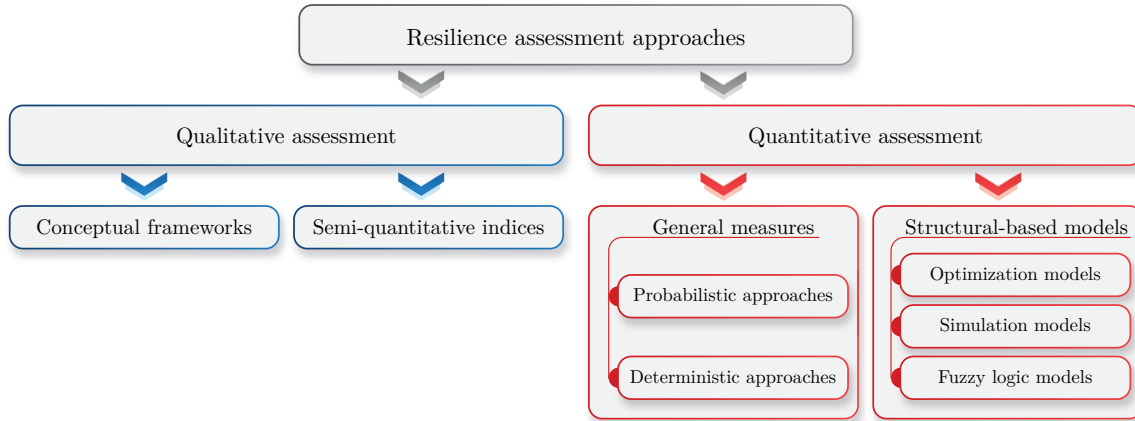


Figure 1.4: Categorization scheme for resilience metrics and resilience assessment methodologies according to Hosseini et al. [12].

- B. Semi-quantitative indices: These are often constructed by expert assessments which focus on distinct qualitative facets of resilience. They represent a bridge between purely qualitative and quantitative analysis, utilizing expert judgment and specifically designed questions to derive numerical scores, e.g., in percentage scale, based on qualitative data.
2. Quantitative approaches: These methods involve the use of numerical descriptors to quantify resilience. This category is further divided into two sub-categories:
- A. General measures: These are domain-agnostic measures, meaning they can be applied across various domains or sectors to quantify resilience. This universality allows for broader applicability and comparability across different system types. They provide a quantitative approach to evaluate resilience by measuring the system’s performance before and after a disruptive event, regardless of the system’s structure. Furthermore, these general measures are further characterized as deterministic and stochastic, each capable of describing static and dynamic system behavior:
- Deterministic measures: These measures do not incorporate uncertainty, such as the probability of disruption, into the metric.
 - Probabilistic (or stochastic) measures: These measures capture the uncertainty associated with system behavior.

Dynamic measures account for time-dependent behavior, whereas static measures do not consider time-dependency.

- B. Structural-based models: These are domain-specific and utilize mathematical and computational models to represent and analyze resilience within a particular domain. They examine how the resilience of a system is affected by its structure. Such methods

are often complex, requiring significant expertise, observation, data, and simulation, but can offer detailed, system-specific insights. Hosseini et al. define three sub-classes of structural-based approaches:

- Optimization models
- Simulation models
- Fuzzy logic models

The categorization scheme by Hosseini et al. reflects the diversity of approaches and methodologies within the realm of resilience quantification, underscoring the complexity of measuring resilience and the multitude of perspectives that contribute to it. It is instrumental in providing a nuanced understanding of the diverse methodologies employed in this field.

Another indication of the dynamic and complex nature of the research field of resilience assessment approaches is provided by the fact that not one but numerous categorization schemes exist in the literature. For instance, Cheng et al. in [74], recently presented, along with a review of existing approaches to quantitatively assessing resilience, a novel categorization scheme. In this scheme they group, numerous established and recently developed resilience metrics into the following categories and subcategories:

1. Length of hazard and recovery periods: These measures quantify resilience as the ratio between the expected recovery and the realized recovery period.
2. Performance over a time period: Metrics in this category measure the robustness of the system and its recovery capacity in terms of performance degradation and recovery during hazard and recovery phases. This category is divided into six subcategories.
 - Performance during the hazard period
 - Difference between actual and desired performance during a period
 - Ratio of actual and desired performance during a period
 - Ratio of performance loss and desired performance during a period
 - Recovered performance
 - Average performance (loss)
3. Performance at a time instant: These measures assess resilience as an immediate indicator at a specific moment in time. In the case of certain service-oriented systems, the system resilience is evaluated directly by the performance status at a particular instant. Three subcategories characterize this category.
 - Performance at a time instant
 - Normalized performance at a time instant
 - Ratio of the recovered and degraded performance

4. Probabilistic metrics: In real-world scenarios, hazards occur randomly, and consequently, system performance degrades at random as well. Moreover, in practice, recovery is a stochastic process, subject to numerous uncertainties. This requires describing system resilience from a probabilistic perspective, which is realized by the metrics in the following six subcategories.
 - Probability that performance is recovered to a level within a period
 - Reliability
 - Complement of failure probability
 - Reliability improvement
 - Probability that performance loss and recovery rapidity meet certain thresholds
 - Conditional probability that performance is recovered to a level within a period
5. Multiple indicators: The resilience of a system can be divided into different segments. Measures in this category combine these individual segments into aggregate resilience. The category is divided into two subcategories.
 - Sum of reliability and recovery ability
 - Other indicators

Although both their review study and categorization scheme are extensive, some problematic inconsistencies can be identified in the scheme proposed by Cheng et al. Especially in comparison to the categorization scheme provided by Hosseini et al. in [12], it is noticeable that the categories and subcategories do not have sufficient selectivity. All investigated metrics are assigned to a single subcategory, even though it would be feasible or even necessary to assign numerous metrics to multiple subcategories. For example, the resilience metric introduced by Ayyub in [6] and presented in Sec. 1.3.4, is categorized in Cheng et al.'s scheme as a metric with "multiple indicators" rather than a "probabilistic metric" or a "performance over a time period" metric, although clearly all three attributes are accurate, according to Ayyub, and according to Hosseini et al.'s scheme in [12]. Similarly, the metric by Ouyang et al. in [86], also presented in Sec. 1.3.4, is not declared to be a "probabilistic metric" in the scheme by Cheng et al., contrary to the authors themselves and Hosseini et al. Instead, in [74], it is only declared as a "performance over a time period" metric. Even though this is undoubtedly correct, this declaration is incomplete and misleading. This ambiguity or inconsistency can be identified for multiple metrics and can be objected to as a clear weakness of this categorization scheme. Other categorization schemes for resilience metrics are provided, e.g., by Johansen et al. in [87] for the domain of community resilience, by Raoufi et al. in [72] for field of power systems, and by Sun et al. in [73] in the context of transportation infrastructure.

Among the categories of resilience assessment approaches proposed in Hosseini et al.'s scheme, the group of performance-based, i.e., general measures is one of the most prevalent in the literature.

These approaches can be ratio-based, integral-based, or both. In particular, probabilistic, time-dependent resilience metrics allow for comprehensive resilience analyses and are capable of taking into account all three essential dimensions of resilience quantification shown in Fig. 1.3. The subsequent sections, Sec. 1.3.3 and Sec. 1.3.4, in which selected and in the literature highly respected time-dependent deterministic and probabilistic resilience metrics are specifically addressed, are guided by the widely recognized categorization scheme according to Hosseini et al.

1.3.3 Deterministic resilience metrics

In the following, two deterministic and time-dependent resilience metrics that have received significant attention in the literature are presented. These metrics are highly relevant in this new and dynamic field of research. Other widely considered developments in the domain of deterministic resilience metrics include, for example, the works of Francis & Bekera [43] and Omer et al. [88] in the field of urban infrastructure, Cox et al. [89], Enjalbert et al. [90], Chen & Miller-Hooks [91], and Henry & Ramirez-Marquez [76] on transportation, Ouedraogo et al. [92] for human-machine systems, Cimellaro et al. [5] in the healthcare sector and Zou & Chen [93] on traffic and electrical power systems.

Metric by Bruneau et al.

Along with the concept of the resilience triangle, see Fig. 1.1, Bruneau et al. introduce in [48] a time-dependent deterministic metric for assessing the resilience of communities subjected to seismic disruption. Given that t_0 represents the moment of the disruptive event's occurrence and t_1 denotes the time point of the system's full recovery, their proposed metric is formulated as:

$$R = \int_{t_0}^{t_1} [100 - Q(t)] dt, \quad (1.3)$$

while $Q(t)$ indicates the quality of the community infrastructure at time t in relation to a specific type of system performance. It should be noted that, analogous to the concept of the resilience triangle, their resilience metric does not refer to the resilience of a system, but to the loss of resilience compared to an ideal system performance over time, which Bruneau et al. determine to be 100. R , therefore, does not represent a system resilience, but a loss of resilience and is equivalent to the area of the resilience triangle.

A major advantage of this approach is its broad applicability. Although the metric was originally developed for measuring seismic resilience of communities, it can be effortlessly applied to other system types. Moreover, the limitation to a static benchmark of a pre-disaster performance of 100% can be easily adapted. The metric of Bruneau et al. was one of the first and is now one of the most widely referenced quantification approaches for systemic resilience in the literature and has had a major influence on numerous metrics that followed, see, e.g., [94–96].

Metric by Rose

In [97] Rose provides a deterministic resilience metric in the context of economic systems that is focused on recovery and denoted as dynamic resilience. Rose notes, “*In the literature on resilience, dynamics often refers to the issue of stability or to the speed of recovery. The real interesting question here is the pattern of recovery – how much recovery takes place in each time period and why.*” The performance of a system, in this approach, is assumed to be the time-dependent economic activity $Y(t_i)$. Dynamic resilience DR , according to Rose, is defined as the loss-reducing effect of hastened recovery and accelerated reconstruction of the capital stock, opposed to a standard recovery procedure:

$$DR = \sum_{t=0}^n Y_{DR}(t_i) - \sum_{t=0}^m Y_{DU}(t_i), \quad (1.4)$$

with n and m representing the number of considered time steps and $m > n$, time period t_i , $Y_{DR}(t_i)$ denoting the economic activity of the system under hastened recovery and $Y_{DU}(t_i)$ representing the economic activity of the system under standard recovery. The concept is illustrated in Fig. 1.5. The area spanned between the resilient, loss-reducing recovery path of $Y_{DR}(t_i)$ and the path of standard recovery $Y_{DU}(t_i)$ can be interpreted as the loss area, similar to the interpretation of the loss triangle by Bruneau et al. [48], as illustrated in Fig. 1.1 and described in Sec. 1.3. Rose’s resilience approach emphasizes the vast importance of incorporating monetary aspects in the context of resilience analysis and focuses on practical decision-making.

1.3.4 Probabilistic resilience metrics

In the following, two particularly sophisticated probabilistic and time-dependent resilience metrics that have received much attention in the literature and are widely applicable are presented as examples. Other widely cited probabilistic resilience metrics include, for example, the works of Franchin & Cavalieri [98], Attoh-Okine et al. [99], and Guidotti et al [100] in the field of urban infrastructure, Pant et al. [78] on transportation, Hashimoto et al. [101] on water resource systems, Chang & Shinozuka [49] and Guidotti et al. [100] on community resilience, Youn et al. [57] on engineering design, Barker et al. [102] on network resilience, Zeng et al. [103] on energy systems and Xu et al. [104] on multi-state networks.

Metric by Ayyub

A sophisticated, comprehensive, and widely referenced probabilistic resilience metric is presented by Ayyub in [6] and [10]. This performance-based metric is time-dependent and can account for any negative as well as positive factors influencing the performance of a system over any period of time. Consequently, it is capable of capturing all relevant phases of system resilience quantification outlined in Fig. 1.3. According to Ayyub, the metric can be vividly explained by means of Fig. 1.6. The figure schematically illustrates a time-dependent system performance

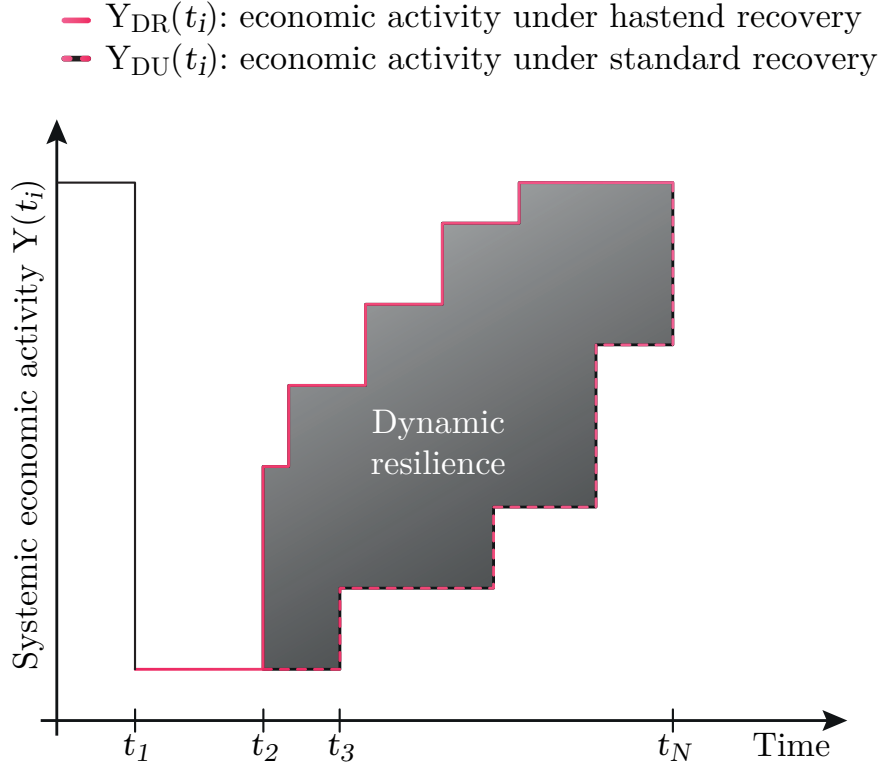


Figure 1.5: Recovery-based resilience metric; adapted from [97] and [12].

$Q(t)$, subjected to aging effects and the occurrence of disruptive events at a rate λ that follows a Poisson process. A potential failure event occurring at time t_i lasts for a duration of ΔT_f and ends at time t_f . Subsequently, a period of recovery begins that lasts for a duration of ΔT_r and concludes at time t_r . For illustrative purposes, the diagram shows three different types of failure events: brittle (f.1), ductile (f.2), and graceful (f.3), as well as six unique recovery events: expeditious recovery to a state better than the original (r.1), expeditious recovery to the original state (r.2), expeditious recovery to a state better than the aged state (r.3), expeditious recovery to as good as the aged state (r.4), recovery to the original aged state (r.5), and recovery to a state worse than the original aged state (r.6). Together, these events represent different rates of change in the performance of the system. In addition, the figure illustrates the performance trajectory of the system during aging and the expected trajectory after recovery. The cumulative disruption D is characterized by a duration of ΔT_d , which is calculated as the sum of ΔT_f and ΔT_r as:

$$\Delta T_d = \Delta T_f + \Delta T_r, \quad (1.5)$$

with

$$\Delta T_f = T_f - T_i, \quad (1.6)$$

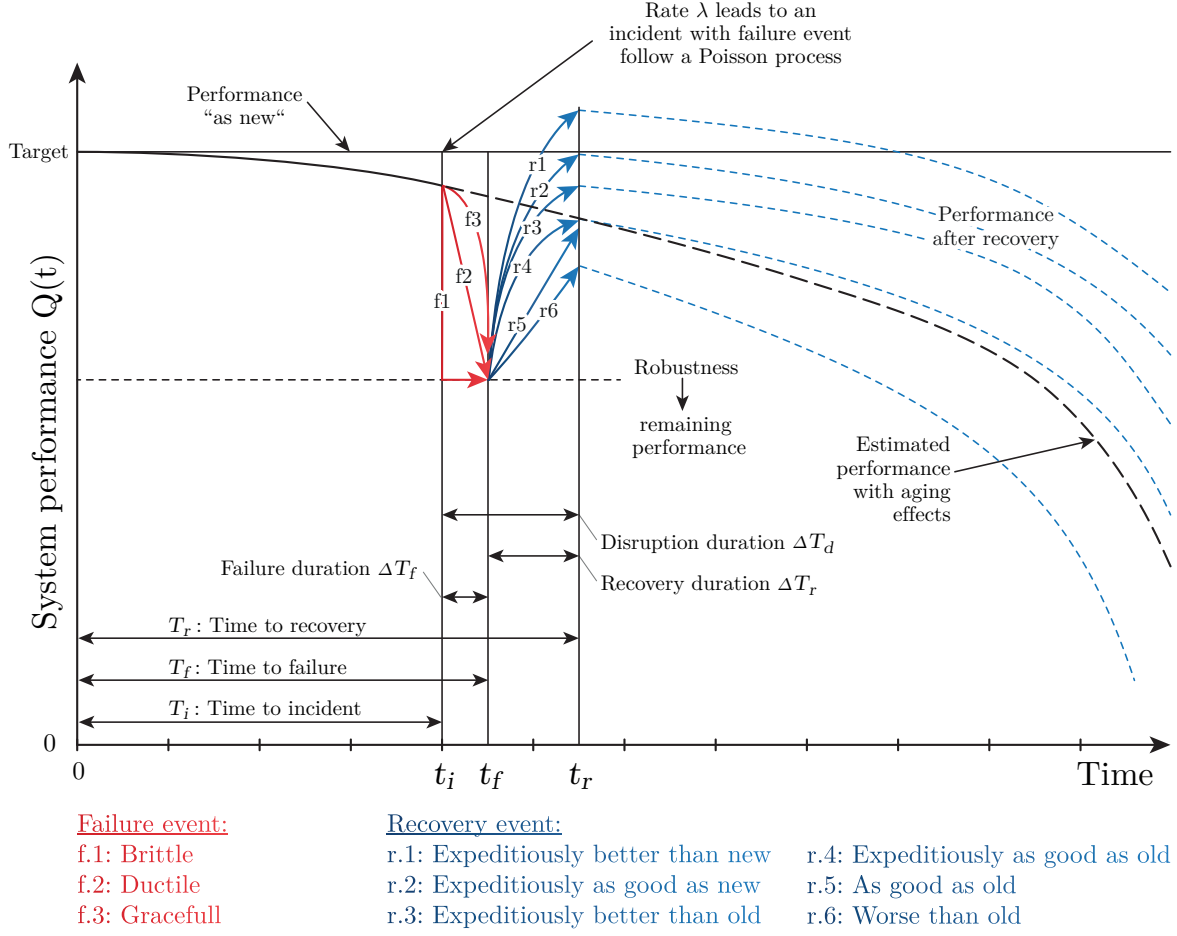


Figure 1.6: Resilience metrics and definitions; adapted from [6].

and

$$\Delta T_r = T_r - T_f. \quad (1.7)$$

The time to incident T_i , the time to failure T_f , as well as the time to recovery T_r , shown in Fig. 1.6, are all assumed to be random variables.

Following these definitions and illustrations, Ayyub's resilience metric is provided as:

$$Resilience (R_e) = \frac{T_i + F\Delta T_f + R\Delta T_r}{T_i + \Delta T_f + \Delta T_r}, \quad (1.8)$$

with F denoting the failure profile, defined for each failure event f as:

$$Failure(F) = \frac{\int_{t_i}^{t_f} f dt}{\int_{t_i}^{t_f} Q dt}. \quad (1.9)$$

The value of the failure profile F can be considered with respect to the four dimensions of resilience introduced by Bruneau et al., see Sec. 1.2, both as a measure of the system property robustness, i.e. the difference of the performance points C and B in Fig. 1.1, see Eq. 1.1, that is the remaining system performance, and as the redundancy of the system. Analogous to F , for each recovery event r , the corresponding recovery profile R is defined as:

$$Recovery(R) = \frac{\int_{t_f}^{t_r} r dt}{\int_{t_f}^{t_r} Q dt}. \quad (1.10)$$

The recovery profile value R , again with respect to the four R's, see Sec. 1.2, can be considered as a measure of resourcefulness and rapidity, proposed to cover the notion in Eq. 1.2 and as illustrated in Fig. 1.1. The time to failure T_f is characterized by its probability density function f_{T_f} , described by the following function that is, according to Ayyub, derived from [105] and is based on a Poisson process:

$$f_{T_f} = -\frac{d}{dt} \int_{s=0}^{\infty} \exp \left[-\lambda t \left(1 - \frac{1}{t} \int_{\tau=0}^t F_L(\alpha(\tau)s) d\tau \right) \right] f_{S_0}(s) ds, \quad (1.11)$$

with λ , the incident occurrence rate, $\alpha(t)$, embodying the aging effects, that constitute a time-dependent degradation mechanism, and $Q(t)$, the time-dependent system performance, defined as the difference between the system's strength S and the corresponding load effect L with $Q = S - L$. L and S are considered to be stochastic variables, with F_L representing the cumulative probability distribution function of L , and f_S representing the probability density function of S . Note that $\alpha(t)$, theoretically, can also reflect performance improvements over time. This resilience metric by Ayyub is coherent with the conditions on a definitional concept of resilience presented by him, and consequently coherent with his proposed definition of resilience as both shown in Sec. 1.2. It should be noted that in addition to the sophisticated resilience metric provided here, Ayyub, in [10], presents also a simplified, more practical version of this metric. Ayyub states that although the metric, see Eqs. 1.5 to 1.11 and Fig. 1.6 “[...] offer a comprehensive capture of the resilience attributes according to the resilience definition; it is complex and might be impractical.”

Metric by Ouyang et al.

Ouyang et al. provide in [86] a time-dependent resilience metric that determines the expected annual resilience of infrastructure systems. The general formulation of the metric allows for easy adaptation to other time periods as well as application to any type of system. The metric is defined as the mean proportion of the area enclosed by the real performance function $P(t)$ and the time axis relative to the area enclosed by the target performance function $TP(t)$ and the time axis as

$$AR = E \left[\frac{\int_0^T P(t) dt}{\int_0^T TP(t) dt} \right] = E \left[\frac{\int_0^T TP(t) dt - \sum_{n=1}^{N(T)} AIA_n(t_n)}{\int_0^T TP(t) dt} \right], \quad (1.12)$$

with $E(\cdot)$ representing the expected value and T denoting a time interval of one year. n refers to the event occurrence number, encompassing co-occurrences of different hazard types and $N(T)$ signifying the aggregate number of event occurrences throughout the time interval T . Furthermore, t_n is a random variable, representing the occurrence time of the n -th event. Lastly, $AIA_n(t_n)$ is a random variable as well and denotes the impact area for the n -th event occurrence at time t_n , which is the area between the actual performance curve $P(t)$ and the targeted performance curve $TP(t)$. Note that both the actual performance function and the target performance function are stochastic processes, although the target performance function can also be assumed to be a constant for practical reasons, i.e., $TP(t) = TP$. If in addition it is assumed that the system returns to its original performance level after each disruptive event, Eq. 1.12 simplifies to:

$$AR = \frac{TP \cdot T - E \left[\sum_{n=1}^{N(T)} AIA_n(t_n) \right]}{TP \cdot T} = \frac{TP - E \left[\frac{1}{T} \sum_{n=1}^{N(T)} AIA_n(t_n) \right]}{TP}. \quad (1.13)$$

In their work, Ouyang et al. provide further specification for the calculation of $AIA_n(t_n)$ for various hazard scenarios involving both single hazard type and multiple joint hazard types. Nevertheless, in both cases, Eq. 1.12 and Eq. 1.13 are appropriate quantitative resilience functions, capable of addressing the possibility of simultaneous hazard type occurrences. Thereby, the equations account for potential variations in frequency within $N(T)$, as well as for variations in $AIA_n(t_n)$ that may occur for the n -th event as a result of resource allocation or preventive measures for other hazard events.

1.4 System reliability

From Sec. 1.2 and Sec. 1.3, it is clear that there is a wide consensus in the literature that reliability is an essential component of a definitional concept of resilience and, consequently, must be considered in resilience quantification, see, e.g., Fig. 1.3. In practice, during analysis, the reliability phase typically requires a considerable number of system evaluations, especially when various simulations of different system configurations are needed. These simulations influence the probability structure of the system components and subsystems and consequently affect the overall system. Therefore, particularly efficient analysis approaches are required for this phase. It is therefore logical, if not necessary, to explore the well-researched and extensive domain of system reliability engineering for tools that can meaningfully assist the emerging field of systems resilience analysis in areas such as quantification, decision-making, efficiency, etc.

1.4.1 Assessment approaches and quantification

Traditional methods for system reliability assessment and quantification encompass failure mode and effect analyses, see, e.g., [106, 107], and mathematical representations such as reliability block diagrams [108], as well as fault tree and success tree methods, see [109–111]. In [112]

and [113], the authors employ master logic diagrams to describe the behavior of systems and assess their reliability. However, various of these methodologies may encounter limitations in handling large, complex systems where the calculations required – for example, for identifying minimal path sets or cut sets – become computationally prohibitive [114]. Furthermore, Markov models [115], Bayesian analysis [116], Bayesian networks [117–119] and Petri nets [120] represent other established approaches. Kabir & Papadopoulos [121] provide a comprehensive overview on the applications of Bayesian networks and Petri nets in safety, reliability, and risk assessments. More recent research has introduced advanced methods for system reliability assessment. For instance, multi-state systems are considered from various perspectives in [122–124], while in [125], Guo et al. employ the Bayesian melding method, integrating data from various sources at both system and subsystem levels. Additionally, novel approaches based on learning Kriging models are proposed by Yang et al. and Xiao et al. in [126, 127], respectively, incorporating multiple failure modes and a multiple response model and in [128] Xiao et al. provide a reliability analysis methodology based on dependent Kriging predictions and a parallel learning strategy. In the context of systems composed of repairable components with intricate failure distribution structures, Li et al. offer a distinct reliability approach in [129]. In [130], Luo et al. provide a novel statistical model for system reliability assessment that incorporates correlated component lifetimes and lifetime ordering constraints, integrating dynamic environmental effects and using the maximum likelihood method for parameter estimation and generalized pivots for confidence intervals. Mellal & Zio present in [131] an enhanced nest cuckoo optimization algorithm, a novel approach for system reliability-redundancy allocation using a cold-standby strategy. Note that this is only a short sample of novel developments in the extensive research field of system reliability analysis and has no claim of completeness. A broad review of numerous system reliability methodologies and the evolution of reliability optimization is furnished in publications such as [132–137]. These collective efforts contribute to a robust and evolving body of knowledge on system reliability assessment in increasingly complex environments.

1.4.2 Concept of survival signature

Numerous system reliability methodologies rely on the mathematical principle of the structure function, which depicts a system’s functional state based on its components’ states, or state vectors [138–143]. However, the structure function can become convoluted or unfeasible, particularly for large and complex systems [144, 145]. Patelli et al. state in [114] that the structure function has a Boolean format and can only be employed to determine a particular output of the system. However, multiple structure functions can be used to capture all possible states of the system, which is typically necessary but severely increases the complexity of the analysis and thus its computational cost, see, e.g., [146]. For coherent systems, i.e., systems with a monotonic structure function whose functional state depends on the functionality of their components [147], and which contain only a single type of component, the system signature serves as a summary of the structure function and thus constitutes a valuable tool [148].

The survival signature concept, pioneered by Coolen and Coolen-Maturi [149], has emerged as a promising technique for effectively modeling the reliability of systems with multiple component types. Introduced as a generalization of the system signature, the survival signature overcomes the limitation to single-component-type systems during reliability analysis. The principal advantage of this approach, compared to conventional methods, is its capacity to separate the system's structure and the time-dependent probabilistic properties of its components. Once the system structure has been evaluated, typically a computationally demanding process, any required probabilistic characterizations can be examined without necessitating a reassessment of the system structure. Consequently, this technique alleviates the computational demands associated with repeated model evaluations in reliability engineering processes, typically encountered in design and maintenance processes, when compared to traditional methods [114, 150]. Furthermore, it condenses the system structure by aggregating state vectors into individual survival signature entries with associated reliabilities, resulting in substantially reduced storage needs and simplified data access [151]. These features are what make the survival signature unique and valuable in the context of system reliability analysis [152]. Comprehensive information on the concept and its derivation can be found in [149, 153, 154].

As noted by [114], a purely analytical application of the survival signature to real-world complex systems is frequently infeasible, necessitating the use of simulations. Accordingly, Patelli et al. propose simulation algorithms based on the survival signature concept and Monte Carlo simulation [114]. Nevertheless, the computational effort required to determine the survival signature for large systems may be prohibitively high. To address this issue, Behrensdorf et al. recently provide an approach that focuses on approximating survival signature entries by estimating associated reliability values over a subset of relevant state vectors, significantly reducing the computational cost of the singular topological system evaluation [155]. Moreover, [156] provides an efficient algorithm for the precise computation of system and survival signatures using binary decision diagrams. Further, the process of substructuring a system into smaller serial or parallel subsystems and subsequently merging their survival signatures has been explored [157]. Other current research incorporates the concept of survival signature with multiple failure modes and dependent failures [158], common cause failures [159], interconnected networks [160], reliability analyses under consideration of imprecision [152], systems with shared components [161], systems subject to internal failures and external shocks [162], direct partial logic derivatives [163], reliability-redundancy allocation problems [164], multi-state components [114, 165], and continuous-state components as well as continuous-state systems [166].

Structure function

Consider a system composed of m components belonging to a single type. The state vector of these components is represented by $\mathbf{x} = (x_1, x_2, \dots, x_m) \in \{0, 1\}^m$, where $x_i = 1$ signifies a functioning state for the i -th component and $x_i = 0$ indicates a non-functioning state. The structure function, denoted by ϕ , is a function of the state vector that describes the operating

state of the system under investigation: $\phi = \phi(\mathbf{x}) : \{0, 1\}^m \rightarrow \{0, 1\}$. Consequently, $\phi(\mathbf{x}) = 1$ indicates a functioning system, while $\phi(\mathbf{x}) = 0$ signifies a non-functioning system with respect to the state vector \mathbf{x} .

In the case of a system composed of components of multiple types, i.e., $K \geq 2$, the total number of system components is given by $m = \sum_{k=1}^K m_k$, where m_k represents the number of components of type $k \in \{1, 2, \dots, K\}$. The state vector for each type can then be defined analogously to systems with only a single component type as $\mathbf{x}^k = (x_1^k, x_2^k, \dots, x_{m_k}^k)$.

Survival signature and survival function

The survival signature characterizes the probability of a system remaining in a functioning state, depending solely on the number of functioning components l_k for each type k . Assuming the failure times of components of the same type to be independent, identically distributed (*iid*) or exchangeable within this type, the survival signature can be expressed as:

$$\Phi(l_1, l_2, \dots, l_K) = \left[\prod_{k=1}^K \binom{m_k}{l_k}^{-1} \right] \times \sum_{\mathbf{x} \in S_{l_1, l_2, \dots, l_K}} \phi(\mathbf{x}), \quad (1.14)$$

where $\binom{m_k}{l_k}$ denotes the total number of state vectors \mathbf{x}^k of type k and S_{l_1, l_2, \dots, l_K} represents the set of all state vectors of the entire system for which $l_k = \sum_{i=1}^{m_k} x_i^k$. Thus, the survival signature is dependent solely on the system's topology, irrespective of any time-dependent failure behavior of its components. It is important to note that the concept of exchangeability, as outlined in [167], implies that the input ordering of random quantities is inconsequential. Therefore, in practical applications, rearranging the components assumed to be exchangeable should be irrelevant to the actual system. The assumption of exchangeability is reasonable for components that share the same functionality, are produced by the same manufacturer, and operate under the same environmental conditions. However, when environmental factors change, components of the same type might be subjected to varying environmental stresses, such as significantly different temperatures, influencing their behavior and lifetime probability distribution function. In such cases, assuming exchangeability would be inappropriate, as discussed in [114].

Let $C_k(t) \in \{0, 1, \dots, m_k\}$ denote the number of components of type k in a functioning state at time t , and assume the probability distribution for the failure times of type k to be known, with $F_k(t)$ representing the corresponding cumulative distribution function. Then,

$$\begin{aligned} P\left(\bigcap_{k=1}^K \{C_k(t) = l_k\}\right) &= \prod_{k=1}^K P(C_k(t) = l_k) \\ &= \prod_{k=1}^K \binom{m_k}{l_k} [F_k(t)]^{m_k - l_k} [1 - F_k(t)]^{l_k} \end{aligned} \quad (1.15)$$

describes the probabilistic structure of the system, i.e., the time-dependent failure behavior of the system components, without considering its topology. The survival function, which describes the probability of a given system remaining in a functioning state at time t , is calculated as:

$$P(T_s > t) = \sum_{l_1=0}^{m_1} \dots \sum_{l_K=0}^{m_K} \Phi(l_1, l_2, \dots, l_K) \times P\left(\bigcap_{k=1}^K \{C_k(t) = l_k\}\right), \quad (1.16)$$

with T_s denoting the random system failure time. Figure 1.7 illustrates an exemplary survival function for an arbitrary system with arbitrarily chosen distribution functions and distribution function parameters that describe the failure behavior of the system components, i.e., the system's reliability.

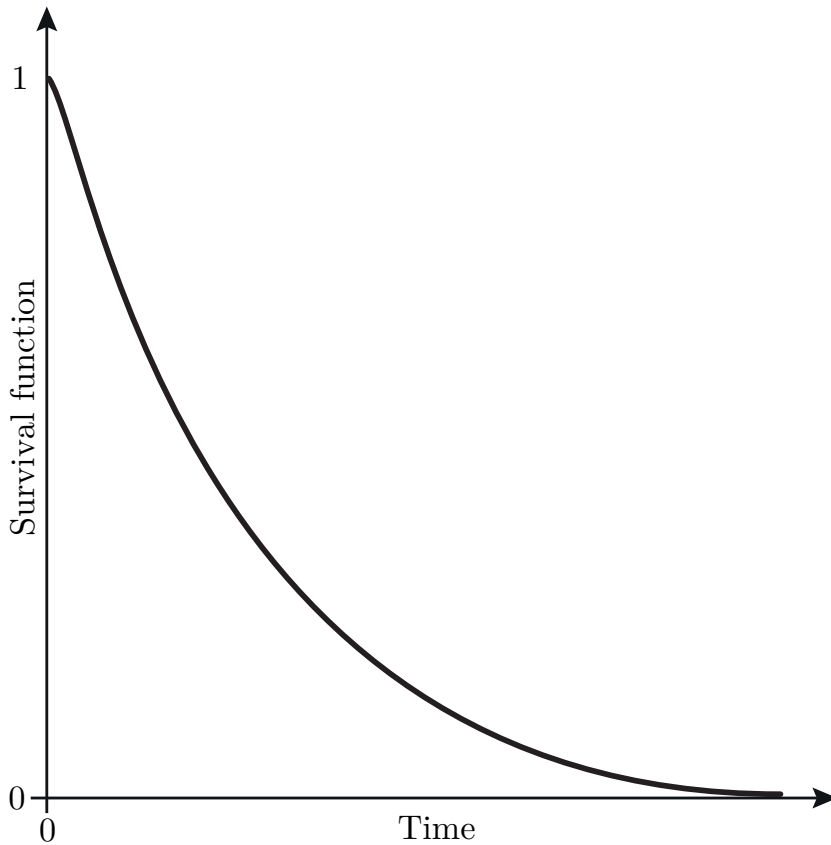


Figure 1.7: Arbitrary survival function.

1.5 Uncertainty

The analysis of complex systems, necessary for scenarios such as design and maintenance decisions, relies not only on the quality of the model but also on the quality of the available data. In the real world, the collection of exact data is often not feasible, as, e.g., lifetime data measurements and expert assessments are naturally subject to different kinds of uncertainty. Consequently, both the model's parameters and its inputs are burdened by inherent uncertainties propagated through the model. This unavoidable limitation necessitates a detailed understanding of uncertain system behavior. A complex and major challenge engineers face is how to accurately incorporate these

uncertainties into their models.

1.5.1 Definition and classification

In the academic literature, there is an ongoing debate about various aspects of uncertainty modeling, such as nomenclature, interpretation [168, 169], and their representation [170, 171]. Building on Nikolaidis' perspective in [172], uncertainty can be interpreted indirectly through the lens of decision theory, by considering the definition of certainty and its absence. This interpretation, along with its corresponding states, is illustrated in Fig. 1.8(a). Expanding this concept into a broader interpretation, certainty – symbolized by state 4 in Fig. 1.8 – denotes the condition wherein full knowledge concerning model input is present. Such a condition is an idealistic one, where deterministic models can be utilized. Accordingly, uncertainty signifies the presence of incomplete knowledge in terms of, for instance, component behavior or relevant decision measures and their resulting outcomes, as discussed in [172]. Maximum uncertainty corresponds to a state of total ignorance, i.e., state 1, where no knowledge exists. Though this state exists only theoretically, in actual practice, the current state of information, represented as state 2, typically comprises a combination of known and unknown variables. The gap between total ignorance and the present state of information represents knowledge deemed certain, which can be deterministically implemented in the model. Conversely, the gap between the present state and certainty corresponds to residual uncertainty. In decision-making, stakeholders aim to mitigate dangerous uncertainties maximally, pushing the present state of information as close to certainty as practicality and cost-effectiveness permit.

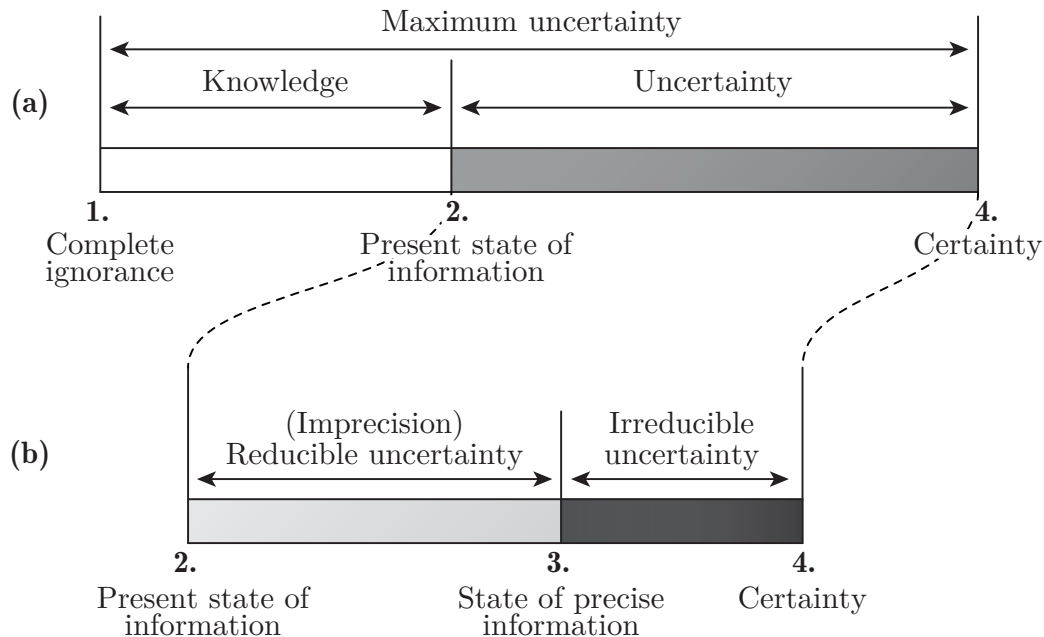


Figure 1.8: Elements and interpretation of uncertainty; adapted from [172] and [168].

Appropriate handling of uncertainties in analyses necessitates a proper classification, such as the two-part taxonomy proposed by Der Kiureghian & Ditlevsen in [169]: “*The advantage of separating the uncertainties into aleatory and epistemic is that we thereby make clear which uncertainties can be reduced and which uncertainties are less prone to reduction, at least in the near-term, i.e., before major advances occur in scientific knowledge*”. Nikolaidis, in [172], observes that further taxonomies of uncertainty can be found in the literature. However, a general agreement prevails that differentiating these two types of uncertainty is advantageous and adequate in the engineering domain [168, 169, 173]. Concentrating on this dual classification, the first type is often referred to as irreducible, aleatoric, or objective uncertainty, and the second is termed as imprecision, epistemic uncertainty, reducible or subjective uncertainty. These terms are typically used interchangeably across the literature [168, 174]. However, this terminology is subject to ongoing discussions, as evidenced by comparisons among [168, 175, 176]. Aughenbaugh & Paredis, in [168], clarify the existence of aleatoric uncertainty as a philosophical debate, emphasizing the practical application of the terms irreducible uncertainty and imprecision. Hence, these terms are adopted henceforth.

Fig. 1.8(b) demarcates the two types of uncertainty. Here, the state of precise information, illustrated as state 3, defines the boundary between irreducible uncertainty and imprecision. The space between state 3 and certainty represents the uncertainty currently considered irreducible. This type originates from assumed variability and randomness, which prevents certainty during the evaluation process [173]. In contrast, the space between the present state of information and the state of precise information denotes imprecision, which can, e.g., result from limited sample sizes or subjective, fuzzy evaluations by experts. Further origins of imprecision and their considerations are discussed in [169] and [177]. Actions can be taken to improve information quality and thus reduce imprecision [173]. However, these actions typically involve effort and costs, and achieving the state of precise information may be unattainable.

1.5.2 Approaches to uncertainty incorporation and handling

In the field of resilience analysis, there are only a few sporadic approaches that adequately account for uncertainty at the present, such as in the work of Azadeh et al. [178] on modeling and improving supply chains with imprecise transportation delays and resilience factors, Rocchetta et al. [179] in the field of (imprecise) probabilistic assessments of power system resilience, and Filippi et al. [180] on optimizing the resilience of space systems under epistemic uncertainty. However, the few existing approaches rarely address the direct integration of uncertainty into fundamental resilience quantification approaches such as presented in Sec. 1.3.

In contrast, in the established domain of system reliability analysis, research has long been conducted on the direct integration of uncertainties into existing models. Existing recognized methods include, e.g., Dempster-Shafer theory [181–183], Bayesian methods [124, 184, 185], info-gap theory [186], p-boxes [187–189], and fuzzy probabilities [124, 190]. Comprehensive studies on uncertainty engineering in general and reviews on reliability analysis approaches

considering uncertainties in a systemic context, in particular, are provided, e.g., in [191–199]. Regarding the concept of survival signature, see Sec. 1.4.2, several studies [114, 145, 154, 200–202] have successfully merged the advantages of the survival signature with uncertainty considerations and provided holistic frameworks for reliability analysis. In order to account for both irreducible uncertainty and imprecision, appropriate system analysis approaches are required. A common approach is a two-phase simulation, often referred to as a “double-loop” approach. In this approach, variables with imprecision are propagated in an “outer loop” while variables with irreducible uncertainty are sampled within an “inner loop” [203]. Conversely, irreducible variables can be sampled in the outer loop, with the propagation of imprecision occurring within the inner loop [204]. For clarifying definition and distinction of aleatory and epistemic uncertainties, see Sec. 1.5.1. A resulting survival function, compared to the precise survival function shown in Fig. 1.7, could for instance appear as in Fig. 1.9, i.e., an arbitrary, imprecise survival function with an upper and a lower bound. However, this simplified approach leads to large sample sizes,

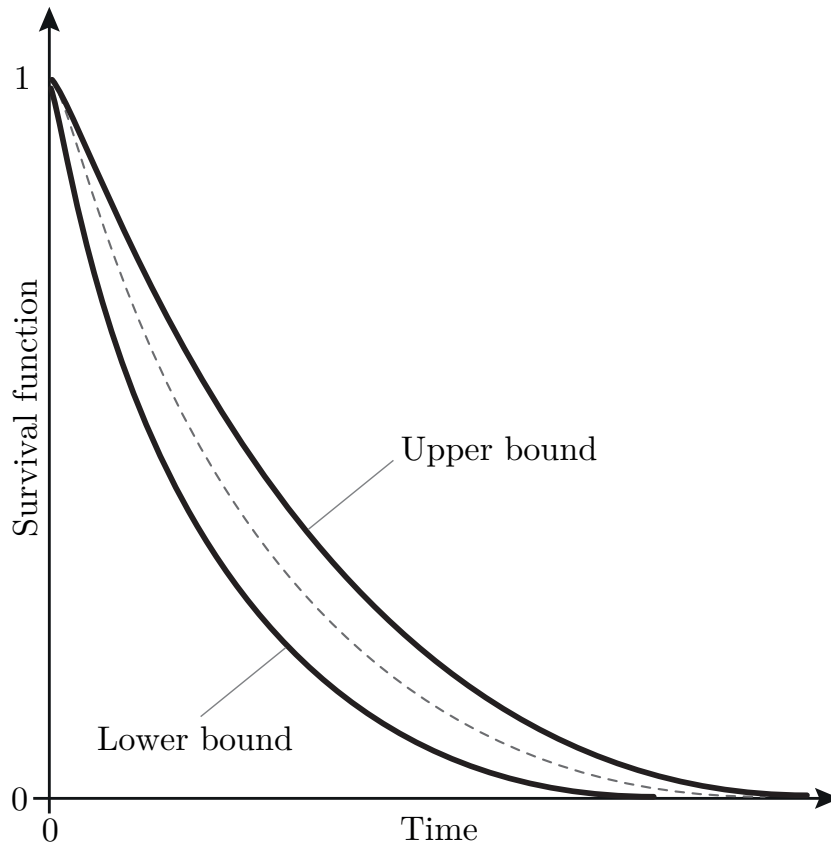


Figure 1.9: Imprecise survival function with lower and upper bound.

especially for complex systems, and thus requires significant computational resources, as [205, 206] confirm. Therefore, there is a need for simulation methods that increase computational efficiency while maintaining high accuracy with the smallest possible sample size.

Several methods have been proposed to circumvent exhaustive double-loop simulations, such

as interval Monte Carlo simulations and interval impact sampling [207, 208], approximation in the context of novel reliability design theory under parametric uncertainty [209], stochastic extensions, and optimization-based interval estimation [210], in addition to sequential optimization and reliability assessment approaches [211], single-loop methods [212, 213], and decoupling approaches [214, 215]. Novel techniques to increase computational efficiency in uncertainty quantification include the fusion of p-boxes, univariate dimensionality reduction methods, and optimization [216], as well as the implementation of the augmented space integral [217], the application of line failure distribution factors [218], and equivalent reliability index utilization for surrogate model uncertainty quantification [219]. Wei et al. recently introduced non-intrusive stochastic simulation (NISS) in [220], an innovative approach to efficiently compute imprecise structural models while significantly reducing the sample size. This methodology is divided into two primary methods, local extended Monte Carlo simulation (LEMCS) and global extended Monte Carlo simulation (GEMCS), each of which offers significant advantages in terms of precision and variability.

Generally, it can be assumed that three distinctive strategies exist for handling uncertainty in a model: non-probabilistic approaches, precise probability approaches, and imprecise probability approaches [220]. To maintain a clear distinction between irreducible uncertainty and imprecision throughout the analysis, only imprecise probability approaches seem suitable [220, 221]. This strategy combines set-theoretical concepts describing imprecision, such as intervals or fuzzy sets, with traditional probability theory distributions that represent irreducible uncertainty [168, 222]. Among various approaches, the utilization of fuzzy sets has demonstrated particular advantages in this context [194, 223].

1.5.3 Fuzzy probability

In the discipline of system reliability engineering, ambiguities and imprecision often arise from limitations present in practice, such as scarcity of data or unclear expert knowledge regarding the probability distribution types and parameters that determine, for example, the lifetime of system components. This is where fuzzy probability theory comes into play, providing a suitable tool for accounting for these uncertainties.

Imprecise distribution parameters can be modeled, for instance, by triangular fuzzy numbers, defined as $\tilde{\theta} = (a/b/c)$, where $a < b < c$, $[a, c]$ represents the base of $\tilde{\theta}$, and b signifies its peak. Suppose $F(x)$ is a probability distribution function, which characterizes the failure probability of a system component within a time period x . Further, assume that the understanding of the parameters of this distribution function is imprecise. Under these conditions, the fuzzy probability distribution function symbolized as $\tilde{F}(x)$, encapsulates this phenomena, as depicted in Fig. 1.10. Here, the membership function of $F(x)$ is represented by $\mu(F(x))$, while $\text{supp}(\tilde{F}(x)) = [\underline{F}^{\alpha_0}(x), \overline{F}^{\alpha_0}(x)]$ signifies the support of $\tilde{F}(x)$. An important point to highlight is that for $\mu(F(x)) = 1$, corresponding to an α -level of $\alpha = 1$, $\tilde{F}(x)$ equals $F(x)$.

For an assumed arbitrary system with arbitrarily chosen imprecise distribution functions describ-

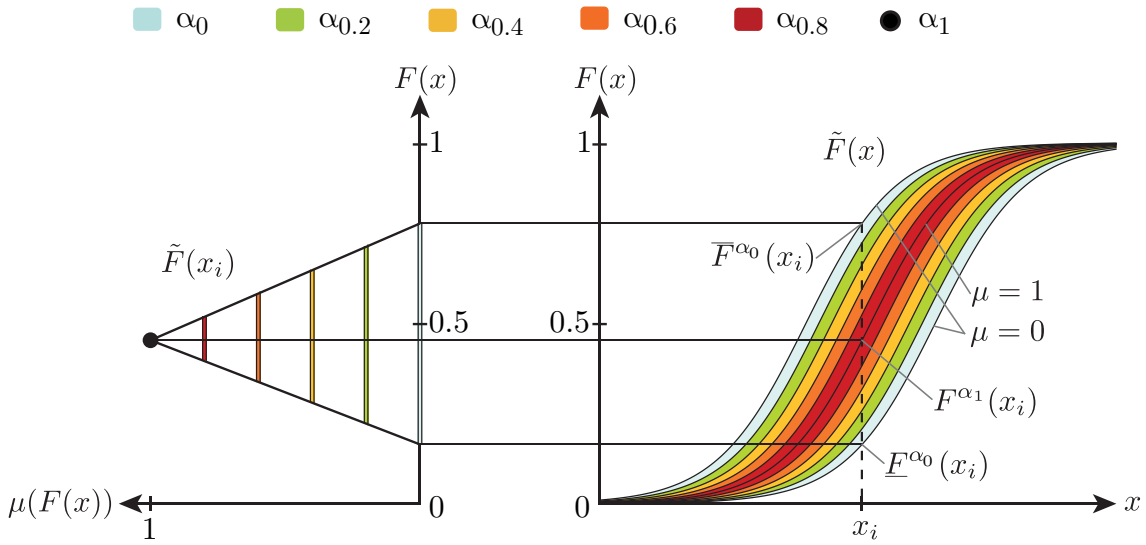


Figure 1.10: Arbitrary fuzzy probability distribution function based on continuous, triangular fuzzy parameters; adapted from [224].

ing the failure behavior of the system components and corresponding distribution parameters described by triangular fuzzy numbers, Fig. 1.11 represents the, analogous to Fig. 1.7 and Fig. 1.9, resulting fuzzy survival function. Detailed insight into fuzzy probability theory and its practical usage can be found in works such as [124, 194, 224–227].

1.6 Decision-making and economic aspects

A fundamental requirement for practical resilience analysis, based on resilience quantification approaches presented in Sec. 1.3 for real-world systems, is the ability to balance different allocations and options that enhance the system’s resilience. In the context of critical infrastructures, Liu et al. recently stated in [228] that existing approaches for decision-making between resilience-enhancing measures commonly use an ad hoc approach via optimization. These approaches can generally be divided into two categories: 1. optimization of investments before a disruptive event [229–231], aimed at enhancing resilience through preventive measures such as hardening of vulnerable components, and 2. acute emergency response and recovery planning after a disruptive event [232–234], aimed at minimizing losses through quick and efficient recovery actions, such as optimized resource allocation. However, according to Liu et al., these methods lack comprehensive consideration, balancing, and coordination of resilience measures across all phases of a system’s life cycle. Thus, there is a scientific gap in resilience frameworks that are able to provide decision-makers with a comprehensive and quantitative scheme for enhancing system resilience during the designing, upgrading, and reconstructing of critical infrastructure. This statement can be generalized to other types of systems. There is a lack of generally formulated approaches in the literature that can be applied to any system type, easily integrated into existing frameworks, and

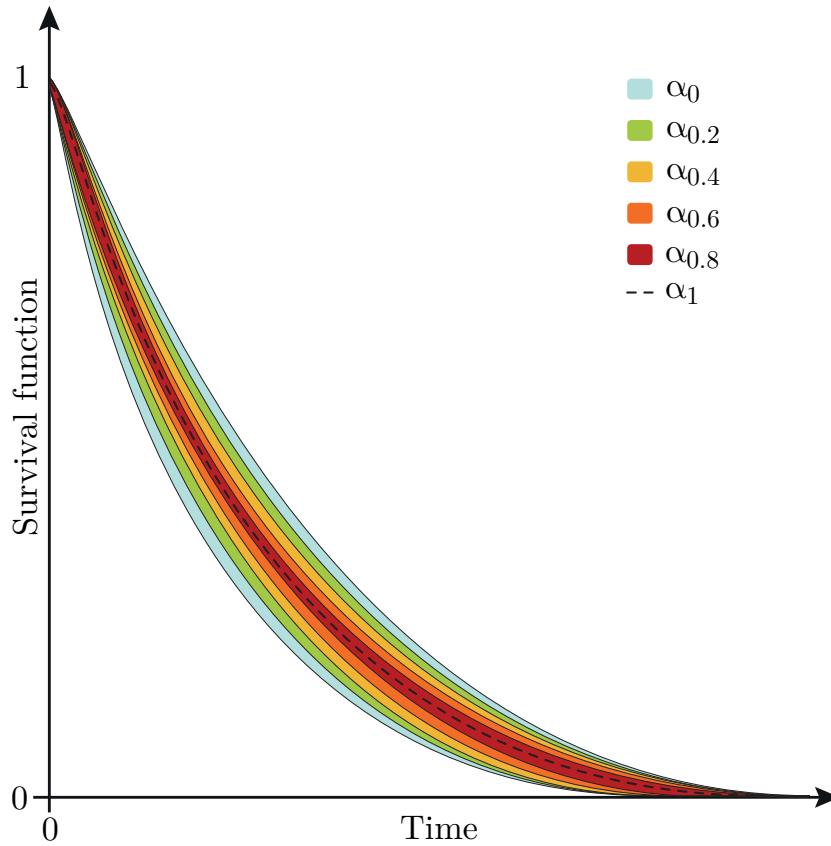


Figure 1.11: Fuzzy survival function.

adapted for any kind of use cases. Liu et al. present such a comprehensive resilience framework in [228], albeit specifically designed for the critical infrastructure domain. Further resilience decision-making frameworks for specific domains include the artificial intelligence-based decision-making framework for resilience building of supply chains by Belhadi et al. provided in [235], and the adaptive robust framework for optimizing resilience of interdependent infrastructures under the impact of natural disasters presented by Fang & Zio presented in [236]. Extensive discussion on the topic is provided in works such as [237] by Attoh-Okine, [238] by Larkin et al., and [239] by Wilson.

Another essential and evident prerequisite for resilience decision-making on practical applications is the inclusion of monetary aspects. Otherwise, the trivial and obvious outcome of the analysis of a system's resilience would always be the simultaneous maximization of all resilience-enhancing measures. However, as such measures are associated with monetary costs in reality, this solution is purely theoretical. In this context, Ayyub, in [6], states: “*Improving the resiliency of a system to meet target levels requires the examination of system enhancement alternatives in economic terms, within a decision-making framework.*” Therefore, in addition to the resilience metric presented in Sec. 1.3.4, Ayyub presents in [6] a broad discussion and an approach on comprehensively

integrating monetary aspects into resilience decision-making processes. As shown in Fig. 1.12 resilience assessment can be based on the savings of potential direct and indirect losses as well as the recovery costs. Resilience measures that can reduce these potential losses can be analyzed by benefit-cost analysis models. The benefits B are the sum of potential savings in losses and

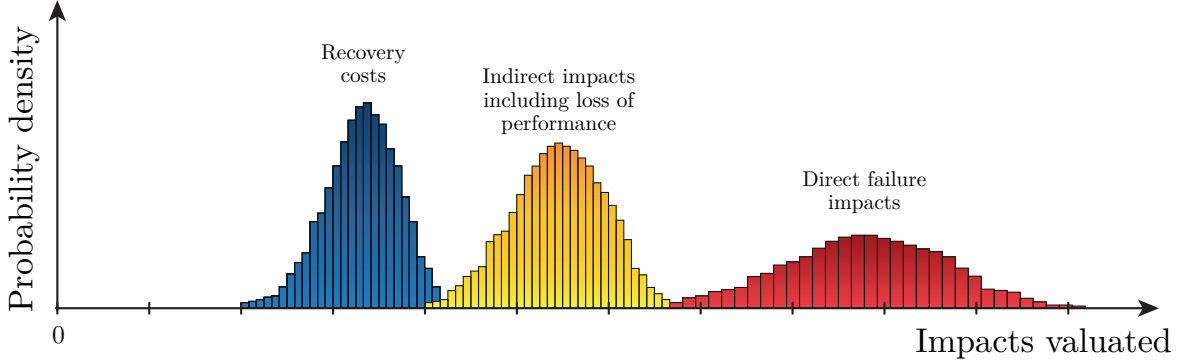


Figure 1.12: Probability densities over the level of recovery costs as well as direct and indirect losses; adapted from [6].

recovery costs due to the implementation of a measure. The costs C correspond to the costs for the implementation of the measure itself. The benefits and costs are assumed to be random variables. Given that B and C are normally distributed and independent, a benefit-cost index $\beta_{B/C}$ is defined as:

$$\beta_{B/C} = \frac{\mu_B - \mu_C}{\sqrt{\sigma_B^2 + \sigma_C^2}}, \quad (1.17)$$

where μ is the mean and σ the standard deviation. The probability $P_{f,B/C}$ that the costs outweigh the benefits can be determined as:

$$P_{f,B/C} = P(C > B) = 1 - \Phi(\beta), \quad (1.18)$$

with Φ being the standard normal cumulative distribution function. For lognormally distributed benefits and costs, Eq. 1.17 can be written as:

$$\beta_{B/C} = \frac{\ln \left(\frac{\mu_B}{\mu_C} \sqrt{\frac{\delta_C^2 + 1}{\delta_B^2 + 1}} \right)}{\sqrt{\ln [(\delta_B^2 + 1)(\delta_C^2 + 1)]}}, \quad (1.19)$$

with δ , the coefficient of variation. Note that in times when various types of systems in modern societies are interconnected and interdependent, determining indirect or secondary costs in practice can be particularly challenging.

More economic models in a resilience context and discussion about them are provided, e.g., by Gilbert & Ayyub in [240], Moslehi & Reddy in [82], Rose in [97] and Pant et al. in [241]. However, it should be noted that the cost of resilience should not be solely reduced to an economic

perspective. Numerous publications [6, 16, 48, 242] point out that in addition to pure economic costs, non-monetarily quantifiable “costs” must be incorporated in resilience decision-making as well. These include, for instance, effects on the environment, on people’s social lives, on the health care system, and on other community systems. However, due to the tremendous complexity, there is a lack of specific approaches to comprehensively incorporate the full range of these non-monetarily quantifiable “costs” into resilience decision-making frameworks. Further fundamental research is needed to address this gap.

As indicated in Sec. 1.5, in the context of existing resilience decision-making frameworks, the imprecision of all influencing factors is widely neglected in the literature. However, for a comprehensive decision-making process, this must be taken into account. Thus, decision-makers need to be provided with information about not only which level of system resilience is acceptable but also which level of imprecision can be tolerated and at which specific points imprecision needs to be reduced in order to identify an appropriate equilibrium point. Since the reductions are beneficial but come typically with unavoidable monetary costs due to the conduction of experimental trials, destructive testing, and similar procedures, for a thorough analysis, these costs must be taken into account in the decision-making process as well.

1.7 Aims and objectives

This dissertation aims to address critical gaps in the understanding and practice of resilience analysis in complex engineering systems. The objective of this research is to develop and improve a decision-making framework that can utilize quantifiable measures, enhance cost and computational efficiency in resilience management, incorporate monetary aspects and uncertainties, and ensure the methodologies are applicable and transferable to any type of complex system. This is achieved through specific research targets set for each publication.

The primary focus of the first publication is the development of a resilience decision-making procedure designed to address the challenges faced by complex systems. Current research reveals a distinct gap: a shortage of methodologies that enable decision-makers to consider and balance the full range of resilience-enhancing measures at any life cycle stage of a complex system. These measures include, e.g., reliability and robustness-enhancing measures, as well as strategies to improve recoverability. As a result, an adaptable and flexible approach is required that integrates various control mechanisms and strategies, facilitating effective comparisons and decision-making among a variety of resilience-enhancing options. It is important that monetary aspects can be integrated into the decision-making process to account for real-world resource constraints. In addition, there is a clear need to reduce the associated computational burden to enable more efficient application in complex system environments.

The second publication addresses the increasing complexity of modern systems that frequently contain numerous substructures. This complexity requires even more efficient approaches for comprehensive resilience analysis and decision-making. The objective is to merge the resilience framework developed in the first publication in Chap. 2 with the concept of survival

signature into a novel methodology. This approach will offer the best of both worlds: efficient comparisons of resilience-enhancing arrangements and significantly reduced computational effort when addressing underlying component and subsystem failure behavior. All of the benefits of the original methodology must be preserved, such as the inclusion of monetary constraints in the resilience analysis, to ensure that the novel approach can be practically applied in real-world scenarios. In addition, the framework is to be extended such that it is applicable to problems with multidimensional input spaces for resilience-enhancing improvements.

The scope of the third publication is to address the issue of efficiently accounting for imprecision in the analysis of complex systems, along with its impact on reliability and, ultimately, resilience. This area remains largely neglected in current methods of resilience analysis, and in reliability analysis it is often accompanied by major computational costs, indicating the need for a framework that can account for this imprecision. Decision-makers need to be provided with the necessary information to decide what level of imprecision is acceptable in certain issues and where imprecision needs to be reduced, e.g., by specific investments. The goal is to incorporate concepts from several areas, namely survival signature, fuzzy probability theory, and NISS methods. This synthesis is intended to create a methodology that not only copes with imprecision, but also dramatically reduces the computational effort and sample size normally required for such analyses. This novel approach is expected to provide the basis for incorporating uncertainties into the developed resilience decision-making framework for substructured and complex systems from the second publication in Chap. 3, while retaining all the existing benefits.

The principal aim of the fourth publication is to overcome a specific limitation of the existing resilience framework for complex and substructured systems from Chap. 3, which currently allows only a binary component state consideration in subsystem structures due to the limitation of the survival signature. The growing complexity and size of modern systems necessitate more nuanced analyses that encompass continuous performance measures at this level. Hence, the objective is to extend the existing resilience framework to include continuous state consideration by developing a novel approach based on the separation property of the concept of the survival signature. Thereby, the existing advantages shall be maintained in order to enable comprehensive resilience analysis of real-world systems.

The aim of the fifth publication is to clearly demonstrate the complete transferability of all developed methods to any systems and use cases. Using the example of the regeneration of complex capital goods, it is to be shown that the developed methodologies are suitable for designing resilient regeneration processes in two ways. First, to analyze and guarantee the resilience of the regeneration process itself, and second, to provide a basis for decision-makers to decide between multiple (resilient) regeneration paths by resilience analysis of the regarded complex capital good. This resilience analysis, coupled with efficient reliability analyses, lifetime analyses, and consideration of uncertainties, shall form an overall framework for resilience-based decision criteria for optimal regeneration of complex capital goods.

In summary, the ultimate goal of this dissertation is to significantly improve our understanding

and management of resilience in complex systems of any kind in a world where societies are becoming increasingly dependent on them in the face of ongoing crises such as climate change. Each study is designed to address pressing needs in this area, with the overall aim of providing more efficient, comprehensive, cost-effective, practical, and resilient solutions.

1.8 Original contributions

A core innovation of this dissertation is the development of a universally applicable resilience decision-making framework, presented in the first publication, see Chap. 2. This framework can address complex systems of any kind as well as consider any type of system performance, marking a significant advancement in the field. By merging an adapted systemic risk measure with a sophisticated probabilistic and time-dependent resilience metric, it provides an innovative approach for comparing resilience-enhancing measures and investments at any stage, allowing decision-makers to strike an optimal balance not only between failure prevention and recovery improvements, but between improvements of all types.

Significantly, this framework recognizes real-world constraints by incorporating monetary aspects into the decision-making process. This feature is critical as it supports decision-makers in identifying the most cost-effective strategies for enhancing resilience. Employing a grid search algorithm for systemic risk measures increases efficiency and reduces computational effort, enhancing the framework's practicality in real-world applications.

The universal applicability and effectiveness of this framework have been demonstrated in case studies involving a multi-stage axial compressor and Berlin's U-Bahn and S-Bahn system. These examples serve to highlight the broad scope and adaptability of the methodology, demonstrating its potential to enhance the resilience of a wide range of complex systems. As a cornerstone of this dissertation, this innovative resilience decision-making framework promises to significantly enhance the understanding and improvement of resilience in modern society's complex systems. Building on the resilience decision-making framework of the first publication, the second publication in Chap. 3 presents a novel methodology that merges the resilience framework with the concept of survival signature. This improves decision-making, especially for complex, large, and substructured systems, corresponding to the systems of modern societies, and extends the scope of the first publication.

The new approach integrates the beneficial features of its two original components. It enables a direct comparison between various resilience-enhancing options, under consideration of monetary aspects and complexity extensions such as cascading failures and other dependency structures due to time-step accurate simulations, and a significant reduction in computational effort due to the synergy between the survival signature and the grid search algorithm: a majority of the resilience-enhancing endowment properties affect the probability structure of the components of a system. These numerous changes in the probability structure during the resilience analysis, caused by the grid search algorithm and considered to be typically among the most costly parts of the simulation, can be ideally captured with minimal effort due to the separation property of the

survival signature – once a subsystem structure has been computed, any possible characterization of the probabilistic part can be validated without having to recompute the structure.

Embedding the survival signature in the resilience framework further leads to the important advantage that it allows the potential exploitation of all existing and ongoing developments of this concept, as they can be integrated straight forward. In addition, the novel methodology allows for consideration of multidimensional search spaces achieved by an extension of the grid search algorithm.

The novel methodology integrates a substructuring approach for large, complex systems. This, together with the integration of the survival signature, enables the propagation of subsystem reliabilities through any number of system levels up to the top level and leads to a significant reduction in computational effort. In this way, and with the extension of the adapted systemic risk measure, it is now possible to analyze systems with a large number of components for their resilience. This is demonstrated in the second publication by applying the novel methodology for a multidimensional resilience analysis of an infrastructure system consisting of numerous subsystems and more than 2500 individual components.

The original contribution of the third publication, see Chap. 4, is a novelty in the field of reliability analysis considering uncertainties. At the same time, it lays the groundwork for the extensive integration of uncertainties into the comprehensive resilience decision-making framework of Chap. 3. A novel methodology is developed by merging survival signature, fuzzy probability theory, and NISS methods. The advantageous properties of the original ingredients are retained: lower computational cost due to the separation property of the survival signature and significantly smaller sample size in the simulation of imprecise failure behavior due to the adapted NISS methods. Beneficially, these adapted NISS methods require only a single stochastic simulation, bypassing the traditionally used and computationally expensive double-loop simulations.

Integrating fuzzy probabilities incorporates imprecision into the systems' probabilistic structure, addressing another complexity level. This enables a more sophisticated and nuanced identification of critical imprecision in system reliability analysis than traditional approaches allow, which is particularly important in design and maintenance processes.

Again, practical applications demonstrate the effectiveness of the methodology. By applying it to an axial compressor and an arbitrary complex system, the approach proves to be both efficient and widely applicable. Furthermore, the inclusion of an analysis comparing the LEMCS and GEMCS, respectively, provides deeper insight into the applicability of the methodology depending on the specific requirements and the existing knowledge of the uncertain behavior of the system.

In summary, the primary contribution of the third publication constitutes a novelty in its field and is a potential extension of the resilience decision-making framework towards a consideration of imprecision. It not only acknowledges the inherent uncertainties in complex systems, but also provides practical tools for assessing system reliability despite uncertainties. This achievement enriches the ongoing development of the comprehensive approach in Chap. 3, advancing the

efficient and extensive resilience analysis of complex systems.

Similar to the original contribution of the third publication in Chap. 4, the new developments in the fourth publication in Chap. 5 present a novelty in the field of reliability analysis. However, they also serve as an extension that can be incorporated into the comprehensive resilience decision-making framework of Chap. 3. The core of the innovative contribution lies in addressing the limitations of a binary component and system state consideration on subsystem level in the resilience framework. This limitation needs to be overcome to ensure the comprehensive resilience analysis of real-world systems. This is achieved by introducing the continuous-state survival function and the concept of the Diagonal Approximated Signature (DAS) as a corresponding surrogate model. The introduction of DAS, based on combinatorial decomposition adopted from the survival signature concept, ensures the separation of topological and probabilistic information, providing an enriched perspective for resilience analyses.

Building upon potentially high-dimensional coherent structure functions, and a stochastic process that models the time-dependent degradation of the continuous-state components, this approach enables the direct computation of the continuous-state survival function. An explicit formula and a stored DAS are utilized, avoiding expensive online Monte Carlo simulations. This innovation not only maintains the original resilience framework's advantages but also allows for an efficient continuous performance consideration of components on subsystem level, significantly enhancing resilience optimization for substructured systems. This offers a valuable extension and new dimension to resilience analysis, holding potential for further research and practical applications. The fifth publication in Chap. 6 primarily contributes to the field by creating a comprehensive decision-making framework for the regeneration of complex capital goods. Additionally, the work demonstrates the broad applicability and transferability of all developed methodologies to systems of any type, and the seamless integration into completely different application domains and frameworks than those shown in the core publications, see Chap. 2 and Chap. 3.

The framework tackles two key facets: first, it ensures the resilience of the regeneration process itself; second, it offers decision-makers a robust basis to choose from multiple (resilient) regeneration paths, through the resilience analysis of the complex capital good. This combined approach, integrating resilience, reliability, and lifetime analyses alongside the consideration of uncertainties, provides effective resilience-based decision criteria for optimal regeneration of complex capital goods.

Moreover, the publication builds on the use of functional models for representing physically complex systems, taking into account input parameter dependencies through time-dependent sensitivity analysis and importance indices. Overall, the framework offers an enhanced foundation for decision-making in maintenance, repair and overhaul (MRO) processes, contributing to the better understanding and implementation of resilience in the regeneration paths of complex capital goods.

The presented dissertation delivers innovative contributions to the field of resilience decision-making for complex engineering systems, through the development of universally applicable

methodologies and frameworks, addressing important scientific gaps. At its heart is a resilience framework that integrates monetary considerations, enabling decision-makers to optimally balance different types of resilience-enhancing measures in practice. This is further augmented by the integration of the survival signature concept, leading to more computational efficiency and providing tools for assessing the resilience of substructured systems. A further extension of the survival signature, based on the integration of NISS and fuzzy probability theory, provides the basis for enabling resilience analysis of complex systems with inherent uncertainties. The research then progresses to introduce the continuous-state survival function and DAS, addressing the limitations of binary component and system state consideration on subsystem level, thereby potentially enriching resilience framework's capability. The final original contribution extends the applicability of these methodologies into the realm of MRO processes, thus underlining the wide-ranging potential of the developed tools in enhancing resilience across varied complex systems and application cases.

1.9 Structure of the thesis

The dissertation is composed of four journal articles and one book contribution. The four journal articles represent the core developments and innovations of the dissertation. The book contribution demonstrates the broad applicability, compatibility and transferability of all developed methodologies. Although all developments are novelties in themselves, they complement and build upon each other in the overall context of the developed resilience decision-making framework.

Chapter 2 introduces an approach to resilience-based decision-making for complex systems, comprised of an adapted systemic risk measure and an appropriate resilience metric that enables balancing between any resilience-enhancing measures. In Chap. 3, the resilience decision-making procedure is extended and combined with the concept of survival signature to enable more efficient, multidimensional resilience analyses for complex and substructured systems. Chapter 4 addresses the analysis of reliability of complex systems in the presence of imprecision and fuses methods of the concept of survival signature, fuzzy probabilities, and NISS into a novel approach that significantly reduces the computational cost and sample size. Chapter 5 introduces the continuous survival function and DAS as a model for a more comprehensive resilience analysis that enables a continuous performance consideration at the subsystem level. Chapter 6 demonstrates the transferability and compatibility of all developed methods by embedding them into the context of resilience-based regeneration of complex capital goods, forming a novel framework for analyzing resilient regeneration paths. The final chapter, Chap. 7, concludes the thesis and provides an outlook that identifies future implications and directions for the research presented.

2 | Resilience decision-making for complex systems

Resilience decision-making for complex systems

Julian Salomon^{a,*}, Matteo Broggi^a, Sebastian Kruse^b, Stefan Weber^c, Michael Beer^{a,b,d}

^aInstitute for Risk and Reliability, Leibniz Universität Hannover, Hannover, Germany

^bInstitute for Risk and Uncertainty, University of Liverpool, Liverpool, United Kingdom

^cInstitute of Probability and Statistics, Leibniz Universität Hannover, Hannover, Germany

^dInternational Joint Research Center for Engineering Reliability and Stochastic Mechanics, Tongji University, Shanghai, China

*Corresponding author

Published in *ASCE-ASME Journal of Risk and Uncertainty in Engineering Systems, Part B: Mechanical Engineering* on June 2020

Abstract

Complex systems – such as gas turbines, industrial plants and infrastructure networks – are of paramount importance to modern societies. However, these systems are subject to various threats. Novel research does not only focus on monitoring and improving the robustness and reliability of systems but also focus on their recovery from adverse events. The concept of resilience encompasses these developments. Appropriate quantitative measures of resilience can support decision-makers seeking to improve or to design complex systems. In this paper, we develop comprehensive and widely adaptable instruments for resilience-based decision-making. Integrating an appropriate resilience metric together with a suitable systemic risk measure, we design numerically efficient tools aiding decision-makers in balancing different resilience-enhancing investments. The approach allows for a direct comparison between failure prevention arrangements and recovery improvement procedures, leading to optimal trade-offs with respect to the resilience of a system. In addition, the method is capable of dealing with the monetary aspects involved in the decision-making process. Finally, a grid search algorithm for systemic risk measures significantly reduces the computational effort. In order to demonstrate its wide applicability, the suggested decision-making procedure is applied to a functional model of a multi-stage axial compressor, and to the *U-Bahn* and *S-Bahn* system of Germany’s capital Berlin.

Keywords: Decision-making, Resilience, Algorithms, Risk, Complex systems, Compressors, Robustness, Failure.

2.1 Introduction

Modern societies rely on the operations of various complex systems, such as gas turbines, industrial plants, or infrastructure networks. These form complex capital goods whose construction, improvement, and regeneration are of paramount importance. However, these systems are subject to various threats. Evidence shows that a wide range of natural, technical, and anthropogenic impacts at all scales can severely affect the functionality of these systems. Due to their high and increasing complexity, it is infeasible to identify all potential adverse impacts and to prevent them accordingly. Novel developments are therefore important that do not only focus on monitoring and improving the robustness and reliability of systems but also focus on their recovery from adverse events [243]. The concept of resilience encompasses these developments: analyzing and optimizing robustness, reliability, and recovery of systems – both from a technical and from an economic perspective [5, 7, 10]. Resilience applied to the artificial systems of our modern society

leads to a paradigm shift. Secure systems can not only be based on strategies that prevent failures but must include strategies for the efficient recovery in cases of failure.

The concept of resilience in the context of engineering applications has gained growing popularity in recent years [23, 24]. The term “resilience” appears in several different domains like ecology, economy, psychology as well as in the context of mechanical and infrastructure systems and is derived from the Latin word “resilire” which means “to bounce back”. The concept of resilience first appeared in the domain of ecological systems by Holling [8]. He defined resilience as “[...] *a measure of the persistence of systems and their ability to absorb change and disturbance and still maintain the same relationships between populations or state variables.*”. Although many different definitions of resilience were introduced in the context of engineering and complex systems (e.g., see Refs. [53–57]), the early definition from Holling [8] captures key aspects of all of them.

Ayyub [6] provides a review of the literature and develops a comprehensive definition of resilience in the context of complex systems which is based on the content of the Presidential Policy Directive (PPD) on critical infrastructure security and resilience [62]: “*Resilience notionally means the ability to prepare for and adapt to changing conditions and withstand and recover rapidly from disruptions. Resilience includes the ability to withstand and recover from disturbances of the deliberate attack types, accidents, or naturally occurring threats or incidents. The resilience of a system’s function can be measured based on the persistence of a corresponding functional performance under uncertainty in the face of disturbances.*”. This novel definition embraces the former definitions, and provides a solid basis for the quantification of resilience.

Our paper suggests a novel quantitative approach to resilience enabling decision-makers to efficiently design and improve complex systems present all over our modern communities [12, 243]. Resources are not unlimited, and resiliences cannot arbitrarily be improved in reality; realistic models must reflect constraints and methods must be developed that support decision-makers in choosing between different resilience-enhancing investments [7, 244].

This paper provides an efficient method for identifying the cost-effective allocations of different resilience-enhancing investments by combining the resilience metric of Ouyang et al. [86] and the systemic risk measure of Feinstein et al. [245]. A grid search algorithm for systemic risk measures significantly reduces the computational effort. In order to demonstrate its wide applicability, the suggested decision-making procedure is applied to a functional model of a multi-stage axial compressor, and to the *U-Bahn* and *S-Bahn* system of Germany’s capital Berlin.

The paper is structured as follows: Section 2.2 describes the theoretical foundations: the quantification of resilience, the systemic risk measure and its adaptation to technical systems, and the grid search algorithm. Section 2.3 develops on this basis a novel resilience-based decision-making process. In Section 2.4 and 2.5, the methods are, first, applied to a functional model of an axial compressor and, second, to Berlin’s suburban train (*S-Bahn*) and subway (*U-Bahn*) network. Section 2.6 summarizes the results and discusses questions for future research.

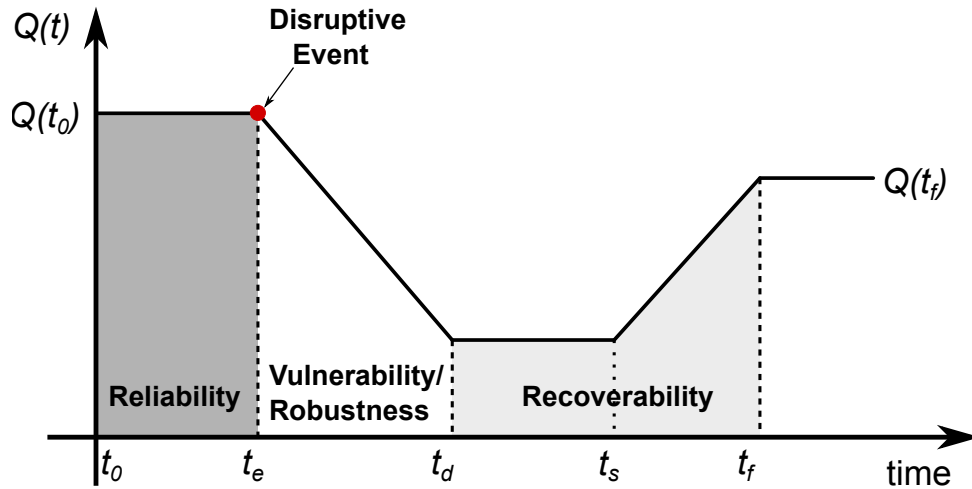


Figure 2.1: In the evolution of a system after the impact of a disruptive event, different phases can be distinguished: (i) the original stable state, (ii) disruptive impact, vulnerability, (iii) disrupted state and recovery. These are separated by the following points in time: t_o - beginning of the original stable state; t_e - end of the original stable state due to the occurrence of a disruptive event; t_d - end of disruptive impact and beginning of disrupted state; t_s - end of disrupted state and beginning of system recovery; t_f - end of system recovery and beginning of new stable state; adapted from [76].

2.2 Theoretical fundamentals

2.2.1 Resilience quantification

Applications of resilience to engineering problems rely on the availability of quantitative measures of resilience. Within the last two decades, various methodologies have been developed. Comprehensive discussions of different resilience metrics are provided by Bergstöm et al. [23], Hosseini et al. [12], and Linkov & Palma-Oliveira [45]. In addition, Hosseini et al. [12] propose a specific classification system for these metrics. Most resilience metrics are performance-based, and the majority of performance-based measures of resilience are assigned to the category of “generic resilience metrics”. These determine resilience by comparing the performance of a system before and after a disruptive event. Further subcategories are constructed by distinguishing between time-dependent or time-independent and deterministic or probabilistic metrics, respectively.

Performance-based approaches may be ratio-based, integral-based, or both. When a system is exposed to a disruptive event and recovers its functionality afterward, it passes through three essential phases: (i) The original stable state whose duration can be interpreted as the reliability of the system forms the first phase. (ii) The second phase is the vulnerability of the system, represented by a loss of performance after the occurrence of a disruptive event; the robustness of the system mitigates the loss of performance. (iii) The disrupted state of the system and its recovery to a new stable state represent the recoverability and the last phase. The three phases are illustrated in Fig. 2.1, with $Q(t)$ denoting the system performance at time t . The new stable state may differ from the original state, e.g., in terms of its performance which may be higher or lower.

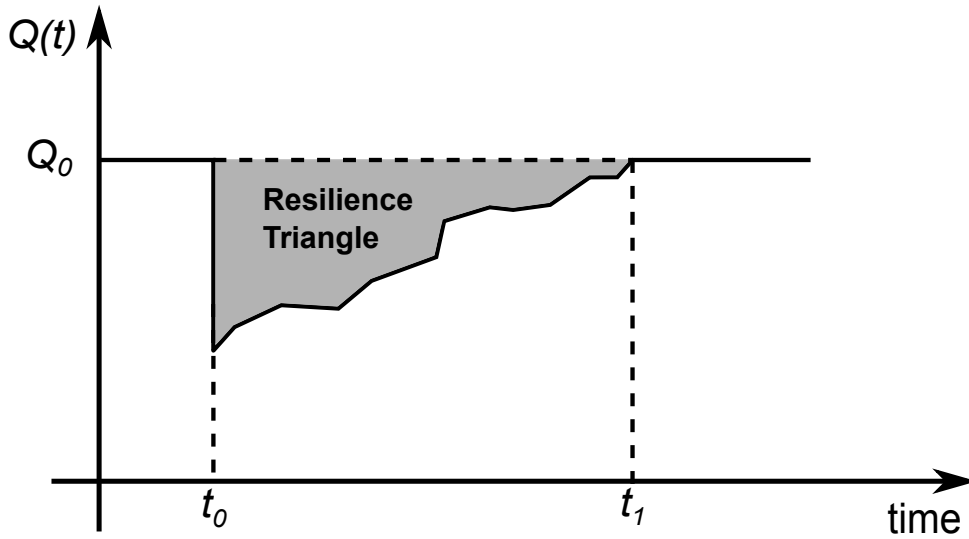


Figure 2.2: Resilience triangle; adapted from [48].

The majority of resilience metrics in the literature is based on system performance, i.e., on these three states and their transitions. A quantitative measure of resilience thus depends on the specific choice and definition of system performance [10].

Bruneau et al. [48] propose a time-dependent metric of the resilience of communities under seismic disruption in a deterministic setting. If t_0 is the time of occurrence of a disruptive event, t_1 the time of complete recovery, and $Q(t)$ the quality of the community infrastructure at time t , a specific type of system performance, their metrics can be expressed in the following form:

$$R_{Br} = \int_{t_0}^{t_1} [100 - Q(t)] dt. \quad (2.1)$$

For systems with random performance, this metric defines a pathwise measure of resilience. Bruneau et al. [48] also introduce the well-known principle of a “*resilience triangle*” as illustrated in Fig. 2.2. Their approach was applied in various contexts and forms a strong basis for several, later proposed metrics [94–96]. Further resilience metrics in the context of deterministic models were e.g. suggested by Refs. [43, 88, 89, 92, 246].

Pathwise metrics do not rely on probabilities and do not capture quantities that depend on probabilities – such as the rates of occurrences of disruptive events and the distributions or moments of the random size of disruptions or the random times of their recovery. Such quantities require the existence and knowledge of a probability measure on the scenario space together with probabilistic resilience metrics, e.g., see Refs. [57, 78, 98, 99, 102]. Very informative resilience metrics were introduced by Ouyang et al. [86] and Ayyub [6]; both metrics are probabilistic, time-dependent, and universally applicable.

In this paper, we utilize the probabilistic resilience metric by Ouyang et al. [86]. Denoted by Res , it is defined as the expectation of the ratio of the integral of the system performance $Q(t)$ over a time interval $[0, T]$ and the integral of the target system performance $\mathcal{T}Q(t)$ during the

same time interval:

$$Res = E[Y], \quad \text{where} \quad Y = \frac{\int_0^T Q(t)dt}{\int_0^T \mathcal{T}Q(t)dt}. \quad (2.2)$$

System performance $Q(t)$ is a stochastic process. The parameter $\mathcal{T}Q(t)$ is generally considered as a stochastic process as well, but for simplicity it is assumed to be a non-random constant $\mathcal{T}Q$ in this work.

Sometimes, it is useful to rewrite Eq. 2.2 in terms of a sum of the impact areas of failure events. If t_1, t_2, t_3, \dots is the sequence of the consecutive occurrences of failures, the random number of failures up to time T is $N(T) = \sup\{n : t_n \leq T\}$. The impact area AIA_n is the expected area between the reduced system performance curve and the target system performance curve caused by the n -th failure within the considered time interval. Under the assumption that the system fully recovers before its next failure, one obtains that $AIA_n = E\left(\int_{t_n}^{t_{n+1}} [\mathcal{T}Q - Q(t)]dt\right)$. In this case, Eq. 2.2 can be written as

$$Y = 1 - \frac{\sum_{n=1}^{N(T)} AIA_n}{\mathcal{T}Q \cdot T}. \quad (2.3)$$

The resilience metric takes values between 0 and 1. The value $Res = 1$ indicates a system performance corresponding to the target performance, while $Res = 0$ captures that the system is not working during the considered time period.

2.2.2 Systemic risk measure

Feinstein et al. [245] propose a novel approach to measure risk inherent in complex systems. Their methodology is based on two key components: first, a suitable descriptive input-output model; and, second, an acceptance criterion representing the normative safety standards of a regulatory authority. These systemic risk measures were, e.g., considered in finance, see Weber & Weske [247], and applied to power transmission, see Cassidy et al. [248].

Let (Ω, F, P) be a probability space, $l \in \mathbb{N}$ the number of entities in the considered system, and $k \in \mathbb{R}^l$ a vector of controls. For each scenario $\omega \in \Omega$ and a control vector k , we denote by $Y_k(\omega)$ the relevant stochastic outcome of the system; for each $k \in \mathbb{R}^l$, Y_k is a random variable.

In the context of financial systems, the vector k is the ‘‘endowment’’ and describes the capital allocation to the entities of the system. The underlying input-output model of the system is given by $Y = (Y_k)_{k \in \mathbb{R}^l}$, a non-decreasing random field taking values in some vector space \mathcal{X} of random variables. The monotonicity property encodes that a larger capital allocation, $k_i \leq m_i \forall i = 1, \dots, l$, increases the random outcome, i.e., $Y_k \leq Y_m$. The acceptance criterion is described by the set $\mathcal{A} \subseteq \mathcal{X}$ of random variables meeting the requirements of a decision-maker; for a survey on acceptance sets and monetary risk measures, we refer to Föllmer & Weber [249]. The systemic risk measure constructed from these two basic ingredients, the input-output model and the acceptance criterion, is the set of allocations of additional capital leading to random

outputs that satisfy the acceptance criterion, i.e.,

$$R(Y; k) = \left\{ m \in \mathbb{R}^l \mid Y_{k+m} \in \mathcal{A} \right\}. \quad (2.4)$$

2.2.3 Adapted systemic risk measure

The systemic risk measure introduced in Sec. 2.2.2 can be applied to engineering systems with components of multiple types with several endowment properties. We consider technical systems for which a meaningful system performance $Q(t)$ can be determined. It is assumed that the system consists of l system components each characterized by their type and n properties that influence the system performance. For convenience, we replace the vector notation of Sec. 2.2.2 by matrix notation.

Consider a component $i \in \{1, \dots, l\}$. Such a component can be characterized by a row vector

$$(a_i; j_i) = (\eta_{i1}, \eta_{i2}, \dots, \eta_{in}; j_i) \in \mathbb{R}^{(1 \times n)} \times \mathbb{N}, \quad (2.5)$$

where $(\eta_{i1}, \eta_{i2}, \dots, \eta_{in})$ are the numerical values of the n relevant properties and $j_i \in \{1, 2, \dots, b\} \subseteq \mathbb{N}$ is its type. Once all components are specified, the system is described by a pair consisting of a matrix $A \in \mathbb{R}^{(l \times n)}$ and a column vector $z \in \mathbb{N}^l$ that captures the types of the components:

$$(A; z) = \begin{pmatrix} \eta_{11} & \eta_{12} & \dots & \eta_{1n}; & z_1 \\ \eta_{21} & \eta_{22} & \dots & \eta_{2n}; & z_2 \\ \vdots & \vdots & & \vdots & \vdots \\ \eta_{l1} & \eta_{l2} & \dots & \eta_{ln}; & z_l \end{pmatrix}. \quad (2.6)$$

The input-output model $Y = (Y_{(A;z)})$ is enumerated by these pairs. In our case studies, we will typically assume that vector z of types is fixed and investigate the impact of a varying matrix A . A corresponding systemic risk measure is now constructed as follows. As a specific example, we choose the acceptance set

$$\mathcal{A} = \{X \in \mathcal{X} \mid E[X] \geq \alpha\} \quad \text{with} \quad \alpha \in [0, 1]. \quad (2.7)$$

A corresponding risk measure is defined by

$$R(Y; K) = R(Y; (K; z)) = \left\{ A \in \mathbb{R}^{l \times n} \mid Y_{(K+A;z)} \in \mathcal{A} \right\}, \quad (2.8)$$

which is the set of all allocations of modifications of the system properties A such that the altered system characterized by $(K + A; z)$ possesses a resilience greater than or equal to α . In order to keep the notation simple and without loss of generality we set $K = 0$, and $R(Y; 0)$ is written as $R(Y)$.

For practical applications, it is often necessary to impose restrictions on the structure of the matrix in Eq. 2.6. For example, it might be required that any component of a specific type is

configured in the same way, meaning that the corresponding row vectors a_i must be equal. As described in Ref. [245], such constraints can be captured by monotonously increasing functions $g_z : \mathbb{R}^p \rightarrow \mathbb{R}^{(l \times n)}$, $a' \mapsto (A; z)$ where $z \in \mathbb{R}^l$ denotes the types of the components; these functions map a lower-dimensional set of parameters $a' \in \mathbb{R}^p$ to the description of the system.

To illustrate this, we consider a system with $l = 5$ components of $b = 2$ types. Each component is characterized by its two endowment properties and its type, i.e. $(\eta_{i1}, \eta_{i2}; j_i)$, and we assume that η_{i2} is a function of the type j_i of the component i . More specifically, we suppose that $\eta_{i2} = 3$ for type 1 and $\eta_{i2} = 5$ for type 2. We choose $p = 5$ and consider as an example the types $z = (1, 1, 1, 2, 2)^\top$. This leads to the following characterization of the system:

$$g \begin{pmatrix} 1 \\ 1 \\ 1 \\ 2 \\ 2 \end{pmatrix} \begin{pmatrix} q_1 \\ q_2 \\ q_3 \\ q_4 \\ q_5 \end{pmatrix} = \begin{pmatrix} q_1 & 3; & 1 \\ q_2 & 3; & 1 \\ q_3 & 3; & 1 \\ q_4 & 5; & 2 \\ q_5 & 5; & 2 \end{pmatrix} = (A; z). \quad (2.9)$$

In this example, the constraint reduces the dimension from $10 = 5 \times 2$ to 5.

The dimension of the space of parameters can be further reduced, if more constraints are introduced. Consider, e.g., the additional condition that the first endowment property η_{i1} is a function of the type of the components, but that it can otherwise freely be chosen. This implies for the given types $z = (1, 1, 1, 2, 2)^\top$ that $q_1 = q_2 = q_3$ and $q_4 = q_5$. In this case, $p = 2$ becomes the appropriate dimension of the parameter space.

2.2.4 Grid search algorithm

Set-valued systemic risk measures can be computed via a combination of a grid search algorithm and stochastic simulation, see Ref. [245]. To employ this algorithm, a box-shaped subset of endowments which are of interest is subdivided by a grid of equally spaced points.

The grid search algorithm proceeds as follows. In a first step, the search is started at the origin of the considered box; we assume that the origin is outside of $R(Y)$; from here, the acceptance criterion is successively evaluated for each adjacent grid point, lying on the diagonal of the grid identified by the direction $(1, 1, \dots, 1)^\top$. Each evaluation typically requires stochastic simulation. The search along the diagonal direction is interrupted as soon as a point satisfying the acceptance criterion is identified. Due to the monotonicity of the input-output model and the properties of the acceptance criterion (cf., Ref. [245]), all grid points representing superior endowments are acceptable as well and belong to $R(Y)$. Analogously, all endowments that are worse than the first identified point are rejected, thus belonging to $R(Y)^c$, the complement of the systemic risk measurement. It is precisely this monotonicity property that makes the algorithm efficient.

Each pair of diagonally adjacent points, one meeting the requirements and the other not, defines a sub-box. The algorithm checks the remaining corners of this sub-box and can quickly assign an acceptance status to dominating, respectively, dominated endowments. Subsequently, new pairs

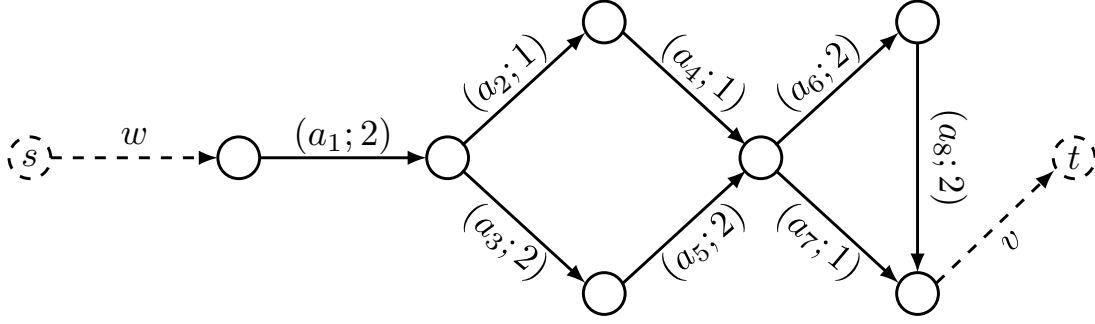


Figure 2.3: Example of a flow network with $b = 2$ component types.

of points can be determined, one in $R(Y)$ and one outside. The successively resulting sub-boxes are checked in the same way as before. The algorithm terminates when all points on the grid are assigned to an acceptance status. It finally determines a discrete grid-approximation of $R(Y)$. For a more detailed description of the grid search algorithm we refer to Ref. [245, Ch. 4].

2.3 Resilience decision-making

The decision-making process for resilience-enhancing endowments in complex systems, developed in this work, integrates resilience metrics and systemic risk measures. As discussed in Zuev et al. [250], complex systems are often described as networks: nodes and edges represent systems as well as the connections between their components. System components may be represented as network edges or nodes – whatever representation is more appropriate.

In order to illustrate our method, we consider a specific flow network as shown in Fig. 2.3. This network consists of seven nodes and eight edges, as well as a source node denoted by s characterized by an initial flow w and a target node denoted by t with a destination flow v , respectively. The network edges represent the essential components of the network. Each component is assigned to one of the two types, i.e., $b = 2$. We set $n = 2$, i.e., two endowment properties are associated with each component: a capacity c and a recovery improvement r^* . Each component $i \in \{1, \dots, 8\}$ is characterized by $(a_i; j_i) = (c_i, r_i^*; j_i) \in \mathbb{R}^{(1 \times 2)} \times \{1, 2\}$.

System performance and resilience are analyzed for a time window $[0, T]$. The interval is partitioned into u parts by the time points $0 = t_0 < \dots < t_{u-1} < t_u = T$. System performance $Q(t)$ is defined as a piecewise constant stochastic process that evaluates the ratio of the destination flow and the initial flow at each time point, i.e.

$$Q(t) = \frac{v(t_h)}{w} \quad \text{with } t \in [t_h, t_{h+1}). \quad (2.10)$$

We assume that partition is equidistant, i.e. $\Delta t = t_{h+1} - t_h = \frac{T}{u} \forall h$. The specification of a notion of system performance is, of course, not uniquely determined by the system; instead, alternative choices may be analyzed simultaneously and should thereby be carefully selected to enable suitable resilience analysis for the intended decision-making process.

The flow for a given endowment $(A; z)$ is simulated as follows: at each time point t_h , the flow of the entire network is computed as follows. The flow starts at the source node and runs iteratively by means of a node-by-node breadth-first search through the entire network up to the destination node. Each node receives the partial flows from all edges leading into it and returns them to all subsequent edges, obeying the following allocation rules: (i) the incoming flow is allocated to all subsequent edges such that 30% runs into edges of type 1 and 70% runs into edges of type 2. Among subsequent edges of the same type, the relevant flow is uniformly allocated; (ii) if the capacity of a subsequent edge is exceeded, this edge is destroyed immediately and the flow is instead reallocated to the remaining edges according to (i); (iii) if a node has no subsequent edge, the flow emanating from this node is lost, i.e. the node becomes a sink.

After the flow has been computed at the time point t_h , the simulation proceeds to time-step $t_{h+1} = t_h + \Delta t$: edges that have been destroyed at time t_h are removed from the network in consecutive time-steps unless they are recovered; the process of recovery will be described below. In addition, each edge can fail at random after the flow has been computed at time t_h and before time t_{h+1} . At time t_{h+1} , the algorithm (i) – (iii) described earlier is then applied to the remaining network.

The failure probability of the edges in the time interval (t_h, t_{h+1}) ,

$$P \{\text{Component } i \text{ fails during } (t_h, t_{h+1})\} = \Delta t \cdot \lambda_i(t_h), \quad (2.11)$$

depends on the utilization of the maximum edge capacity caused by the flow; letting $v_i(t_h)$ be the current flow of the edge i , c_i its capacity, and $\beta > 0$ a mitigation factor, we set

$$\lambda_i(t_h) = \beta \cdot \frac{v_i(t_h)}{c_i}. \quad (2.12)$$

As discussed by Ayyub [6], multiple causes and processes can lead to failures. In this illustrative example and in applications in later sections, we consider only immediate failures due to overload or random impacts; failure might also occur due to a loss of performance in time, e.g., by aging. After failure, each destroyed edge is assumed to be immediately recovered to the original performance level after a certain number of time-steps

$$r = r_{max} - r^* \quad \text{with} \quad r^* < r_{max}, \quad (2.13)$$

where r_{max} is an upper bound for number of time-steps for recovery and r^* is a reduction specific to the component. Since each time-step has a length of $\Delta t = \frac{T}{u}$, the duration of the recovery process is $r \cdot \frac{T}{u}$. This recovery model corresponds to a one-step recovery profile; as discussed before in the context of failure profiles, various characteristic profiles of recovery in time are possible as well, cf., Refs. [6, 10].

In the context of our model, the simulation procedure is executed consecutively for all time points, resulting in a single path of the performance process $t \mapsto Q(t)$ over the time interval

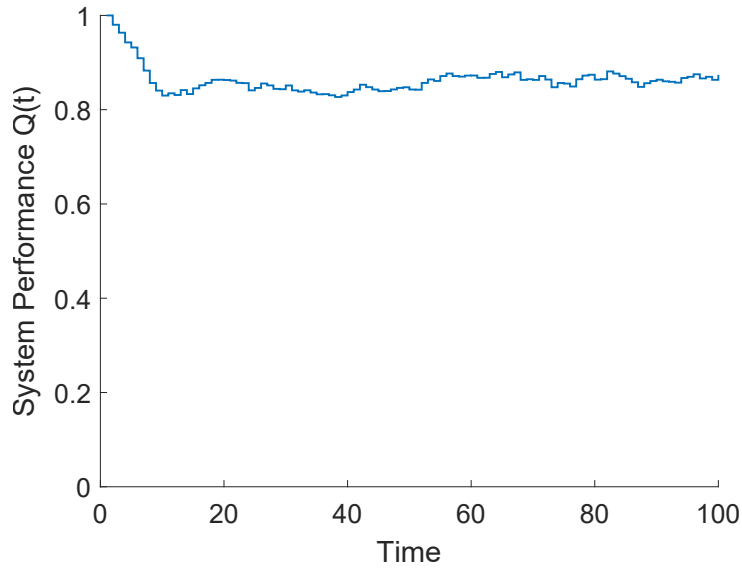


Figure 2.4: Monte Carlo sample average of the system performance $Q(t)$ for the flow network shown in Fig. 2.3, considering the following model and simulation parameter values: $r_{max} = 21$, $r_i^* = 11$ for all edges, $c_i = 12$ for all edges of type $j_i = 1$, $c_i = 8$ for all edges of type $j_i = 2$, $\beta = 0.025$, $u = 100$, $\Delta t = 0.01$.

$[0, T]$. A sample average of the system performance as a function of time T obtained from a Monte Carlo simulation is exemplarily illustrated in Fig. 2.4. The probabilistic resilience metric given in Eq. 2.2 can, of course, also be computed as a suitable average of Monte Carlo samples. When analyzing the resilience of the system, an important task consists in determining the set of all endowment configurations $(A; z)$ that lead to a prescribed acceptable level of system resilience. The numerical procedure is computationally expensive, but tractable due to the grid search algorithm by Feinstein et al. [245]. In addition, the problem is also simplified if restrictions are imposed on the matrix A via a suitable function g_z where z denotes the vector of types; this was discussed in Sec. 2.2.3.

To illustrate this procedure in the context of a flow network model, we fix the vector of types $z \in \{1, 2\}^8$ for the eight edges. Figure 2.3 provides, for example, $z = (2, 1, 2, 1, 2, 2, 1, 2)^\top$. We assume that the constraint function g_z captures the following restrictions: (a) recovery improvements r_i^* are fixed and equal for all components i . (b) Capacities c_i are a function of the type j_i of the components i , i.e., if two components are of the same type, they possess the same capacity. We explore a range of capacities in order to separate acceptable and unacceptable pairs. Figure 2.5 provides an example how the results of the grid search algorithm could look like. The blue dots signify the acceptable pairs of capacities of the two types of components, whereas red dots are unacceptable pairs. Acceptable pairs satisfy the desired resilience criterion, while unacceptable pairs do not. Obviously, the computation of the systemic risk measure significantly facilitates decision-making.

Additionally, the procedure allows the integration of monetary aspects into any decision process that is focusing on the resilience of the system. An important question concerns the identification of a least expensive configuration that is acceptable with respect to the chosen resilience criterion.

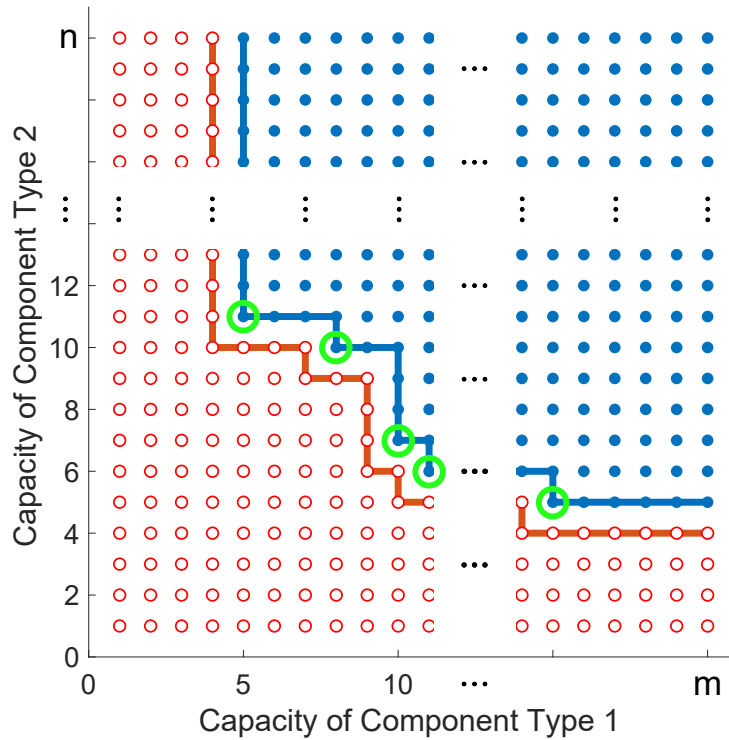


Figure 2.5: Acceptable parameter pairs are marked as blue, filled dots; least expensive acceptable pairs are marked as blue, filled dots that are highlighted in green.

If increasing the endowment values is costly, a least expensive solution will always be at the boundary between the red and the blue area. If the price of the endowments is linearly increasing, prices define a normal vector to this boundary that characterizes the least expensive acceptable configurations on the boundary, as illustrated by the green points in Fig. 2.5. Finding the least expensive configurations corresponds to efficient allocation rules as introduced by Feinstein et al. [245].

2.4 Multistage high-speed axial compressor

Gas turbines are a highly important technology employed in industrial application, e.g., for electricity production, as well as in the military and transportation sector, e.g., as component of aircraft propulsion systems. In particular, axial compressors are one of the key components of gas turbines. For economic and safety reasons, it is of the utmost importance that they are as resilient as possible. In order to illustrate how the decision-making method developed in this paper allows for an analysis of the financial burden of increasing resilience and for an optimal choice between different instruments to enhance resilience, our method is applied to a functional model of an axial compressor.

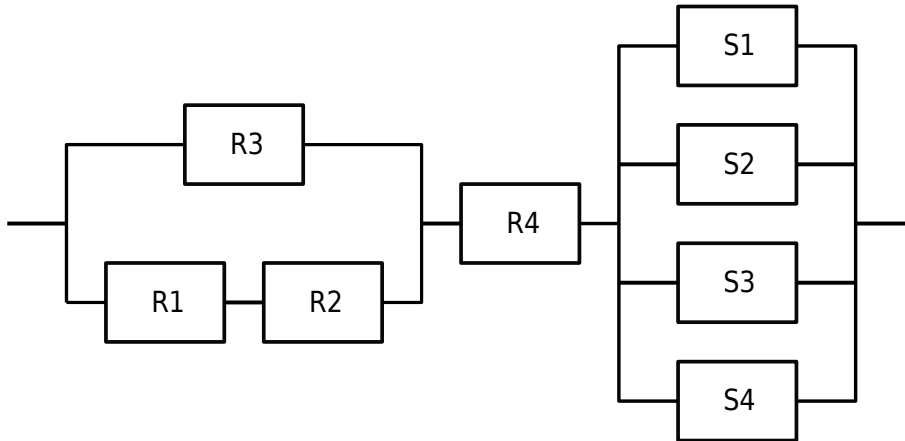


Figure 2.6: Functional model of the multi-stage high-speed axial compressor.

2.4.1 Model

In a previous work by one of the authors of this paper, developed within the Collaborative Research Centre 871, funded by the German Research Foundation [251], a functional model of an axial compressor was created as the foundation for a reliability analysis. This model has been developed to represent the reliability characteristic and functionality of the four-stage high-speed axial compressor of the Institute for Turbomachinery and Fluid Dynamics at Leibniz Universität Hannover. Detailed information about this axial compressor is provided in Refs. [252–254].

The model captures the influence of the roughness of the blades in the individual stator and rotor rows, alternately connected in series, on the performance of the axial compressor, namely, on the total-to-total pressure ratio and on the total-to-total isentropic efficiency. This functional model of the axial compressor has been assembled by applying a sensitivity analysis and identifying the relative important indices from an aerodynamic model of the compressor. The network representing the functional model is shown in Fig. 2.6. Each component of the reliability-based model represents one of the rotor blade rows (R1 - R4) or stator blade rows (S1 - S4). The arrangement of the components was chosen according to the effect of blade roughness on the two performance parameters of the axial compressor. More specifically, an interruption between start and end means a performance variation of at least 25%, corresponding to a nonfunctional compressor. This defines the system performance $Q(t)$ of the functional model for the subsequent application of the resilience decision-making method. The system performance is determined at each time point t_h and is 1 if there is a connection from start to end and 0 if this connection is interrupted. More detailed information on the functional model and its formulation can be obtained from Ref. [251].

For the analysis, as components, we do not distinguish between the stator blade rows and the rotor blade rows and enumerate them by $i \in \{1, \dots, 8\}$. Further, each of them is assigned to the same component type, i.e., it is $j_i = 1 \forall i \in \{1, \dots, 8\}$, and we therefore simplify the notation by $(a_i; j_i) = (a_i; 1) = a_i \forall i \in \{1, \dots, 8\}$. Each row, i.e., each component of the functional model,

is assumed to be characterized by two endowment properties, a roughness resistance re and a recovery improvement r^* , so that a component is fully described by $a_i = (re_i, r_i^*)$. Both, the roughness resistance re_i and the recovery improvement r_i^* of each row i are assumed to be functions of the type j_i , i.e., $re_i = re_{i'}$, $r_i^* = r_{i'}^*$ if $j_i = j_{i'}$ and are therefore in this case study equal for all components. This restriction can be captured by a suitable constraint function g_z , cf., Sec. 2.2.3.

It should be noted that, in order to improve the roughness resistance of a blade, techniques that counteract the roughening of the surface are required. However, such techniques are not clearly identifiable and readily available at the moment. Within the scope of this example, the application of methodologies leading to an improvement of the resistance, e.g., by applying coating techniques, can nevertheless still be envisioned for the scope of the analysis. As an example, in areas not inherent with the mechanical resistance, the principle of blade coatings is already extensively employed, e.g., in the reduction of heat transfer from the gas flow into the blades by means of thermal coatings [255].

Each component of the functional model can fail at random after the system performance has been computed at time t_h . A failed component is treated as no longer present in the model and does not contribute to the overall system performance at time t_{h+1} and all subsequent time points anymore until it is fully recovered. The failure probability of a component i in the time interval (t_h, t_{h+1}) is assumed to be constant in time, cf., Ref. [251], and is given by

$$P \{ \text{Component } i \text{ fails during } (t_h, t_{h+1}) \} = \Delta t \cdot \lambda_i \quad (2.14)$$

with

$$\lambda_i = 0.8 - 0.03 \cdot re_i, \quad (2.15)$$

where λ_i is the time-independent failure rate. An increase of the roughness resistance of a row of blades will reduce the degradation of the surface, and thus, the corresponding failure rate λ_i . In contrast to the flow model in Sec. 2.3, in the functional model of the axial compressor, a component can fail exclusively at random.

If a component i failed, its functionality is assumed to be fully recovered after a number of time-steps according to Eq. 2.13. Single-step failure and recovery profiles are assumed in this application (cf., Sec. 2.3).

2.4.2 Costs of endowment properties

The optimal endowment properties are related to the quality of the components, and an increase in their production quality is associated with large costs. This should be taken in to account in the decision-making process. As discussed in Ref. [256], an increase of the reliability of components in complex networks might be associated with an exponential increase in their costs, and in our analysis, we will make such an assumption.

The endowment property “roughness resistance” affects the failure rate of the blades of a row,

Table 2.1: Parameter values for the resilience decision-making method for the functional model of the multi-stage high-speed axial compressor.

Parameter	Scenario
Number of Rotor/Stator blade rows l	8
Acceptance threshold α	0.8
Number of time steps u	200
Length of a time step Δt	0.05
Maximum recovery time r_{max}	21
Recovery improvement r^*	$r_i^* \in \{1, \dots, 20\}$
Roughness resistance re	$re_i \in \{1, \dots, 20\}$
Recovery improvement price $price^*$	600€
Roughness resistance price $price^{re}$	500€

cf., Eqs. 2.14 and 2.15. Better “roughness resistance” improves reliability, and we assume that its total costs equal

$$cost^{re} = \sum_{i=1}^8 price^{re} \cdot 1.3^{(re_i-1)}, \quad (2.16)$$

where re_i is the “roughness resistance” value of component i and $price^{re}$ a common basic price that does not depend on i in this case study. In a similar way, an exponential relationship is assumed for the cost associated with recovery improvement:

$$cost^* = \sum_{i=1}^8 price^* \cdot 1.3^{(r_i^*-1)}. \quad (2.17)$$

The total cost “ $cost$ ” of an endowment is the sum of these costs:

$$cost = cost^{re} + cost^*. \quad (2.18)$$

2.4.3 Scenario

In order to apply the decision-making method for resilience-enhancing endowments to the multistage high-speed axial compressor, the model parameter and simulation parameter values, shown in Table 2.1, are considered. A resilience acceptance threshold of $\alpha = 0.8$, an arbitrarily selected number of $u = 200$ time-steps as well as an arbitrarily selected time-step length of $\Delta t = 0.05$ are assumed. We first determine the set of all acceptable endowments corresponding to a resilience value of at least $Res = 0.8$ over the considered time period. Second, in practice, any improvement of the axial compressor blades is associated with costs; thus, the least expensive acceptable endowment is characterized as well, denoted by \hat{A} . The roughness resistance re and the recovery improvement r^* are explored over $re_i \in \{1, \dots, 20\}$, $r_i^* \in \{1, \dots, 20\} \forall i \in \{1, \dots, l\}$. These values can be interpreted as increasing quality levels. In terms of recovery, this leads to a recovery time for the components of maximum 20 time-steps to a minimum of one time-step,

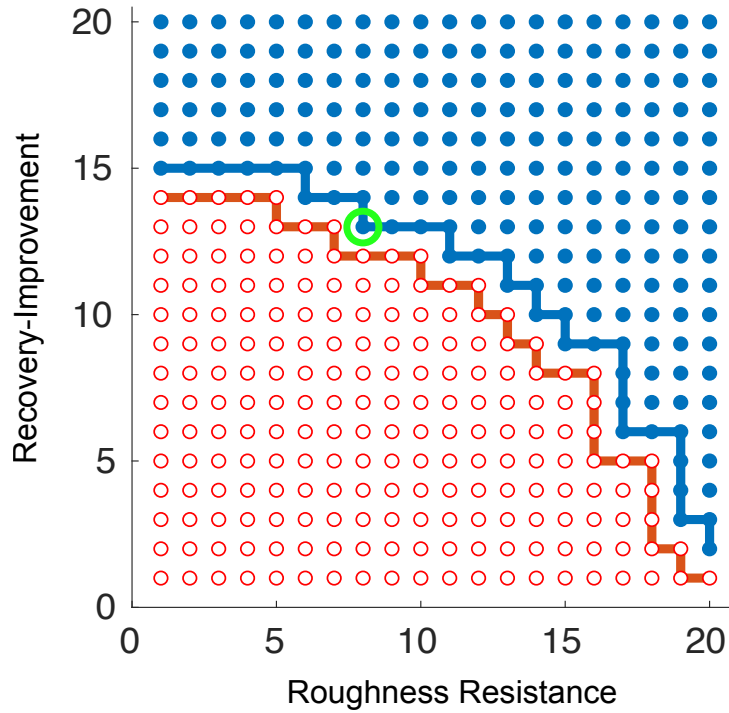


Figure 2.7: Numerical results of the grid search algorithm for the functional model of the axial compressor with explored roughness resistance/recovery improvement values.

depending on the recovery improvement value r_i^* of each component.

The scenario was simulated on the basis of the functional model, following the procedure described in Secs. 2.2.3 and 2.2.4. Figure 2.7 shows the results of the grid search algorithm. The blue, filled dots are the acceptable pairs of roughness resistance and recovery improvement. In terms of system resilience, the impact of the quality of recovery improvement and the quality of the blade coatings can be compared. For example, for recovery improvement values of $r_i^* \geq 15$ time-steps, only the minimum roughness resistance value of $re_i = 1$ is necessary in order to achieve the desired level of system resilience.

By applying the grid search algorithm [245], only about 10% of the possible pairs of roughness resistance and recovery improvement values had to be tested to determine $R(Y)$. As described in Sec. 2.3, the least expensive endowment is an element of the boundary of $R(Y)$. Taking into account the base prices in Table 2.1, the least expensive endowment is characterized by a roughness resistance of $re_i = 8$ and a recovery improvement of $r_i^* = 13$ for each component. In Fig. 2.7 the corresponding pair is highlighted in green. According to Eq. 2.17, its cost is 136 930€.

2.5 Berlin's *U-Bahn* and *S-Bahn* system

Berlin's subway *U-Bahn*, suburban train *S-Bahn*, trams, and buses carry more than 1.5 billion passengers each year. Approximately, two-thirds of these passengers are transported via the

S-Bahn and *U-Bahn* rails ([257], [258]). These are the most used public transport systems in Berlin and of utmost importance for Germany's capital. Obviously, key infrastructures of high social and economic relevance require a large degree of resilience. The method developed in this paper will be applied to a model of the Berlin subway and suburban train system, with the aim of examining suitable resilience-enhancing modifications. Our methodology could also be applied to assess the resilience of new systems that are still in their design phase. This provides an opportunity to characterize *ex ante* adequate system requirements in terms of reliability, robustness and regenerative capacity.

2.5.1 Model

The *U-Bahn* and *S-Bahn* public transportation systems in Berlin are interconnected via multiple train stations. As described in Ref. [250], they may thus be considered as one single public transport network, in the following called "metro network". Zhang et al. [259] explain how a metro network can be mapped into a topological graph: train stations correspond to the nodes and the connecting railway lines to the edges of the graph. For simplicity, we map parallel railway lines between two stations to one single undirected edge. In this way, the complexity of the metro network can be significantly reduced. In the case of the Berlin metro network, this procedure leads to a topological graph with 306 nodes and 350 edges. This representation of the *U-Bahn* and *S-Bahn* system is shown in Fig. 2.8.

We begin our analysis with the definition of a suitable metric of the system performance of the network, as explained in Sec. 2.2.3. Zhang et al. [260] present resilience assessments for large-scale metro networks and apply their approach to the Shanghai metro network. They suggest that the connectivity between the individual stations is an essential criterion for assessing metro operations. Their approach employs the characteristics of topographic networks in order to capture resilience, e.g., the characteristic path length, the network-clustering coefficient, the average node degree, and the network efficiency.

Network efficiency, as described by Latora & Marchiori [261], is a quantitative indicator of the network connectivity:

$$E_f = \frac{1}{N(N-1)} \sum_{i \neq j} \frac{1}{d_{ij}}, \quad (2.19)$$

with N being the number of nodes in the network and d_{ij} being the path length between node i and node j , i.e., the shortest distance between these nodes. We use the network efficiency E_f as system performance of the Berlin metro network in each time point t_h , previously denoted by $Q(t_h)$. Zhan & Noon [262] and Dreyfus [263] provide a good overview of tools for efficiently determining the path length d_{ij} between nodes, e.g., the algorithms of Floyd, Dijkstra's, or Bellman-Ford.

The node degree represents the number of nodes in the graph that have a direct connection to the i -th node. In many useful random graphs, the distribution of node degrees follows a power distribution, see, e.g., Barabási & Albert [264]. Figure 2.9 shows the relative frequencies of

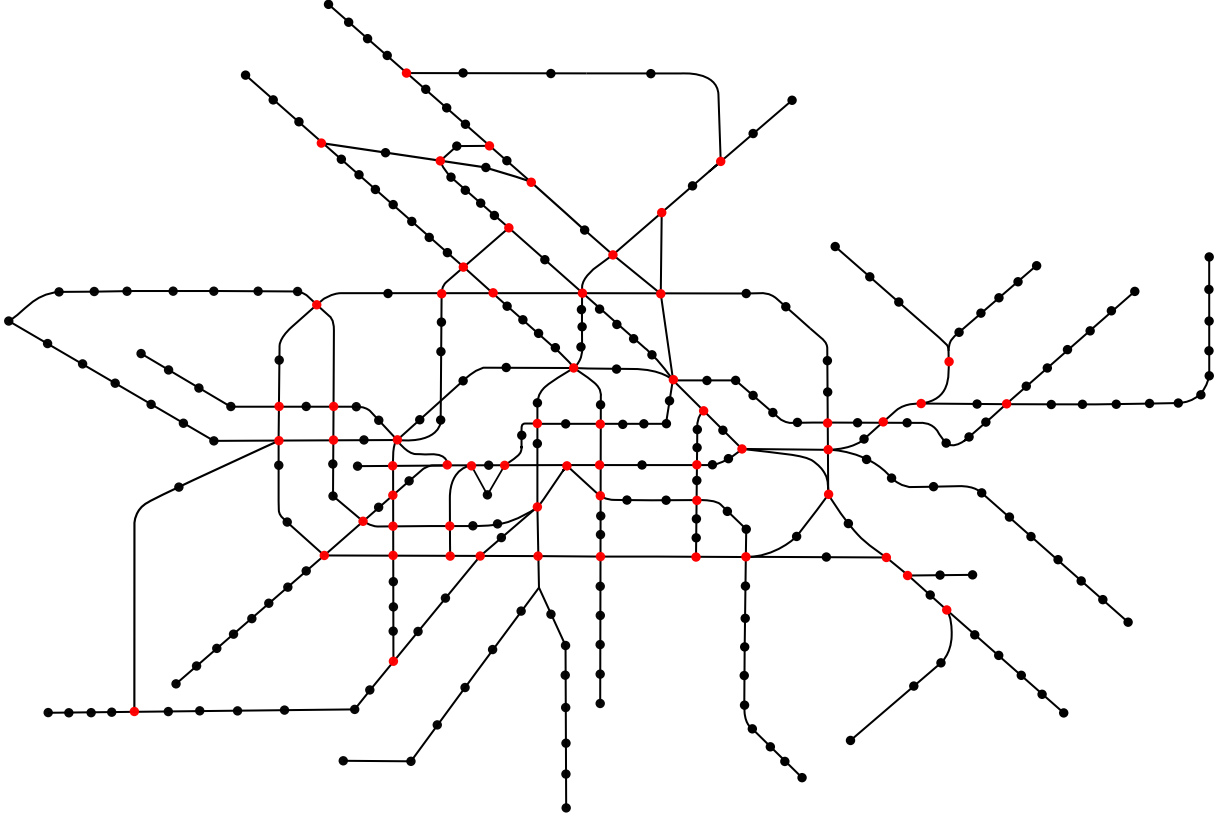


Figure 2.8: Topological network for the Berlin metro system.

the node degrees in case of the Berlin metro network which could be approximated by a power distribution.

Metro stations are modeled as nodes of the network. We assume that each metro station i is characterized by two endowment properties, (a) robustness ro_i and (b) recovery improvement r_i^* ; a component i of type j_i is described by a tuple $(a_i; j_i) = (ro_i, r_i^*; j_i)$. Again both endowment properties are assumed to be functions of their component type j_i only, such that $ro_i = ro_{i'}$ and $r_i^* = r_{i'}^*$ if $j_i = j_{i'}$. These restrictions can again formally be captured by the constraint function g_z that explicitly describes the reduction of the dimension of the problem, cf., Sec. 2.2.3.

Metro stations fail at random. The failure probability for each component i is

$$P \{\text{Component } i \text{ fails during } (t_h, t_{h+1})\} = \Delta t \cdot \lambda_i(t_h) \quad (2.20)$$

with

$$\lambda_i(t_h) = (1 + k_i(t_h) \cdot 0.2) - \frac{ro_i}{ro_{max}}, \quad (2.21)$$

where $\lambda_i(t_h)$ is the failure rate at time t_h , $k_i(t_h)$ is the time-dependent number of direct neighbors of the i -th metro station that are in a failed state at time t_h , ro_i is the robustness of the i -th metro station, and ro_{max} is the maximum value of the robustness. As the robustness of a metro station i increases, its failure rate $\lambda_i(t_h)$ decreases. In the event of failure of a directly adjacent

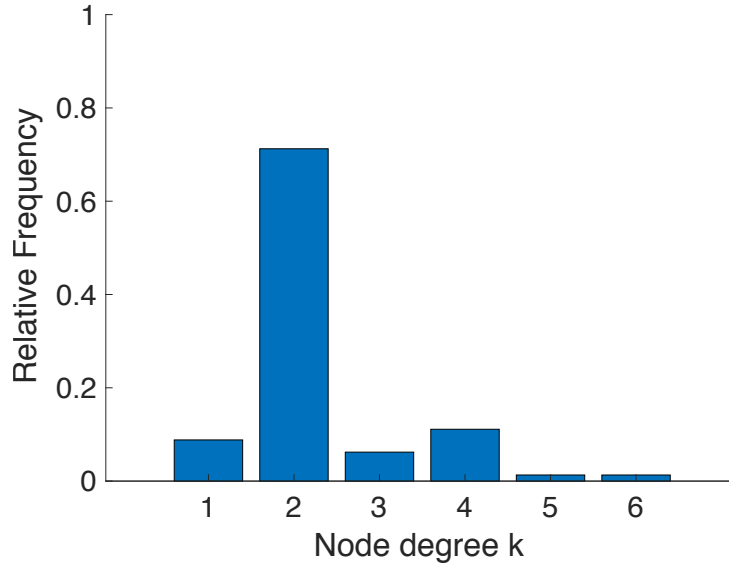


Figure 2.9: Relative frequency of node degrees for the metro network of Berlin.

metro station, its probability of failure increases; a rational for this assumption is that the load on the considered station becomes larger which increases the likelihood of failure. This phenomenon might potentially lead to cascading failures, cf., Refs. [265–267].

The second endowment property, the recovery improvement r_i^* , determines the time to recovery after failure according to Eq. 2.13. Failed metro stations are not removed, but remain in the set of metro stations; however, their node degree becomes 0 in the evolving network structure. This assumption is important, since the computation and interpretation of network efficiency E_f depends on the number of nodes; our case study relies on the fact that the number of nodes is preserved. After recovery, all previous connections to other metro stations are restored, unless these are in a state of failure. Our analysis focuses on determining the optimal endowments in terms of resilience. This is in contrast to Zhang et al. [260] whose focus is – among other things – the optimal order in which connections should be recovered.

2.5.2 Endowment property costs

Improving the endowment properties is costly. We again assume an exponential relationship. The total cost of “robustness” for all stations is

$$cost^{ro} = \sum_i price_{(ro_i; j_i)}^{ro} \cdot 1.2^{ro_i - 1}, \quad (2.22)$$

where j_i is the type of station i , its robustness is ro_i and its basic price of the endowment property “robustness” is $price_{(ro_i; j_i)}^{ro}$. The total cost of “recovery improvement” is given by

$$cost^* = \sum_i price_{(r_i^*; j_i)}^* \cdot 1.2^{r_i^* - 1}, \quad (2.23)$$

Table 2.2: Parameter values for two scenarios of the decision-making method of the Berlin metro network.

Parameter	Scenario 1	Scenario 2
Number of nodes l	306	306
Number of edges	350	350
Acceptance threshold α	0.8	0.8
Number of time steps u	100	100
Length of a time step Δt	0.01	0.01
Maximum recovery time r_{max}	25	25
Maximum robustness ro_{max}	20	20
Number of metro station types	2	1
Recovery improvement r^*	$r_i^* = 15$ for $j_i \in \{1, 2\}$	$r_i^* \in \{1, \dots, 20\}$
Robustness ro	$ro_i \in \{1, \dots, 20\}$ for $j_i \in \{1, 2\}$	$ro_i \in \{1, \dots, 20\}$
Robustness price $price_{(ro_i; j_i)}^{ro}$	$price_{(ro_i; 1)}^{ro} = 1\,000\text{€}$ $price_{(ro_i; 2)}^{ro} = 2\,000\text{€}$	$price_{ro_i}^{ro} = 1\,500\text{€}$
Recovery impr. price $price_{(r_i^*; j_i)}^*$	$price_{(r_i^*; j_i)}^* = 1\,100\text{€}$ for $j_i \in \{1, 2\}$	$price_{r_i^*}^* = 1\,100\text{€}$

where j_i is the type of station i , its recovery improvement is r_i^* and its basic price of the endowment property “recovery improvement” is $price_{(r_i^*; j_i)}^*$. The total cost $cost_{(A; z)}$ of an endowment $(A; z)$ is obtained as

$$cost_{(A; z)} = cost^{ro} + cost^*. \quad (2.24)$$

2.5.3 Scenarios

We consider two different scenarios characterized by the simulation and model parameters in Table 2.2. In both scenarios, we assume a resilience threshold of $\alpha = 0.8$, a number of $u = 100$ time-steps, and a time-step length of $\Delta t = 0.01$. The objective of the analysis is to characterize suitable endowment allocations such that the metro network’s resilience is at least $Res = 0.8$. We will also identify the least expensive acceptable endowments, denoted by $(\hat{A}; z)$ in both cases.

Scenario 1

In the first scenario, each metro station is assigned to one of the two station types, namely, “small” and “large”. The “small” metro stations i (type $j_i = 1$) have only one or two direct neighboring stations, i.e., a node degree of 1, 2, while the “large” metro stations i (type $j_i = 2$) have more than two direct neighboring stations, i.e., a node degree > 2 , and are highlighted in red in Fig. 2.8. Out of all stations, a total of 245 are of type 1 and 61 of type 2.

The endowment properties of all components depend on their type only. We vary robustness with $ro_i \in \{1, \dots, 20\}$ for all i . The recovery improvements of both component types are fixed and equal $r_i^* = 15$ for all components i independent of their types.

Figure 2.10 shows the results of the grid search algorithm for scenario 1. The blue, filled dots signify the pairs of robustness values that lead to acceptable endowments. In terms of system

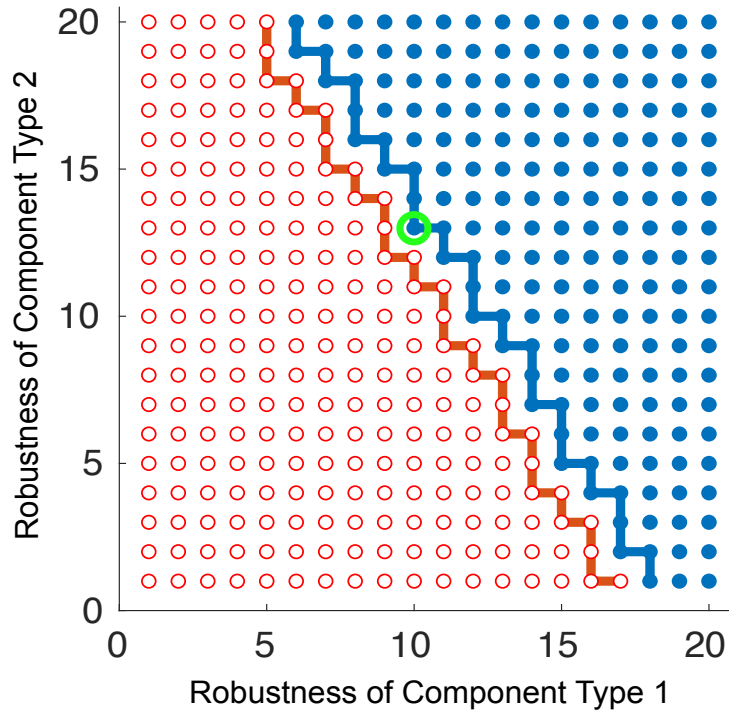


Figure 2.10: Numerical results of scenario 1 of the Berlin metro network, varying robustness.

resilience the robustness of the “small” metro stations is more important than the one of the “large” stations in this case study. For example with large robustness values for the “small” stations, i.e., $ro_i \geq 18$ for $j_i = 1$, acceptability may be achieved even with a minimal robustness value of $ro_i = 1$ of “large” stations, i.e. $j_i = 2$. The slope of the almost linear boundary indicates that in order to compensate for the reduction of one robustness unit of the endowments of the “small” stations, an increase of approximately 1.7 robustness units of the endowments of the “large” stations is necessary.

This observation can be explained as follows: first, the number of “small” stations (245) is significantly larger than the number of “large” stations (61), and thus, their overall influence is large. Second, “small” stations are often arranged in chains. If a station within such a chain fails, all stations further out of town are automatically cut off from the main network, which has a major impact on network efficiency.

Thanks to the grid search algorithm only about 10% of all pairs of robustness values had to be tested to determine the set of all accepted endowments. As described in Sec. 2.3, the least expensive endowment is an element of the boundary of the acceptable endowment allocations. For the parameters in Table 2.2, the least expensive endowment corresponds to a robustness of $ro_i = 10$ for all “small” stations i of type $j_i = 1$ and a robustness of $ro_i = 13$ for all “large” stations of type $j_i = 2$. The corresponding pair of parameters is highlighted in green in Fig. 2.10. The total endowment cost, computed according to Eq. 2.24, equals 6 673 579€.

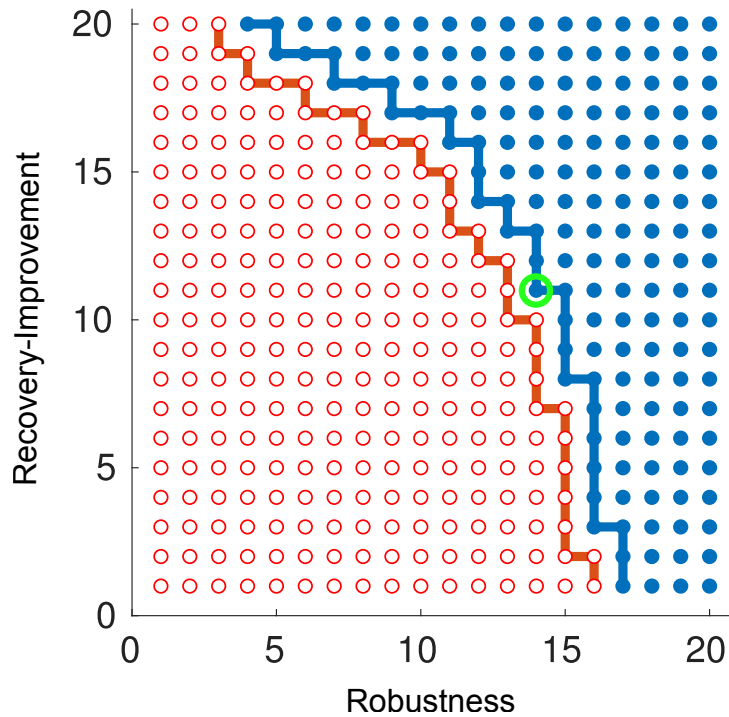


Figure 2.11: Numerical results of scenario 2 of the Berlin metro network, varying robustness/recovery-improvement.

Scenario 2

In the second scenario, all metro stations are assigned to the same station type, and $(a_i; j_i)$ can simply be written as a_i . We vary both recovery improvement and robustness, i.e. $r_i^*, ro_i \in \{1, \dots, 20\} \forall i$.

Figure 2.11 shows the results of the grid search algorithm for scenario 2. The blue, filled dots signify the pairs of robustness and recovery improvement values that lead to acceptable endowments. The application of the grid search algorithm leads to a similar reduction of the computing effort as in scenario 1. For the parameters in Table 2.2 the least expensive endowment corresponds to robustness $ro_i = 14$ and recovery improvement $r_i^* = 11$ for all stations i ; this is highlighted in green in Fig. 2.11. Its cost is computed according to Eq. 2.24 and equals 6 995 127€.

2.6 Conclusion

This paper introduces a procedure for decision-making in complex systems that enables the optimal allocation of scarce resources to resilience-enhancing endowments. The methodology integrates systemic risk measures with time-dependent and probabilistic resilience metrics. Our approach is not limited to controls of the same type, but allows for a direct comparison of the impact of heterogeneous controls on the resilience of the system, e.g., failure prevention and recovery improvement arrangements, over any period of time. The system behavior itself may depend on a wide variety of stochastic variables that influence its performance. Our method

characterizes, in a first step, all acceptable endowments of system components that lead to a desired level of resilience. In a second step, it is capable of incorporating monetary aspects into the decision-making process and admits the identification of the least expensive controls. In addition, we explain a grid search algorithm for systemic risk measures that significantly reduces the required computational effort.

The suggested methodology is not limited to a certain type of networks. This paper illustrates that the approach is easily adaptable and universally applicable. Examples in this paper include technical systems such as axial compressors as well as infrastructure networks such as the Berlin metro system. Many other applications are possible, thereby supporting decision-makers in improving the complex systems of our modern society and increasing their resilience.

Future research may apply the suggested methodology to highly complex systems. In this paper, many simplifying assumptions were made in order to be able to focus on the basic concepts and to demonstrate the versatility of the approach in concrete examples. More challenging problems, e.g., higher dimensions of the parameter space, are left to future developments. From a conceptual point of view, real-world problems involve multiple objectives and are not limited to a finite time horizon. Future work should not only focus on system resilience and the costs of the controls but also on long-term effects, such as different expected profits under a modified system resilience. Comprehensive decisions require a deep understanding of the tradeoff between the costs and the gains of resilience. Further work will also have to address the balancing between monetary and safety-related criteria for decision-making. The proposed method provides powerful instruments for one important aspect: the characterization of acceptable resilience-enhancing endowments and the identification of the most cost-efficient allocation. This tool box will be a prerequisite for future answers to many challenging questions.

Acknowledgment

The authors kindly thank the German Research Foundation (DFG) for the financial support to accomplish the research project D5 “Resilience Based Decision Criteria for Optimal Regeneration” within the Collaborative Research Center (CRC) 871 - Regeneration of Complex Capital Goods.

3 | Multidimensional resilience decision-making for complex and substructured systems

Multidimensional resilience decision-making for complex and substructured systems

Julian Salomon^{a,*}, Jasper Behrendorf^a, Niklas Winnewisser^a, Matteo Broggi^a, Michael Beer^{a,b,c}

^aInstitute for Risk and Reliability, Leibniz Universität Hannover, Hannover, Germany

^bInstitute for Risk and Uncertainty, University of Liverpool, Liverpool, United Kingdom

^cInternational Joint Research Center for Resilient Infrastructure & International Joint Research Center for Engineering Reliability and Stochastic Mechanics, Tongji University, Shanghai, China

*Corresponding author

Published in *Resilient Cities and Structures* on September 2022

Abstract

Complex systems, such as infrastructure networks, industrial plants and jet engines, are of paramount importance to modern societies. However, these systems are subject to a variety of different threats. Novel research focuses not only on monitoring and improving the robustness and reliability of systems, but also on their recoverability from adverse events. The concept of resilience encompasses precisely these aspects. However, efficient resilience analysis for the modern systems of our societies is becoming more and more challenging. Due to their increasing complexity, system components frequently exhibit significant complexity of their own, requiring them to be modeled as systems, i.e., subsystems. Therefore, efficient resilience analysis approaches are needed to address this emerging challenge. This work presents an efficient resilience decision-making procedure for complex and substructured systems. A novel methodology is derived by bringing together two methods from the fields of reliability analysis and modern resilience assessment. A resilience decision-making framework and the concept of survival signature are extended and merged, providing an efficient approach for quantifying the resilience of complex, large and substructured systems subject to monetary restrictions. The new approach combines both of the advantageous characteristics of its two original components: A direct comparison between various resilience-enhancing options from a multidimensional search space, leading to an optimal trade-off with respect to the system resilience and a significant reduction of the computational effort due to the separation property of the survival signature, once a subsystem structure has been computed, any possible characterization of the probabilistic part can be validated with no need to recompute the structure.

The developed methods are applied to the functional model of a multistage high-speed axial compressor and two substructured systems of increasing complexity, providing accurate results and demonstrating efficiency and general applicability.

Keywords: Resilience, Decision-making, Survival signature, Reliability, Complex systems, Substructured systems.

3.1 Introduction

In today's highly developed societies, complex systems, such as infrastructure networks, industrial plants and jet engines are both ubiquitous and of paramount importance to the functioning of these modern societies. It is evident that these systems are exposed to a variety of harmful influences of natural, technical and anthropogenic origin. At the same time, as Punzo et al. highlight in [17], "It is an undeniable fact that modern day systems are more integrated, more interdependent, evolve at faster pace and, in a word, are more complex than the systems of the

previous century [...]” Considering this high and increasing system complexity, it is impractical to detect and prevent all potential negative impacts. Therefore, it is essential that new developments in engineering focus not only on monitoring and improving the robustness and reliability of systems, but also on their recoverability after adverse events [243]. The concept of resilience encompasses these aspects: analyzing and optimizing robustness, reliability and recovery of systems, from a technical and economic perspective [5, 7, 10]. Applying resilience to engineered systems leads to a paradigm shift. Secure systems cannot solely rely on strategies to prevent failures, but must include strategies for efficient recovery in the event of failure as well, see, e.g., [11, 13].

In engineering, the concept of resilience has steadily gained popularity in recent years [17, 23, 24]. The notion of “resilience” appears in various fields such as ecology, economics, and psychology, as well as in the context of mechanical systems, and is derived from the Latin word “resilire,” which means “to bounce back.” The concept of resilience was first introduced by Holling in the field of ecological systems [8]. Although several other definitions by various scientists followed, most of them have certain key aspects in common that were already captured by Holling’s early definition [53–57]. In [6], Ayyub provides a literature review and develops a comprehensive definition of resilience in the context of complex systems based on the content of the Presidential Policy Directive (PPD) on critical infrastructure security and resilience [62]. His definition provides a solid foundation for quantifying resilience.

Numerous options exist for improving the resilience of complex systems. However, resources are not unlimited and resilience cannot be increased at will. Therefore, it is essential not only to be able to distinguish and weigh between a variety of different resilience-enhancing measures, but to also consider their monetary aspects [240, 244]. In [268], Salomon et al. present a method for identifying the most cost-effective allocation of resilience-enhancing investments by merging the resilience metric of [86] and an adaptation of the systemic risk measure of [245]. Their approach allows for a direct comparison of the effects of heterogeneous controls on the resilience of a system over an arbitrary time period in a two-dimensional parameter space.

Additionally, current research in the context of resilience focuses on improved resilience quantification measures, as proposed in [84], and overarching frameworks for stakeholder decision-making, e.g., for transportation networks in the presence of seismic hazards [269]. For a comprehensive literature review on resilience assessment frameworks that balance resources and performance, see [270]. Other researchers recently studied the complexity of realistic infrastructure systems, failure consequences, recovery sequences, and varying external effects. In [271], for example, the authors revealed the vast complexity of modern critical infrastructures and their multi-factorial nature as cyber-human-physical systems and studied appropriate modeling and resilience analysis approaches. Further, the works [272] and [273] are concerned with the effects on decision-making when considering stakeholder preferences or enhancement and recovery strategies. External effects and challenges arising from climate change were studied in the context of resilience, e.g., in [274].

Various technical and infrastructural systems in today’s society are large and complex in nature. In particular, when system components have such complexity that they themselves need to be modeled as systems, so-called systems of systems [275, 276], resulting in a significantly high number of components. This is in accordance to Batty, who highlights “A very simple definition of a complex system is ‘a system that is composed of complex systems’” [277]. As each of the subsystems affects the top-level system under consideration, this causes a significant increase in computational effort for system analysis and constitutes a major challenge [278, 279]. Therefore, it is particularly important to have tools capable of efficiently assessing all three resilience phases. Typically the reliability phase involves the most system evaluations, in particular when various different system configurations need to be assessed that have an impact on the probability structure of the subsystems and thus on the overall system. Therefore, a particularly efficient analysis approach is required for this phase.

An efficient approach to modeling the reliability of systems with multiple component types is provided by the concept of survival signature, introduced and discussed in [149, 153] by Coolen and Coolen-Maturi. Its major benefit over conventional approaches is the separation of the system structure from the probabilistic properties of the system components. Once the system structure has been analyzed, any possible probabilistic characterization can be tested without having to reevaluate any system states. Consequently, this approach reduces the computational cost of repeated model evaluations typically required in design and maintenance processes [114]. Current research is focused on multi-state components [114], common cause failures [159], multiple failure modes and dependent failures [158], approximation techniques for large systems [155] and reliability analysis in consideration of imprecision [152].

In this paper, theoretical fundamentals are summarized and the resilience decision-making method introduced in [268] is extended to multidimensional parameter spaces. Next, a novel and encompassing methodology is developed, consisting of its two major ingredients, the extended resilience decision-making method and the survival signature. This allows for an efficient and multidimensional resilience analysis of complex, large and substructured systems. The extension and novel methodology are then applied to a functional model of a multistage high-speed axial compressor, an arbitrary complex system as well as the U-Bahn and S-Bahn system of Berlin, to prove general applicability.

3.2 Resilience decision-making

Assessing the resilience of complex systems subject to technical or monetary constraints requires a sophisticated methodology to efficiently derive optimal decisions. In [268], Salomon et al. propose a versatile approach with three key elements, including a metric for resilience quantification, an adapted systemic risk measure, and a grid search algorithm that increases computational efficiency.

3.2.1 Resilience quantification

A suitable quantitative measure of resilience is a fundamental prerequisite for assessing resilience in engineering. In [12, 23, 73], the authors provide a comprehensive overview of resilience metrics in a systemic context. While Bergström et al. emphasize the general concept of resilience in the current literature as a critical link between increasing complexity of systems and their risk [23], Sun et al. focus on resilience of infrastructures and highlight the close link between resilience and functionality respectively performance measures [73]. Hosseini et al. proposed a general scheme for categorizing resilience quantification approaches [12]. In summary, performance-based resilience metrics are most widely used. These determine the resilience of a system by comparing its performance before and after a destructive event. Further subcategories relate to time in-/dependence and characterization as deterministic or probabilistic processes.

According to [76] and [12], performance-based and time-dependent metrics are capable of considering the following system and transition states before and after a disruptive event:

- The original stable state, i.e., the duration until a disruptive event occurs, relying on the reliability of the system.
- The system vulnerability, represented by a loss of performance after the occurrence of a disruptive event and the robustness counteracting the vulnerability and mitigating this performance loss. Both are governed by degradation characteristics of the system components.
- The system recoverability, characterized by the disrupted state of the system and its recovery to a new stable state.

An illustration of these phases and transitions is shown in Fig. 3.1. The performance level of the new stable state might differ from the performance level of the original state.

The area of performance loss between original and new stable state in Fig. 3.1 refers to the well-known principle of “*resilience triangle*” introduced by Bruneau et al. [48], as illustrated in Fig. 3.2. In their work, Bruneau et al. proposed a time-dependent, performance-based, and deterministic metric for resilience loss of a community due to seismic disasters as follows. Let t_0 be the time a disruptive event occurs and t_1 be the time of completed recovery. Further, $Q(t)$ denotes the quality of the community infrastructure at time t , specifying the type of system performance. Then, the metric is defined as:

$$R_{Br} = \int_{t_0}^{t_1} [100 - Q(t)] dt. \quad (3.1)$$

Note that the system performance is compared with a time-independent ideal performance of 100 in the considered interval of performance loss. The approach forms a strong basis for several, later proposed metrics in various contexts, see [94–96].

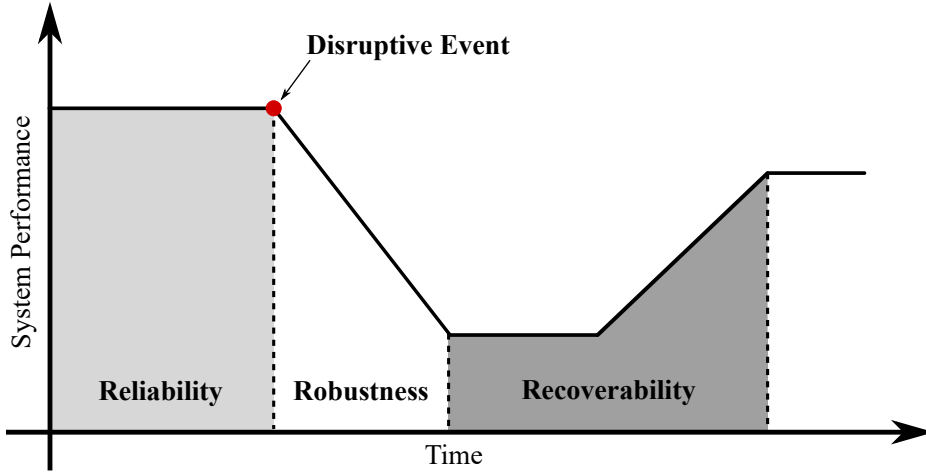


Figure 3.1: In the evolution of a system before and after the impact of a disruptive event, different phases can be distinguished: (i) the original stable state, (ii) disruptive impact, vulnerability, robustness, (iii) disrupted state and recovery; adapted from [76].

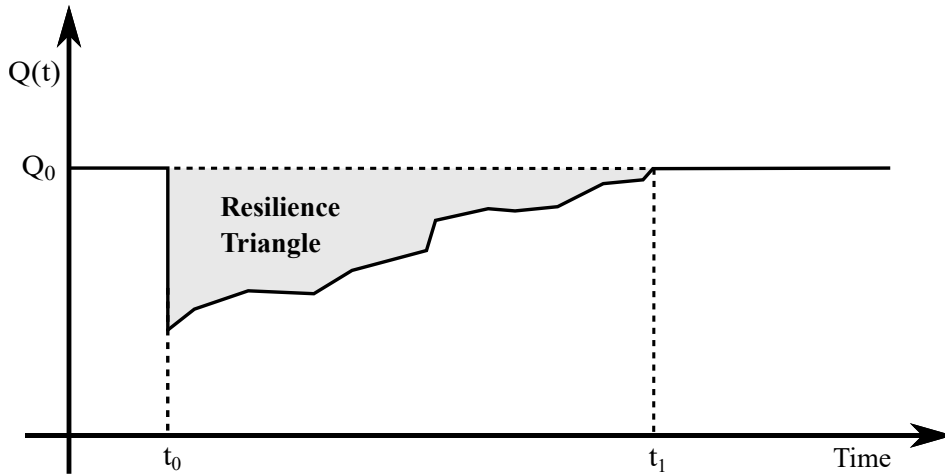


Figure 3.2: Resilience triangle; adapted from [48].

In [268], Salomon et al. utilize the probabilistic and time-dependent metric developed by Ouyang et al. [86]. The metric is defined as the expected ratio of the integral over the actual system performance $Q(t)$ from 0 to a given time T and the corresponding integral of a target system performance $\mathcal{T}Q(t)$ over the same time interval:

$$Res = E[Y], \quad (3.2)$$

where

$$Y = \frac{\int_0^T Q(t)dt}{\int_0^T \mathcal{T}Q(t)dt}. \quad (3.3)$$

Thereby, the system performance $Q(t)$ is a stochastic process. The target system performance $\mathcal{T}Q(t)$ can be generally considered as a stochastic process as well, however, for simplicity, $\mathcal{T}Q(t)$

may be assumed as a non-random and constant quantity $\mathcal{T}Q$. Assuming that the actual system performance does not exceed the target performance, the metric takes values between 0 and 1. For $Res = 1$, the system performance is equal to the target system performance, while $Res = 0$ indicates that the system is not functioning during the entire period under consideration.

3.2.2 Adapted systemic risk measure

In [245], Feinstein et al. proposed a general approach to measuring systemic risk, e.g., pursued in finance [247]. In [268], this risk measure was adapted and extended for the application to engineering systems as summarized in this section. The adapted systemic risk measure comprises a descriptive input-output model and an acceptance criterion that represents normative resilience standards of a regulatory authority.

Let a system be given with m components $i \in \{1, \dots, m\}$ of type $k_i \in \{1, 2, \dots, K\} \subseteq \mathbb{N}$ with e properties that influence the system performance $Q(t)$. These properties, hereafter referred to as "endowment properties", affect system resilience and can be improved through capital allocations. Then, the component i is characterized by

$$(\mathbf{a}_i; k_i) = (\eta_{i1}, \eta_{i2}, \dots, \eta_{ie}; k_i) \in \mathbb{R}^{(1 \times e)} \times \mathbb{N}, \quad (3.4)$$

where $(\eta_{i1}, \eta_{i2}, \dots, \eta_{ie})$ are the numerical values of the e relevant endowment properties. Consequently, the entire system can be described by a tuple, consisting of the matrix $\mathbf{A} \in \mathbb{R}^{(m \times e)}$ and the column vector $\mathbf{z} \in \mathbb{N}^m$ that captures the component types:

$$(\mathbf{A}; \mathbf{z}) = \begin{pmatrix} \eta_{11} & \eta_{12} & \cdots & \eta_{1e} & z_1 \\ \eta_{21} & \eta_{22} & \cdots & \eta_{2e} & z_2 \\ \vdots & \vdots & & \vdots & \vdots \\ \eta_{m1} & \eta_{m2} & \cdots & \eta_{me} & z_m \end{pmatrix}. \quad (3.5)$$

The system under consideration is defined via a descriptive, non-decreasing input-output model $Y = Y_{(\mathbf{A}; \mathbf{z})}$ that is specified by this tuple and relates endowment properties to system performance. With respect to Eq. 3.2, the model output is specified as $Y = Y_{(\mathbf{A}; \mathbf{z})}$ dependent on the current endowment allocation $(\mathbf{A}; \mathbf{z})$.

Further, consider the following specific acceptance set

$$\mathcal{A} = \{X \in \mathcal{X} \mid E[X] \geq \alpha\} \quad (3.6)$$

for a normalized model output X and its expected value $E[X]$ with $\alpha \in [0, 1]$. Correspondingly, the risk measure is defined as

$$R(Y) = \left\{ \mathbf{A} \in \mathbb{R}^{m \times e} \mid Y_{(\mathbf{A}; \mathbf{z})} \in \mathcal{A} \right\}, \quad (3.7)$$

that is the set of all endowment property allocations \mathbf{A} such that the system reaches a resilience

value greater or equal to α .

In practice, it might be necessary to impose structural restrictions on the matrix in Eq. 3.5. For example, consider the case that any component i of a specific type should be configured in the same way, i.e., the row vectors \mathbf{a}_i are claimed to be equal. In [245], Feinstein et al. capture such constraints by monotonously increasing functions $g_z : \mathbb{R}^p \rightarrow \mathbb{R}^{(m \times e)}$, $a' \mapsto (A; z)$ with $z \in \mathbb{R}^m$ denoting the component types. Such a function maps a lower-dimensional set of parameters $a' \in \mathbb{R}^p$ to the system description given in Eq. 3.5.

3.2.3 Grid search algorithm and the curse of dimensionality

According to [245] and [268], the measure of systemic risk might be determined via a combination of a grid search algorithm and stochastic simulations. The grid search algorithm operates in the space of all possible endowments, while stochastic simulations are employed to evaluate system resilience for the endowment allocations according to the grid search algorithm. The probabilistic resilience metric (Eq. 3.2 and Eq. 3.3) is estimated by means of Monte Carlo simulation. The grid search algorithm given in [245] consists of two phases and can be recapitulated as follows:

- (I) Search along the main diagonal of the space of endowment properties until the first acceptable combination is found based on the adapted systemic risk measure.
- (II) Identify the Pareto front between the set of acceptable endowments $R(Y)$ and its complement $R(Y)^c$ starting at the first accepted allocation.

The algorithm allows to compute the entirety of $R(Y)$ while significantly reducing the computational cost due to the assumed monotonicity property of the input-output model $Y_{(A; z)}$ given in Sec. 3.2.2. For a detailed description of a grid search algorithm for two dimensional problems, see [245], Ch. 4.

In [268] this algorithm was included in the resilience decision-making method and applied to case studies with two dimensional parameter spaces. In their work [245], Feinstein et al. point out that the grid search algorithm is applicable to higher dimensional problems “[...] *at the price of substantially larger computation times and required memory capacity.*”. However, when analyzing real technical systems, it is often inevitable to consider a large number of influencing factors and thus a higher dimensionality of the parameter space. Therefore, in Sec. 3.5, an extension of the previously proposed resilience decision-making methodology to n -dimensional problems is applied to a four-dimensional functional model of an axial compressor and, in Sec. 3.7, as part of the novel methodology proposed in Sec. 3.4, it is applied to the *U-Bahn* and *S-Bahn* system of Berlin, addressing a five-dimensional problem.

3.3 Concept of survival signature

Introduced in [149], the concept of survival signature allows to compute the survival function of a system with multiple component types and attracted increasing attention for its advantageous

features over the last decade. One of its merits is the high efficiency in repeated model evaluations due to the separation of the topological system reliability and the probability structure of system component failures. At the same time, the survival signature radically condenses information on topology. System components are of one type if their failure times are independent and identically distributed (*iid*) or exchangeable. This differentiation is important when it comes to modeling dependent component failure times [153]. A brief recap of the concept is provided in the following subsections. Detailed information about both the derivation of the concept and further applications can be found in [149, 153, 154].

3.3.1 Structure function

Let a system be given consisting of m components of a single type. Further, let $\mathbf{x} = (x_1, x_2, \dots, x_m) \in \{0, 1\}^m$ define the corresponding state vector of the m components, where $x_i = 1$ indicates a functioning state of the i -th component and $x_i = 0$ indicates a non-functioning state. Then, the structure function ϕ is a function of the state vector \mathbf{x} defining the operating status of the considered system: $\phi = \phi(\mathbf{x}) : \{0, 1\}^m \rightarrow \{0, 1\}$. Accordingly, $\phi(\mathbf{x}) = 1$ denotes a functioning system and $\phi(\mathbf{x}) = 0$ specifies a non-functioning system.

Suppose that a system consists of components of more than one type, i.e., $K \geq 2$. Then, the quantity of system components is denoted by $m = \sum_{k=1}^K m_k$, where m_k is the number of components of type $k \in \{1, 2, \dots, K\}$. Correspondingly, the state vector for each type is given by $\mathbf{x}^k = (x_1^k, x_2^k, \dots, x_{m_k}^k)$.

3.3.2 Survival signature

The survival signature summarizes the probability that a system is functioning as a function solely depending on the number of functioning components l_k per component type $k \in \{1, 2, \dots, K\}$. Assuming the failure times within a component type to be *iid* or exchangeable, the survival signature is defined as:

$$\Phi(l_1, l_2, \dots, l_K) = \left[\prod_{k=1}^K \binom{m_k}{l_k}^{-1} \right] \times \sum_{\mathbf{x} \in S_{l_1, l_2, \dots, l_K}} \phi(\mathbf{x}), \quad (3.8)$$

where $\binom{m_k}{l_k}$ corresponds to the total number of state vectors \mathbf{x}^k of type k and S_{l_1, l_2, \dots, l_K} denotes the set of all state vectors of the entire system for which $l_k = \sum_{i=1}^{m_k} x_i^k$. Consequently, the survival signature depends only on the topological reliability of the system, independent of the time-dependent failure behavior of its components that is described in Sec. 3.3.3. For more information on claimed exchangeability in practice, see [152, 153].

3.3.3 Probability structure

The probability structure of system components specifies the probability that a certain number of components of type k is functioning at time t . Accordingly, $C_k(t) \in \{0, 1, \dots, m_k\}$ represents the

number of components of type k in a functioning state at time t . Further, assume the probability distribution for the failure times of type k to be known with $F_k(t)$, denoting the corresponding cumulative distribution function. Then,

$$\begin{aligned} P\left(\bigcap_{k=1}^K \{C_k(t) = l_k\}\right) &= \prod_{k=1}^K P(C_k(t) = l_k) \\ &= \prod_{k=1}^K \binom{m_k}{l_k} [F_k(t)]^{m_k - l_k} [1 - F_k(t)]^{l_k} \end{aligned} \quad (3.9)$$

describes the probability structure of the system, regardless of its topology.

3.3.4 Survival function

The survival function describes the probability of a system being in a functioning state at time t and results from Sec. 3.3.2 and 3.3.3 as:

$$P(T_s > t) = \sum_{l_1=0}^{m_1} \dots \sum_{l_K=0}^{m_K} \Phi(l_1, l_2, \dots, l_K) \times P\left(\bigcap_{k=1}^K \{C_k(t) = l_k\}\right), \quad (3.10)$$

where T_s denotes the random system failure time. Clearly, the concept of survival signature separates the time-independent topological reliability and the time-dependent probability structure. Thus, the survival signature, calculated once in a pre-processing step, can be reused for further evaluations of the survival function, which are necessary, for example, when analyzing a variety of different system configurations that affect the probability structure given a constant system topology. The survival signature can be stored in a matrix, thereby summarizing the topological reliability. The utilization of this matrix circumvents the repeated evaluation of the often computationally expensive structure function. Note that it is precisely these properties of the survival signature concept that provide an important advantage over conventional methods when system simulations need to be performed repeatedly [114]. In terms of computational demand, Monte Carlo simulation may be used to approximate the survival signature of large systems [155].

3.4 Proposed methodology

In this section, the proposed methodology for computationally efficient resilience analysis in the context of complex substructured systems is illustrated. The approach integrates the concept of survival signature described in Sec. 3.3 into the resilience decision-making framework recapped in Sec. 3.2. First, the preparation of the complex system by means of a formalized substructuring approach is presented. Second, the novel methodology is proposed.

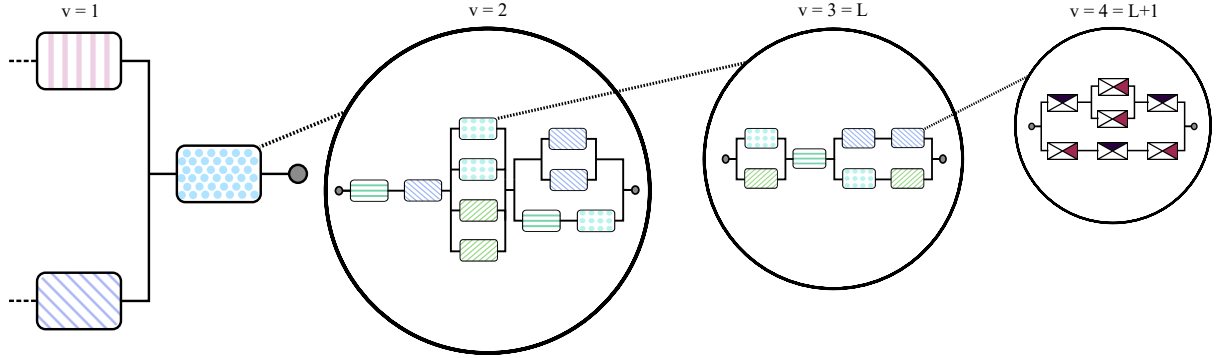


Figure 3.3: Illustration of the proposed substructuring concept.

3.4.1 Definition of substructured systems

Assume a substructured system \mathcal{S} that is composed of a set of subsystems and a set of components. The subsystems can again be comprised of further subsystems and components. This substructuring approach can be conducted for $L \geq 1$ levels of subsystems, where only components exist at level $L + 1$. Components are directly associated with probability distributions describing their time-dependent probabilistic behavior. Note that the level 1 relates to the overall system level. Figure 3.3 illustrates the substructuring concept.

Let there be n^v subsystems $\mathcal{S}_1^v, \mathcal{S}_2^v, \dots, \mathcal{S}_{n^v}^v$ and m^v components $\mathcal{C}_1^v, \mathcal{C}_2^v, \dots, \mathcal{C}_{m^v}^v$ at level $v = 1, 2, \dots, L$. During the analysis, the information on component behavior is propagated from level $L + 1$ to level 1 before determining the state s^0 of the overall system \mathcal{S} in dependence on various topological (sub)system structures. In the context of the resilience framework in Sec. 3.2, the state $s^0 \in S \subseteq \mathbb{R}^+$ with state space S of the overall system \mathcal{S} corresponds to the system performance $Q(t)$ that is basis for the resilience measure Res , see Eq. 3.2. Note that multiple resilience analyses might be conducted for various $Q(t)$. The quantity s^0 indicates system functionality from an ordered perspective and depends on the functionality of its directly subordinate subsystems and components. Given level $v = 1, \dots, L$, the dependency of the (sub)system state s_j^v on the state vector \mathbf{x}_j^v is modeled via the mapping $s_j^v = \phi_j^v(\mathbf{x}_j^v) \in \{0, 1\}$, where ϕ_j^v is a structure function, i.e., a topological rule for system functioning as presented in Sec. 3.3.1. The state vector is introduced as $\mathbf{x}_j^v = (s_1^w, s_2^w, \dots, s_{n_j^w}^w, c_1^w, c_2^w, \dots, c_{m_j^w}^w)$ for the j -th subsystem at level v with $j = 1, 2, \dots, n^v$ and $w = v + 1$. Thereby, $s_p^w, c_q^w \in \{0, 1\}$ denote the functionality of the p -th subsystem and q -th component, respectively. Further, n_j^w is the number of subsystems at level w contained in subsystem j at level v and $\sum_j^{n^v} n_j^w = n^w$. Analogously, m_j^w has the equivalent interpretation for components. At level $v = 1$, the notation reduces to $s^0 = \phi^0(\mathbf{x}^0)$. The state vectors at level L comprises only component states as $\mathbf{x}_j^L = (c_1^w, c_2^w, \dots, c_{m_j^w}^w)$ with $j = 1, 2, \dots, n^L$, $c_i^w \in \{0, 1\}$ and $w = L + 1$.

The probability distributions governing the component states c_i^v are assumed to be known as CDF $F_k(t)$ for given component type k according to Sec. 3.3.3. Note that different subsystems might rely on the same component types. The assumption $s_j^v, c_i^v \in \{0, 1\}$ is due to the fact that

the concept of survival signature is based on a binary-state consideration. However, multiple researchers work on extensions of the concept to a discrete or continuous multi-state consideration, see e.g. [165, 216, 280, 281].

3.4.2 Extension of the adapted systemic risk measure

In the resilience analysis of complex, substructured systems, it may be important that endowments can be formally assigned not only to system components but to other system structures, such as subsystems. To enable the incorporation of such endowment assignments in the novel methodology, the adapted systemic risk measure, cf. Sec. 3.2.2, is extended as follows.

Let a system, in addition to its m components, be given with a total of n subsystems $j \in \{1, \dots, n\}$ of $b_j \in \{1, 2, \dots, B\} \subseteq \mathbb{N}$ types over all system levels L with d endowment properties that influence the system performance $Q(t)$. Then, the subsystem j is characterized by

$$(\mathcal{S}_j; b_j) = (\xi_{j1}, \xi_{j2}, \dots, \xi_{jd}; b_j) \in \mathbb{R}^{(1 \times d)} \times \mathbb{N}, \quad (3.11)$$

where $(\xi_{j1}, \xi_{j2}, \dots, \xi_{jd}; b_j)$ are the numerical values of the d relevant endowment properties. The entire system is then, in addition to the description by the tuple consisting of the matrix $\mathbf{A} \in \mathbb{R}^{(m \times e)}$ and the column vector $\mathbf{z} \in \mathbb{N}^m$, capturing the components, described by the tuple composed of the matrix $\mathbf{D} \in \mathbb{R}^{(n \times d)}$ and the column vector $\mathbf{h} \in \mathbb{N}^n$, capturing the subsystems:

$$(\mathbf{D}; \mathbf{h}) = \begin{pmatrix} \xi_{11} & \xi_{12} & \cdots & \xi_{1d}; & h_1 \\ \xi_{21} & \xi_{22} & \cdots & \xi_{2d}; & h_2 \\ \vdots & \vdots & & \vdots & \vdots \\ \xi_{n1} & \xi_{n2} & \cdots & \xi_{nd}; & h_n \end{pmatrix}. \quad (3.12)$$

The system under consideration is defined via the descriptive, non-decreasing input-output model $Y = Y_{(\mathbf{A}; \mathbf{z}), (\mathbf{D}; \mathbf{h})}$ that is specified by both tuples and relates endowment properties to system performance. Again, with respect to Eq. 3.2, the model output is specified as $Y = Y_{(\mathbf{A}; \mathbf{z}), (\mathbf{D}; \mathbf{h})}$ dependent on the current endowment allocation for components $(\mathbf{A}; \mathbf{z})$ and subsystems $(\mathbf{D}; \mathbf{h})$. Then, with the specific acceptance set \mathcal{A} from Eq. 3.6, the extended adapted systemic risk measure is defined as

$$R(Y) = \left\{ \mathbf{A} \in \mathbb{R}^{m \times e}, \mathbf{D} \in \mathbb{R}^{(n \times d)} \mid Y_{(\mathbf{A}; \mathbf{z}), (\mathbf{D}; \mathbf{h})} \in \mathcal{A} \right\}, \quad (3.13)$$

that is the set of all endowment property allocations \mathbf{A} and \mathbf{D} such that the system reaches a resilience value greater or equal to α . Note that in this manner, equivalently, any performance-influencing endowments, of any system structures, or even endowments independent of system structures, can be incorporated into the resilience decision-making analysis.

3.4.3 Augmentation of the resilience analysis

The system resilience Res is governed by the reliability, robustness and recoverability of a system as illustrated in Fig. 3.1. The magnitude of these quantities is influenced by the endowment allocations that are captured in the tuples $(A; z)$ and $(D; h)$. The assigned resilience-enhancing endowment properties $(\eta_{i1}, \eta_{i2}, \dots, \eta_{im})$ and $(\xi_{j1}, \xi_{j2}, \dots, \xi_{jd})$ can either relate to a specific quantity or a subset of the three quantities and correspond to different implementations in the overall system performance model, i.e., input-output model $Y_{(A;z),(D;h)}$.

The reliability is typically the most computationally challenging quantity when evaluating system resilience Res . Thus, this part of the computation is augmented by the concept of survival signature with its advantageous separation and compact storage properties as well as the fundamental substructuring approach proposed in the previous Sec. 3.4.1 in order to enable efficient resilience analyses of large and highly complex systems.

In a pre-processing step, the survival signatures $\Phi_j^v(l_1, l_2, \dots, l_K)$ of the $n = \sum_v^L n^v$ subsystems \mathcal{S}_j^v are computed based on the corresponding structure functions ϕ_j^v as described in Sec. 3.3.2. Subsequently, the survival signatures are utilized to efficiently retrieve the topological subsystem reliability (online) for varying endowment configurations.

In order to identify the set of all acceptable endowments $R(Y)$, repeated evaluations of $Y_{(A;z),(D;h)}$ are required according to the grid search algorithm – various endowment allocations in the search space spanned over discretized numerical values of $A \in \mathbb{R}^{m \times e}$ with $m = \sum_v^{L+1} m^v$ and $D \in \mathbb{R}^{(n \times d)}$ with $n = \sum_v^{L+1} n^v$ need to be evaluated analogous to Sec. 3.2.3. In each evaluation N stochastic simulations of $Y_{(A;z),(D;h)}$ have to be performed to obtain $E[Y]$, see Eq. 3.2, and corresponding status assignments according to the acceptance set \mathcal{A} in Eq. 3.6. Given the number of dimensions that need to be evaluated according to the grid search algorithm as M , the number of evaluations for $Q(t)$ is $M \cdot N \cdot u$ with u being the total number of time steps per simulation. Consequently, simulating system resilience is a complex, demanding and repeating challenge.

Computing the resilience directly relates to the computation of at least one structure function that can be any function that expresses the relation of interacting elements. The structure function can correspond to simple logical expressions, such as Reliability Block Diagrams (RBD) or fault trees, up to sophisticated simulation models, e.g., when assessing the network efficiency of a graph. In fact, such models often become extremely challenging in the context of real world systems. The evaluation of a global structure function including the entirety of all components at once might even be computationally unfeasible. In contrast, given a system in a substructured form \mathcal{S} as proposed in Sec. 3.4.1, the computation of the system functionality splits into the evaluation of multiple hierarchically ordered structure functions. Such a consideration enables a wider range of application in terms of system size and complexity, especially when the computational capacity is limited.

The computational efficiency is further enhanced by application of the survival signature. Given a system, substructured according to Sec. 3.4.1 with $L \geq 2$, the computation of subsystem reliabilities can be propagated from level L to level 1 by evaluating the survival functions of

subsystems \mathcal{S}_j^v based on the survival functions of \mathcal{S}_p^w instead of computing $s_j^v = \phi_j^v(\mathbf{x}_j^v)$ for each level. Coolen et al. proposed a methodology to merge survival signatures of specifically arranged subsystems in the context of substructured systems [157]. However, note that this approach differs from the one developed in the current paper. The survival function $P(T_{s_j^v} > t)$ of the j -th subsystem at level v is then computed according to Eq. 3.10 w.r.t. the survival signature $\Phi_j^v(l_1, l_2, \dots, l_K)$. At top-level 1, the failure rates of the subsystems \mathcal{S}_j^1 with $j = 1, 2, \dots, n^1$, utilized to sample subsystem functionality, can then be obtained via the cumulative hazard function and its derivative:

$$\lambda^{s_j^1}(t) = -\frac{d \ln P(T_{s_j^1} > t)}{dt}. \quad (3.14)$$

This enables to sample the subsystem state s_j^1 for time step (t_h, t_{h+1}) online with significantly reduced computational effort when evaluating the system resilience Res . The computation of Res then only involves $n^1 + m^1$ instead of $\sum_v^{L+1} m^v$ elements. In addition, significantly increased computational efficiency is achieved due to the separation of system topology and probability structure, the latter determined by the current endowment allocation. While the component probability structure varies, the topological reliability, independent of the endowment allocation, is captured in the survival signature in a compact manner and can be retrieved repeatedly with close to no costs. Note that subsystems of the same type share the same survival signature. This can be exploited for increased efficiency as well. In fact, the computational advantage of the proposed approach scales with size and complexity of the considered system \mathcal{S} . The developed and employed algorithm is outlined in Alg. 3.4.3 for illustrative purposes.

In order to prove efficiency and general applicability, the novel approach is applied to an arbitrary complex system in Sec. 3.6 and to the *U-Bahn* and *S-Bahn* system of Berlin in Sec. 3.7.

Algorithm 3.4.3

Step A Computation of the survival signatures for all subsystem \mathcal{S}_j^v with $v = 1, 2, \dots, L$ and $j = 1, 2, \dots, n^v$.

Step B Identification of the Pareto front by executing the grid search algorithm; each endowment allocation is evaluated by performing the following steps:

Step B1. Generation of the failure rate matrix with dimensions $n^1 \times T$ based on Eq. 3.14 for each subsystem and each timestep t_h with $h = 1, 2, \dots, u$ and generation of the failure rate matrix with dimensions $m^1 \times T$ for each component and each timestep; if $L \geq 2$, the failure rate matrix for $v = 1$ for each subsystem is generated recursively from bottom to top by computing the survival functions.

Step B2. Perform N samples with time $t_h = 0$:

- a) Evaluate the system performance $Q(t_h)$.
- b) Sample possible failures of subsystems \mathcal{S}_j^1 for $j = 1, 2, \dots, n^1$ and components \mathcal{C}_i^1 for $i = 1, 2, \dots, m^1$ based on the failure rate matrices computed in

Step B1.

- c) Check if any failed subsystem/component has recovered;
if a subsystem/component recovers, set the time counter of its specific failure rate to 0.
- d) Set $t_h = t_{h+1} = t_h + \Delta t$ and repeat Steps a) – d) until $t_h = T$, i.e., the maximum time is reached.

Step B3. Obtain Res for the current endowment configuration via Eq. 3.2 and Eq. 3.3 over all time steps u and all samples N .

The complete algorithm has been implemented in the Julia package *ResilienceDecisionMaking.jl* and made publicly available on Github [282].

3.5 Multistage high-speed axial compressor

Axial compressors are complex, multi-component key elements of gas turbines. Therefore, it is critical in both design and maintenance to consider as many factors affecting system performance as possible to efficiently maximize compressor resilience. To address this challenge, the decision-making analysis proposed in [268] regarding system resilience is extended in order to deal with components, respectively factors, of different types.

3.5.1 Model

In [251], the authors present a functional model of a four-stage high-speed axial compressor from the Institute of Turbomachinery and Fluid Dynamics at Leibniz Universität Hannover, Germany, depicting its functionality as well as reliability characteristics. For detailed information about this particular axial compressor see [252–254].

The model captures the dependence of the overall performance of the compressor, i.e., the total-to-total pressure ratio and the total-to-total isentropic efficiency, on the surface roughness of the individual blades. These are arranged in rotor and stator rows. The model is based on the results of a sensitivity analysis of an aerodynamic model of the compressor and the so-called Relative Important Indices, cf. [154]. A network representation of the functional model is shown in Fig. 3.4. Each component represents either a stator (S1 - S4) or rotor (R1 - R4) row.

The rows are classified into $K = 4$ component types $k_i \in \{1, 2, 3, 4\} \forall i \in \{1, \dots, 8\}$. This classification, as well as the arrangement of the components, is based on the resulting effect of their blade roughness on the two performance parameters of the compressor. More precisely, an interruption between start and end implies that a roughness-induced performance variation of at least 25% is exceeded, corresponding to a non-functional compressor. This defines the system performance $Q(t)$ of the functional model for subsequent application of the resilience decision-making method. The system performance is determined at each time point t_h and is

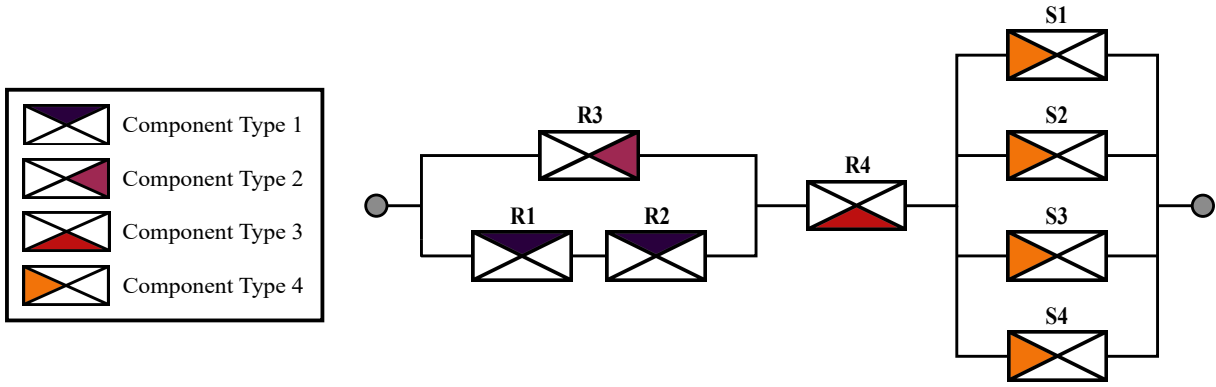


Figure 3.4: Functional model of the multistage high-speed axial compressor.

1 if there is a path from start to end and 0 if this connection is interrupted. More detailed information about the functional model and its derivation can be obtained from [251].

For the resilience analysis, it is assumed that each row, i.e., each component of the functional model, is characterized by two endowment properties, a roughness resistance re and a recovery improvement rec , such that a component is fully described by $(a_i; k_i) = (re_i, rec_i; k_i)$. In this context, the roughness resistance can be interpreted as a qualitative coating that counteracts the roughening of the blade surfaces. Both the roughness resistance re_i and the recovery improvement rec_i of each row i are assumed to be functions of the component type k_i , i.e., $re_i = re_{i'}$, $rec_i = rec_{i'}$ if $k_i = k_{i'}$.

Each component of the functional model can fail randomly after system performance is calculated at time t_h . A failed component is considered as no longer being part of the model and does not contribute to the overall system performance at time t_{h+1} and at all subsequent times until it is completely recovered. The failure probability of a component i in the time interval (t_h, t_{h+1}) is assumed to be constant in time, cf. [251], and is specified by

$$P\{(a_i; k_i) \text{ fails during } (t_h, t_{h+1})\} = \Delta t \cdot \lambda_i \quad (3.15)$$

with

$$\lambda_i = 0.8 - 0.03 \cdot re_i, \quad (3.16)$$

where λ_i is the time-independent failure rate. Increasing the roughness resistance of a blade row reduces the degradation of the surface and consequently the corresponding failure rate λ_i .

When a component i fails, its functionality is assumed to be immediately and completely recovered after a certain number of time steps, according to

$$r = r_{max} - rec_i \quad \text{with} \quad rec_i < r_{max} \quad (3.17)$$

where r_{max} is an upper bound on the number of time steps for recovery and rec_i is the recovery improvement that reduces the recovery duration. Note, that this recovery model corresponds to

a one-step recovery profile and various alternative characteristic profiles of recovery are possible as well, cf., [6] and [10].

3.5.2 Costs of endowment properties

Optimal endowment properties are related to the quality of the components, and an increase in their production quality is associated with increasing costs. This should be taken into account in resilience decision-making. As discussed in [256], increasing the reliability of components in complex networks can be associated with an exponential increase in cost.

Increasing the endowment property of roughness resistance reduces the failure rate of blades in a row and thus improves reliability, see Eq. 3.15 and Eq. 3.16. Thus, its total cost is assumed to be

$$cost^{re} = \sum_{i=1}^8 price_{(re_i; k_i)}^{re} \cdot 1.2^{(re_i-1)}, \quad (3.18)$$

where re_i is the roughness resistance value of component i , k_i its type and $price_{(re_i; k_i)}^{re}$ an arbitrary common basic price. Accordingly an exponential relationship is assumed for the cost associated with recovery improvement:

$$cost^{rec} = \sum_{i=1}^8 price_{(rec; k_i)}^{rec} \cdot 1.2^{(rec_i-1)}. \quad (3.19)$$

The total cost $cost_{(A; z)}$ of an endowment is the sum of these costs:

$$cost_{(A; z)} = cost^{re} + cost^{rec}. \quad (3.20)$$

3.5.3 Scenario

In order to apply the decision-making method for resilience-enhancing endowments to the multistage high-speed axial compressor, the model parameter values and simulation parameter values shown in Tab. 3.1 are considered.

In a first step, the set of all acceptable endowments corresponding to a resilience value of at least $Res = 0.85$ over the considered time period is determined. Since any axial compressor blade improvement involves costs, the second step is to identify the most cost-efficient acceptable endowment, denoted as \hat{A} . The recovery improvement rec is assumed to be fixed for all components, regardless of the type, $rec_i = 11 \forall i \in \{1, \dots, m\}$ and the roughness resistance re is examined over $re_i \in \{1, \dots, 20\} \forall i \in \{1, \dots, m\}$. The roughness resistance values may be interpreted in ascending order as increasing quality levels of coatings.

Figure 3.5 illustrates the results of the grid search algorithm. It shows the roughness resistance combinations contained in $R(Y)$, i.e., all combinations that lead to a satisfying system resilience of at least $Res = 0.85$. It can be clearly seen that the roughness resistance of the blades of the fourth stage (component type 3) has the greatest influence on the system resilience. Combinations

Table 3.1: Parameter values for the resilience decision-making method for the functional model of the multistage high-speed axial compressor.

Parameter	Scenario
Acceptance threshold α	0.85
Number of time steps u	200
Length of a time step Δt	0.05
Maximum time T	10
Base failure rate λ	0.8
Roughness resistance re	$re_i \in \{1, \dots, 20\}$
Roughness resistance price $price_{(re_i; k_i)}^{re}$:	$800\text{€} \forall k_i \in \{1, 2, 3\}$ $500\text{€} \forall k_i = 4$
Maximum recovery time r_{max}	21
Recovery improvement rec	11
Recovery improvement price $price_{(rec; k_i)}^{rec}$:	600€
Sample size N	500

with coating qualities of $re_i \leq 15$ at the fourth stage are generally not sufficient to achieve an acceptable level of resilience, regardless of the endowment property values of the other component types. In addition, the roughness resistance of the four stators (component type 4) has the least influence on system resilience of all types. Here, a minimum coating quality of $re_i = 1$ as endowment is in various combinations already sufficient to achieve acceptable resilience values. The same applies to the rotors of component type 1 and type 2. However, the components of the other types require significantly higher coating qualities compared to the stators in order to compensate for the small roughness resistance values in these both types.

The design, maintenance and optimization of complex systems, such as an axial compressor, are invariably subject to monetary limitations. It is crucial for decision-making to be able to take these financial constraints into account. Therefore, Fig. 3.6 shows only those roughness resistance combinations included in $R(Y)$ that result in an acceptable system resilience of at least $Res = 0.85$ and are less expensive than a predefined cost limit for the total roughness resistance, that is arbitrarily assumed to be $cost^{re} = 40\,000\text{€}$ in this case study.

The results reveal that only configurations with low coating qualities for stators (component type 4) are below the cost limit. On the one hand, this is due to their aforementioned low influence on system resilience, and on the other hand to the high cost of the quality levels for the stators. Although the base price of 500€ is rather low, it is significantly higher in terms of cost for the entire component type than for the other types due to the higher total number of components of this type. In addition, only configurations that provide the highest quality levels of $re_i \geq 18$ for the type 3 rotor are acceptable and below the price limit. The roughness resistance of this rotor has such a large impact on system resilience that at lower quality levels, compensation by higher quality levels of the remaining stages would exceed the given budget. Although the roughness resistance of the rotor of component type 2 has a lower influence on the system resilience than

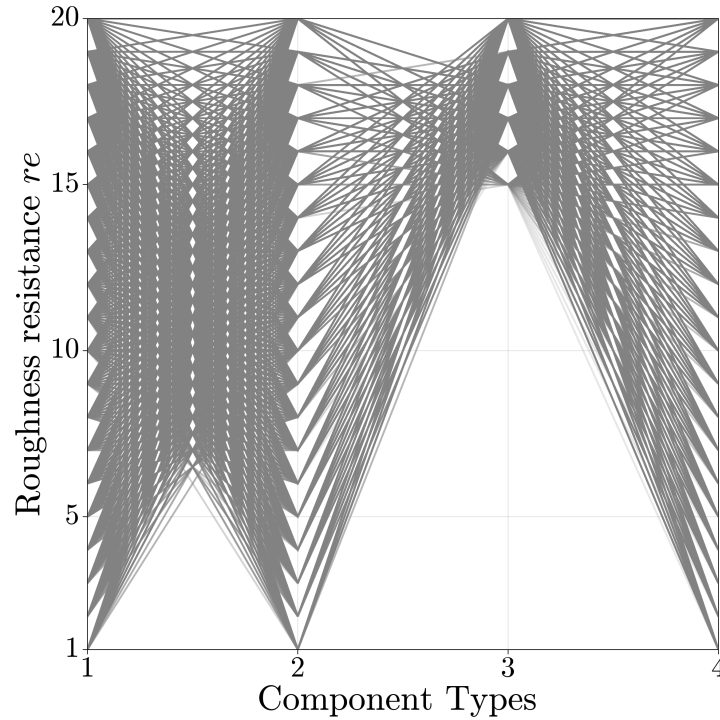


Figure 3.5: Numerical results of the 4D grid search algorithm for the functional model of the axial compressor with explored roughness resistance values.

that of component type 3, minimal quality levels of the coating can not be compensated by high qualities of the other components. Therefore, at least $re_i = 5$ for $k_i = 2$ is required to fulfill the acceptance criterion.

The grid search algorithm is able to reduce the numerical effort for the calculation of $R(Y)$ by about 98%. As a result, only 2% of the potential combinations of roughness resistance values need to be evaluated.

Taking into account the base prices in Tab. 3.1, the most cost-efficient endowment is characterized by roughness resistances of $re_i = 7$ for $k_i = 1$, $re_i = 13$ for $k_i = 2$, $re_i = 19$ for $k_i = 3$ and $re_i = 1$ for $k_i = 4$ for the respective components. In Fig. 3.6 the corresponding configuration is highlighted in blue. The final cost results from Eq. 3.20 as $cost_{(\hat{A};z)} = cost^{re} + cost^{rec} = 35\,209\text{€} + 29\,720\text{€} = 64\,929\text{€}$.

3.6 Complex system

In [114] and [152] the authors apply their introduced simulation approaches for reliability analysis on an arbitrary complex system. In order to demonstrate the wide applicability and efficiency of the proposed methodology developed in this paper, this complex system is considered, adapted by means of substructuring, and an efficient resilience decision-making analysis is conducted.

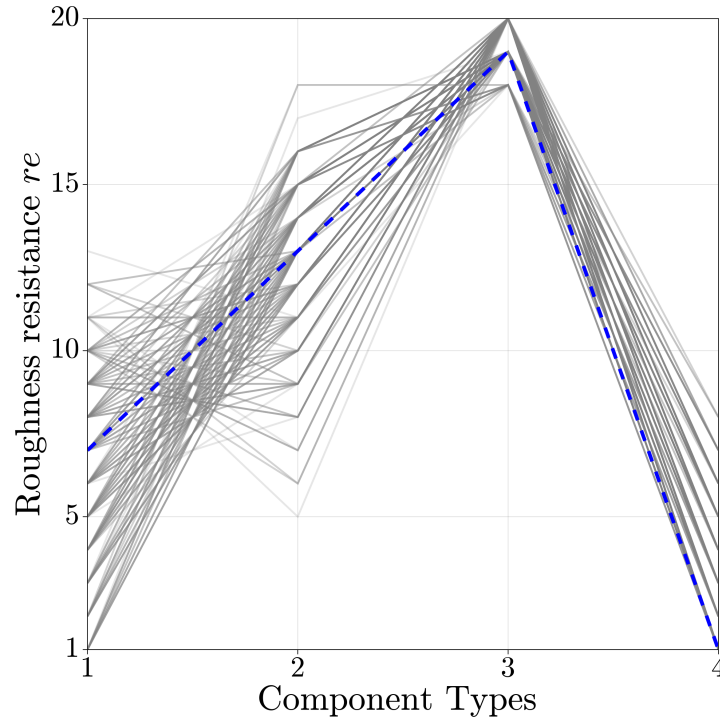


Figure 3.6: Numerical results of the 4D grid search algorithm for the functional model of the axial compressor with explored roughness resistance values and a cost threshold for roughness resistance of 40 000€.

3.6.1 Model

The arbitrary complex system consists of $n = 14$ subsystems, each assigned to one of $B = 6$ subsystem types. Figure 3.7 illustrates the complex system and the assignment of subsystems to their types. A connection between start node and target node indicates a functioning state and an interruption of this connection indicates a non-functioning state of the overall system. This defines the system performance $Q(t)$ of the functional model for subsequent application of the resilience decision-making method. The system performance is determined at each time point t_h and is 1 if there is a path from start to end and 0 if this connection is interrupted. Note that the complex system is thus formally an RBD. For illustration and simplicity, it is assumed that there is only one level of subsystems, i.e., $l = L = 1$, and thus $\mathbf{x}^s = (s_1, s_2, \dots, s_{14})$, $\mathcal{S}_j^1 = \mathcal{S}_j$, and $\lambda^{s_j^1}(t) = \lambda^{s_j}(t)$. Figure 3.8 illustrates the structure of the six subsystem types. These are formally RBDs as well. It is assumed that each subsystem of the same type is represented by the same RBD. A subsystem \mathcal{S}_j is considered to be functional if a connection exists from start to end and non-functional if this connection is interrupted, i.e., $s_j \in \{0, 1\} \forall j \in \{1, \dots, 14\}$. Depending on the type, the subsystems consist of seven to ten components. Thus, the overall system is composed of $m = 106$ individual components.

The components are classified into $K = 2$ types $k_i \in \{1, 2\} \forall i \in \{1, \dots, 106\}$, i.e., 50 components of type 1 and 56 components of type 2. For the resilience analysis, each component of the model, is assumed to be characterized by an endowment property, that is the reliability improvement

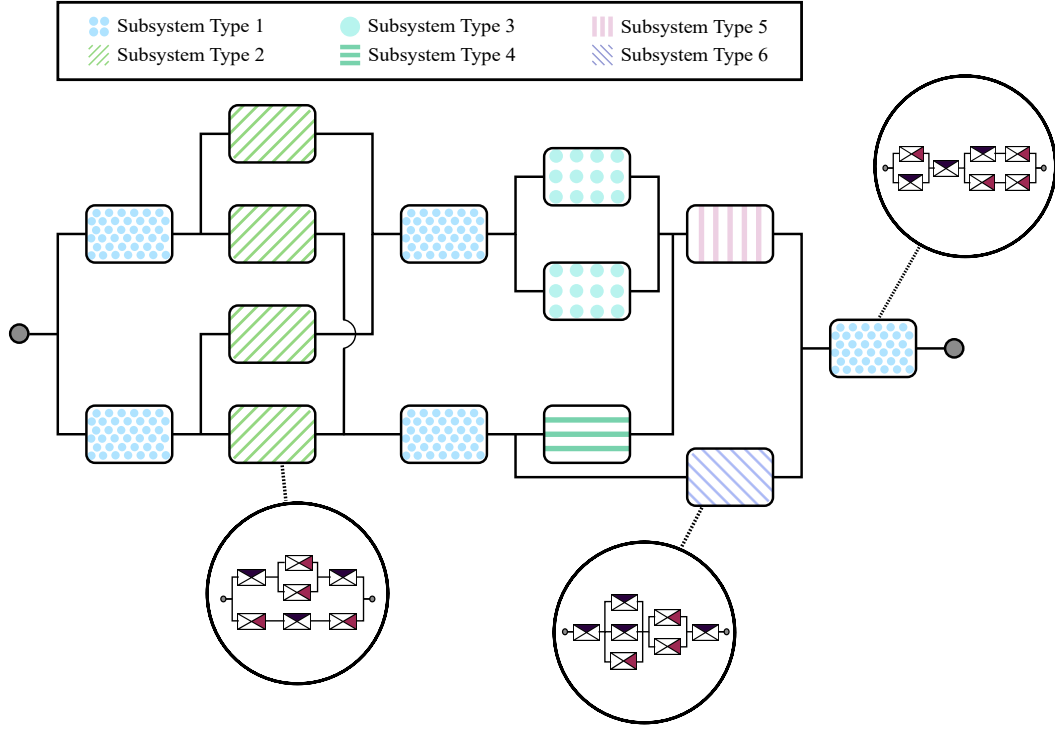


Figure 3.7: Representation of the arbitrary complex system with 14 components, adapted from [114].

rel_i , such that a component is fully described by $(a_i; k_i) = (rel_i; k_i)$. Note that the reliability improvement rel_i of each component i is assumed to be function of the component type k_i , i.e., $rel_i = rel_{i'}$ if $k_i = k_{i'}$. Further, each component type, and thus each component, is characterized by a specific time-dependent failure behavior. In practice, the underlying distribution functions, describing this behavior, need to be derived from existing operational data. However, the consideration of real data is often highly challenging due to the inherent uncertainty caused by, e.g., lack of data, measurement inaccuracies, subjective expert knowledge, small sample sizes, etc. New developments in the context of the survival signature as introduced, e.g., in [152], allow for the efficient consideration and propagation of uncertainties through the entire model. They will be incorporated into the proposed methodology towards an imprecise resilience approach in future work of the authors. However, for the purpose of proof of concept and applicability, exponential distributions are considered for both component types in this case study as

$$F_i(t; \lambda_i(rel_i)) = 1 - e^{-\lambda_i(rel_i)t} \text{ for } t \geq 0, \quad (3.21)$$

with

$$\lambda_i(rel_i) = \lambda_{i,\max} - \Delta\lambda_i \cdot rel_i, \quad (3.22)$$

being the failure rate of component i of type k depending on the corresponding reliability improvement rel_i . $\lambda_{i,\max}$ is the maximum failure rate and $\Delta\lambda_i$ denotes the failure rate reduction

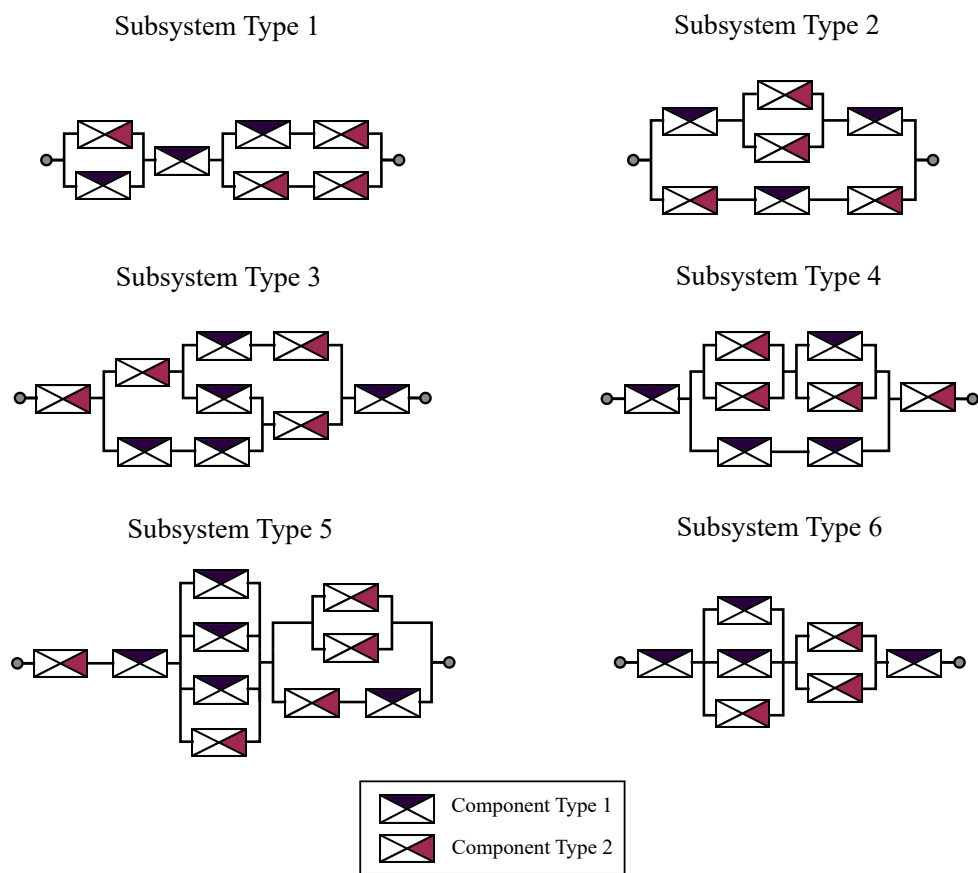


Figure 3.8: Representation of the $B = 6$ subsystem types of the complex system.

per reliability improvement rel_i that is assumed to be constant for each component type, leading to equidistant failure rate variations.

The simulation can be summarized as follows: after the system performance has been computed at time t_h , each subsystem \mathcal{S}_j of the complex system can fail at random based on the extracted and time-dependent failure rate $\lambda^{s_j}(t_h)$ from corresponding survival function, cf. Eq. 3.14. A failed subsystem is treated as no longer present in the model and does not contribute to the overall system performance $Q(t)$ at time t_{h+1} and all subsequent time points until it is fully recovered. The failure probability of a subsystem \mathcal{S}_j in the time interval (t_h, t_{h+1}) is

$$P\{\mathcal{S}_j \text{ fails during } (t_h, t_{h+1})\} = \Delta t \cdot \lambda^{s_j}(t_h). \quad (3.23)$$

If a subsystem \mathcal{S}_j failed, its functionality is assumed to be immediately and fully recovered after r time steps, again corresponding to a one-step recovery profile. It is assumed that a repaired subsystem and thus all components of the subsystem are in as-new original condition after repair. Note that this is an assumption for the sake of demonstration, and in reality deviating states might be obtained after repair, possibly depending on further endowment properties that affect the duration and quality of recovery. After recovery, the survival function of a subsystem is time-zeroed, such that the resulting failure rate per simulation step $\lambda^{s_j}(t_h)$ evolves over time equivalent to that of a subsystem in new condition.

3.6.2 Costs of endowment properties

The improvement of endowment properties is inevitably associated with costs. Increasing the endowment property “reliability improvement” reduces the failure rate of components and consequently of corresponding subsystems. Again, an exponential relationship between costs and improvements is assumed. Then the total costs can be defined as

$$cost_{(A;z)} = cost^{rel} = \sum_{i=1}^{106} price_{(rel_i;k_i)}^{rel} \cdot 1.2^{(rel_i-1)}, \quad (3.24)$$

where $(rel_i; k_i)$ is the reliability improvement value of component i , k_i its type and $price_{(rel_i;k_i)}^{rel}$ is an arbitrary common basic price.

3.6.3 Scenario

The considered model parameters and simulation parameters values for the application of the resilience decision-making method for complex and substructured systems to the arbitrary complex system illustrated in Fig. 3.7, are shown in Tab. 3.2. The recovery is assumed to be fixed with $r = 20$ time steps for all subsystems, regardless of the type. The reliability improvement rel_i is explored over $rel_i \in \{1, \dots, 10\} \forall i \in \{1, \dots, m\}$.

In a pre-processing step, the survival signatures of all 14 subsystems are determined. As an example, Tab. 3.3 depicts the survival signature values of subsystem type 5 of the complex

Table 3.2: Parameter values for the resilience decision-making method on the arbitrary complex system.

Parameter	Scenario
Acceptance threshold α	0.90
Number of time steps u	200
Length of time step Δt	0.05
Maximum time T	10
Maximum failure rate $\lambda_{i,\max}$	$\lambda_{i,\max} = 0.15$ for $k_i = 1$ $\lambda_{i,\max} = 0.20$ for $k_i = 2$
Failure rate reduction $\Delta\lambda_i$	$\Delta\lambda_i = 0.014$ for $k_i = 1$ $\Delta\lambda_i = 0.019$ for $k_i = 2$
Reliability improvement rel_i	$rel_i \in \{1, \dots, 10\}$ for $k_i \in \{1, 2\}$
Reliability improvement price $price_{(rel_i;k_i)}^{rel}$	$price_{(rel_i;1)}^{rel} = 1\,000\text{€}$ $price_{(rel_i;2)}^{rel} = 2\,000\text{€}$
Recovery time steps r	20
Sample size N	500

system. For clarity, only the non-trivial survival signature values are shown, i.e., all values that are neither zero or one. Then the analysis starts as follows: In a first step, the set of all acceptable endowment configurations $R(Y)$, corresponding to a resilience value of at least $Res = 0.9$ over the considered time period, is determined according to Algorithm 3.4.3. Since any improvement of the system components is associated with costs, the second step is to identify the most cost-efficient acceptable endowment \hat{A} .

Figure 3.9 illustrates the results of the grid search algorithm. It shows the reliability improvement combinations contained in $R(Y)$, i.e. all combinations that lead to a satisfying system resilience. It can be seen, that the reliability improvement of components of type 1 is more important, i.e., has a higher impact on the overall system resilience than the reliability improvement of components of type 2. For maximum reliability improvement values for type 1, i.e., $rel_i = 10$ for $k_i = 1$, even low reliability improvement values for type 2, i.e., $rel_i = 2$ for $k_i = 2$, are sufficient in order to fulfill the acceptance criterion and reach system resilience values of at least $Res = 0.90$. On the other hand, with maximum reliability improvement for components of type 2, i.e., $rel_i = 10$ for $k_i = 2$, a moderate reliability improvement for type 1 of at least $rel_i = 4$ for $k_i = 1$ is required to meet the acceptance criterion.

These results are plausible, since a detailed examination of the subsystem types and their topology, cf. Fig. 3.8, reveals that components of type 1 hold a total of six so-called bottleneck positions within the subsystems, i.e., positions where the failure of a single component interrupts the functioning of the entire subsystem, while components of type 2 occupy only three of these positions. This results in a higher influence of component type 1 on the functionality of the subsystems and thus ultimately in a higher influence on overall system resilience. Accordingly, the quality of reliability improvement of component type 1 is more relevant than that of component type 2. Looking at the probabilistic structure of the components, it is noticeable that the failure

Table 3.3: Non-trivial survival signature values of subsystems with $b_j = 5$ of the complex system, shown in Fig. 3.7 and Fig. 3.8.

l_1	l_2	$\Phi(l_1, l_2)$
2	4	1/25
3	3	3/50
2	5	3/25
4	3	3/20
3	4	9/50
2	6	1/5
5	3	11/50
6	3	3/10
3	5	3/10
4	4	33/100
3	6	2/5
5	4	23/50
4	5	12/25
6	4	3/5
4	6	3/5
5	5	16/25
6	5	4/5
5	6	4/5

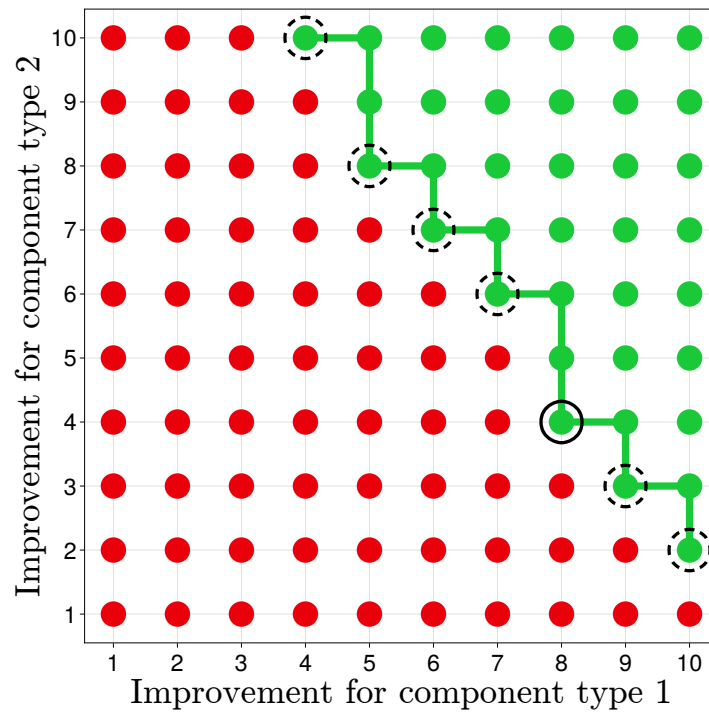


Figure 3.9: Numerical results of the 2D grid search algorithm for the complex system with explored reliability improvement values.

rate reduction for components of type 2 is greater than for components of type 1, i.e., the increase in reliability improvement for type 2 probabilistically generates a higher surplus value compared to improvements of type 1. However, this obviously cannot balance the influence gradient between both types and thus underlines the critical topological importance of type 1 components.

The design, maintenance and optimization of complex systems is typically restricted by economic limitations. It is crucial for decision-making to be able to take these monetary constraints into account. Assuming the arbitrary base prices in Tab. 3.2, the most cost-effective acceptable endowment \hat{A} is specified by a reliability improvement configuration of $rel_i = 8$ for $k_i = 1$ and $rel_i = 4$ for $k_i = 2$ for the respective components. In Fig. 3.9, the corresponding configuration is highlighted. Note that due to the monotonicity of the input-output model and the monotonically increasing endowment costs, the most cost-efficient endowment can only be located on the dominant vertices of the Pareto front. Therefore, only these configurations need to be examined in terms of cost. The final cost results from Eq. 3.24 as $cost_{(\hat{A};z)} = 372\,695\text{€}$.

Due to the utilization of the grid search algorithm, the numerical effort required to compute $R(Y)$ is reduced. Only 23% of all possible configurations of reliability improvement values need to be evaluated. This reduction effect scales with the size and dimensionality of the endowment search space. By means of the novel resilience decision-making method, the considered complex system could be reduced from its entirety of 106 individual components to 14 components on the top-level with respect to the resilience analysis and the associated identification of all acceptable endowment configurations, which drastically reduces the computational effort. Nevertheless, all 106 components and their influence were considered by incorporating and propagating the subsystems' survival functions. Again, this effect scales with increasing complexity and size of the investigated systems.

3.7 U-Bahn and S-Bahn system of Berlin

About two thirds of the total of 1.5 billion passengers per year are transported by Berlin's subway U-Bahn and suburban trains S-Bahn [257, 258], making these two transport services the most used means of public transport in Berlin and thus of utmost importance for the German capital. Key infrastructures that are of such significant social and economic relevance to modern societies obviously and inevitably need to be as resilient as humanly possible. The applicability of the methodology developed in this work to large complex systems is demonstrated on a comprehensive model of the Berlin U-Bahn and S-Bahn system. The objective is to identify suitable resilience-enhancing properties for all stations in the system, taking into account monetary constraints. This allows the characterization of acceptable endowments for the system in terms of reliability, robustness, and recoverability. This approach can be applied not only to any phase during the life cycle of existing systems, but also to systems in the design phase, in order to optimize their resilience.

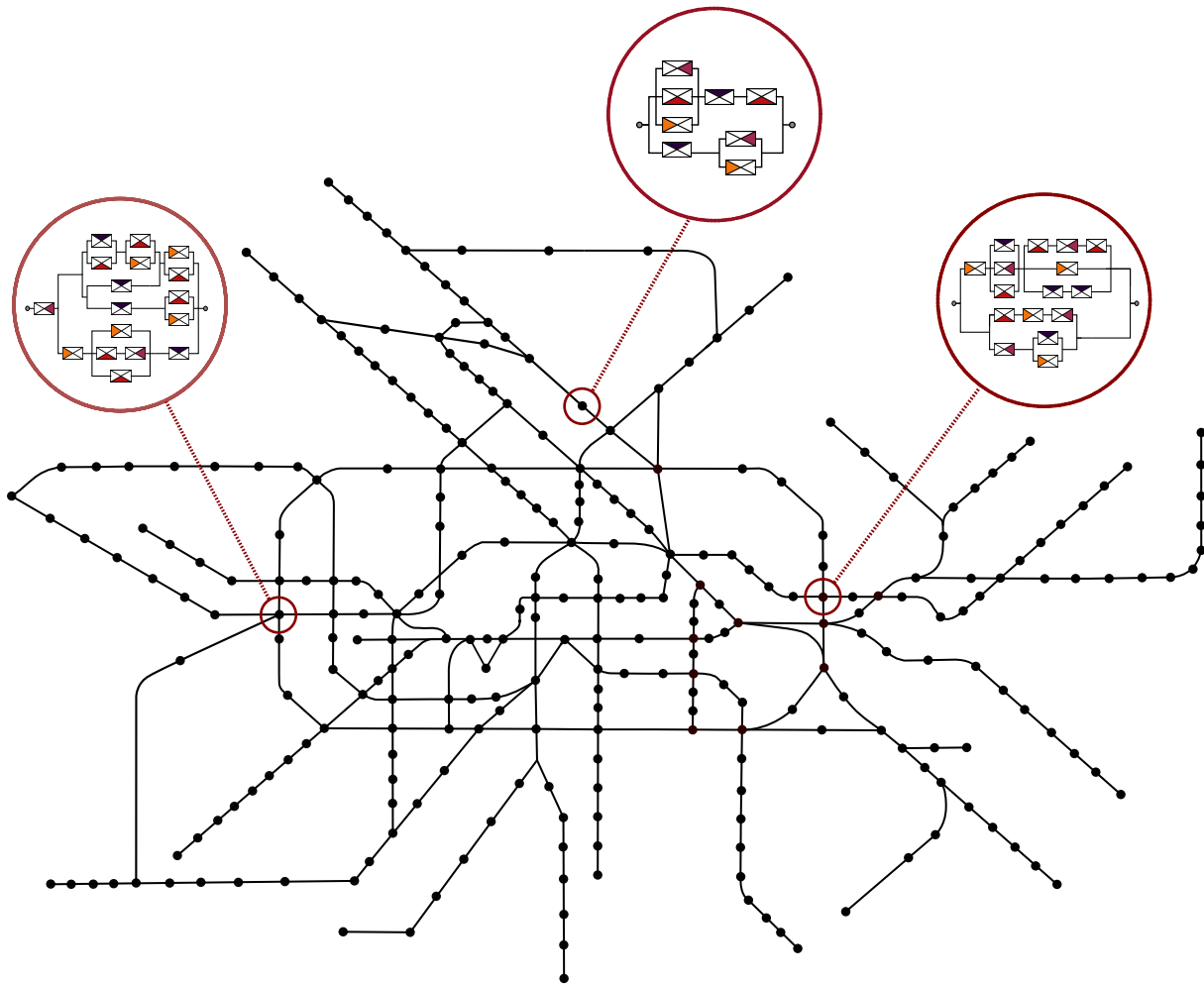


Figure 3.10: Topological network for the Berlin metro system.

3.7.1 Model

Berlin’s U-Bahn and S-Bahn systems are highly interconnected systems that are linked by numerous stations. According to [250], they may therefore be considered as a unified system, hereafter referred to as “metro system”. In [268] the authors apply their introduced approach for resilience decision-making to a model of the Berlin metro system. In order to demonstrate the wide applicability and efficiency of the proposed methodology developed in this work, this model is considered, extended and adapted by means of substructuring, and an efficient and multidimensional resilience decision-making analysis is conducted.

In [259], Zhang et al. proposed how mapping of metro networks into topological graphs can be conducted. Based on this, the Berlin metro system consists of 306 nodes for 306 metro stations and 350 edges for 350 connections between these stations. For simplicity, parallel connections are mapped to single edges in the model, and are assumed to be undirected. These assumptions reduce the complexity of the metro system. Figure 3.10 illustrates the graph representation.

The functionality of systems depends on the functionality of its components. However, the

functionality of these components often depends again on the functionality of a variety of subcomponents, etc. A major challenge in modeling is therefore determining an appropriate level of detail.

The resilience decision-making methodology proposed in this paper allows for the incorporation of such subsystem structures by live propagation of corresponding reliability characteristics up to the top-level. Therefore, for the resilience analysis of the metro system, each metro station is modeled as a subsystem with own functionality and performance function. Again, for illustrative purposes and sake of convenience, assume that there is only one level of subsystems, i.e., $l = L = 1$, and thus $\mathbf{x}^s = (s_1, s_2, \dots, s_{306})$, $\mathcal{S}_j^1 = \mathcal{S}_j$ and $\lambda^{s_j^1}(t) = \lambda^{s_j}(t)$ with $n = 306$ subsystems respectively metro stations.

In terms of reliability modeling, subcomponents could correspond to structural elements, such as stairs, columns, ceilings, station rails as well as electric facilities, such as railway power supply, elevators, escalators, ventilation plants, information systems and illuminations. These subcomponents can be subdivided in terms of their functionality and relevance to the metro station, such as in rail operations related components and user accessibility related components. For illustrative purpose, the analysis is restricted to reliability modeling of metro stations. Therefore, functional models are defined for the metro station subsystems that are, as in the previous case study, formally RBDs. Again, a subsystem \mathcal{S}_j is considered to be functional if a connection from start to end exists and non-functional if this connection is interrupted, i.e., $s_j \in \{0, 1\} \forall j \in \{1, \dots, 306\}$. Figure 3.10 illustrates three of these subsystems for three different metro stations as an example. The metro stations are classified into $B = 6$ types, depending on the number of their connections to direct neighbors, i.e., stations with only one connection form subsystem type 1, stations with two direct neighbors form subsystem type 2, etc. For the analysis, each subsystem is assumed to be characterized by an endowment property, that is the recovery improvement rec , such that a metro station j with type b_j is described by $(\mathcal{S}_j; b_j) = (rec_j; b_j)$. Note, that the recovery improvement rec_j of each metro station is assumed to be a function of the station type b_j , i.e., $rec_j = rec_{j'}$ if $b_j = b_{j'}$. For simplicity, it is assumed that each metro station of a type is represented by the same RBD. Figure 3.11 displays the structure of all six subsystem types and Fig. 3.12 tabulates the number of individual metro stations per type.

Depending on the type and thus with increasing complexity related to the number of direct neighbors, also known as node degree, the subsystems consist of four up to twenty-one components. Taking into account the information from Fig. 3.12, the overall system therefore consists of a total of $m = 2776$ considered individual components.

The components are classified into $K = 4$ types $k_i \in \{1, 2, 3, 4\} \forall i \in \{1, \dots, 2776\}$. For the analysis, each component is assumed to be characterized by an endowment property, that is the reliability improvement rel , such that a component is fully described by $(a_i; k_i) = (rel_i; k_i)$. Note, that the reliability improvement rel_i of each component is assumed to be a function of the component type k_i , i.e., $rel_i = rel_{i'}$ if $k_i = k_{i'}$. Further, each component is characterized by a specific time-dependent failure behavior. For the purpose of proof of concept and applicability,

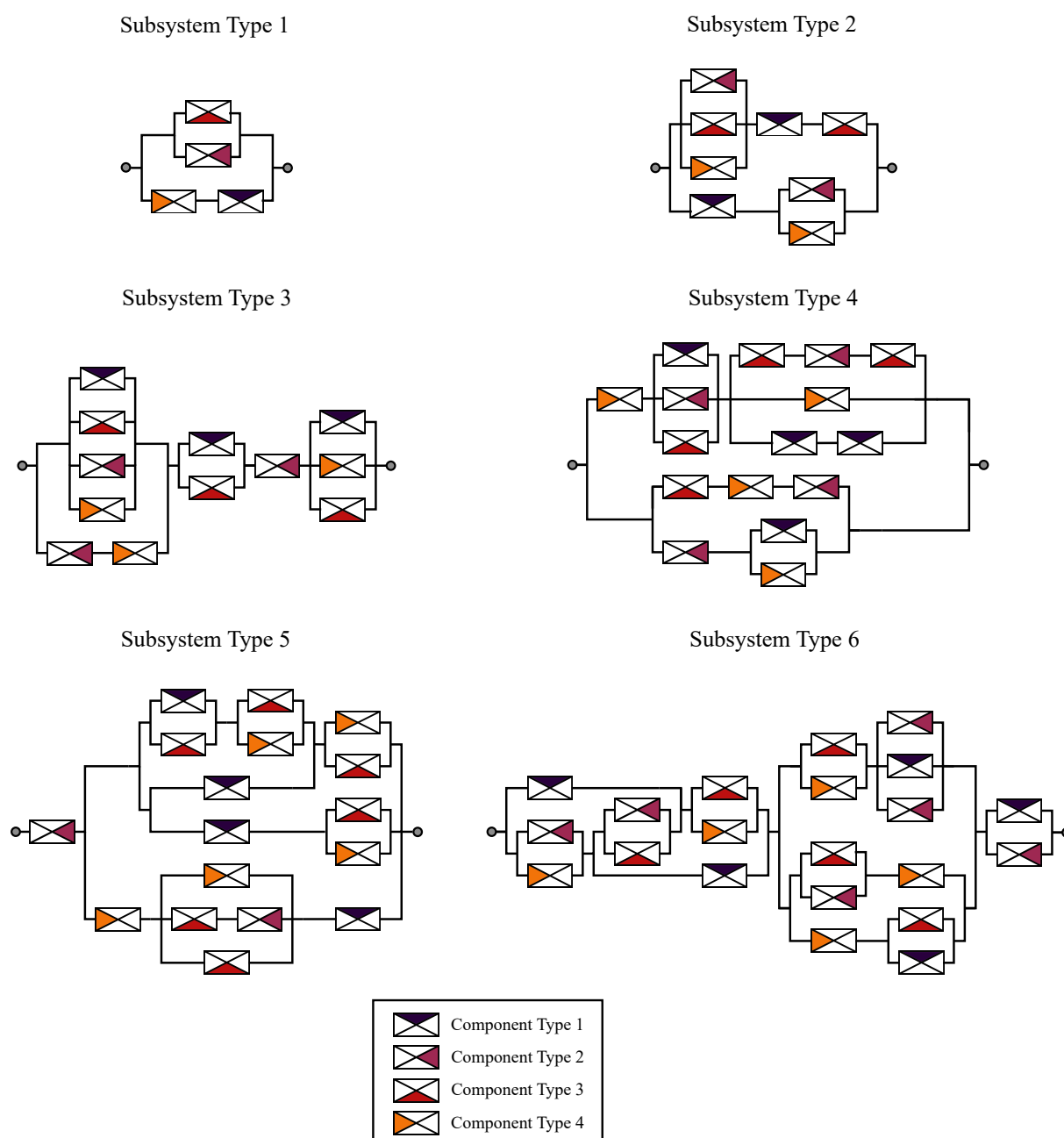


Figure 3.11: Representation of the $B = 6$ station types of the Berlin metro system.

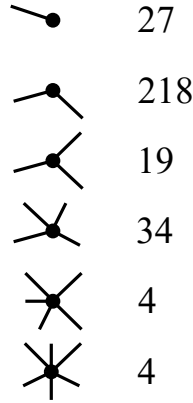


Figure 3.12: Number of individual metro stations per type.

for component type 1 and 3, i.e., $k_i = 1$ and $k_i = 3$, exponential distributions are considered according to Eq. 3.21 and Eq. 3.22. For component type 2 and 4, i.e., $k_i = 2$ and $k_i = 4$, two parametric gamma distributions are considered. The cumulative distribution function of the gamma distribution can be derived based on its probability density function that is given in terms of the rate parameter $\lambda_i(reli_i)$ depending on the current reliability endowment value rel_i of component i of type k_i as

$$f(t; \alpha_i, \lambda_i(reli_i)) = \frac{t^{\alpha_i-1} e^{-\lambda_i(reli_i)t} \lambda_i(reli_i)^{\alpha_i}}{\Gamma(\alpha_i)}, \quad (3.25)$$

for $t, \alpha_i, \lambda_i(reli_i) > 0$, where α_i is the shape parameter, $\lambda_i(reli_i)$ is the rate parameter, and $\Gamma(\alpha_i)$ is the well-known Gamma function. Consequently, the cumulative distribution function can be obtained by integration and with respect to the current endowment of component i it can be formulated as

$$F(t; \alpha_i, \lambda_i(reli_i)) = \int_0^t f(u; \alpha_i, \lambda_i(reli_i)) du. \quad (3.26)$$

$\lambda_i(reli_i)$ is again a function of the component specific reliability improvement and given by Eq. 3.22.

In order to perform a resilience analysis, the definition of an appropriate system performance measure for the metro system is imperative. As in [259] and [268], in this case study, the so-called network efficiency E_f is adopted as the relevant performance measure, i.e., $Q(t) = E_f(t)$. Zhang et al. justified in [259] their choice by stating that connectivity between individual metro stations is an essential criterion for evaluating metro operations. As described by Latora and Marchiori in [261], network efficiency is a quantitative indicator of network connectivity and is defined as:

$$E_f = \frac{1}{n(n-1)} \sum_{u \neq v} \frac{1}{d_{uv}} \quad (3.27)$$

with n the number of subsystems, i.e., metro stations in the network and d_{uv} the path length between metro station u and metro station v , i.e., the shortest distance between these stations.

A comprehensive overview of algorithms to efficiently determining the path length d_{uv} between stations, such as the algorithms of Floyd, Dijkstra's, or Bellman-Ford, is provided in [263] and [262].

The simulation procedure corresponds to that from the previous case study and the failure probability of a subsystem \mathcal{S}_j , i.e., metro station, in the time interval (t_h, t_{h+1}) is defined by Eq. 3.23. Unlike in the previous case study, a failed metro station is not entirely removed from the system, but remains in the set of metro stations; however, their node degree becomes 0, i.e., all existing connections to direct neighbors are removed. This assumption is essential, as the computation and interpretation of the system performance network efficiency depends on the number of nodes. The case study therefore relies on the fact that the number of nodes is constant.

If a subsystem \mathcal{S}_j failed, its functionality is assumed to be immediately and fully recovered after a certain number of time steps r :

$$r = r_{\max} - 2 \cdot rec_j \quad \text{with} \quad rec_j < r_{\max}, \quad (3.28)$$

where rec_j is the recovery improvement specific to the station \mathcal{S}_j and r_{\max} is an upper bound for number of time-steps for recovery. After recovery, all previous connections to other metro stations are assumed to be restored, unless these are in a state of failure. As each time-step has a specific length of $\Delta t = (T/u)$, the duration of the recovery process is $r \cdot (T/u)$. Again, this recovery model corresponds to a one-step recovery profile and as mentioned before, various alternative characteristic profiles of recovery are possible as well. A repaired station and thus all components of the station are assumed to be in a as-new original condition after repair. This is an assumption for the sake of demonstration, and deviating states are possible. After recovery, the survival function of a metro station is time-zeroed, such that the resulting failure rate per simulation step $\lambda^{s_j}(t_h)$ evolves over time equivalent to that of a station in new condition.

3.7.2 Costs of endowment properties

The improvement of both endowment properties, "reliability improvement" and "recovery improvement", is inevitably associated with costs. Again, exponential relationships between total costs and improvements are assumed:

$$cost^{rel} = \sum_{i=1}^{2776} price_{(rel_i; k_i)}^{rel} \cdot 1.2^{(rel_i-1)}, \quad (3.29)$$

where rel_i is the reliability improvement value of component i , k_i its type and $price_{(rel_i; k_i)}^{rel}$ an arbitrary common basic price. Accordingly an exponential relationship is assumed for the total cost associated with recovery improvement:

$$cost^{rec} = \sum_{j=1}^{306} price_{(rec_j; b_j)}^{rec} \cdot 1.2^{(rec_j-1)}, \quad (3.30)$$

where rec_j is the recovery improvement value of station j , b_j its type and $price_{(rec_j; b_j)}^{rec}$ an arbitrary common basic price. The total cost $cost_{(A; z), (D; h)}$ of an endowment is the sum of these costs:

$$cost_{(A; z), (D; h)} = cost^{rel} + cost^{rec}. \quad (3.31)$$

In practice, it is crucial to include the economic aspects of failure and recovery processes in detail in the resilience assessment. Mitigating resilience losses through system improvements imposes direct costs on stakeholders, such as improving component properties. Note, however, that for a comprehensive analysis, it is important to also consider indirect costs to the affected population and businesses, when the performance of a key system declines, as stated in [273]. Further, it is reasonable to incorporate the subjective preferences of stakeholders into the resilience assessment, as suggested in [272]. These considerations have the potential to significantly influence the outcome of a resilience decision-making process. Therefore, they should be integrated into the proposed methodology in future work by including additional cost conditions and discount rates for the corresponding deterioration and recovery sequences.

3.7.3 Scenario

In order to apply the resilience decision-making method to the Berlin metro system illustrated in Fig. 3.10, the model parameter and simulation parameter values, shown in Tab. 3.4, are considered. The recovery improvement rec_j is explored over $rec_j \in \{1, \dots, 10\} \forall j \in \{1, \dots, 306\}$, but considered to be equal for each station, regardless of the type b_j . The reliability improvement rel_i again is explored over $rel_i \in \{1, \dots, 10\} \forall i \in \{1, \dots, 2776\}$ for $k_i \in \{1, \dots, 4\}$.

In a pre-processing step, the survival signatures of all 306 metro stations are determined. As an example, Tab. 3.5 illustrates the non-trivial survival signature values, i.e., $\Phi(l_1, \dots, l_4) \neq 0$ and $\Phi(l_1, \dots, l_4) \neq 1$, of station type 2 of the metro system. Then, the set of all acceptable endowment configurations $R(Y)$, corresponding to a resilience value of at least $Res = 0.99$ over the considered time period, is determined according to Algorithm 3.4.3. Further, as any improvement of the system components and stations is associated with costs, the most cost-efficient acceptable endowment, denoted by the tuple (\hat{A}, \hat{D}) , is determined.

In Fig. 3.13 the results of the grid search algorithm are illustrated. It shows the accepted endowments contained in $R(Y)$, i.e. all combinations that lead to a satisfying resilience of the metro system. It is clearly visible that type 1 components as well as the recovery improvement of the metro stations have the greatest influence and thus the highest importance for the metro system. Only endowments with a reliability improvement of at least $rel_i = 8$ for type 1 components and endowments with a recovery improvement for all metro stations of at least $rec_j = 8$ lead to a system resilience meeting the acceptance criterion. In addition, type 2 components are of considerable relevance. Here, only endowments with a reliability improvement of at least $rel_i = 6$ are acceptable. The reliability improvements of type 3 and 4 components, on the other hand, are of less significance. For both types of components, there are numerous

Table 3.4: Parameter values for the resilience decision-making method on the metro system of Berlin.

Parameter	Scenario
Acceptance threshold α	0.99
Length of time step Δt	0.05
Number of time steps u	200
Maximum time T	10
Shape parameter gamma distribution α_i	$\alpha_i = 1.2$ for $k_i = 2$ $\alpha_i = 2.6$ for $k_i = 4$
Maximum failure rate $\lambda_{i,\max}$	$\lambda_{i,\max} = 0.34$ for $k_i = 1$ $\lambda_{i,\max} = 0.43$ for $k_i = 2$ $\lambda_{i,\max} = 0.36$ for $k_i = 3$ $\lambda_{i,\max} = 0.66$ for $k_i = 4$
Failure rate reduction $\Delta\lambda_i$	$\Delta\lambda_i = 0.03$ for $k_i = 1$ $\Delta\lambda_i = 0.04$ for $k_i = 2$ $\Delta\lambda_i = 0.034$ for $k_i = 3$ $\Delta\lambda_i = 0.051$ for $k_i = 4$
Reliability improvement rel_i	$rel_i \in \{1, \dots, 10\}$ for $k_i \in \{1, \dots, 4\}$
Reliability improvement price $price_{(rel_i;k_i)}^{rel}$	$price_{(rel_i;1)}^{rel} = 100\text{€}$ $price_{(rel_i;2)}^{rel} = 200\text{€}$ $price_{(rel_i;3)}^{rel} = 200\text{€}$ $price_{(rel_i;4)}^{rel} = 400\text{€}$
Maximum recovery time r_{max}	22
Recovery improvement rec_j	$rec_j \in \{1, \dots, 10\}$
Recovery improvement price $price_{(rec_j;b_i)}^{rec}$	$price_{(rec_j;1)}^{rec} = 100\text{€}$ $price_{(rec_j;2)}^{rec} = 200\text{€}$ $price_{(rec_j;3)}^{rec} = 300\text{€}$ $price_{(rec_j;4)}^{rec} = 400\text{€}$ $price_{(rec_j;5)}^{rec} = 500\text{€}$ $price_{(rec_j;6)}^{rec} = 600\text{€}$
Sample size N	500

Table 3.5: Non-trivial survival signature values of stations with $b_j = 2$ of the metro system, shown in Fig. 3.11.

l_1	l_2	l_3	l_4	$\Phi(l_1, \dots, l_4)$
2	2	1	1	1/4
2	1	1	2	1/4
2	2	2	1	3/8
2	2	1	2	3/8
2	1	2	2	3/8
3	2	1	1	1/2
2	3	1	1	1/2
2	1	3	1	1/2
3	1	1	2	1/2
2	3	1	2	1/2
2	1	1	3	1/2
2	2	1	3	1/2
2	3	1	3	1/2
2	2	2	2	9/16
3	2	2	1	3/4
2	3	2	1	3/4
2	2	3	1	3/4
3	2	1	2	3/4
3	1	2	2	3/4
2	3	2	2	3/4
2	1	3	2	3/4
2	1	2	3	3/4
2	2	2	3	3/4
2	3	2	3	3/4
3	2	2	2	7/8
2	2	3	2	7/8

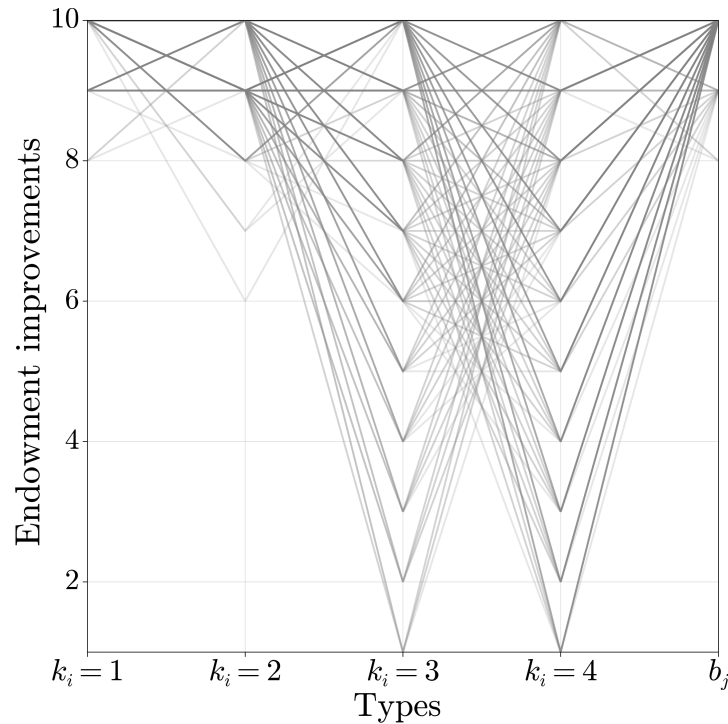


Figure 3.13: The set of all accepted endowments $R(Y)$ evaluated via the 5D grid search algorithm for the Berlin metro system with explored reliability improvement and recovery improvement values.

acceptable configurations that include minimum reliability improvement values for one of these types.

These results again prove to be plausible, as in the previous case study, upon closer examination of the topological structures of the metro system and its subsystems. Several U-Bahn and S-Bahn lines start and end in long chains of directly interconnected type 2 stations, see Fig. 3.10. The resilience analysis of the Berlin metro system published in [268] revealed that especially an interruption of these chains has a major negative impact on the network efficiency and thus on the resilience of the metro system. Accordingly, the importance of type 2 stations is particularly high not only due to their multiplicity in the system, but due to their topological contribution in terms of connectivity as well. Consequently, components of this station type have a significant impact on the resilience of the overall system. An examination of the type 2 subsystem model, see Fig. 3.11, shows that type 1 components take on a predominant position. Once both type 1 components in this subsystem fail, the entire metro station fails. No other components of a single type can cause this in station type 2.

The significant influence of type 2 components can easily be explained by examining the type 3 and 5 station systems, see again Fig. 3.11. Of all stations, only here bottleneck positions exist, where the failure of a single component interrupts the functioning of the entire station. Both of these positions, in type 3 and type 5 stations, are occupied by type 2 components. Since both station types have three and five direct connections to other stations, they can be considered to be particularly interconnected and thus of high relevance to network efficiency and thus of high

relevance to system resilience.

Type 3 and 4 components, on the other hand, do not occupy any particularly significant positions in the stations' systems. This explains their low influence. The enormous influence of the recovery improvement is intuitively explainable. As resilience is established via the integral of the actual system performance, each recovered metro station contributes directly and immediately to the network efficiency and thus to the resilience of the system. Therefore, improvement of this property results in an immediate and intuitive increase in resilience.

Assuming the arbitrary base prices in Tab. 3.4, the most cost-efficient acceptable endowment (\hat{A}, \hat{D}) results from a reliability improvement configuration of $rel_i = 10$ for $k_i = 1$, $rel_i = 9$ for $k_i = 2$, $rel_i = 7$ for $k_i = 3$, $rel_i = 2$ for $k_i = 4$ for components of type 1 to 4 and a maximum recovery improvement configuration of $rec_j = 10$ for $b_j \in \{1, 2, 3, 4\}$, i.e., all stations, regardless of their type. In Fig. 3.14, the corresponding configuration is highlighted. Due to the monotonicity of the input-output model and the assumed monotonically increasing endowment costs, only the endowment configurations on the dominant vertices of the Pareto front have to be examined for the identification of the most cost-efficient endowment. Therefore, only these endowment configurations are shown in Fig. 3.14. The resulting costs are given by Eq. (3.29, 3.30, 3.31) with $cost_{(\hat{A}, \hat{D})} = 1\,700\,829\text{€} + 361\,185\text{€} = 2\,062\,014\text{€}$.

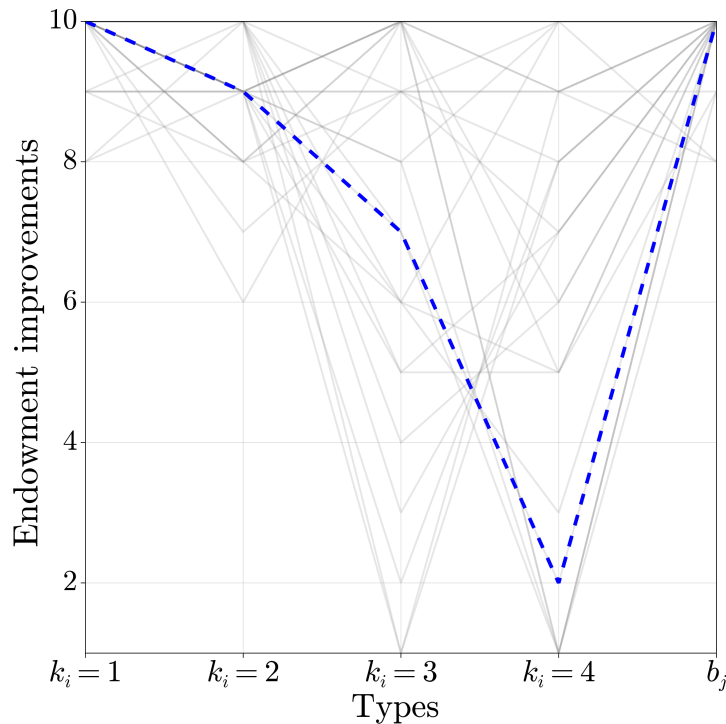


Figure 3.14: Dominant Pareto front endowments of the 5D grid search algorithm for the Berlin metro system with explored reliability improvement and recovery improvement values and the most cost-efficient endowment (\hat{A}, \hat{D}) is highlighted.

Due to the utilization of the grid search algorithm, the computational effort could be significantly reduced in this case study as well – only 0.159% of all potential endowment configurations had

to be examined in order to assign a distinct state to each configuration in the search space as accepted or not accepted. By means of the novel approach, the metro system could be reduced from its entirety of 2776 individual components to 306 components on the top-level with respect to the resilience analysis, drastically reducing the computational effort. Nevertheless, all 2776 components and their influence were considered. As in the case study of the axial compressor, not only the most cost-efficient endowment configuration can be identified but also investigations on configurations that are below certain budget limits can be conducted.

Note that, in this case study, as well as in the previous ones, various complexity variations such as so-called cascading failures, see [265–267], are possible to implement due to the time-step-accurate simulation. In the case of infrastructure systems, e.g., the increasingly frequent natural disasters can thus be considered, that typically have an impact as local phenomena and affect stations that are geographically close to each other. It has already been shown in [268] that these can be taken into account in the resilience decision-making analysis of infrastructure systems.

3.8 Conclusion and outlook

This paper addresses the challenge of efficient multidimensional decision-making for complex and substructured systems between resilience-influencing parameters. By merging an extension of the resilience framework proposed in [268] with the survival signature, an efficient and novel methodology is derived. The approach allows for direct comparison of the impact of heterogeneous controls on system resilience, such as failure prevention and recovery improvement arrangements, both during the design phase as well as during any phase in the life cycle of already existing complex systems.

Due to the time-step accurate simulation of the system performance on system level during the resilience analysis, complexity extensions such as cascading failures and other dependency structures can be considered without difficulties. The new methodology has a high numerical efficiency. The majority of the endowment properties examined affect the probability structure of the system components. The numerous changes in the probability structure caused by constantly changing endowment properties during the resilience analysis can be ideally covered with minimal effort due to the separation property of the survival signature.

The novel approach includes a substructuring approach for large, complex systems. This and the integration of the survival signature allow for the propagation of subsystem reliabilities through any number of system levels to the top-level and lead to a significant reduction of the computational load. This way, and with the extension of the adapted systemic risk measure, it is now possible to analyze systems with a large number of components in terms of their resilience. Monetary restrictions can easily be included in the analysis. More precisely, not only the most cost-efficient, accepted endowment is identified, but subsets of the set of all accepted endowments below defined price levels can be formed. Budget limits can thus be specifically taken into account in the decision-making process.

The methodology is applied to three entirely distinct systems: A functional model of a multi-

stage high-speed axial compressor, an arbitrary system consisting of numerous subsystems and components and a comprehensive substructured model of the metro system of Berlin, proofing wide and general applicability. All results obtained are plausible with the corresponding assumed model parameters. Note, that the approach can be utilized to systems of any kind.

In the development of our proposed methodology, some simplifying assumptions were made that do not accurately reflect reality. However, the authors strongly believe that the presented approach can be considered as a meaningful core development that, for a reality-based application on highly multifactorial systems, such as cyber-human-physical systems, should be combined with future as well as existing developments to ensure an efficient and comprehensive resilience decision-making analysis taking into account all technical and monetary aspects of modern societies.

Future work will address the incorporation of various existing extensions of the concept of survival signature, such as accounting for uncertainty and propagating it toward imprecise system resilience and considering multiple state or continuous component functionality. Further, future work regarding multidimensional parameter spaces must deal with the limitations in computing time and storage capacity in order to enable application to even higher-dimensional problems. Namely, techniques such as advanced sampling methods, e.g. Subset Simulation, see [283], must be investigated to further reduce numerical effort.

Acknowledgment

Funded by the Deutsche Forschungsgemeinschaft (DFG, German Research Foundation) SFB 871/3 119193472 and SPP 2388 501624329.

4 | Efficient reliability analysis of complex systems in consideration of imprecision

Efficient reliability analysis of complex systems in consideration of imprecision

Julian Salomon^{a,*}, Niklas Winnewisser^a, Pengfei Wei^{a,b}, Matteo Broggi^a, Michael Beer^{a,c,d}

^aInstitute for Risk and Reliability, Leibniz Universität Hannover, Hannover, Germany

^bSchool of Mechanics, Civil Engineering and Architecture, Northwestern Polytechnical University, Xi'an, China

^cInstitute for Risk and Uncertainty, University of Liverpool, Liverpool, United Kingdom

^dInternational Joint Research Center for Resilient Infrastructure & International Joint Research Center for Engineering Reliability and Stochastic Mechanics, Tongji University, Shanghai, China

*Corresponding author

Published in *Reliability Engineering & System Safety* on December 2021

Abstract

In this work, the reliability of complex systems under consideration of imprecision is addressed. By joining two methods coming from different fields, namely, structural reliability and system reliability, a novel methodology is derived. The concepts of survival signature, fuzzy probability theory and the two versions of non-intrusive stochastic simulation (NISS) methods are adapted and merged, providing an efficient approach to quantify the reliability of complex systems taking into account the whole uncertainty spectrum. The new approach combines both of the advantageous characteristics of its two original components: 1. a significant reduction of the computational effort due to the separation property of the survival signature, i.e., once the system structure has been computed, any possible characterization of the probabilistic part can be tested with no need to recompute the structure and 2. a dramatically reduced sample size due to the adapted NISS methods, for which only a single stochastic simulation is required, avoiding the double loop simulations traditionally employed.

Beyond the merging of the theoretical aspects, the approach is employed to analyze a functional model of an axial compressor and an arbitrary complex system, providing accurate results and demonstrating efficiency and broad applicability.

Keywords: Survival signature, System reliability, Complex systems, Reliability analysis, Epistemic uncertainty, Imprecision, Fuzzy probabilities, Extended Monte Carlo methods, Non-intrusive imprecise stochastic simulation.

4.1 Introduction

Engineering systems constitute a key factor for the state of development and progress of modern societies. Typical examples are infrastructure networks, industrial plants or machines, e.g., gas turbines. Closely integrated into society, the functionality of such complex capital goods has a significant impact on the economy as well as on everyday life. However, in reality, engineering systems deteriorate due to environmental and operational influences. As a result, their overall performance decreases over time or, in the worst case, they fail entirely. Consequently, for economic and safety-related reasons the reliability of a system, i.e., its continuous functionality, is of utmost importance. In order to ensure this reliability, appropriate decisions must be made in both design and maintenance. However, since societal growth and progress is accompanied by increasing size and complexity of societies' systems [284] and since "Global population growth

will continue for decades, reaching around 9.2 billion in 2050 and peaking still higher later in the century,” [285], this task, i.e., the identification of appropriate decisions towards maximum reliability, is becoming increasingly challenging. For this reason, the development of sophisticated methods for quantifying and assessing system reliability gained more and more importance over the past decades [132, 286–288] and will receive even more attention in the future.

Conventional tools in system reliability assessment are failure mode and effect analyses, see, e.g., [106, 107], as well as more mathematical representations, such as reliability block diagrams, see, e.g., [108], fault tree and success tree methods, see, e.g., [109, 110]. However, as stated in [114], the calculations for identifying minimal path sets or cut sets might be too arduous for large complex systems, limiting the applicability of such methods. Further traditional approaches are Markov models, see, e.g., [115] and Petri nets, see, e.g., [120]. In recent research, system reliability assessment methods are provided, e.g., in [289] and [122] for multi-state systems, in [125], using Bayesian melding method, including various available sources on system, as well as subsystem level and in [126, 127], where Yang et al. as well as Xiao et al. propose approaches based on an active learning Kriging model, considering multiple failure modes and a multiple response model, respectively. Furthermore, Li et al. propose in [129] a reliability approach for analyzing systems composed of repairable components with complex failure distribution structure. A comprehensive review on numerous system reliability methods and the evolution of reliability optimization is provided in, e.g., [133, 136, 137].

Various system reliability approaches are based on the mathematical concept of the structure function that represents a functional state of a system in dependence on its components states, i.e., its state vectors, see, e.g., [140, 142]. Nevertheless, not only for large systems the structure function might become complicated or impractical [144, 145]. For coherent systems with components of only a single type, i.e., exchangeable components, the system signature represents a summarization of the structure function, providing an advantageous tool, see, e.g., [148].

In current research, the concept of survival signature is a promising approach to efficiently model the reliability of systems with multiple component types. The survival signature was introduced and discussed in [149, 153] as a generalization of the system signature. Apart from overcoming the restriction to systems with only one type of components, similar to the signature, the key feature of the survival signature is a clear separation between the structure of a system and the probabilistic properties of its components [290]. In addition, it summarizes the system structure by aggregating state vectors into single survival signature entries with associated reliabilities, resulting in significantly reduced storage requirements and simplified data access. Once the system structure has been evaluated – usually a demanding task – any number of calculations for various probability properties can be performed without having to recalculate it. Thus, compared to traditional approaches, the survival signature reduces the computational effort associated with repetitive model evaluations that are typically required in reliability engineering processes. A direct comparison between fault tree, Markov chain and survival signature modeling is presented in [150].

As stated in [114], a purely analytical implementation of the survival signature to real-life complex systems is often not feasible and simulations are required instead. Therefore, in [114], Patelli et al. provide simulation algorithms based on the concept of survival signature and Monte Carlo simulation (MCS). However, for large systems the computational effort of determining the survival signature might be prohibitive. Thus, current research addresses the approximation of survival signature entries by estimating the associated reliability values over a subset of corresponding state vectors, reducing computational expense for the single required topological system evaluation significantly [291]. Furthermore, in [156] an efficient algorithm for exact computation of system and survival signatures using binary decision diagrams is provided. In addition, sub-structuring the system in serial or parallel subsystems of smaller size and the subsequent merging of the survival signatures of these subsystems may be conducted [157]. Further research combines the notion of survival signature with multiple failure modes and dependent failures [158], common cause failures [159], interconnected networks [160] and multi-state components [114].

In reality, design and maintenance decisions determining the reliability of a system have to be made under the presence of uncertain conditions. Gathering precise information is typically unfeasible, since, for instance, measurements of lifetime data and subjective assessments by experts are governed by uncertainty. Thus, comprehensive details, providing insight into the uncertain system behavior, are required. Consequently, a challenging task for engineers is how uncertainty can be integrated into reliability models. In the systemic context, current approaches to propagate uncertainty in the model are, e.g., Dempster-Shafer theory [182, 292], info-gap theory [186], p-boxes [188, 218] and fuzzy probabilities [190, 293]. It shall be noted that a lot of debate is present in the literature on various aspects of modeling uncertainties, such as the terminology and interpretation [168, 169] as well as their representation [170, 171]. In practice, the reduction of uncertainty is desired but associated with unavoidable costs, involving for example experimental campaigns, destructive testing, etc. Therefore, a trade-off is required by decision-makers, where a critical level of uncertainty needs to be identified among various design and maintenance measures in order to balance uncertainty and the costs associated with its reduction. This can be achieved by utilizing fuzzy probabilities as an appropriate uncertainty representation, as, e.g., Beer et al. propose in [194].

In the context of survival signature, several works, such as in [114, 145, 154, 157], have already demonstrated how the numerous advantages of the concept of survival signature and the consideration of uncertainties can be merged in an encompassing reliability analysis framework. Accounting for both aleatoric and epistemic uncertainties requires an adequate treatment in system analysis. An often conducted approach is a two-staged simulation, known as “double loop” approach, where variables with epistemic uncertainty are propagated in an “outer loop” and variables with aleatoric uncertainty are sampled in an “inner loop” [203], or, vice versa, aleatory variables are sampled in an “outer loop” and epistemic uncertainty is propagated in the “inner loop” [204]. It is obvious that for complex systems this naive approach leads to an extraordinarily large sample size and thus to high computational effort, see, e.g., [294]. Consequently, simulation

methods that enhance computational efficiency and provide high accuracy with minimal sample size are desired.

Approaches to circumvent the exhaustive double loop simulation include interval MCS and interval importance sampling [207, 208], stochastic expansions and optimization-based interval estimation [210] as well as surrogate modeling via optimization and approximation techniques [295]. Latest methods to improve computational performance for uncertainty quantification, for instance, combine p-boxes, univariate dimension reduction method and optimization [216], utilize the augmented space integral [217] or apply line outage distribution factors [218]. Recently, Wei et al. introduced in [220] the non-intrusive stochastic simulation (NISS), a promising approach for efficient computation of imprecise structural models with a drastically reduced sample size. The method splits into two basic approaches, the local extended Monte Carlo simulation (LEMCS) and the global extended Monte Carlo simulation (GEMCS), coming along with different advantages in accuracy and variation.

In the present work, two methodologies from different fields, namely, structural reliability and system reliability, are joined to derive a novel and comprehensive approach for system reliability analysis taking into account imprecisions. More specifically, both, LEMCS and GEMCS, are adapted and merged with the concept of survival signature. Through the complex amalgamation, a new methodology is derived, combining the advantages of both original methods: a significant storage reduction of system topological information and major efficiency advantages in repeated model evaluations as well as an extensive consideration of uncertainties with just a single stochastic simulation needed, reducing the sample size dramatically. The combination of these advantages leads to beneficial synergy effects, increasing the efficiency even more. The representation of uncertainties is achieved by integrating fuzzy probabilities.

The paper proceeds as follows: Section 2 briefly reviews the fundamental theory of survival signature, uncertainty, fuzzy probability and NISS method. Based on this, Section 3 develops the proposed novel approach. In Section 4 the method is applied to a functional model of a multi-stage high-speed axial compressor as well as to an arbitrary complex system. Section 5 summarizes the results and discusses questions for future research.

4.2 Theoretical fundamentals

4.2.1 Survival signature

The survival signature according to [149] is a concept for efficiently determining the time-dependent reliability of systems that are composed of components of different types. Detailed information about the concept and its derivation can be found, e.g., in [149, 153, 154].

Structure function

Suppose a system composed of m components of a single type. Then, $\mathbf{x} = (x_1, x_2, \dots, x_m) \in \{0, 1\}^m$ defines the state vector of these components with $x_i = 1$ indicating a functioning state

of the i th component and $x_i = 0$ indicating a non-functioning state. The structure function ϕ is a function of the state vector, describing the operating state of the regarded system: $\phi = \phi(\mathbf{x}) : \{0, 1\}^m \rightarrow \{0, 1\}$. Accordingly, $\phi(\mathbf{x}) = 1$ indicates a functioning system and $\phi(\mathbf{x}) = 0$ indicates a non-functioning system with respect to the state vector \mathbf{x} .

Suppose a system composed of components of multiple types, i.e., $K \geq 2$, then the number of system components is given by $m = \sum_{k=1}^K m_k$ with m_k denoting the number of components of type $k \in \{1, 2, \dots, K\}$. Then, the state vector for each type can be defined, equivalent to systems with only a single component type, as $\mathbf{x}^k = (x_1^k, x_2^k, \dots, x_{m_k}^k)$.

Survival signature and survival function

The survival signature describes the probability of a system being in a functioning state, purely depending on the number of functioning components l_k for each type k . Assuming the failure times of components of the same type to be independent, identically distributed (*iid*) or exchangeable within this type, the survival signature can be defined as:

$$\Phi(l_1, l_2, \dots, l_K) = \left[\prod_{k=1}^K \binom{m_k}{l_k}^{-1} \right] \times \sum_{\mathbf{x} \in S_{l_1, l_2, \dots, l_K}} \phi(\mathbf{x}), \quad (4.1)$$

with $\binom{m_k}{l_k}$ denoting the total number of state vectors \mathbf{x}^k of type k and S_{l_1, l_2, \dots, l_K} denoting the set of all state vectors of the entire system for which $l_k = \sum_{i=1}^{m_k} x_i^k$. Thus, the survival signature only depends on the topology of the system, regardless of any time-dependent failure behavior of its components. Note that the notion exchangeability, following [167], implies the input ordering of the random quantities being irrelevant. As a consequence in practice, rearranging the exchangeable assumed components should be irrelevant to real systems. For components that have the same functionality, come from the same manufacturer and operate in the same environment, the assumption of exchangeability is reasonable. However, as the environment changes, components of the same kind are exposed to different environmental stresses as, e.g., significantly different temperatures, affecting their behavior and further their lifetime probability distribution function. Here, assuming exchangeability would be inappropriate, see [114].

Let $C_k(t) \in \{0, 1, \dots, m_k\}$ denote the number of components of type k in a working state at time t and suppose the probability distribution for the failure times of type k to be known with $F_k(t)$, being the corresponding cumulative distribution function. Then

$$\begin{aligned} P\left(\bigcap_{k=1}^K \{C_k(t) = l_k\}\right) &= \prod_{k=1}^K P(C_k(t) = l_k) \\ &= \prod_{k=1}^K \binom{m_k}{l_k} [F_k(t)]^{m_k - l_k} [1 - F_k(t)]^{l_k} \end{aligned} \quad (4.2)$$

describes the probabilistic structure of the system, i.e., the time-dependent failure behavior of the system components, regardless of its topology. The survival function, describing the probability of a regarded system being in a functioning state at time t , results as:

$$P(T_s > t) = \sum_{l_1=0}^{m_1} \dots \sum_{l_K=0}^{m_K} \Phi(l_1, l_2, \dots, l_K) \times P\left(\bigcap_{k=1}^K \{C_k(t) = l_k\}\right), \quad (4.3)$$

with T_s denoting the random system failure time. Thereby, the concept of survival signature separates the topology and the time-dependent probability structure. In addition, the survival signature is a summary of the structure function and, therefore, is advantageous compared to traditional methods when model simulations have to be conducted repeatedly, especially, if the system failure evaluation is computational expensive [114, 149]. Note that these are precisely the features that make the survival signature so unique and beneficial.

4.2.2 Uncertainty

In literature, various concepts concerning uncertainty are spread. Therefore, a brief clarification of the notion of uncertainty, its interpretation, classification and further a hint of how uncertainties can be advantageously implemented into the probability structure of a system, as presented in Section 4.2.1, is given in the following.

Interpretation of uncertainty

Initially, a fundamental notion of uncertainty must be established. Following Nikolaidis in [172], uncertainty can be defined indirectly by the definition of certainty known from decision theory and its absence. This interpretation and its associated states are illustrated in Fig. 4.1(a). In this sense but extended to a more general interpretation, certainty, represented by state 4 in Fig. 4.1, is the state in which complete knowledge, e.g., concerning model input, is given. This state is ideal and a deterministic model can be utilized. Accordingly, uncertainty implies incomplete knowledge concerning, e.g., corresponding measures of a decision and their outcome as addressed in [172] or component behavior. Further, maximum uncertainty refers to complete ignorance, i.e., state 1, in which no knowledge is available at all. This is the worst case scenario yet appearing only in the theoretical sense. In practice, the present state of information, shown as state 2, typically includes both knowledge and uncertainty. The gap between complete ignorance and the present state of information relates to knowledge stated to be certain, i.e., it can be implemented in the model deterministically, while the gap between the present state and certainty corresponds to remaining uncertainty. Concerning decision-making, stakeholders intend, among other things, a maximum reduction of hazardous uncertainties, i.e., shifting the present state of information as close to certainty as cost and feasibility allow.

Classification of uncertainty

In order to deal with uncertainties in analyses properly, e.g., Der Kiureghian & Ditlevsen propose a two-part classification of uncertainty in [169]: “The advantage of separating the uncertainties into aleatory and epistemic is that we thereby make clear which uncertainties can be reduced and which uncertainties are less prone to reduction, at least in the near-term, i.e., before major

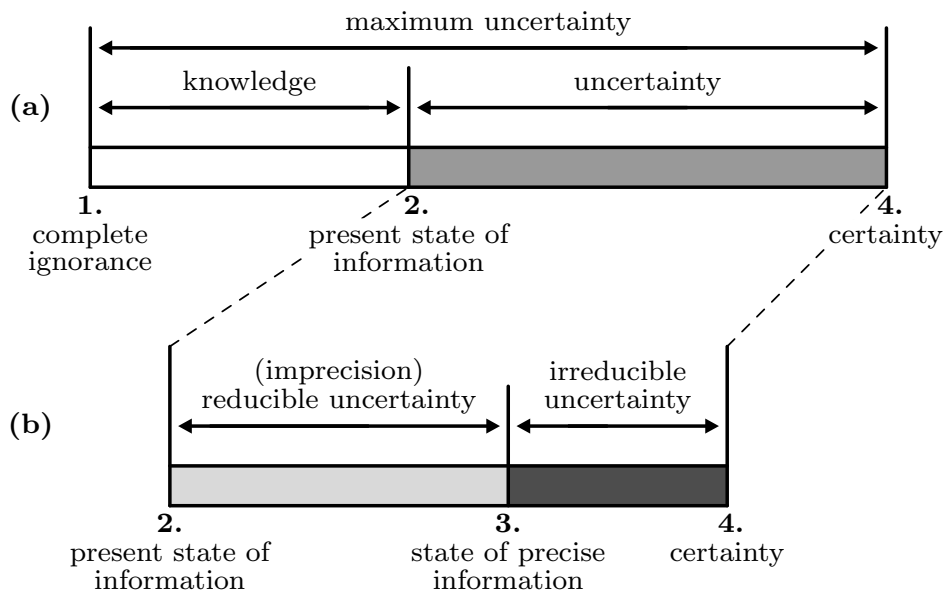


Figure 4.1: Interpretation of uncertainty; adapted from [172] and [168].

advances occur in scientific knowledge”. Nikolaidis remarks in [172] that further uncertainty taxonomies can be found in the literature. However, a broad consensus exists that in engineering practice a distinction between these two types of uncertainty is beneficial and sufficient [168, 169, 173]. Focusing on this two-part classification, for the first type frequently used terms are irreducible, aleatoric or objective uncertainty and the second is denoted as imprecision, epistemic uncertainty, reducible or subjective uncertainty. These terms are respectively utilized interchangeably among literature [168, 174]. However, the terminologies are up for debate as can be seen by comparing, e.g., [168, 175, 176]. Aughenbaugh & Paredis clarify in [168] the existence of aleatoric uncertainty as a controversial but philosophical issue and emphasize the terms irreducible uncertainty and imprecision with regard to practical application. Accordingly, these terms are used in the following.

Fig. 4.1 (b) illustrates the distinction into the above-mentioned two uncertainty types. Here, the state of precise information, shown as state 3, delimits irreducible uncertainty and imprecision. Thereby, the gap between state 3 and certainty denotes uncertainty that is claimed to be irreducible from the current perspective. This type arises from presumed variability and randomness and impedes the analyst from being certain throughout the evaluation process [173]. In contrast, the gap between the present state of information and state of precise information denotes imprecision. Imprecision arises, e.g., as only a limited amount of samples or subjective and, thus, fuzzy assessments of experts on component behavior are available. Further sources of imprecision and their consideration are discussed in [169] and [177]. Measures can be implemented to increase the quality of information and, therefore, reduce imprecision [173]. However, these are typically associated with effort and reaching the state of precise information may even be unfeasible.

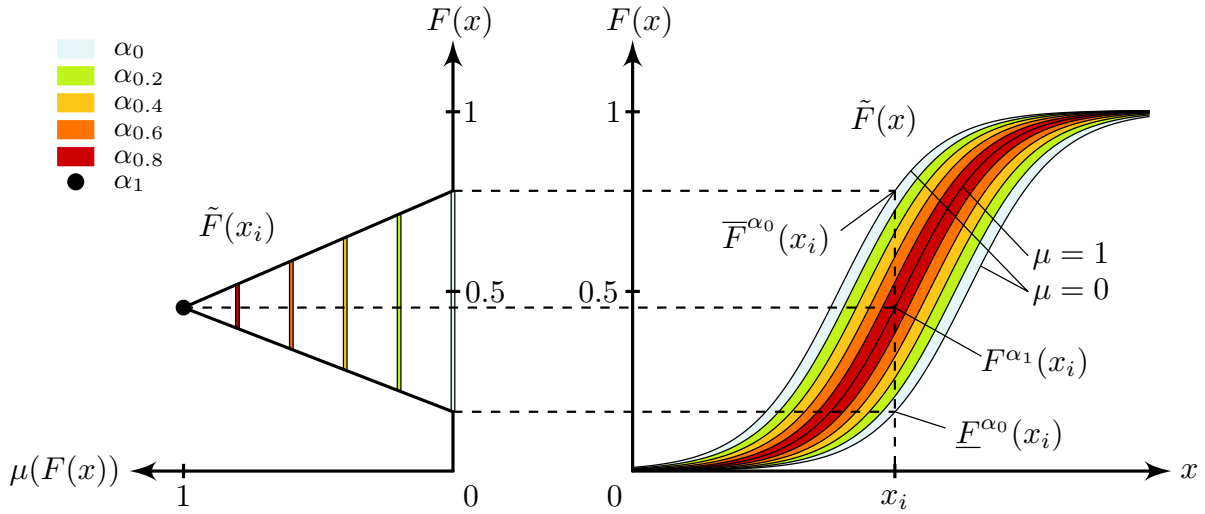


Figure 4.2: Fuzzy probability distribution function of a continuous fuzzy random variable; adapted from [224].

Implementation of uncertainty

Concepts to deal with uncertainty in a model can be distinguished into three groups, namely, non-probabilistic approaches, precise probability approaches and imprecise probability approaches [220]. In order to propagate a clear distinction between irreducible uncertainty and imprecision throughout analysis only the latter appears appropriate [220, 221]. Thereby, set-theoretical concepts describing imprecision, such as intervals or fuzzy sets, and probability distributions from traditional probability theory that represent irreducible uncertainty are combined [168, 222]. Among various alternatives, in this context fuzzy sets are beneficial [194, 223]. For instance, Beer et al. utilize fuzzy sets in reliability analyses and propose two approaches to evaluate these. For more information see [227] as well as [194].

4.2.3 Fuzzy probability

In system reliability engineering, imprecisions frequently occur, e.g., due to scarcity of data or vague expert knowledge regarding the underlying probability distribution types and distribution parameters of component lifetimes. Fuzzy probability theory enables to take these imprecisions into account.

Let $F(x)$ be a probability distribution function, describing the failure probability of a system component up to time x . Further, assume that the knowledge of the parameters of this distribution function is imprecise. Then Fig. 4.2 shows the fuzzy probability distribution function $\tilde{F}(x)$ describing this phenomenon, with $\mu(F(x))$ denoting the membership function of $F(x)$ and $\text{supp}(\tilde{F}(x)) = [\underline{F}^{\alpha_0}(x), \overline{F}^{\alpha_0}(x)]$ denoting the support of $\tilde{F}(x)$. Note that for $\mu(F(x)) = 1$, corresponding to an α -level of $\alpha = 1$, $\tilde{F}(x) = F(x)$.

In this work, all imprecise distribution parameters are modeled by triangular fuzzy numbers $\tilde{\theta} = (a/b/c)$, with $a < b < c$, $[a, c]$ denoting the base of $\tilde{\theta}$ and b denoting its vertex. In practice,

the fuzzy probability model can be learned from (precise or censored) lifetime data by using either frequentist or Bayesian statistical inference methods. For example, given a small number of precise lifetime data, the $(100 \cdot \alpha)\%$ confidence intervals can be inferred for $\tilde{\theta}$ with either confidence interval estimation or bootstrap approach, where α can be taken as the membership level. Comprehensive information on fuzzy probability and its practical applications is provided, e.g., in [224, 225].

4.2.4 Non-intrusive imprecise stochastic simulation

The NISS, according to [220] and [296], provides a general methodological framework for propagating parameterized imprecise probability models through a black-box simulator with only one stochastic simulation. Indeed, any stochastic simulation algorithm can be injected into this framework to tackle different types of problems.

The original extended Monte Carlo simulation (EMCS) method was introduced in [297] for parametric global sensitivity analysis as well as parametric optimization and was further developed in [220] and [296] into the NISS framework for efficient evaluation of moments of imprecise response functions in a structural context. For the classical EMCS, the unbiased estimators are derived by sampling from probability distribution functions of input variables with imprecise distribution parameters fixed at a particular point, hence, it has been referred to as LEMCS in further work. In [220], the GEMCS was established, where no fixed point of distribution parameter is required, but rather an auxiliary sampling distribution. Further, the combination of the LEMCS and GEMCS with high-dimensional model representation (HDMR) was presented in order to efficiently apply the NISS method to more sophisticated and high-dimensional models. Additionally, improvements for rare failure events were introduced to NISS in [296] and further developed in [298, 299].

Note that all NISS methods (including both LEMCS and GEMCS), although inspired by importance sampling, have significant different features, compared to the classical importance sampling including the one developed in [208]. The specific features of NISS can be summarized as follows: First, global NISS methods utilize samples generated from the joint space of component lifetimes and their imprecise parameters and show better global performance than the classical importance sampling, especially for the cases with large imprecision. Second, when applied to the cases with high-dimensional imprecise parameters, two types of HDMR decomposition are injected into LEMCS and GEMCS with proper truncation for substantial alleviating the expansion of variations of estimators, which is a common phenomenon appeared in all importance sampling based algorithms. Third, all classical stochastic simulation techniques for stochastic analysis, such as subset simulation and line sampling, developed for rare event analysis, can be injected into the NISS framework, following same rationale. This has substantially expended the suitability of NISS framework to different types of imprecise probability analysis tasks.

In this work, the LEMCS and GEMCS are reviewed, where LEMCS is the basis of all local NISS methods, while GEMCS provides a basis for all global NISS methods. The NISS methods are

originally developed for performance and reliability estimation of structures simulated with a black-box model, such as a finite element model.

4.3 Proposed methodology

In the following, the two basic NISS methods, LEMCS and GEMCS, are adapted and merged with the concept of survival signature allowing for efficient system reliability analyses under the constraint of imprecision. These two methods form the basis for all further developments included in the NISS framework.

Let $\mathbf{t} = (t_1, t_2, \dots, t_m)^\top$ denote the failure times of the components of a system and T_s indicates the failure time of the system. For a coherent system a non-decreasing deterministic function, denoted as $T_s = g(\mathbf{t})$, can be uniquely derived for modeling the relationship between system and component failure times. The failure times of all component functions are intrinsically random variables and the conditional joint density function is assumed to be $f(\mathbf{t}|\boldsymbol{\theta})$, where $\boldsymbol{\theta}$ indicates the q -dimensional vector of non-deterministic distribution parameters. The imprecision embodied through $\boldsymbol{\theta}$ might result from a lack of life data on components or expert knowledge and supports can be inferred by, e.g., confidence interval estimation. Based on the above setting, the system failure time is also a random variable with non-deterministic distribution parameters, where the probability distribution reflects the natural variability of system failure time and the bounds of probability reflect the degree of unknown on this variability. The system survival function can then be formulated as:

$$R_s(t, \mathbf{t}|\boldsymbol{\theta}) = \int_{\mathbb{R}^+} I[g(\mathbf{t}) > t] f(\mathbf{t}|\boldsymbol{\theta}) dt, \quad (4.4)$$

where \mathbb{R}^+ indicates the space of non-negative real numbers and $I[\cdot]$ is the indicator function with the values being either one if the argument is true or zero if it is false. With the above setting, the system survival function can be reformulated as:

$$R_s(t, \mathbf{t}|\boldsymbol{\theta}) = \int_{\mathbb{R}^+} I[g(\mathbf{t}) > t] \frac{f(\mathbf{t}|\boldsymbol{\theta})}{f(\mathbf{t}|\boldsymbol{\theta}^*)} f(\mathbf{t}|\boldsymbol{\theta}^*) dt, \quad (4.5)$$

where $\boldsymbol{\theta}^*$ can be any fixed and crisp point of $\boldsymbol{\theta}$. Then, given a set of random samples $\mathbf{t}^{(n)}$ ($n = 1, 2, \dots, N$) following $f(\mathbf{t}|\boldsymbol{\theta}^*)$, the LEMCS estimator of the system survival function is given as:

$$\hat{R}_s(t, \mathbf{t}|\boldsymbol{\theta}) = \frac{1}{N} \sum_{n=1}^N I[g(\mathbf{t}^{(n)}) > t] \frac{f(\mathbf{t}^{(n)}|\boldsymbol{\theta})}{f(\mathbf{t}^{(n)}|\boldsymbol{\theta}^*)}. \quad (4.6)$$

This estimator is unbiased and its variance can be easily derived. Given the above estimator, the bounds of the survival function can be computed by any global optimization algorithm, such as genetic and particle swarm algorithms.

The GEMCS method involves first attributing auxiliary distributions for $\boldsymbol{\theta}$, which, in the simplest case, can be uniform distributions within $[\boldsymbol{\theta}_{low}, \boldsymbol{\theta}_{up}]$. Let $p(\boldsymbol{\theta})$ denote the joint density

function of these auxiliary distributions and $p(\theta_i)$ the marginal density function of θ_i . Then a set of joint random samples $(\mathbf{t}^{(n)}, \boldsymbol{\theta}^{(n)})$ can be generated following the joint density function $f(\mathbf{t}, \boldsymbol{\theta}) = f(\mathbf{t}|\boldsymbol{\theta})p(\boldsymbol{\theta})$ of \mathbf{t} and $\boldsymbol{\theta}$, based on which the GEMCS estimator for the system survival function results as:

$$\hat{R}_s(t, \mathbf{t}|\boldsymbol{\theta}) = \frac{1}{N} \sum_{n=1}^N I[g(\mathbf{t}^{(n)}) > t] \frac{f(\mathbf{t}^{(n)}|\boldsymbol{\theta})}{f(\mathbf{t}^{(n)}|\boldsymbol{\theta}^{(n)})}. \quad (4.7)$$

Both the LEMCS and GEMCS performance might vary for different types of probability distributions or different distribution parameters and can depend on an appropriate choice for $\boldsymbol{\theta}^*$ and $p(\boldsymbol{\theta})$, respectively. More detailed information is provided in [220].

Another key feature of the classical NISS method is the HDMR, see [220, 296], based on which the behavior of the system survival function with respect to $\boldsymbol{\theta}$ can be learned visibly and the variation of estimators can be substantially reduced, especially when the number of components with imprecise distribution parameters is large. However, in this paper, the LEMCS and GEMCS estimator are solely utilized without HDMR decomposition.

4.3.1 LEMCS algorithm

A modified version of the MCS algorithm 2 in [114] is utilized as the stochastic simulation module for implementing LEMCS and GEMCS. The LEMCS algorithm is then described as follows:

Step A1. Discretize the support $[0, \bar{t}]$ of system failure time uniformly as $0 = t_{z1} < t_{z2} < \dots < t_{zd} = \bar{t}$ and initialize the value of $\boldsymbol{\theta}^*$ and the number N of deterministic simulations. Let $n = 1$.

Step A2. Sample the failure times $\mathbf{t}^{(n)} = (t_1^{(n)}, t_2^{(n)}, \dots, t_m^{(n)})$ for all components following $f(\mathbf{t}|\boldsymbol{\theta}^*)$ randomly.

Step A3. At each time instant t_{zi} , count the number of components working for each component type as $C_k(t_{zi})$, where $k = 1, 2, \dots, K$ denotes the component type.

Step A4. Evaluate the survival signature at each time instant as:

$$\Phi_{zi}^{(n)} = \Phi(C_1(t_{zi}), C_2(t_{zi}), \dots, C_K(t_{zi})).$$

Step A5. Define the weight function for the sample $\mathbf{t}^{(n)}$ as $w^{(n)}(\boldsymbol{\theta}) = \frac{f(\mathbf{t}^{(n)}|\boldsymbol{\theta})}{f(\mathbf{t}^{(n)}|\boldsymbol{\theta}^*)}$. If $n = N$, finish the simulation; else, let $n = n + 1$ and go back to Step A2.

Based on the samples $\Phi_{zi}^{(n)}$, the LEMCS estimator for the system survival function at time t_{zi} is formulated as:

$$\hat{R}_s(t_{zi}, \boldsymbol{\theta}) = \frac{1}{N} \sum_{n=1}^N \Phi_{zi}^{(n)} w^{(n)}(\boldsymbol{\theta}). \quad (4.8)$$

Computing at each time instant the minimum and maximum values of the estimator in Eq. 4.8, by utilizing any global optimization algorithm, leads to the estimated upper and lower bound of the system survival function.

4.3.2 GEMCS algorithm

The GEMCS algorithm is similar to the LEMCS algorithm except that the stochastic simulation needs to be implemented in the joint space of \mathbf{t} and $\boldsymbol{\theta}$. Given the auxiliary density function $p(\boldsymbol{\theta})$, the GEMCS algorithm is described as follows:

- Step B1. Discretize the support $[0, \bar{t}]$ of system failure time uniformly as $0 = t_{z1} < t_{z2} < \dots < t_{zd} = \bar{t}$ and initialize the number N of deterministic simulations. Let $n = 1$.
- Step B2. Generate a joint random sample $(\mathbf{t}^{(n)}, \boldsymbol{\theta}^{(n)})$ following the joint density $f(\mathbf{t}|\boldsymbol{\theta})p(\boldsymbol{\theta})$.
- Step B3. Same as Steps A3 and A4.
- Step B4. Evaluate the weight function for the joint sample $(\mathbf{t}^{(n)}, \boldsymbol{\theta}^{(n)})$ as $w^{(n)}(\boldsymbol{\theta}) = \frac{f(\mathbf{t}^{(n)}|\boldsymbol{\theta})}{f(\mathbf{t}^{(n)}|\boldsymbol{\theta}^{(n)})}$. If $n = N$, finish the simulation; else, let $n = n + 1$ and go back to Step B2.

The GEMCS estimator for the system survival function is formulated equivalently to the LEMCS estimator in Eq. 4.8 and the estimated upper and lower bound of the system survival function can be computed at each time instant by utilizing any optimization algorithm. Note that the upper and lower distribution parameter vectors $\bar{\boldsymbol{\theta}}(t_{zi})$ and $\underline{\boldsymbol{\theta}}(t_{zi})$, corresponding to the maximum and minimum survival function values at time t_{zi} , are time-dependent and might vary for different time points.

One of the factors when performing the GEMCS method is the pre-specification of the auxiliary density $p(\boldsymbol{\theta})$. It has been demonstrated that the type of auxiliary distribution has minor effect on the performance of GEMCS estimators [300]. In this work, it is set as the uniform distribution within the support of $\boldsymbol{\theta}$.

The most appealing aspect of both the LEMCS and GEMCS algorithm is that only a single stochastic simulation is required in order to deal with the imprecisions. Therefore, the traditional utilized double loop simulation can be avoided. For both LEMCS and GEMCS, the interval analysis and stochastic analysis has been successfully decoupled and the computational cost is mainly governed by the one stochastic simulation performed. Furthermore, due to the merging with the survival signature, the stochastic analysis has been separated from the system topology, thus, only one reliability analysis with respect to the topology is required for generating the survival signature. Besides these advantageous properties of the survival signature, it is precisely the feature of only a single required stochastic simulation, that makes the proposed methodology so efficient and clearly distinguishes it from traditional approaches. Due to this approach, for any NISS method combined with the concept of survival signature, the imprecise stochastic analysis for estimating the bounds of system survival function has been simplified significantly.

4.3.3 Repeated p-box analysis for fuzzy probability approximation

In order to compute the survival function of a system with components whose random failure times are based on distribution functions with imprecise distribution parameters modeled by independent fuzzy numbers with support $[a, c]$, a procedure is needed to handle these in probabilistic models. In [194] such a procedure is provided, that is based on a repeated p-box analysis. The procedure is shown in Fig. 4.3. Each x^α denotes an α -level set of the fuzzy number

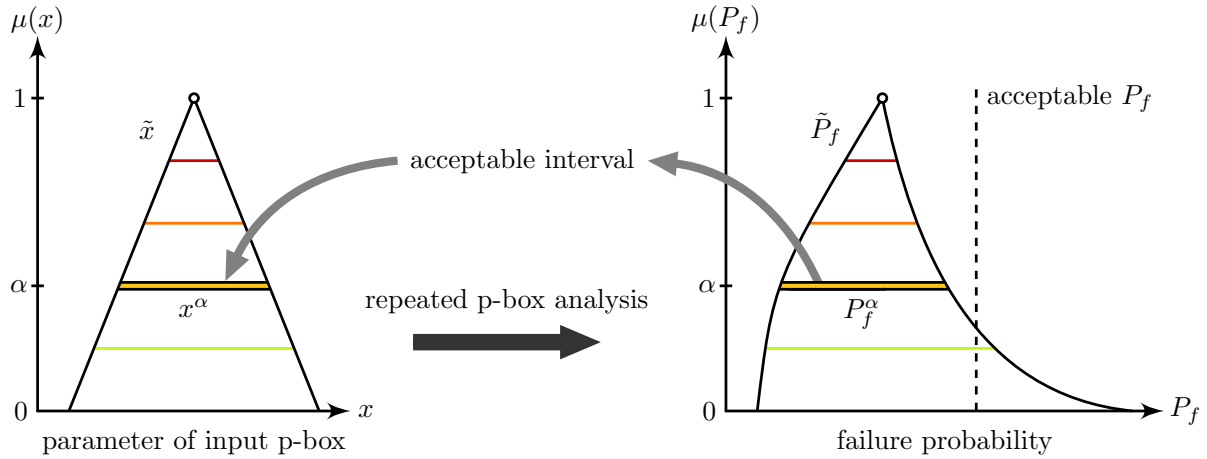


Figure 4.3: Nested p-box analysis to determine a fuzzy failure probability; adapted from [194].

\tilde{x} , representing an interval parameter of a probability distribution and, therefore, defining a p-box. This leads to an interval P_f^α associated with the same α -level. Repeating this p-box analysis with different α -levels leads to the fuzzy failure probability \tilde{P}_f . For more detailed information, see [194]. Note that the combined advantages of the proposed methodology, originating from the advantages of both the NISS methods and the concept of survival signature, as well as the beneficial synergy effects emerging from this combination, facilitate the nested p-box analysis with significantly reduced computational effort.

4.3.4 Decision-making procedure

In reality, decision-makers typically encounter situations of imprecise knowledge about component behavior as starting point. This might be the case in design and maintenance, if, e.g., only insufficient information on the installed components has been collected so far. Depending on the budget, gathering precise information for each component type, e.g., via experimental campaigns, might not be feasible, impeding proper reliability analyses. In fact, a complete elimination of imprecision is in most cases neither necessary nor cost-efficient. Thus, a procedure for identifying a critical level of imprecision is crucial for cost-efficient decision-making, balancing the amount of imprecision and costs associated with its reduction. Integral parts of such a procedure are illustrated in Fig. 4.4.

To establish a basis for this procedure, the spectrum of imprecision can be represented by

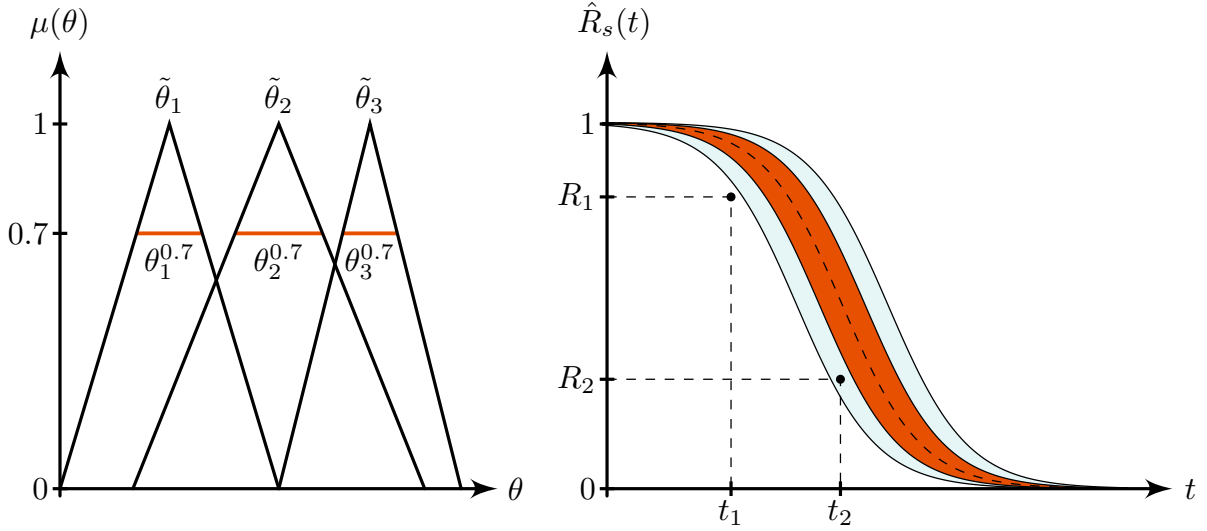


Figure 4.4: Decision-making procedure.

means of nested p-boxes, as proposed in Section 4.3.3. Further, a certain number of α -levels is determined. Note that a higher number of α -levels yields a more comprehensive imprecision analysis. In the simplest case, each upper and lower parameter bound is relatively changed to the same extent per α -level. Then, each $\theta^\alpha = (\theta_1^\alpha, \theta_2^\alpha, \dots, \theta_q^\alpha)$, with $\alpha \in [0, 1]$ and the number of distribution parameters q , is a tuple of parameter intervals θ_i^α of the fuzzy distribution parameters $\tilde{\theta}_i$. Such an implementation allows the identification of a global critical imprecision level, as the imprecisions for each component type are altered simultaneously. A more detailed critical imprecision identification can be conducted by considering various mixed combinations of imprecision levels or, in a more sophisticated manner, e.g., by means of importance measures in a sensitivity analysis. However, this is beyond the scope of this paper. According to the simplest case, for each θ^α the imprecise model is evaluated, resulting in the lower survival functions $\hat{R}_s^\alpha(t_{zi}) = \hat{R}_s^\alpha(t_{zi}, \underline{\theta}^\alpha(t_{zi}))$ and upper survival functions $\bar{R}_s^\alpha(t_{zi}) = \hat{R}_s^\alpha(t_{zi}, \bar{\theta}^\alpha(t_{zi}))$ at each time step t_{zi} . Correspondingly, the time-dependent upper and lower distribution parameter vectors are $\bar{\theta}^\alpha(t_{zi}) \in \mathcal{I} = \{(\theta_1, \theta_2, \dots, \theta_q) | \theta_i \in \theta_i^\alpha \forall i = 1, 2, \dots, q\}$ and $\underline{\theta}^\alpha(t_{zi}) \in \mathcal{I}$. Further, a set of reliability requirements $\mathcal{R} = \{(t_1, R_1), (t_2, R_2), \dots, (t_r, R_r)\}$ is established, where the tuple (t_j, R_j) , with $j = 1, 2, \dots, r$, specifies a pair of time and reliability values for r requirements. Typically, in practice, only $\hat{R}_s^\alpha(t_{zi})$ is relevant with respect to \mathcal{R} . Then, $\hat{R}_s^{cr}(t_{zi}) = \min_\alpha \{\hat{R}_s^\alpha(t_{zi}) | \hat{R}_s^\alpha(t_j) \geq R_j, (t_j, R_j) \in \mathcal{R} \forall j = 1, 2, \dots, r\}$ is the critical, i.e., last acceptable, lower survival function. Thereby, $\alpha_{cr} = \arg \min_\alpha \{\hat{R}_s^\alpha(t) | \hat{R}_s^\alpha(t_j) \geq R_j, (t_j, R_j) \in \mathcal{R} \forall j = 1, 2, \dots, r\} \in [0, 1]$ indicates the critical α -level. Note that lower distribution bounds not necessarily yield lower response function bounds and vice versa. In accordance, $\theta_{cr} = [\underline{\theta}^{\alpha_{cr}}, \bar{\theta}^{\alpha_{cr}}]$ is the interval of acceptable imprecision. As a consequence, imprecision has to be reduced at least up to the bounds of θ_{cr} . This reduction can be achieved for instance by investing more budget in experimental campaigns, destructive testing, etc.

The procedure allows decision-makers the straightforward and reliable identification of acceptable levels of imprecision in the underlying failure probabilities, e.g., in the design of new systems. Corresponding to the requirements defined in the right graph of Fig. 4.4, the acceptable α -level is $\alpha_{cr} = 0.7$ with the tuple of parameter intervals $\theta_{cr} = (\theta_1^{0.7}, \theta_2^{0.7}, \theta_3^{0.7})$ contained in the tuple of fuzzy numbers $\tilde{\theta} = (\tilde{\theta}_1, \tilde{\theta}_2, \tilde{\theta}_3)$. This decision-making procedure is demonstrated for the case study in Section 4.5.3.

4.4 Multistage high-speed axial compressor

Axial compressors are complex multi-component machines that are employed in major sectors of society, e.g., in the industrial sector, as a key component of gas turbines for electricity production or as part of aircraft engines in the public transport or military sector. Therefore, in both design and maintenance, it is critical to consider as many system performance influencing, certain and uncertain, information as possible to maximize the reliability of the compressor efficiently. In order to illustrate this, the proposed method is applied to a functional model of an axial compressor.

4.4.1 Model

In [251] a functional model of an axial compressor is developed as the foundation for a reliability analysis. This model has been created to represent the reliability characteristic and functionality of the four-stage high-speed axial compressor of the Institute for Turbomachinery and Fluid Dynamics at Leibniz Universität Hannover. Detailed information about this axial compressor is provided in [253].

The functional model captures the dependence of the overall compressor performance, namely, the total-to-total pressure ratio and the total-to-total isentropic efficiency, on the surface roughness of the individual blades, arranged in rotor and stator rows. It is based on the results of a sensitivity analysis of an aerodynamic model of the compressor. A network representation of the functional model is shown in Fig. 4.5. Each component represents either a stator (S1 — S4) or rotor row (R1 — R4).

The rows are classified into four component types. This classification as well as the component arrangement is chosen based on the effect of their blade roughness on the two performance parameters of the axial compressor. More specifically, a connection between start and end implies a functioning state of the compressor and an interruption of this connection means exceeding a roughness-related performance variation of at least 25%, corresponding to a non-functioning state. More detailed information on the functional model and its formulation can be obtained from [251].

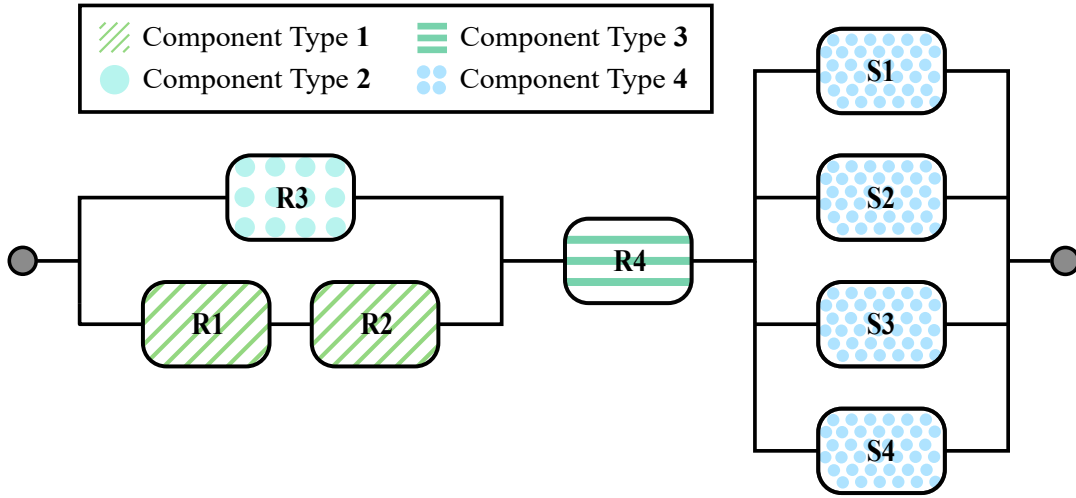


Figure 4.5: Functional model of the multi-stage high-speed axial compressor.

4.4.2 Reliability analysis

For the time-dependent reliability analysis, each row, i.e., each component of the functional model, is characterized by a failure probability depending on its component type. Note that the model is thus formally a reliability block diagram (RBD) [108]. In practice, the underlying distribution functions have to be derived from existing operational data. However, in order to prove the usability of the proposed method and the capability of dealing with imprecisions, exponential functions with imprecise parameters are assumed for all components. The imprecise parameters are modeled by triangular fuzzy numbers. Depending on the respective component type, the following parameters are assumed: $\lambda_1 = (0.1/0.15/0.2)$ for type 1; $\lambda_2 = (0.2/0.25/0.3)$ for type 2; $\lambda_3 = (0.4/0.5/0.6)$ for type 3; $\lambda_4 = (0.6/0.7/0.8)$ for type 4.

After determining the survival signature of the compressor, in a first step, the imprecise parameters are taken into account by approximating them with a single p-box, being the base of each triangle fuzzy parameter, corresponding to an α -level of $\alpha = 0$. The imprecise parameters result as: $\lambda_1 \in [0.1, 0.2]$ for type 1; $\lambda_2 \in [0.2, 0.3]$ for type 2; $\lambda_3 \in [0.4, 0.6]$ for type 3; $\lambda_4 \in [0.6, 0.8]$ for type 4. Based on the functional compressor representation, shown in Fig. 4.5, the upper and lower bounds of the survival function of the compressor are obtained and displayed in Fig. 4.6: 1. via traditional double loop approach; 2. via LEMCS algorithm with $\lambda_1^* = 0.1$, $\lambda_2^* = 0.2$, $\lambda_3^* = 0.4$, $\lambda_4^* = 0.6$ as the best fits for λ_i^* ; 3. via GEMCS algorithm with $p(\boldsymbol{\lambda})$ assumed to be uniform; 4. analytically. Note that the sampling density for LEMCS estimation is generated by setting λ_i^* at their lower bounds. For exponential distribution, only with this setting, the support of the sampling density will coincide with the support of the imprecise probability models when their distribution parameters vary in their imprecise intervals. This principle for specifying the sampling density is referred to in [220]. The double loop approach is conducted with 5 000 samples (failure times) on the inner loop and 1 000 samples (λ -values) on the outer loop. In other words: 1 000 λ -vectors are sampled (epistemic space), representing 1 000 different probabilistic

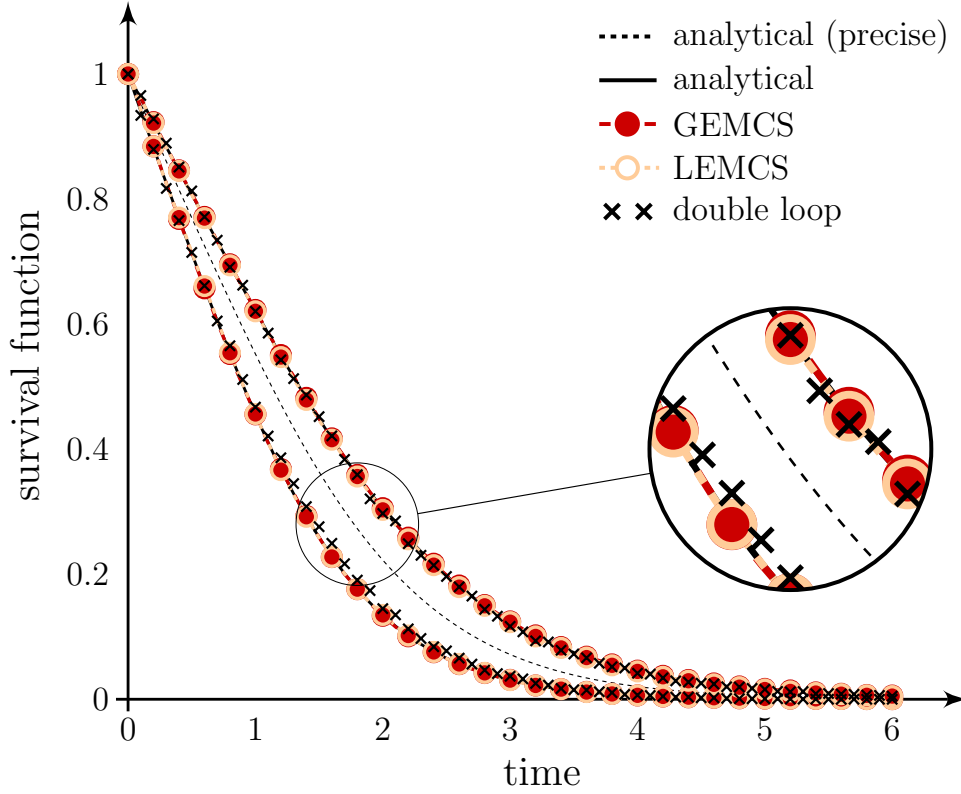


Figure 4.6: Survival function bounds of the functional compressor model via double loop approach, LEMCS algorithm, GEMCS algorithm and analytically.

models. Each model is solved by MCS algorithm 2 in [114], generating 5 000 failure time vectors per model, i.e., a total of 5 000 000 samples. Then the enveloping system reliability is determined by identifying the minimum and maximum survival function value for each time step. Note that the number of samples for the double loop approach, i.e., the number of failure times as well as the number of samples in epistemic space, is adopted from [114]. For both LEMCS and GEMCS where only one simulation is required, 100 000 samples (failure times) are generated each, i.e., only 1/50th of the sample size compared to the double loop approach. Time discretization is set to $\Delta t = 0.05$. Furthermore, the precise survival function of the axial compressor model, i.e., with distribution parameters $\lambda_i = b_i$, is determined and displayed in Fig. 4.6 as well.

Clearly, both the LEMCS and GEMCS algorithm approximate the analytically calculated upper and lower bound of the survival function accurately with relative errors of: $\bar{\delta}_{LEMCS} = 0.23\%$, $\underline{\delta}_{LEMCS} = 0.23\%$ and $\bar{\delta}_{GEMCS} = 0.29\%$, $\underline{\delta}_{GEMCS} = 0.3\%$, where $\bar{\delta}$ relates to the upper and $\underline{\delta}$ to the lower bound of the survival function. Despite a 50-times increased sample size, the double loop approach performs significantly worse and does not capture the outer boundaries of the survival function correctly, see Fig. 4.6. Correspondingly, the relative errors are larger with: $\bar{\delta}_{DoubleLoop} = 0.98\%$ and $\underline{\delta}_{DoubleLoop} = 2.58\%$. To achieve the same quality of results with the double loop approach as with the LEMCS or GEMCS, significantly more samples than the 5 000 000 would be required.

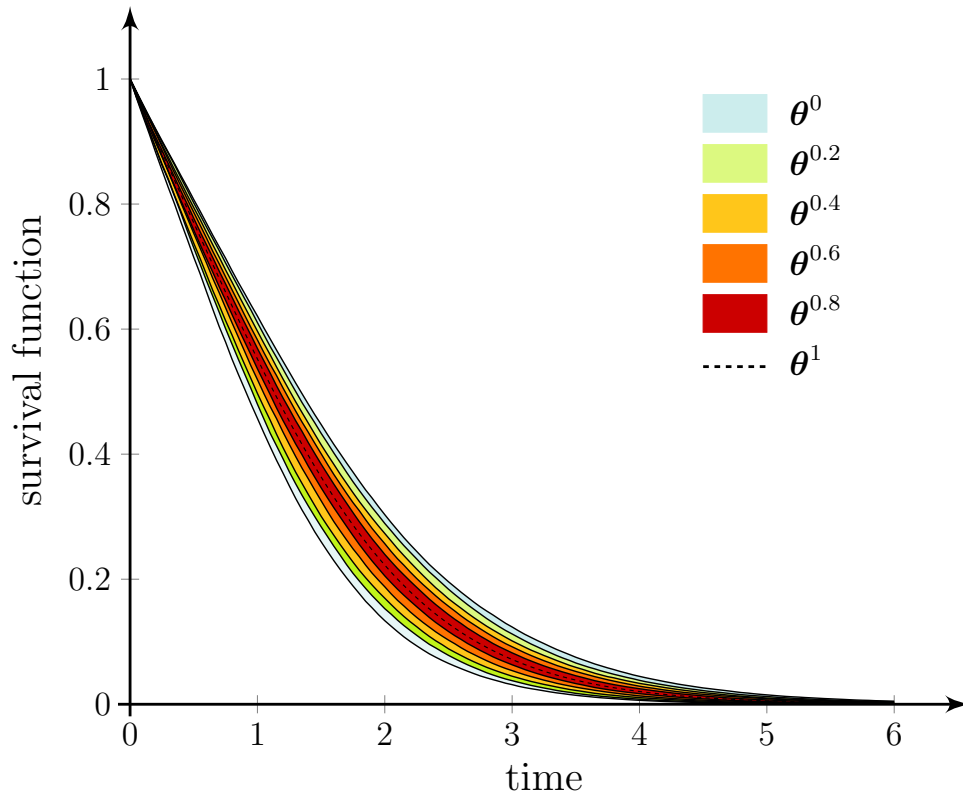


Figure 4.7: Survival function bounds of a functional compressor model via LEMCS algorithm with fuzzy probability approximation.

It shall be noted, that, in general, the GEMCS algorithm has better global performance than the LEMCS algorithm, as demonstrated and discussed in the following, second case study. Further, the approximation quality of the LEMCS algorithm highly depends on the choice, respectively, on the knowledge of the preselected distribution parameters λ_i^* .

In a second step, by performing a nested p-box analysis to determine fuzzy failure probabilities, described in Section 4.3.3, further bounds of the survival function for different imprecision levels can now be determined, based on various α -levels. With regard to the survival signature, these only represent a change in the probability structure. Due to the separation between topological and probability structure, the survival signature does not have to be recalculated, neither for parameter variations within an α -level, nor for each new α -level, only the probability structure has to be adapted. This results in a substantial reduction of the computational effort.

The results of the LEMCS algorithm for different α -levels are shown in Fig. 4.7. Note that for each α -level just one single stochastic simulation, according to Section 4.3.1, has to be performed. Clearly, these results support decision-makers in design and maintenance processes of complex capital goods to estimate the level of imprecision that is bearable and still ensures acceptable reliability.

4.5 Complex system

In [114] the authors test their introduced simulation approaches for reliability analysis on an arbitrary complex system. In order to demonstrate the broad applicability as well as efficiency of the method proposed in this work, the complex system from [114] is considered and a reliability analysis is conducted, taking into account imprecisions.

4.5.1 Model

The complex system consists of 14 components each of which is assigned to one of six component types. Figure 4.8 illustrates the complex system and the assignment of components to their types. A connection between the start and destination node indicates a functioning and an interruption of this connection a non-functioning state of the system.

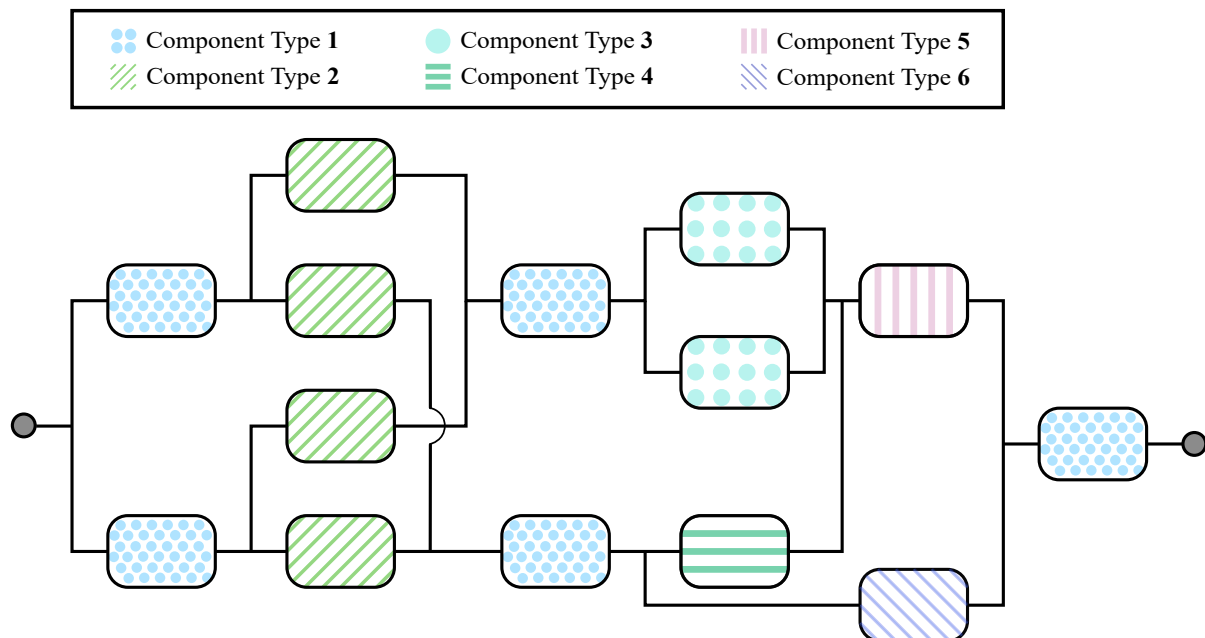


Figure 4.8: Representation of the arbitrary complex system with 14 components, adapted from [114].

4.5.2 Reliability analysis

Each system component is characterized by a specific time-dependent failure behavior depending on its assigned component type. Again, in practice, the underlying distribution functions, describing this behavior, need to be derived from existing operational data. However, for the purpose of proof of concept and applicability, the arbitrary distributions and corresponding imprecise parameters shown in Tab. 4.1 are assumed. Note that thus the complex system is formally an RBD. As for the reliability analysis in the previous section, the imprecise distribution parameters are modeled by triangular fuzzy numbers.

Table 4.1: Distribution functions and parameters for each component type of the complex system.

Component type	Distribution	Parameters	Triangular fuzzy numbers
1	Weibull	[scale, shape]	[(3.6/4.0/4.4), (2.1/2.25/2.4)]
2	Exponential	[λ]	[(0.1/0.15/0.2)]
3	Weibull	[scale, shape]	[(2.9/3.05/3.2), (0.8/0.95/1.1)]
4	Log-normal	[μ, σ]	[(2.2/2.35/2.5), (3.3/3.4/3.5)]
5	Exponential	[λ]	[(0.2/0.25/0.3)]
6	Gamma	[scale, shape]	[(2.1/2.2/2.3), (3.2/3.35/3.5)]

The survival signature of the complex system is provided in Tab. 4.2 and Tab. 4.3. For the sake of conciseness, only the non-trivial survival signature values are shown, i.e., all values that are not equal to zero or one.

For the time-dependent reliability analysis, the imprecise distribution parameters are first assumed to be precise by considering just the vertex b of each triangular fuzzy number. Second, the analysis is conducted by approximating the distribution parameters with a single p-box, corresponding to the base boundaries a and c of the fuzzy numbers. Third, the full imprecision is addressed in Section 4.5.3 by considering the fuzzy numbers according to the repeated p-box analysis described in Section 4.3.3.

In Fig. 4.9 the resulting survival function bounds of the complex system are displayed: 1. via traditional double loop approach; 2. via LEMCS algorithm with θ_i^* corresponding to the upper base bounds c_i of each fuzzy parameter for all two-parametric distributions and with θ_i^* corresponding to the lower base bounds a_i for both exponential distributions, see Tab. 4.1; 3. via GEMCS algorithm with $p(\theta)$ assumed to be uniform; 4. analytically. Again, the double loop approach is conducted with 5 000 samples (failure times) on the inner loop and 1 000 samples (θ -values) on the outer loop. As in the previous case study, the number of samples for the double loop approach is adopted from [114]. For the one required LEMCS and GEMCS simulation, 200 000 samples (failure times) are generated each, i.e., only 1/25th of the sample size compared to the double loop approach. Time discretization is again set to $\Delta t = 0.05$. In addition, the precise survival function of the complex system, i.e., with distribution parameters $\theta_i = b_i$, is determined and displayed in Fig. 4.9.

As in the previous analysis of the axial compressor, both the LEMCS and GEMCS algorithm approximate the analytically determined bounds of the survival function of the complex system with high accuracy, see Fig. 4.9. However, considering the relative errors of both algorithms, it is noticeable that the GEMCS approximates both bounds equally well, with errors of $\bar{\delta}_{GEMCS} = 0.15\%$ and $\underline{\delta}_{GEMCS} = 0.12\%$, whereas the LEMCS algorithm provides a deviation in the quality of the bound approximation that is more significant with $\bar{\delta}_{LEMCS} = 0.06\%$ and $\underline{\delta}_{LEMCS} = 0.32\%$. The different bound qualities provided by the LEMCS are due to its locality property that is determined by the choice of the preselected θ^* . The LEMCS performs locally, i.e., in the region

Table 4.2: Non-trivial survival signature values of the complex system, shown in Fig. 4.8 — Part 1.

l_1	l_2	l_3	l_4	l_5	l_6	$\Phi(l_1, \dots, l_6)$
3	1	[1,2]	0	1	0	1/20
3	1	[0,1,2]	[0,1]	0	1	1/20
3	1	0	1	1	[0,1]	1/20
3	1	0	0	1	1	1/20
3	2	[1,2]	[0,1]	0	1	1/10
3	2	[1,2]	0	1	0	1/10
3	2	0	1	1	[0,1]	1/10
3	2	0	1	0	1	1/10
3	2	0	0	[0,1]	1	1/10
3	1	[1,2]	1	1	[0,1]	1/10
3	1	[1,2]	0	1	1	1/10
3	3	[0,1,2]	[0,1]	0	1	3/20
3	3	[1,2]	0	1	0	3/20
3	3	0	1	1	[0,1]	3/20
3	3	0	0	1	1	3/20
3	4	[0,1,2]	[0,1]	0	1	1/5
3	4	[1,2]	0	1	0	1/5
3	4	0	1	1	[0,1]	1/5
3	4	0	0	1	1	1/5
3	2	[1,2]	1	1	[0,1]	1/5
3	2	[1,2]	0	1	1	1/5
4	1	[1,2]	[0,1]	0	1	1/5
4	1	[1,2]	0	1	0	1/5
4	1	0	1	1	[0,1]	1/5
4	1	0	0	[0,1]	1	1/5
4	1	0	1	0	1	1/5
3	3	[1,2]	1	1	[0,1]	3/10
3	3	[1,2]	0	1	1	3/10

of θ^* excellent but worse on a global scale. However, since with the GEMCS all failure times are sampled uniformly over the entire range of θ , it has better global performance, as shown by these results. It shall be noted that in case of rare failure events, as stated in [220] for both original NISS methods, also for the adapted method proposed in this work, instabilities may occur, depending on the sample size. Guidance on selecting an appropriate sample size is provided at the end of this section. If rare failure events are of special concern, it is recommended to use the NISS methods driven by advanced stochastic simulation techniques such as subset simulation and line sampling, see [296, 298, 299] for more details.

The difference between both algorithms is especially apparent for complex systems such as the one considered in Fig. 4.8, with various component types and various underlying multi-parametric and imprecise failure distribution functions. However, for less complex systems with single-

Table 4.3: Non-trivial survival signature values of the complex system, shown in Fig. 4.8 — Part 2.

l_1	l_2	l_3	l_4	l_5	l_6	$\Phi(l_1, \dots, l_6)$
4	2	[0,1,2]	[0,1]	0	1	11/30
4	2	[1,2]	0	1	0	11/30
4	2	0	1	1	[0,1]	11/30
4	2	0	0	1	1	11/30
3	4	[1,2]	1	1	[0,1]	2/5
3	4	[1,2]	0	1	1	2/5
4	1	[1,2]	1	1	[0,1]	2/5
4	1	[1,2]	0	1	1	2/5
4	3	[0,1,2]	[0,1]	0	1	1/2
4	3	[1,2]	0	1	0	1/2
4	3	0	1	1	[0,1]	1/2
4	3	0	0	1	1	1/2
5	1	[0,1,2]	[0,1]	0	1	1/2
5	1	[1,2]	0	1	0	1/2
5	1	0	1	1	[0,1]	1/2
5	1	0	0	1	1	1/2
4	4	[0,1,2]	[0,1]	0	1	3/5
4	4	[1,2]	0	1	0	3/5
4	4	0	1	1	[0,1]	3/5
4	4	0	0	1	1	3/5
4	2	[1,2]	1	1	[0,1]	2/3
4	2	[1,2]	0	1	1	2/3
4	[3,4]	[1,2]	1	1	[0,1]	4/5
4	[3,4]	[1,2]	0	1	1	4/5
5	2	[0,1,2]	[0,1]	0	1	5/6
5	2	[1,2]	0	1	0	5/6
5	2	0	1	1	[0,1]	5/6
5	2	0	0	1	1	5/6

parametric distribution functions of the same type as given for the axial compressor model in the previous section, the LEMCS performs equally well at both bounds and the errors are barely different from those of the GEMCS. Similar to the previous analysis of the axial compressor, the traditional double loop approach provides substantially worse approximations despite a significantly larger sample size, as clearly shown in Fig. 4.9, with errors of $\bar{\delta}_{DoubleLoop} = 2.07\%$ and $\underline{\delta}_{DoubleLoop} = 1.93\%$. Again, as in the previous case study, to achieve the same quality of results with the double loop approach as with the LEMCS or GEMCS, significantly more samples than the 5 000 000 would be required.

In Fig. 4.10 a convergence study for the complex system, illustrated in Fig. 4.8, is shown. Both algorithms are considered: On the left, the results of the GEMCS and, on the right, the results of the LEMCS algorithm are depicted. The graphs display the relative error between the

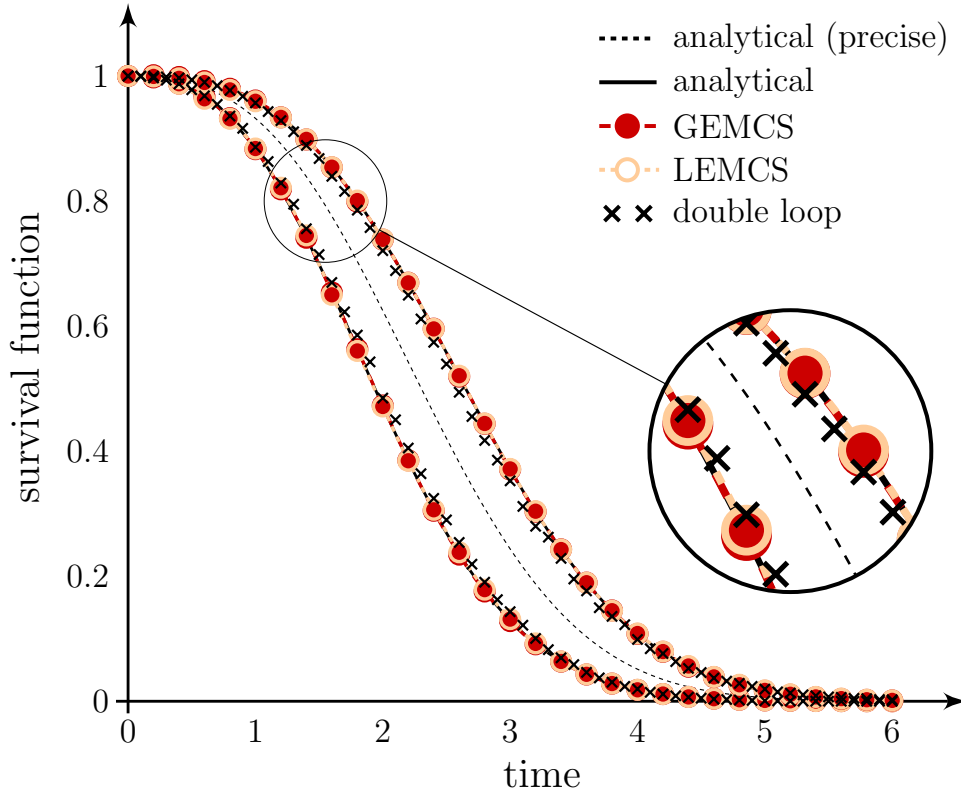


Figure 4.9: Survival function bounds of the complex system, displayed in Fig. 4.8, via double loop approach, LEMCS algorithm, GEMCS algorithm and analytically.

results of the proposed estimator algorithms and the analytically evaluated survival function bounds, plotted over various sample sizes with 500 evaluations each, reaching from 100 up to 250 000 samples. On the top, the relative error is evaluated for the upper survival function bound and, on the bottom, the relative error is evaluated for the lower survival function bound. The errors decrease significantly with increasing sample size and, clearly, for both algorithms and both bounds convergence is to observe. For the upper bound of the survival function via LEMCS algorithm, even small sample sizes are sufficient to yield low median errors and variances compared to the GEMCS results due to the specific choice of θ^* . In contrast, for the lower bound, the LEMCS performs significantly worse than the GEMCS. This demonstrates the superior global performance of the GEMCS algorithm compared to the LEMCS, while the LEMCS algorithm shows better local performance. However, considering the GEMCS algorithm, the slightly larger upper median error indicates the upper survival function bound as a more challenging region for the global estimator. As stated in Section 4.4.2 for exponential distributions, this observation relates to the point that the support of the sampling density should ideally coincide with the support of the density with parameters varying in their imprecise intervals, see [220]. However, this condition is not given for the majority of GEMCS samples at the upper bound, leading to the slightly worse results compared to the lower bound.

As a supplementary decision-making indicator, the coefficient of variation can be considered to

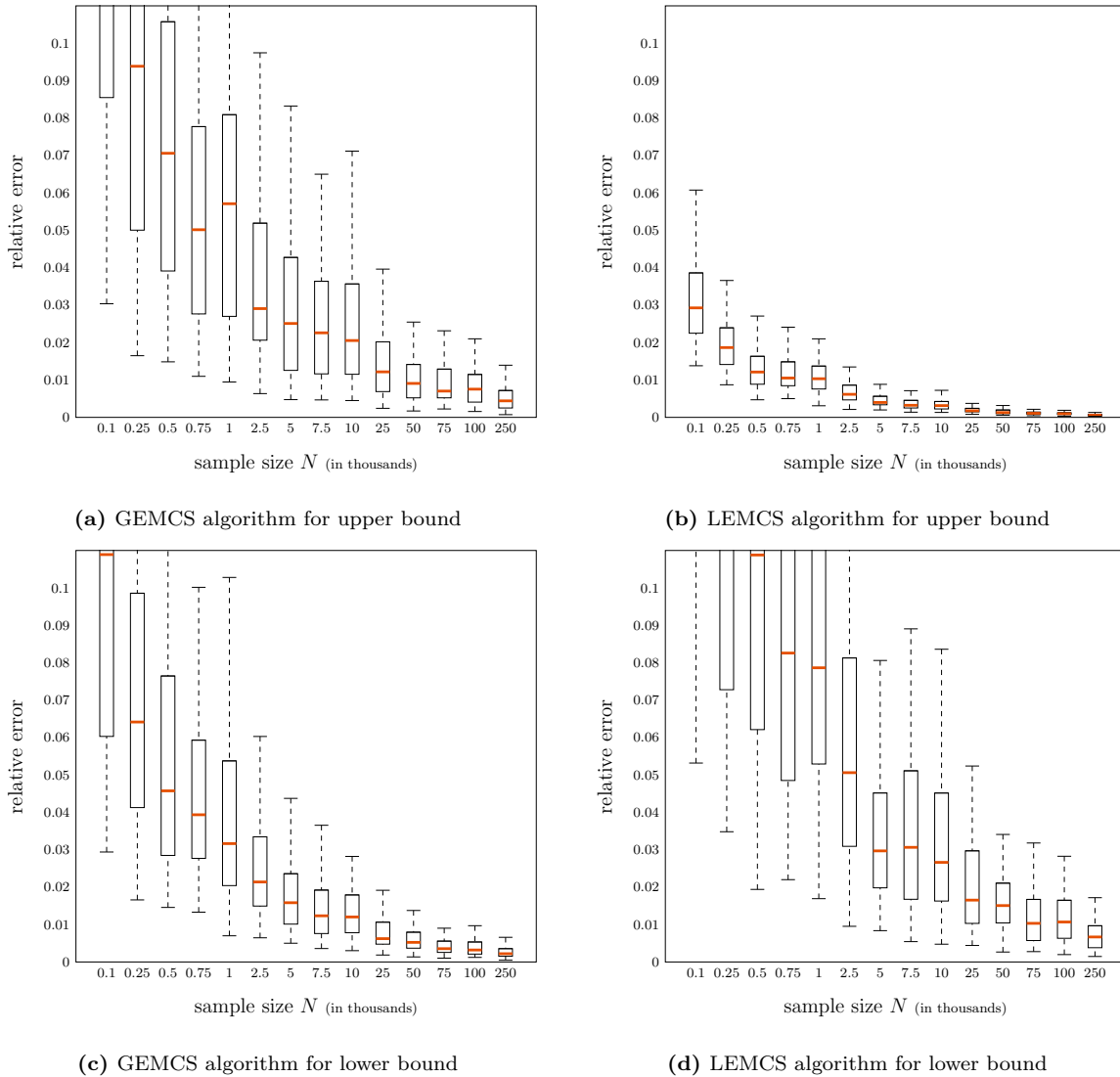


Figure 4.10: Convergence study of the GEMCS and LEMCS algorithms with the relative error of the corresponding survival function bounds with respect to the sample size over 500 evaluations each.

adaptively specify the required sample size. For instance, a threshold can be set for the coefficient of variation, e.g., (5%). If the estimated coefficient is above this threshold, more samples should be considered in order to reduce the variation.

4.5.3 Imprecision decision-making

Given the fuzzy numbers specified in Tab. 4.1, the spectrum of imprecision is represented by means of a repeated p-box analysis as described in Section 4.3.3. The nested p-box analysis conducted via the GEMCS algorithm provides further survival function bounds of the complex system, corresponding to different α -levels, as shown in Fig. 4.11. Due to the separation between topological and probability structure, the survival signature does not have to be recalculated,

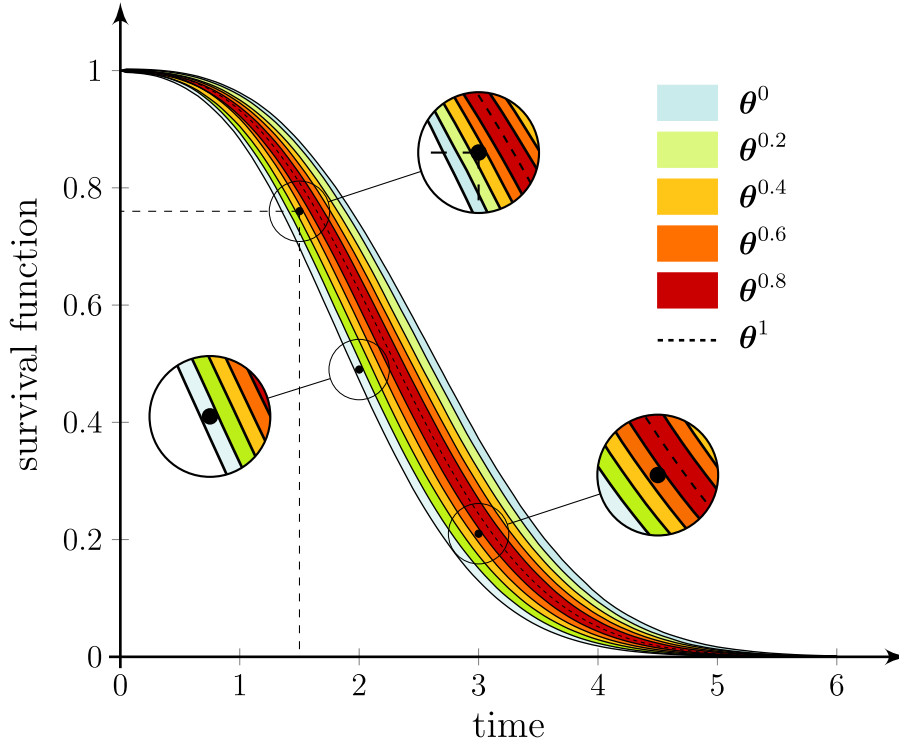


Figure 4.11: Survival function bounds of the complex system, displayed in Fig. 4.8, via GEMCS algorithm with fuzzy probability approximation.

neither for parameter variations within an α -level, nor for each new α -level, only the probability structure has to be adapted. Consequently, for each α -level only a single stochastic simulation, according to Section 4.3.2, has to be performed. This enables comprehensive reliability analyses with substantially reduced cost compared to traditional approaches. In order to perform decision-making concerning the reduction of system components inherent imprecision, reliability requirements can be established, according to Section 4.3.4. In this case study, requirements are arbitrarily assumed with $\mathcal{R} = \{(t_1, R_1), (t_2, R_2), (t_3, R_3)\} = \{(1.5, 0.76), (2, 0.49), (3, 0.21)\}$, as illustrated in Fig. 4.11. Due to $\alpha_{cr} = \arg \min_{\alpha} \{\hat{R}_s^{\alpha}(t) | \hat{R}_s^{\alpha}(t_j) \geq R_j, (t_j, R_j) \in \mathcal{R} \forall j = 1, 2, 3\} = \arg \min_{\alpha} \{\hat{R}_s^{\alpha}(t) | \hat{R}_s^{\alpha}(1.5) \geq 0.76, \hat{R}_s^{\alpha}(2) \geq 0.49, \hat{R}_s^{\alpha}(3) \geq 0.21\} = \arg \min_{\alpha} \{\hat{R}_s^{0.8}(t), \hat{R}_s^1(t)\} = 0.8$. Note that $\hat{R}_s^1(t) = \hat{R}_s^1(t) = \overline{\hat{R}_s^1}(t)$. Imprecision should be reduced at least up to a level of $\alpha = 0.8$ for all component types corresponding to the tuple of parameter intervals of $\theta_{cr} = (\theta_1^{0.8}, \theta_2^{0.8}, \dots, \theta_{10}^{0.8})$ with $\theta_1^{0.8} = [3.92, 4.08]$, $\theta_2^{0.8} = [2.22, 2.28]$, $\theta_3^{0.8} = [0.12, 0.18]$, $\theta_4^{0.8} = [3.02, 3.08]$, $\theta_5^{0.8} = [0.92, 0.98]$, $\theta_6^{0.8} = [2.32, 2.38]$, $\theta_7^{0.8} = [3.38, 3.42]$, $\theta_8^{0.8} = [4.00, 4.33]$, $\theta_9^{0.8} = [3.32, 3.38]$, $\theta_{10}^{0.8} = [2.18, 2.22]$.

4.6 Conclusion and outlook

The present paper introduces a novel methodology supporting decision-making in the context of system reliability analysis, taking into account imprecisions. It allows to efficiently estimate the system reliability in design and maintenance processes, considering uncertainty in various levels, underlying the system component behavior. Thereby, decision-makers are enabled to identify a bearable level of imprecision that still ensures acceptable system reliability.

The proposed method consists of the sophisticated union of the concept of survival signature with two adapted extended MCS methods (NISS methods), thus representing a novel development combining two approaches from two different fields. Considering imprecision into the probabilistic structure by means of fuzzy probabilities and utilizing a nested p-box analysis for approximating this fuzziness allows for the ability of critical imprecision identification. The provided method combines both tremendous advantages of its two main components: 1. the application of the concept of survival signature dramatically reduces the computational effort for the analysis, since once it has been computed, any number of probability structures can be tested without having to recompute it and 2. the utilization of both adapted NISS methods is accompanied by the necessity of only a single stochastic simulation per considered uncertainty level and consequently a substantially reduced sample size compared to traditional approaches, leading to another significant improvement of efficiency. Precisely these two characteristics and the symbiosis between them make the proposed methodology so efficient and widely applicable.

The novel approach is employed to the functional model of an axial compressor as well as to an arbitrary complex system. A comparison of analytical and numerical results proves the applicability of the method. However, in general, the LEMCS exhibits more local accuracy, while the GEMCS possesses better global performance and leads to superior results, especially for systems with complex imprecise probability structure. In terms of choice of method and application area, the LEMCS is preferable if accurate local performance is required and the knowledge for an educated guess of θ^* is available. While GEMCS should be applied if no prior knowledge about the uncertain system behavior is present. Further, a combination of both methods can be practical as well. First, GEMCS can be utilized to evaluate the neighborhood in which the parameter vector θ yields the critical survival function bound. Second, LEMCS can be applied to compute the results in the desired area of interest more accurately.

Further research should address the challenge of computing the survival signature for lifelike, large and complex systems with components of various types since it is highly demanding or even unfeasible. Thus, improved methods for determining the survival signature or enhanced methods for approximations are required. In addition, future work of the authors will address an improved rare failure event estimation and further performance improvements, such as the utilization of an HDMR.

Acknowledgment

Funded by the Deutsche Forschungsgemeinschaft (DFG, German Research Foundation) SFB 871/3 119193472, the National Natural Science Foundation of China (NSFC 72171194) and Sino-German Center for Research Promotion (Sino-German Mobility Program), Project number M-0175.

- 5 | **The concept of diagonal approximated signature: new surrogate modeling approach for continuous-state systems in the context of resilience optimization**

The concept of diagonal approximated signature: new surrogate modeling approach for continuous-state systems in the context of resilience optimization

Niklas R. Winnewisser^{a,*}, Julian Salomon^a, Matteo Broggi^a, Michael Beer^{a,b,c}

^aInstitute for Risk and Reliability, Leibniz Universität Hannover, Hannover, Germany

^bInstitute for Risk and Uncertainty, University of Liverpool, Liverpool, United Kingdom

^cInternational Joint Research Center for Resilient Infrastructure & International Joint Research Center for Engineering Reliability and Stochastic Mechanics, Tongji University, Shanghai, China

*Corresponding author

Published in *Disaster Prevention and Resilience* on April 2023

Abstract

The increasing size and complexity of modern systems presents engineers with the inevitable challenge of developing more efficient yet comprehensive computational tools that enable sound analyses and ensure stable system operation. The previously introduced resilience framework for complex and sub-structured systems provides a solid foundation for comprehensive stakeholder decision-making, taking into account limited resources. In their work, a survival function approach based on the concept of survival signature models the reliability of system components and subsystems. However, it is limited to a binary component and system state consideration. This limitation needs to be overcome to ensure comprehensive resilience analyses of real world systems. An extension is needed that guarantees both maintaining the existing advantages of the original resilience framework, yet enables continuous performance consideration.

This work introduces the continuous-state survival function and concept of the Diagonal Approximated Signature (DAS) as a corresponding surrogate model. The proposed concept is based on combinatorial decomposition adapted from the concept of survival signature. This allows for the advantageous property of separating topological and probabilistic information. Potentially high-dimensional coherent structure functions are the foundation. A stochastic process models the time-dependent degradation of the continuous-state components. The proposed approach enables direct computation of the continuous-state survival function by means of an explicit formula and a stored DAS, avoiding costly online Monte Carlo Simulation (MCS) and overcoming the limitation of a binary component and system state consideration during resilience optimization for sub-structured systems. A proof of concept is provided for multi-dimensional systems and an arbitrary infrastructure system.

Keywords: Surrogate modeling, Continuous-state system, Survival function, Coherent structure function, Resilience optimization, System reliability, Monte Carlo simulation.

5.1 Introduction

Engineering systems, such as infrastructure networks and complex machines, are ubiquitous worldwide and form the backbone of modern societies. As societies grow, these systems become increasingly sophisticated in size and complexity. Evidently, the stable operation of such systems is crucial for the economy and an undisturbed and safe everyday life of civilians. This challenge is exacerbated by exposure to an increasingly inhospitable, changing and uncertain environment. It is evident that it is exceedingly difficult if not impossible to identify and prevent all potential

adverse impacts. The focus in design and maintenance of complex systems has to be extended from a pure failure prevention and failure persistence strategy to the capabilities of adaptation and recovery. The concept of resilience meets exactly these needs both from a technical and economic point of view and ensures steady functioning [5, 7, 10]. Consequently, there is an increasing need for sophisticated and efficient computational tools that adapt this perspective in order to exploit the potential emerging benefits in engineering practice.

A fundamental precondition for the assessment of resilience of complex systems is an appropriate quantitative resilience metric. In [12, 23, 73], the authors present a broad review of current resilience metrics. In [301], Linkov and Trump provided a critical analysis of resilience definitions and metrics found in literature, their practical application and specifically compare them to the concept of the traditional notion of risk. Hosseini et al. presented in [12] a categorization scheme for resilience quantification approaches. Among these, performance-based resilience metrics are the most common and are based on comparing the performance of a system before and after an adverse event. Theoretically, such an adverse event could correspond to rare shock events on a large time scale or persistent degrading effects on an infinitesimally small time scale. Further subcategories distinguish between time in-/dependence and characterization as deterministic or probabilistic. As motivated in [12] and [76], it is assumed that a performance-based and time-dependent metric is capable of considering the following system states before and after a disruptive event:

- The initial state that remains unchanged until the occurrence of an effectively disruptive event, characterized by system reliability, that is interpreted as the ability of the system to sustain typical performance prior to a disruptive event [12, 302].
- The disrupted state, determined by the system robustness, i.e., the ability of the system to mitigate an effectively disruptive event and its counterpart, vulnerability, represented by a potential loss of performance after the occurrence of a disruptive event [6, 52].
- The recoverability of the system characterizes the duration of the degraded state and the recovery to a new stable state [6, 76].

5.1 illustrates these system states and their transitions simplified for a single effectively disruptive event and its potentially infinitesimal small period. Note that the terminologies concerning the governing properties, phases and states presented here, although in their physical interpretation perceived alike or at least similarly, are discussed in literature partly controversially. Thus, for example, what is described here, and, e.g., in [52], as system robustness is referred to as resistance of a system, as in [79]. In fact, the boundaries between the interpretations of reliability and robustness are fluid when extending the conventional perspective as shall be seen in the further course of this work. For the developments subsequently proposed, it is critical to define a concise interpretation of reliability from a probabilistic perspective. In accordance with [303], let reliability refer to the probability of a system or some entity under consideration

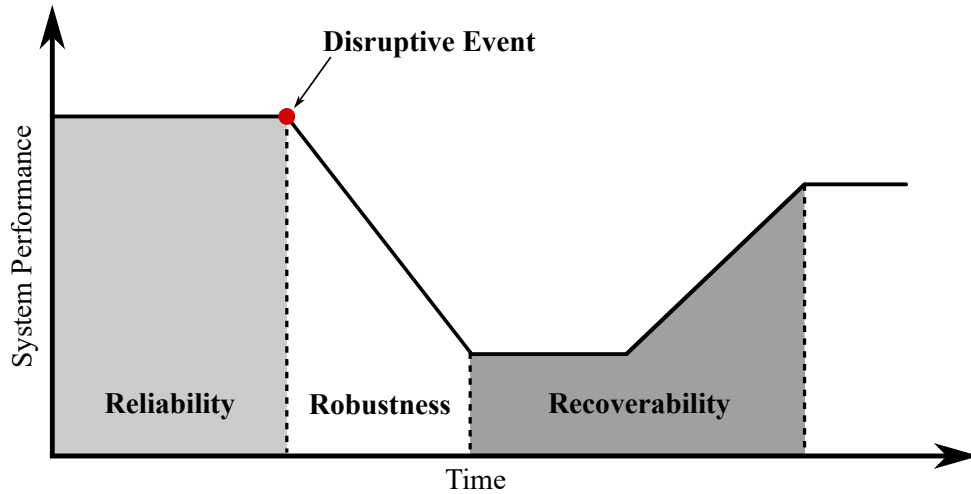


Figure 5.1: The concept of resilience - three essential phases, adapted from [76].

to uninterruptedly perform a certain specified function during a stated interval of a life variable, e.g., time, within a certain specified environment.

In the field of engineering, resilience as a concept has consistently gained popularity in recent years [17, 23]. There are numerous ways to improve the resilience of systems. However, there are limits to available resources, and resilience cannot be increased indefinitely. Therefore, it is important not only to be able to differentiate and balance between different resilience-enhancing measures, but also to take into account their monetary aspects [240, 244]. In [268], Salomon et al. present a method for determining the most cost-efficient allocation of resilience-enhancing investments. Further, current research related to resilience focuses on improved metrics for quantifying resilience, such as those proposed in [84], and overarching frameworks for stakeholder decision-making, such as for transportation networks in the presence of seismic hazards [269]. Other recent studies have examined the complexity of real-world infrastructure systems, the consequences of failures, recovery sequences, and various externalities. For instance, in [271], the authors demonstrated the tremendous complexity of modern critical infrastructures and their multifactorial nature as cyber-human-physical systems, and explored appropriate modeling and resilience analysis techniques. Moreover, the studies [272] and [273] address the implications for decision-making considering stakeholder priorities and enhancement or recovery strategies. Climate change challenges have been explored in the context of resilience, e.g., in [274]. A comprehensive literature review of resilience assessment frameworks balancing both resources and performance can be found in [270].

Salomon et al. recently introduced in [304] an efficient resilience framework for large, complex and sub-structured systems, providing a solid foundation for comprehensive stakeholder decision-making, taking into account limited resources. In their work, a survival function approach based on the concept of survival signature, first introduced in [149], models the reliability of system components and subsystems of investigated systems. This reliability approach separates

information on the topological (sub)system reliability and the component failure time behavior. Thereby, the survival signature captures the topological information in an efficient manner [114] and thus, can be seen as a type of surrogate modeling technique. This allows for significantly reduced computational effort when it comes to repeated model evaluations, as the demanding evaluation of the topological system model is circumvented [152]. This is all the more relevant the larger and more complex the system under consideration is. The repeated model evaluations are of crucial importance when the parameters examined during the resilience optimization affect the probability structure of the system components. This results in a high number of changes in the probability structure during the resilience analysis, which can be ideally covered by the separation property of the survival signature with minimal computational effort.

A major restriction of the survival signature in its original form is the limitation to a binary component and system state consideration. Consequently, the resilience framework for complex and sub-structured systems in [304] is subject to the same constraints during resilience optimization. However, for a comprehensive resilience analysis of real world systems, a continuous component and system performance state consideration is an indispensable prerequisite. Therefore, an extension is needed that guarantees both the already existing advantages of the resilience framework in [304] based on the original form of the survival signature, yet enables continuous performance consideration.

The most widespread reliability assessment methods follow a binary-state consideration, i.e., reducing the consideration of system performance to the set of the two states of either perfect functioning or complete failure, compare [305]. Jain et al. states that the “Majority of the existing models have computed system reliability at a holistic level but fail to consider the interactions at component and sub-system levels [...]” In [306], Yang & Xue highlight the importance of a continuous-state consideration in reliability analysis. It is evident that the consideration of continuous component and (sub)system states is equally important for resilience analysis and thus indispensable for realistic resilience optimization. In the last years several researchers proposed various concepts that bring the survival signature to a multi-state consideration, e.g., see [165, 216, 280, 281], which can be seen as a first step in development, towards continuous consideration and potential implementation into proposed resilience framework for sub-structured complex systems [304].

In the current work, theoretical fundamentals are first summarized. Then the concept of the DAS is introduced as a new surrogate modeling approach, based on the concept of survival signature and potentially high-dimensional coherent structure functions describing the relationship between degrading components and corresponding continuous-state system performance. The proposed approach enables direct computation of continuous-state survival function by means of an explicit formula and a stored DAS, thus avoiding a costly online MCS and overcoming the limitation of a binary component and system state consideration. A proof of concept is provided for multi-dimensional systems consisting of min- and max-operators, where exact results are obtained. Further, the applicability of the concept is investigated for an arbitrary infrastructure system.

Finally, a conclusions and outlook are presented.

5.2 Theoretical fundamentals

5.2.1 Structure function

According to [307], the performance of a system depends only on its components, i.e., their states, and their interactions. Then, a vector $\mathbf{x}(t)$ can be seen as the component state vector of the system assigning a state to each component. $\mathbf{x}(t)$ should dependent on the environmental conditions. As a result, the system performance can be described as a function of the component state vector. Suppose that a component state is modeled via probability distributions in dependence on component properties, environmental effects, and time. Then, the system performance function solely describes the system structure, corresponding to the arrangement of the components and their interactions. Such a system performance model can be considered as the well-known system structure function. In the current work, the structure function is assumed to be time-independent.

Binary-state structure function

The structure function of a system is a fundamental concept to represent system topology in reliability analysis. For a binary-state system the structure function can be defined as follows. Let a system consist of n components of the same type. Further, let $\mathbf{x} = (x_1, x_2, \dots, x_n) \in \{0, 1\}^n$ be the corresponding state vector of the n components, where $x_i = 1$ indicates a working state of the i -th component and $x_i = 0$ indicates a nonworking state. Then, the structure function ϕ is a function of the state vector defining the operating status of the considered system:

$$\phi := \phi(\mathbf{x}) : \{0, 1\}^n \rightarrow \{0, 1\}, \quad (5.1)$$

as proposed, e.g., in [149] Accordingly, $\phi(\mathbf{x}) = 1$ denotes a working system and $\phi(\mathbf{x}) = 0$ specifies a nonworking system relative to the state vector \mathbf{x} .

Let a system consist of components of different types, i.e., $K \geq 2$. Then, the number of system components is denoted by $n = \sum_{k=1}^K n_k$, where n_k is the number of components of type $k \in \{1, 2, \dots, K\}$. Accordingly, the state vector for each type is specified by $\mathbf{x}_k = (x_{k,1}, x_{k,2}, \dots, x_{k,n_k})$.

Multi-state structure function

Analogously, the structure function can be defined for a discrete multi-state consideration. Then, the system and component states degrade from a perfect state over a set of intermediate states to the state of complete failure:

$$\phi := \phi(\mathbf{x}) : \{0, \dots, M\}^n \rightarrow \{0, \dots, M\}, \quad (5.2)$$

compare [308].

Continuous-state structure function

When following a continuous multi-state consideration, the set of possible system and component states are all elements of the interval between 0 and 1. Such a consideration relates to the performance function well-known in structural reliability when normalized for minimum and maximum parameter values, e.g., as proposed in [309]:

$$\phi := \phi(\mathbf{x}) : [0, 1]^n \rightarrow [0, 1]. \quad (5.3)$$

5.2.2 Coherent system

A special case of the general system is the class of coherent systems. Note that binary-state, discrete multi-state, as well as continuous multi-state structure functions can be coherent. In accordance with Hudson & Kapur [310], this class can be defined as follows. A (discrete or continuous multi-state) system is defined to be coherent if the three subsequent conditions are fulfilled:

- $\phi(\mathbf{x})$ is surjective. Consequently, for each system state m there exists at least one state vector \mathbf{x} for which $\phi(\mathbf{x}) = m$.
- $\phi(\mathbf{x}) \leq \phi(\mathbf{y})$ if $\mathbf{x} \leq \mathbf{y}$, i.e., ϕ is monotone and non-decreasing.
- The set C of all components contains no inessential components, i.e., each component influences the system performance at some point.

5.2.3 Concept of binary-state survival signature

The concept of the survival signature is a promising approach for a more efficient evaluation of system reliability, especially when it comes to repeated model evaluations. Introduced in [149], this concept enables to compute the survival function of a system. The approach attracted increasing attention over the last decade due to its advantageous features compared to traditional methods [114]. One of its benefits is the efficiency in repeated model evaluations due to a separation of the probability structure of system components and the topological system reliability. In addition, the survival signature significantly condenses information on the topological reliability for systems with multiple component types. Components are of the same type if their failure times are independent and identically distributed (*iid*) or exchangeable. This distinction is important when modeling dependent component failure times [153]. For more information on claimed exchangeability in practice, see [152, 153]. In the following the derivation of the concept of survival signature is shown for a binary-state system with a single component type and multiple component types, respectively, based on Coolen et al. [149]. More detailed

information about further applications and the derivation of the concept can be found in [149, 153, 154].

Consider a coherent system with a given structure function as described in 5.2.1. Given a binary-state vector specifying the state of n components in total, there are $\binom{n}{l}$ state vectors \mathbf{x} with exactly l components with $x_i = 1$, i.e., $\sum_{i=1}^n x_i = l$. Let the set of these state vectors refer to as S_l . Assume that the failure times of the components specifying \mathbf{x} over time are *iid*. Consequently, all possible state vectors are equally likely to occur and, hence, it can be stated that

$$\Phi(l) = \binom{n}{l}^{-1} \sum_{\mathbf{x} \in S_l} \phi(\mathbf{x}), \quad (5.4)$$

where $\phi(\mathbf{x})$ is the binary-state structure function. Then, $\Phi(l)$ denotes the probability that a system is working given that exactly l of its components working for $l = 1, \dots, n$. Note that the survival signature depends only on the topological reliability of the system, independent of the time-dependent failure behavior of its components, hereafter referred to as the probability structure of the system. It holds that $\Phi(0) = 0$ and $\Phi(n) = 1$ due to the coherent system property. The expression given in 5.4 closely relates to the signature, introduced by Samaniego in [148]. The probability structure of system components specifies the probability that a certain number of components of type k are working at time t . Let $C_t \in \{0, 1, \dots, n\}$ be the number of components functioning at time $t > 0$. Further, the probability distribution of the component failure time is described by the cumulative density function (CDF) $F(t)$. Therefore, the probability structure for $l \in \{0, 1, \dots, n\}$ is given as

$$P(C_t = l) = \binom{n}{l} [F(t)]^{n-l} [1 - F(t)]^l. \quad (5.5)$$

The topological reliability described by Eq. 5.4 and the probability structure characterizing the component failure times can be brought together to obtain the survival function as

$$R(t) = P(T_f > t) = \sum_{l=0}^n \Phi(l) P(C_t = l), \quad (5.6)$$

where T_f denotes the random system failure time. Clearly, the two terms on the right-hand side of the equation have different roles: The term $\Phi(l)$ represents the topological reliability and is determined by the structure function of the system, defining how the system functionality depends on the function of its components. The other term $P(C_t = l)$ describes component failure behavior and is referred to as the probability structure of the system. Consequently, the concept of survival signature separates the time-independent topological reliability and the time-dependent probability structure. Thus, the survival signature computed once in a pre-processing step can be reused for further evaluations of the survival function. The survival signature can be stored in a matrix, summarizing the topological reliability. The utilization of this matrix circumvents the repeated evaluation of the typically computationally expensive

structure function. Note that precisely these properties give the concept of survival signature an advantage over conventional methods when system simulations must be performed repeatedly [114].

The survival function $R(t)$ is a well-known concept in reliability engineering that is also referred to as reliability function [311, 312]. It is typically interpreted as the mathematical formalization of the definition of reliability provided in 5.1 and quantifies the system failure time to be greater or equal to t . It relates to the CDF $F(t)$ as $R(t) = 1 - F(t)$.

It is also possible to define the concept of survival signature for $K \geq 2$, with K being the number of component types. In this case, the survival signature summarizes the probability that a system is working as a function depending on the number of working components l_k for each type $k = 1, \dots, K$, see [149] for more details.

5.2.4 Concept of continuous-state survival signature

The original concept of survival signature achieves considerable efficiency advantages when computing system reliability but is limited to a binary-state consideration. However, a multi-state or even continuous-state consideration might be beneficial for the assessment of most real-world systems in terms of safety and cost efficiency. In the last years several researchers proposed various concepts that bring the survival signature to a multi-state consideration, see [165, 280, 281].

In [216], Liu et al. introduced an approach for the concept of survival signature in the context of continuous-state systems, for which the component functionality is characterized by a stress-strength relation. The strength of the components are assumed to be *iid*, while the strength X and the stress Y acting on the components are statistically independent. The state of a component is defined via a kernel function $K : \mathbb{R}^+ \rightarrow S$ through the relation $\eta = K(Z)$ with the random variable $Z = X/Y$. Thereby, $S \in \{0, 1, 2, \dots, M\}$ and $S \in [0, 1]$, respectively, depending on a discrete or continuous multi-state consideration. The researchers provided formulas to compute the survival signature for discrete multi-state systems similar to [280] in a combinatorial manner but directly based on the number of path sets. Analogously, the survival signature for continuous multi-state systems is given as

$$\begin{aligned} \rho_{n_s}(n) &= P(\varepsilon \geq s \mid N(s, n) = n_s) \\ &= \delta_{n_s}(n) / \binom{n}{n_s} \end{aligned} \quad (5.7)$$

with

$$N(s, n) = \sum_{i=1}^n I(\eta \geq s) \quad (5.8)$$

that is the number of components in state s of in total n components and $\delta_{n_s}(n)$ being the number of path sets for which exactly n_s components are in state s or above. The time-independent

probability that the system is at least in state s or above can then be given as

$$R(s) = \sum_{l_s=0}^n \rho_{l_s}(n) \binom{n}{l_s} P(N(s, n) = n_s), \quad (5.9)$$

where l_s is the number of components functioning in state s . Again, the left term represents the inherently time-independent topological reliability, while the right term refers to the probability structure that is time-independent in this case due to specific the stress-strength relation of components established in [216].

Despite an extension to discrete and continuous multi-state consideration, the authors limited their considerations in [216] to a time-independent reliability analyses. Thereby, $R(s)$ quantifies the probability that the entity under consideration performs in state s , compare $R(t)$ that measures the probability of the system failure time is greater or equal to time t . In addition, a stress-strength relation characterizing probabilistic properties of components must be established as prerequisite in order to determine the component probability structure $P(N(s, n) = n_s)$.

5.3 Proposed methodology

In this section, the continuous-state survival function is defined. In contrast to the previously outlined approaches that are either probability measures of state s or time t , this notion depends on both s and t simultaneously. For comparison with the subsequently presented methodology, a true solution estimate based on MCS is proposed in order to evaluate the continuous-state survival function. Eventually, the DAS is introduced as surrogate model to compute the continuous-state survival function efficiently.

5.3.1 Continuous-state survival function

In this work, the probability $P(u_s \geq s|t)$ that the state of some entity under consideration u_s is greater or equal to s at given time t is referred to as the continuous-state survival function of this entity and is denoted by

$$R(s, t) = P(U_s \geq s|t). \quad (5.10)$$

Thereby, the continuous-state survival function constitutes a time-dependent probability measure that characterizes the distribution of performance states of the considered entity over time. From another perspective, the continuous-state survival function can be interpreted as

$$R(s, t) = P(U_t \geq t|s), \quad (5.11)$$

where U_t is the random variable characterizing the time to failure of the condition that the state of the entity is greater than s . Despite this perspective does not find application in this work, the consideration is decisive for the terminology. In fact, the original and well-known survival function can be extended to this notion when conditioning the considered lifetime to a state s in

the interval $[0, 1]$ instead of a binary condition of operating or not operating.

In the context of systems that consist of components facing disruptive events, the entity under consideration may correspond to either a system or one of its components. Thereby, $R(s, t)$ can be established in several ways. The first attempt to quantify $R(s, t)$ could be a fully empirical approach, measuring the frequency of the system or component state u_s . Given the typically limited number of samples, engineers in most cases face the challenge of modeling a stochastic process based on limited data or expert knowledge and to utilize it as basis for sampling performances as an alternative. Besides that, the continuous-state survival function can be evaluated based on a given structure function $\phi(\mathbf{x})$, as presented in 5.2.1, that represents system topology, i.e., component interaction, and a given probability structure describing the degrading component performance over time. The latter approach involving $\phi(\mathbf{x})$ will be focal point for all subsequent developments.

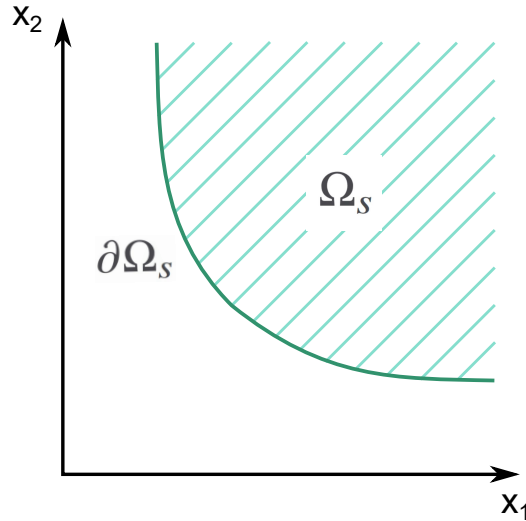


Figure 5.2: Examples for $\partial\Omega_s$ and Ω_s shown in a contour plot of an exemplary 2D-system with the structure function $\phi(\mathbf{x})$ evaluated for an arbitrary state s .

Consider a system with a coherent and time-invariant structure function $\phi(\mathbf{x})$. Then $u_s = \phi(\mathbf{x})$ and the corresponding continuous-state survival function can be given by $R(s, t) = P(\phi(\mathbf{x}) \geq s | t)$. 5.2 shows the contour line of an exemplary 2D system for a given state s . Thereby, $\partial\Omega_s := \{\mathbf{x} \mid \phi(\mathbf{x}) = s\}$ represents this contour line as the set of state vectors that meet exactly the system performance $\phi(\mathbf{x}) = s$ with $\mathbf{x} = (x_1, x_2, \dots, x_n)$ and $x_i \in [0, 1]$. $\Omega_s := \{\mathbf{x} \mid \phi(\mathbf{x}) \geq s\}$ corresponds to the set of state vectors that fulfill the criteria $\phi(\mathbf{x}) \geq s$. Given $\phi(\mathbf{x})$, an exact solution for $R(s, t)$ can be obtained by evaluating the integral of the time-dependent probability density at the state vectors belonging to Ω_s . Denote the underlying probability distribution as $f_{x_i}(x_i | t)$ – potentially time-dependent – describing the state x_i of component i . Further, let $\Omega = [0, 1]^n$ be the set of all possible component states and assume the component states to be

independently distributed. Then, the true solution of the continuous-state survival function is given as the integral over $\Omega_s \subseteq \Omega$:

$$\begin{aligned} R(s, t) &= \int_{\Omega_s} f_{\mathbf{x}}(\mathbf{x} | t) d\mathbf{x} \\ &= \int_{\Omega} I(\phi(\mathbf{x}) \geq s) f_{\mathbf{x}}(\mathbf{x} | t) d\mathbf{x}, \end{aligned} \quad (5.12)$$

where $f_{\mathbf{x}}(\mathbf{x} | t) = \prod_{i=1}^n f_{x_i}(x_i | t)$ is the conditional joint probability density characterizing the probability of the component state vector \mathbf{x} . Further, $I(\cdot) \in \{0, 1\}$ denotes the indicator function. In fact, the identification of $\partial\Omega_s := \{\mathbf{x} | \phi(\mathbf{x}) = s\}$, that corresponds to the well-known limit state function, in order to quantify the probability mass assigned to the elements in Ω_s is a challenging task, particularly for nonlinear functions. MCS is applied to obtain an estimate of the true solution, since there is no closed form available to solve this general and possibly multi-dimensional problem. It holds true that

$$\begin{aligned} R(s, t) &= \int_{\Omega} I(\phi(\mathbf{x}) \geq s) f_{\mathbf{x}}(\mathbf{x} | t) d\mathbf{x} \\ &= \frac{1}{N_{MCS}} \sum_{j=1}^{N_{MCS}} I(\phi(\mathbf{x}_j) \geq s | t), \end{aligned} \quad (5.13)$$

where N_{MCS} is the number of component state samples $\mathbf{x}_j \in \Omega \sim f_{\mathbf{x}}(\mathbf{x} | t)$ used for MCS, when $N_{MCS} \rightarrow \infty$.

5.3.2 Surrogate model: the concept of diagonal approximated signature

The concept of the DAS is introduced as a surrogate modeling approach that enables the computation of the true continuous-state survival function or at least an approximation of it depending on the characteristics of $\phi(\mathbf{x})$. Similarly to the concepts of binary- and discrete/continuous multi-state survival signatures, the concept of the DAS is based on a decomposition of working components, compare l that is the number of components working, as in 5.6, and l_s that is the number of components functioning in state s , as in 5.9, respectively. This leads to a separation property of these concepts that enables to store information on the system topology, i.e., the functional interaction of components, and retrieve it in repeated model evaluations more efficiently than compared to the evaluation via the original structure function.

Fundamental statement

With regard to the current developments, several categorizations for three properties of a coherent system structure function are introduced. As first property, the diagonal state sign can be defined: A coherent structure function is referred to as diagonally state positive if it holds that $\phi(x_s) > s \forall s \in [0, 1]$ with $x_s = (x_1, x_2, \dots, x_n)$ and $x_i = s$ where n is the number of system components. Analogously, the terms diagonally state neutral and diagonally state negative

correspond to the conditions $\phi(x_s) = s$ and $\phi(x_s) < s$, respectively. Secondly, note that a structure function is called diagonally state invariant in particular if it is diagonally state neutral. In contrast, the property of the diagonal state variance can also be assigned as diagonally state variant if the structure function is partly diagonally state positive, neutral and negative. The third property can be assigned as diagonally state extreme if it holds that $\phi(x_s) \geq s \ \forall s \in [0, 1]$ with $x_s = (x_1, x_2, \dots, x_n)$ and $x_i \in \{0, s\}$. This condition would imply that the structure function is also diagonally state constant, i.e., $\phi(x_s) \geq s \ \forall s \in [0, 1]$ with $x_s = (x_1, x_2, \dots, x_n)$ and $x_i \in [0, s]$. Let these specifications relate to the diagonal state order. As an example, both of these properties can be specified as diagonally state neutral and diagonally state extreme for structure functions that are solely composed by min- or max-operators, i.e., compositions of $\phi_e(\mathbf{x}) = \min(x_f, x_g) \in [0, 1]$ and $\phi_h(\mathbf{x}) = \max(x_j, x_k) \in [0, 1]$ with $x_f, x_g, x_j, x_k \in [0, 1]$. In addition to such systems, Liu et al. also investigated *k – consecutive – out – of – n – systems* which are diagonally state neutral and diagonally state extreme, compare [216]. The min- and max-operators can be interpreted as analogy of series and parallel operators known from the binary-state consideration, as stated in [306]. The binary operators often appear in reliability block diagrams.

Assume a coherent structure function to be diagonally state neutral or at least positive and at least diagonally state constant. Then, the basic concept of the DAS can be stated as

$$\begin{aligned} R(s, t) &= \int_{\Omega_s} f_{\mathbf{x}}(\mathbf{x} | t) d\mathbf{x} \\ &= \sum_{l_s=0}^n \sum_{p=1}^{\binom{n}{l_s}} [R_{\mathbf{x}}(\Phi(l_s, p) | t) - R_{\mathbf{x}}(s | t)]^{n-l_s} [R_{\mathbf{x}}(s | t)]^{l_s}, \end{aligned} \quad (5.14)$$

where $\Phi(l_s, p)$ represents the DAS and $R_{\mathbf{x}}(s | t) = R_{x_i}(s | t) = P\{x_i | x_i \geq s, t\}$ corresponds to the probability that a component is in state s or above at time t given that all component states are *iid* or exchangeable. Thereby, $\Phi(l_s, p)$ stores values representing an approximation of the limit state function, i.e., $\partial\Omega_s$ that is the set of component state vectors fulfilling the condition $\phi(\mathbf{x}) = s$. For a given state s , the p -th permutation of the overall $\binom{n}{l_s}$ permutations defines a subspace $\Omega_{s, l_s, p} \subseteq \Omega_{s, l_s} \subseteq \Omega_s \subseteq \Omega$ determined by l_s that is the number of components working in state s . All state vectors in the set of $\Omega_{s, l_s, p}$ fulfill the condition $\phi(\mathbf{x}) \geq s$. Let the value of $\Phi(l_s, p)$ for subspace $\Omega_{s, l_s, p}$ be the minimum value of $n - l_s$ components of the state vector \mathbf{x} in the interval $[0, s]^{n-l_s}$ for which the condition $\phi(\mathbf{x}) \geq s$ is met, while l_s components are fixed in state s . The developed algorithm for computing the values $\Phi(l_s, p)$ ensures that the continuous-state survival function $R(s, t)$ can only be underestimated in the worst case.

Derivation of the fundamental statement

The derivation of 5.14 can be given as follows. Let $I = \{1, 2, \dots, n\}$, where $n = |I|$, and $(k_1, k_2, \dots, k_n) \in K_p := \binom{I}{l_s}$. Then, K_p is the index set of all possible permutations of the state vector for a given number of components functioning in state s with in total $\binom{n}{l_s}$ elements,

and the index $p \in \{1, 2, \dots, \binom{n}{l_s}\}$ corresponds to the p -th permutation. At first, consider the decomposition of Ω_s , the set of state vectors for which the condition $\phi(\mathbf{x}) \geq s$ is fulfilled, into its subspaces when given l_s components functioning in state s . The decomposition is formulated as

$$\begin{aligned}
 \Omega_s &= \{\mathbf{x} \mid \phi(\mathbf{x}) \geq s\} = \bigcup_{l_s=0}^n \Omega_{s,l_s} = \Omega_{s,0} \cup \bigcup_{l_s=1}^{n-1} \Omega_{s,l_s} \cup \Omega_{s,n} \\
 &= \bigcup_{p=1}^{\binom{n}{0}} \{x_{k_1}, \dots, x_{k_n} < s \wedge \phi(\mathbf{x}) \geq s\} \\
 &\cup \bigcup_{l_s=1}^{n-1} \bigcup_{p=1}^{\binom{n}{l_s}} \{x_{k_1}, \dots, x_{k_i} \geq s \wedge x_{k_{i+1}}, \dots, x_{k_n} < s \wedge \phi(\mathbf{x}) \geq s\} \\
 &\cup \bigcup_{p=1}^{\binom{n}{n}} \{x_{k_1}, \dots, x_{k_n} \geq s \wedge \phi(\mathbf{x}) \geq s\} \\
 &= \bigcup_{l_s=0}^n \bigcup_{p=1}^{\binom{n}{l_s}} \Omega_{s,l_s,p},
 \end{aligned} \tag{5.15}$$

where $\{k_{i+1}, \dots, k_n\} = (I/K_p)$. Note that the subspace Ω_{s,l_s} is also decomposed into the subspaces $\Omega_{s,l_s,p}$ defined via all possible permutations p of the state vector for l_s given components functioning in state s or above and the corresponding $n - l_s$ components functioning in state $< s$. Secondly, the set-theoretical decomposition $\bigcup_{l_s=0}^n \bigcup_{p=1}^{\binom{n}{l_s}} \Omega_{s,l_s,p}$ proposed in 5.15 is utilized to decompose the time-dependent state probability and to separate the probability structure and the information on the limit state function. This spatial decomposition depending on a given state s and time t is now utilized to form sums of mutually exclusive event sets as:

$$\begin{aligned}
 R(s, t) &= \int_{\Omega_s} f(\mathbf{x} \mid t) d\mathbf{x} \\
 &= P(\Omega_s \mid t) = P\left(\bigcup_{l_s=0}^n \bigcup_{K_p=\binom{n}{l_s}}^{\binom{n}{l_s}} \Omega_{s,l_s,p} \mid t\right) \\
 &= \sum_{l_s=0}^n \sum_{p=1}^{\binom{n}{l_s}} \int_{\Omega_{s,l_s,p}} f(\mathbf{x} \mid t) d\mathbf{x}.
 \end{aligned} \tag{5.16}$$

The claim that the coherent structure function is diagonally state neutral or positive and at least diagonally state constant implies that $\Omega_{s,l_s,p} = [a_i(l_s, p), b_i(l_s, p)]^n$. The boundary points $a_i(l_s, p)$ and $b_i(l_s, p)$ characterize the subspace $\Omega_{s,l_s,p}$ and depend on l_s the number of components functioning in state s and the permutation p . Further, assume that the components are independent and identically distributed, i.e., $x_1, x_2, \dots, x_n = x \sim f_x(x_i \mid t)$. Consequently, it

can be stated that

$$\begin{aligned}
 \int_{\Omega_{s,l_s,p}} f(\mathbf{x} | t) d\mathbf{x} &= \int_{\Omega_{s,l_s,p}} f_1(x_1 | t) f_2(x_2 | t) \cdots f_n(x_n | t) dx_1 dx_2 \dots dx_n \\
 &= \prod_{i=1}^n \int_{a_i(l_s,p)}^{b_i(l_s,p)} f_i(x_i | t) dx_i = \prod_{i=1}^n \int_{a_i(l_s,p)}^{b_i(l_s,p)} f_x(x_i | t) dx_i \\
 &= \prod_{i=1}^n F_x(b_i(l_s,p) | t) - F_x(a_i(l_s,p) | t) \\
 &= \prod_{i=1}^n 1 - R_x(b_i(l_s,p) | t) - (1 - R_x(a_i(l_s,p) | t)) \\
 &= \prod_{i=1}^n R_x(a_i(l_s,p) | t) - R_x(b_i(l_s,p) | t).
 \end{aligned} \tag{5.17}$$

The expression proposed in 5.14 involving the time-dependent state probability distribution results from 5.17 when considering two reformulations: At first, note the simplification $R_x(a_j(l_s,p)) - R_x(b_j(l_s,p)) = R_x(s) - R_x(1) = R_x(s)$ for the j -th component of the overall $l_s \in \{0, 1, \dots, n\}$ components functioning in state greater or equal to s . At second, it can be stated that the DAS $\Phi(l_s,p) = a_k(l_s,p)$ as $R_x(a_k(l_s,p)) - R_x(b_k(l_s,p)) = R_x(\Phi(l_s,p)) - R_x(s)$ for the k -th component of the overall $n - l_s$ components in state $< s$. Consequently,

$$\begin{aligned}
 \int_{\Omega_{s,l_s,p}} f(\mathbf{x} | t) d\mathbf{x} &= \prod_{i=1}^n R_x(a_i(l_s,p) | t) - R_x(b_i(l_s,p) | t) \\
 &= [R_x(\Phi(l_s,p) | t) - R_x(s | t)]^{n-l_s} [R_x(s | t)]^{l_s}.
 \end{aligned} \tag{5.18}$$

Then, 5.16 and 5.18 are brought together to finally obtain the expression presented in 5.14:

$$\begin{aligned}
 R(s,t) &= \sum_{l_s=0}^n \sum_{p=1}^{\binom{n}{l_s}} \int_{\Omega_{s,l_s,p}} f(\mathbf{x} | t) d\mathbf{x} \\
 &= \sum_{l_s=0}^n \sum_{p=1}^{\binom{n}{l_s}} [R_x(\Phi(l_s,p) | t) - R_x(s | t)]^{n-l_s} [R_x(s | t)]^{l_s}.
 \end{aligned} \tag{5.19}$$

Note that the topological information captured beforehand in $\Phi(l_s,p)$ is then retrieved and inserted into the probability structure in order to evaluate $R(s,t)$.

Basic algorithm for evaluating the DAS

At a first attempt, the approximation of $\Phi(l_s,p)$ can be achieved via the numerical scheme proposed in Algorithm 1. The presented Algorithm 1 poses a basic optimization scheme for finding the values $\Phi(l_s,p)$ for given state s . The proposed algorithm yields an exact representation of the limit state function at state s if the coherent structure function is diagonally state extreme and an approximated representation for diagonally state constant systems.

Pseudocode 1 Evaluation of $\Phi(l_s, p)$

```

function EVALUATEDIAGONALAPPROXIMATEDSIGNATURE( $\phi()$ ,  $\mathbf{x}_0$ ,  $s$ ,  $h_{max}$ )
     $\triangleright$  fixed point evaluation
    if  $all(\mathbf{x}_0. == s)$  then
        if  $\phi(\mathbf{x}_0) \geq s$  then
            return  $s$ 
        end if
    end if
     $\triangleright$  start iteration
     $v, v_1 \leftarrow s$ 
     $h \leftarrow 0$ 
     $\triangleright$  initialize auxiliary iteration variables
     $\triangleright$  initialize iteration counter
     $systemstate \leftarrow \phi(\text{DETERMINESTATEVECTOR}(\mathbf{x}_0, v_1))$ 
    while  $h \leq h_{max}$  do
        if  $systemstate < s$  then
             $v_1 \leftarrow v - \frac{s}{2^h}$ 
        else if  $systemstate \geq s$  then
             $v \leftarrow v_1$ 
             $v_1 \leftarrow v - \frac{s}{2^h}$ 
        end if
         $systemstate \leftarrow \phi(\text{DETERMINESTATEVECTOR}(\mathbf{x}_0, v_1))$ 
         $h \leftarrow h + 1$ 
    end while
    return  $v_1$ 
end function
     $\triangleright$  auxiliary function

function DETERMINESTATEVECTOR( $\mathbf{x}_0, v_1$ )
    return  $fill(\mathbf{x}_0[\mathbf{x}_0. == NaN], v_1)$ 
end function

```

Considering Algorithm 1, $\phi(\cdot)$ corresponds to the coherent structure function of the system and $\mathbf{x}_0 = (x_1, x_2, \dots, x_n)$ with $x_i \in \{NaN, s\}$, where \mathbf{x}_0 contains l_s times s and $n - l_s$ times NaN . Further, s indicates the state under consideration. The tuple (l_s, p) is characterized by the number of components in state s and their arrangement in the vector \mathbf{x}_0 . If the vector $\mathbf{x}_0 = (x_1, x_2, \dots, x_n)$ with $x_i = s$ fulfills the condition $\phi(\mathbf{x}_0) \geq s$, the structure function is at least diagonally state neutral for the given state s and s can be returned as value for $\Phi(l_s, 1)$ with $l_s = n$. For every other vector, the algorithm starts its search at s , next it checks the minimum value 0 and then evaluates the interval in between until it stops. The algorithm stops when meeting the condition $\phi(\mathbf{x}_0) = s$ or after a specified number of iterations h_{max} . Thereby, the step size is reduced in each iteration by 1/2 and the last value v that met the requirement $\phi(\text{DETERMINESTATEVECTOR}(\mathbf{x}_0, v_1)) \geq s$ is maintained and candidates are rejected if $\phi(\text{DETERMINESTATEVECTOR}(\mathbf{x}_0, v_1)) < s$. The Algorithm 1 yields exact results if the system is diagonally state extreme, since both extreme cases, i.e., $\Phi(l_s, p) = s$ and $\Phi(l_s, p) = 0$, are evaluated. For diagonally state constant structure functions the iteration achieves an underestimating approximation with an accuracy depending on h . The algorithm can be further improved by including the stopping criteria for a sufficiently small improvement between h and $h + 1$.

Extended statements

5.14 and 5.19, respectively, as well as the Algorithm 1 form the basis for all further developments of the concept of DAS. However, the established expression still appears to be computationally expensive, as the sum over all permutations becomes increasingly demanding for systems comprising a large number of components. Therefore, a naive approach is introduced based on counting the occurrences of equal values of $\Phi_c(l_s, p)$ in the subspace Ω_{s, l_s} to further reduce the computational effort: Let $\Psi(l_s, j) = (|C_j|, v_j)$ be the so-called condensed DAS that assigns a tuple for $l_s \in \{0, 1, \dots, n\}$ and $j \in \{1, 2, \dots, J\}$, where J is the number of unique values v_j of $\Phi(l_s, p)$ for a fixed l_s and $p \in \{1, 2, \dots, \binom{n}{l_s}\}$. Thereby, v_j indicates the j -th unique element in the set C_j that is formally defined as $C_j := \{(l_s, p) : \Phi(l_s, p) = v_j\}$. Then,

$$\begin{aligned}
 R(s, t) &= \sum_{l_s=0}^n \sum_{p=1}^{\binom{n}{l_s}} [R_x(\Phi(l_s, p) | t) - R_x(s | t)]^{n-l_s} [R_x(s | t)]^{l_s} \\
 &= \sum_{l_s=0}^n \sum_{j=1}^J \Psi(l_s, j)[1] [R_x(\Psi(l_s, j)[2] | t) - R_x(s | t)]^{n-l_s} [R_x(s | t)]^{l_s} \quad (5.20) \\
 &= \sum_{l_s=0}^n \sum_{j=1}^J |C_j| [R_x(v_j | t) - R_x(s | t)]^{n-l_s} [R_x(s | t)]^{l_s}.
 \end{aligned}$$

For most systems, the application of 5.20 will lead to a tremendous reduction of computational cost since typically $J \ll |\{(l_s, p)\}|$ for a fixed l_s and $p \in \{1, 2, \dots, \binom{n}{l_s}\}$.

For systems with high $|C_j|$ per l_s but many values of $v_j \in [0, 1]$ in direct neighborhood to each other, v_j can be rounded up for r digits. Formally, this is defined as $C_{j,r} := \{(l_s, p) : \Phi(l_s, p) = v_{j,r}\}$,

where $v_{j,r}$ is a rounded value of v_j up to r -th digit. Correspondingly, $\Psi_r(l_s, j) = (|C_{j,r}|, v_{j,r})$. Considering the Algorithm 1, the corresponding values $\Phi(l_s, p)$ were evaluated during the iteration and yield an approximation. This introduces an approximation error and a trade-off between computational cost and accuracy has to be made. The continuous-state survival function will be underestimated in the worst case, since $v_{j,r} > v_j \Rightarrow R(v_{j,r}) - R(s) \leq R(v_j) - R(s)$. Consequently, the concept of DAS can be formulated as an inequality for at least diagonally state neutral coherent structure functions that are not diagonally state constant. For such systems a subspace of $\Omega_{s,l_s,p}$ might be neglected. The hypervolume that is neglected and consequently by which the continuous-state survival function is underestimated depends on the shape and curvature of the corresponding limit state function. This probably large-scale approximation error results from the facts that these systems are no longer diagonally state constant and the DAS values are evaluated along the state diagonals of the individual subspaces $\Omega_{s,l_s,p}$. Nevertheless, an underestimation of the continuous-state survival function is provided in the worst case. This property is of crucial importance in engineering practice to prevent an unconscious risk from being taken. Let the following inequality be referred to as the concept of the naive first-order DAS. It holds true that

$$\begin{aligned} R(s, t) &\geq \sum_{l_s=1}^n \sum_{p=1}^{\binom{n}{l_s}} [R_x(\Phi(l_s, p) | t) - R_X(s | t)]^{n-l_s} [R_x(s | t)]^{l_s} \\ &\geq \sum_{l_s=0}^n \sum_{j=1}^J \Psi_r(l_s, j)[1] [R_x(\Psi_r(l_s, j)[2] | t) - R_x(s | t)]^{n-l_s} [R_x(s | t)]^{l_s}, \end{aligned} \quad (5.21)$$

where $R_x(s | t) = R_{x_i}(s | t) = P\{x_i | x_i \geq s, t\}$, i.e., all component states are *iid*. The statement above refers to as first-order approach since higher-order approaches are plausible. One could consider convolutions of subspaces via a recursive formula. Let $\Phi^1(l_s, p)$ denote the first-order DAS. Then, statements involving higher-order DAS such as $\Phi^h(l_s, p)$ would rely on the subordinate values $\Phi^{h-1}(l_s, p)$. However, the development of such higher-order schemes is beyond the scope of this paper.

5.4 Case studies

In this section, various system models are established that are designed for a proof of concept and a test of applicability of the developed approaches. Subsequently, the numerical results are presented.

5.4.1 System structure functions

Here, the structure functions are presented that will be studied to achieve a proof of concept and test the applicability of the approach. Note that the structure functions model the system topology, i.e., the functional interaction of components with each other.

Proof of concept: min- and max-systems

The min- and the max-operator are crucial in the context of continuous-state system reliability as these correspond to the fundamental series- and parallel-operator well-known from the binary-state consideration of system functionality. Typically, they appear in the context of reliability block diagrams. Several systems composed by these operators are established in order to proof the fundamental methodologies proposed in 5.3. The following coherent structure functions composed by min- and max-operators are considered:

- 2-component-min-system

The system is composed by two continuous-state components with $x_i \in [0, 1]$. The components are linked by a min-operator. Both components are considered to be of the same type. The 2-Component-Min-System can be interpreted as the analog to a series-connection in the binary-state case. The structure function $\phi(\mathbf{x}) \in [0, 1]$ can be defined in a functional form as

$$\phi(\mathbf{x}) = \min(x_1, x_2). \quad (5.22)$$

This structure function is diagonally state neutral, consequently, also diagonally state invariant, and diagonally state extreme. A graphical representation is given in 5.3.



Figure 5.3: System composed by a min-operator with two components.

- 2-component-max-system

The system is composed by two continuous-state components with $x_i \in [0, 1]$. The components are linked by a max-operator. Both components are considered to be of the same type. The 2-Component-Max-System can be interpreted as the analog to a parallel-connection in the binary-state case. The structure function $\phi(\mathbf{x}) \in [0, 1]$ can be defined in a functional form as

$$\phi(\mathbf{x}) = \max(x_1, x_2). \quad (5.23)$$

This structure function is diagonally state neutral, consequently, also diagonally state invariant, and diagonally state extreme. A graphical representation is given in 5.4.

- 8-component-minmax-system

The system is composed by eight continuous-state components with $x_i \in [0, 1]$. The components are linked by min-operators, as well as, max-operators. All components are considered to be of the same type. This system can be interpreted as the analog to a

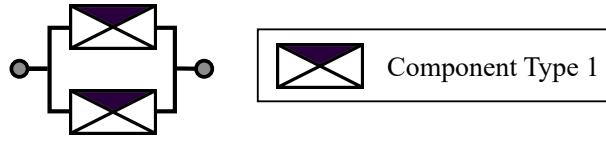


Figure 5.4: System composed by a max-operator with two components.

reliability block diagram that is composed by eight components. The structure function $\phi(\mathbf{x}) \in [0, 1]$ can be defined in a functional form as

$$\phi(\mathbf{x}) = \max(\min(\max(x_1, x_2, x_3), x_5, x_8), \min(x_4, \max(x_6, x_7))). \quad (5.24)$$

This structure function is diagonally state neutral, consequently, also diagonally state invariant, and diagonally state extreme. A graphical representation is given in 5.5.

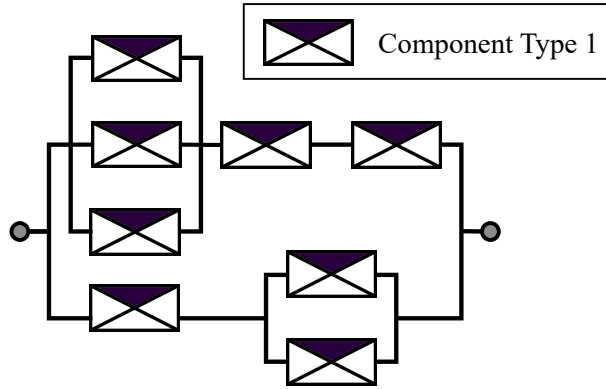


Figure 5.5: System composed by min- and max-operators with eight components, adapted from [304].

- 21-component-minmax-system

The system is composed by 21 continuous-state components with $x_i \in [0, 1]$. The components are linked by min-operators, as well as, max-operators. All components are considered to be of the same type. This system can be interpreted as the analog to a reliability block diagram that is composed by 21 components. The structure function $\phi(\mathbf{x}) \in [0, 1]$ can be defined in a functional form as

$$\begin{aligned} \phi(\mathbf{x}) = & \min(\max(\min(x_1, \max(x_6, x_7)), \min(\max(x_2, x_3), \min(\max(x_4, x_5), \\ & \max(x_6, x_7)), x_8)), \max(\min(\max(x_9, x_{10}), \max(x_{14}, x_{15}, x_{16})), \\ & \max(\min(\max(x_{11}, x_{12}), x_{17}), \min(x_{13}, \max(x_{18}, x_{19}))))), \max(x_{20}, x_{21})). \end{aligned} \quad (5.25)$$

This structure function is diagonally state neutral, consequently, also diagonally state invariant, and diagonally state extreme. A graphical representation is given in 5.6.

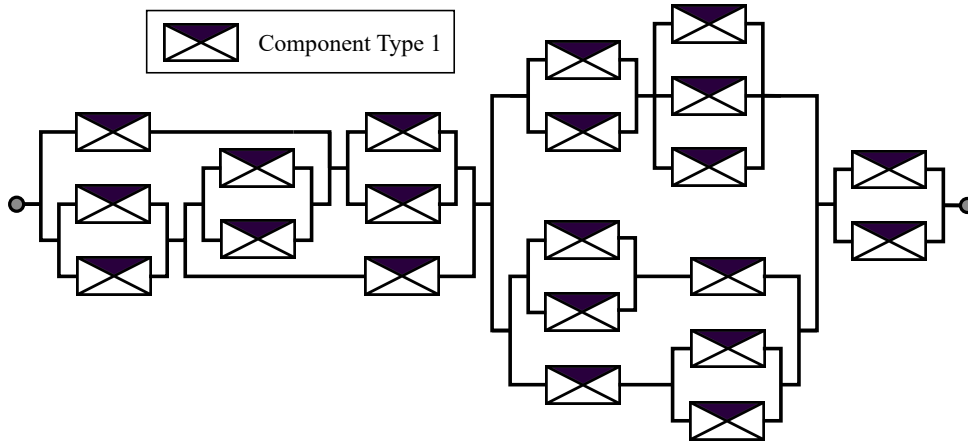


Figure 5.6: System composed by min- and max-operators with 21 components, adapted from [304].

Test of applicability: infrastructure system

In today's highly developed world, complex systems such as infrastructure networks and industrial plants are omnipresent and of vital importance to the functioning of modern societies. Consequently, the resilience of these systems is of utmost importance as well. Therefore, in the following, an arbitrarily chosen infrastructure network, represented by a graph, is considered. 5.7 illustrates the graph of this exemplary system. Hereafter, This system is referred to as 18-Component-Infrastructure-System.

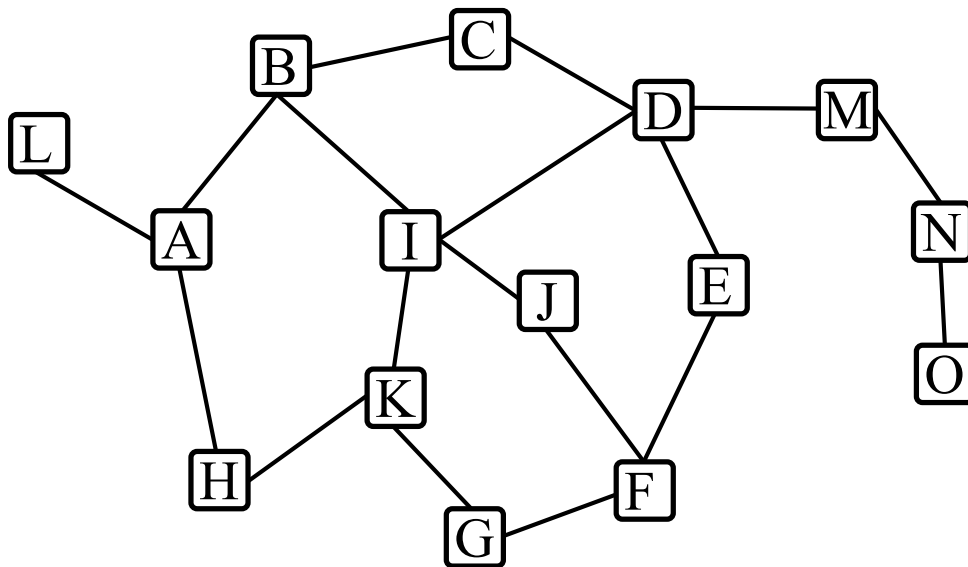


Figure 5.7: Arbitrary infrastructure system.

The graph consists of 15 nodes (capital letters, e.g., A) and 18 weighted edges (links between, e.g., $A - B$), where the nodes may represent cities in the system and the edges may represent transit links, as an example. The weights of the traffic routes can be interpreted as the travel

time T required to complete this route.

As, e.g., in [259], [268] and [304], for the analysis of this infrastructure system it is assumed that it has a performance function defined by the so-called network efficiency. According to Latora and Marchiori [261], the network efficiency E represents a qualitative indicator of the connectivity of a network and is defined as:

$$E(G) = \frac{1}{N(N-1)} \sum_{i \neq j \in V} \frac{1}{d_{ij}^W}, \quad (5.26)$$

with G denoting the considered graph, V is the set of nodes, i.e., cities, $N = |V|$ the number of cities and d_{ij}^W the weighted path length between city i and city j , that is, the path with shortest travel time between these two cities. A detailed review of algorithms for efficiently determining the path length d_{ij}^W , such as the Floyd, Dijkstra, or Bellman-Ford algorithms, can be found, e.g., in [263] and [262]. Furthermore, the authors in [261] and [313] proposed the utilization of a normalized network efficiency E_{glob} :

$$E_{\text{glob}}(G) = \frac{E(G)}{E(G^{\text{ideal}})}. \quad (5.27)$$

$E(G^{\text{ideal}})$ is here the network efficiency of the graph in ideal state, i.e., all edges and nodes are present and fully operative. As a basis for calculating d_{ij}^W with respect to degrading edges, assume a monotonic functional relationship between the performance of the degrading edge and the travel time assigned to that edge. Therefore, a transformation function that maps

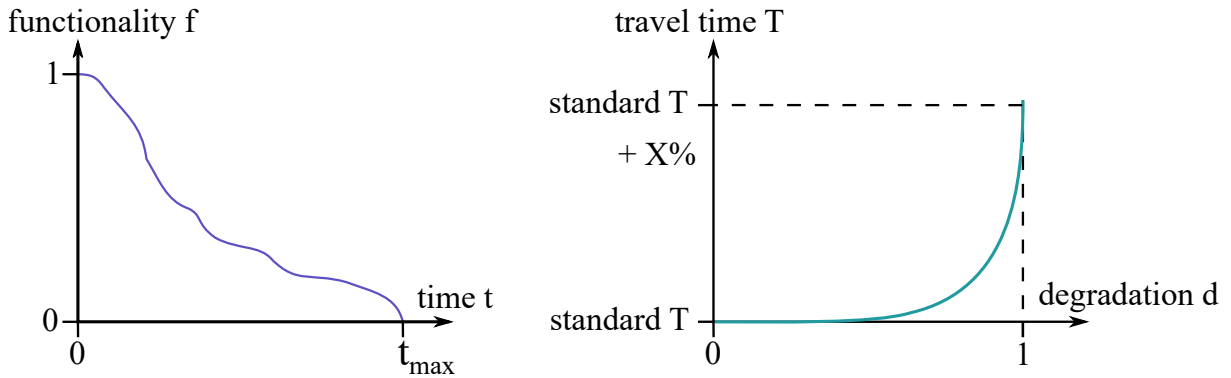


Figure 5.8: Relation of the edge degradation and travel time T for infrastructure graph systems.

the component functionality $f \in [0, 1]$ to a component degradation $d \in [0, 1]$ via $d = 1 - f$ is introduced. Further, the component degradation is mapped to the travel time T via an arbitrary function depicted in 5.8 on the right. Note that the function has to ensure the requirement that the system structure function is at least diagonally state neutral. This function has an exponential shape, For $d = 0$, the travel time of the edge is equal to the standard travel time assigned as weight to the edge beforehand. The travel time increases up to a value of standard

travel time plus 800% of the standard travel time as maximum.

5.4.2 Stochastic modeling of the component degradation process

As fundamental step for computing the continuous-state survival function via a structure function $\phi(\mathbf{x})$, the probability structure characterizing the component state vector \mathbf{x} in a probabilistic manner over time has to be established. In the case of the DAS, this corresponds to the continuous-state survival function, while sampling during MCS requires probability densities as fundamental form. As outlined in 5.3.1, there exist a variety of approaches to generate the basic probability structure. In this work, an arbitrary stochastic process is proposed for illustrative purposes.

The stochastic degradation of components is modeled by combining an inverse Gamma process and a Gamma process. These types of processes are widely spread in stochastic degradation modeling [246, 314, 315]. Correspondingly, let $Z \sim InverseGamma(\alpha, 1)$ and $Y \sim Gamma(\beta, 1)$ be the random variables. Then, a random variable characterizing component degradation following a Beta process results when sampled as

$$X = \frac{Z}{Z + Y} \sim Beta(\alpha, \beta), \quad (5.28)$$

see [316].

MCS is applied to obtain a true solution estimate. In this case, the *iid* component state vector $\mathbf{x} = [0, 1]^n$ is sampled with respect to 5.28 for all obtained numerical results that are subsequently presented. Consequently, the state of the i -th component is characterized as $x_i = X$. Thereby, N_{MCS} state samples are generated for each component in the online phase.

In the case of the DAS, a continuous-state survival function describes the probabilistic characteristics of a component. Accordingly, the continuous-state survival function of a component can be established by solving the integral

$$R_x(s, t) = P(X \geq s | t) = \int_X I(X \geq s | t) = \frac{1}{N_{DAS}} \sum_{j=1}^N I(x_j \geq s | t), \quad (5.29)$$

where X denotes the random performance variable characterizing the component state, I corresponds to the indicator function, s is the considered state threshold, and t corresponds to the currently considered time. Further, N_{DAS} refers to the number of MCS samples utilized to estimate the true solution of the continuous-state survival function for components and x_j is the j -th state sample, compare 5.13. It is possible that $N_{DAS} \neq N_{MCS}$.

As exemplary parameters, $\alpha = 0.15$ and $\alpha = 0.6$ were arbitrarily selected. Further, *InverseGamma*($\alpha, 1.5$) was assumed, skewing the Beta process to the left. These parameters were applied for all presented case studies.

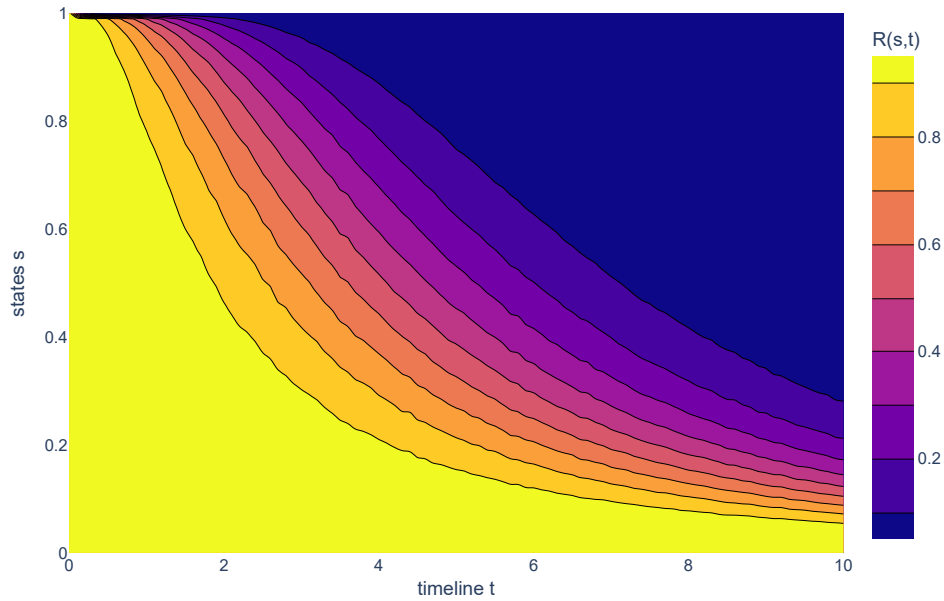
5.4.3 Numerical results

In this section all computed results are presented. Convergence studies for the number of samples as well as studies concerning the computation time with respect to the number of samples and the number of states were conducted. Further, contour plots of the continuous-state survival function approximated by the DAS and contour plots depicting the corresponding error are provided. Note that the code utilized to compute the following numerical results was not optimized in terms of computational efficiency for the DAS and included *print* statements for computations based on MCS and DAS. Further, the code was not parallelized and variations in the capacity of working memory were unavoidable during the studies concerning convergence and computation time. Besides the study of computation time in terms of the number of considered states, all plots were generated with this number set to 101 states.

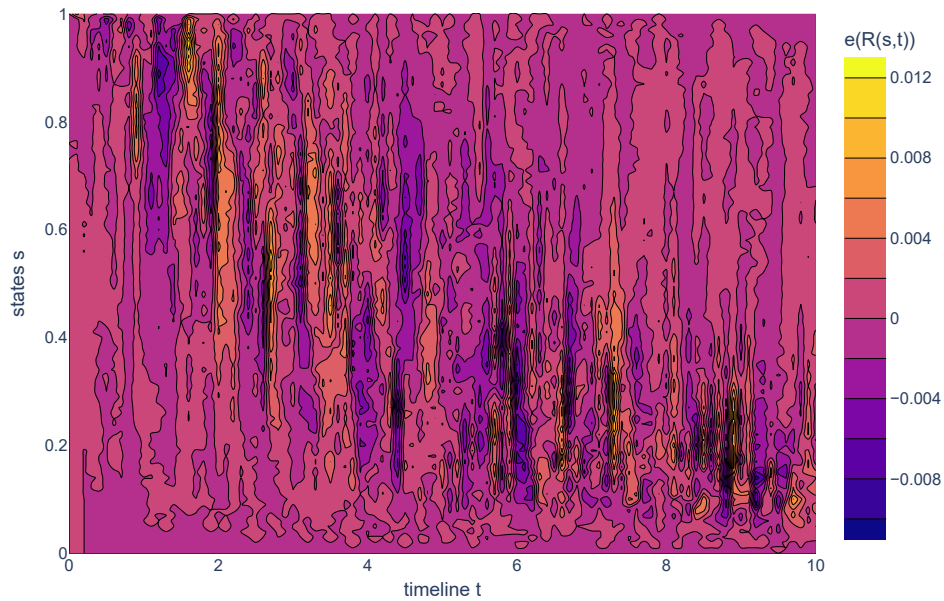
2-component-min-system

At first, consider the results computed for the continuous-state survival function of the 2-Component-Min-System. In 5.9, the approximation of the continuous-state survival function by means of the concept of DAS is depicted. The contour plot shows $R(s, t)$ with a step size of 0.1. In this example, the sample size $N = N_{MCS} = N_{DAS}$ equals 51 000. No significant differences between the computation via MCS, DAS and condensed DAS (indicated by DASC) could be observed during the study. Consequently, it is sufficient to consider a single contour plot out of three. As it can be observed in the figure, slight variations occur along the contour curves. 5.9b shows the error between the true solution estimate obtained by means of MCS and the approximation via the condensed DAS. In theory, the DAS should yield exact results when for the underlying sampling process $N_{DAS} \rightarrow \infty$. This can be verified by the obtained results, as contour plot of the error purely exhibits variations with a maximum magnitude of 0.012 due to the variance in sampling process of the underlying component degradation. It can be presumed that the error vanishes completely for $N_{MCS} = N_{DAS} \rightarrow \infty$.

This becomes even more evident when considering 5.10. The convergence study was conducted for sample sizes in the interval [1 000, 51 000] with a step size of 10 000. Three different error measures were taken into account, namely, the Mean Absolute Error (MAE), the Mean Squared Error (MSE), and the Root Mean Square Error (RMSE). Thereby, the errors between MCS true solution estimate and both the approximations via DAS and via condensed DAS were considered. They represent the total error over the entire spatial and temporal domain under consideration. The error norms are common measures for evaluating the performance of estimators such as the MCS. As expected, all indicators converge against zero for an increasing sample size. The results emphasize that the developed approach neither suffers from significant outliers nor a bad approximation in average. 5.11 shows studies concerning the computation time with respect to the number of samples N , see in 5.11a, as well as to the number of considered states, see 5.11b. The study with respect to sample size were considered analogously to the convergence study with sample sizes N_{MCS} and N_{DAS} between 1 000 and 51 000 with a step size of 1 000. For the



(a) Continuous-state survival function by means of DASC.



(b) Error between MCS estimate and DASC approximation.

Figure 5.9: 2-component-min-system: DAS condensed approximation of continuous-state survival function and the corresponding error.

study of computation time in terms of the number of considered states, the sample size N was set to 11 000. It can be observed that the MCS exhibits a steep linear relation between the total computation time in the online phase and the number of samples as well as a similar factorized

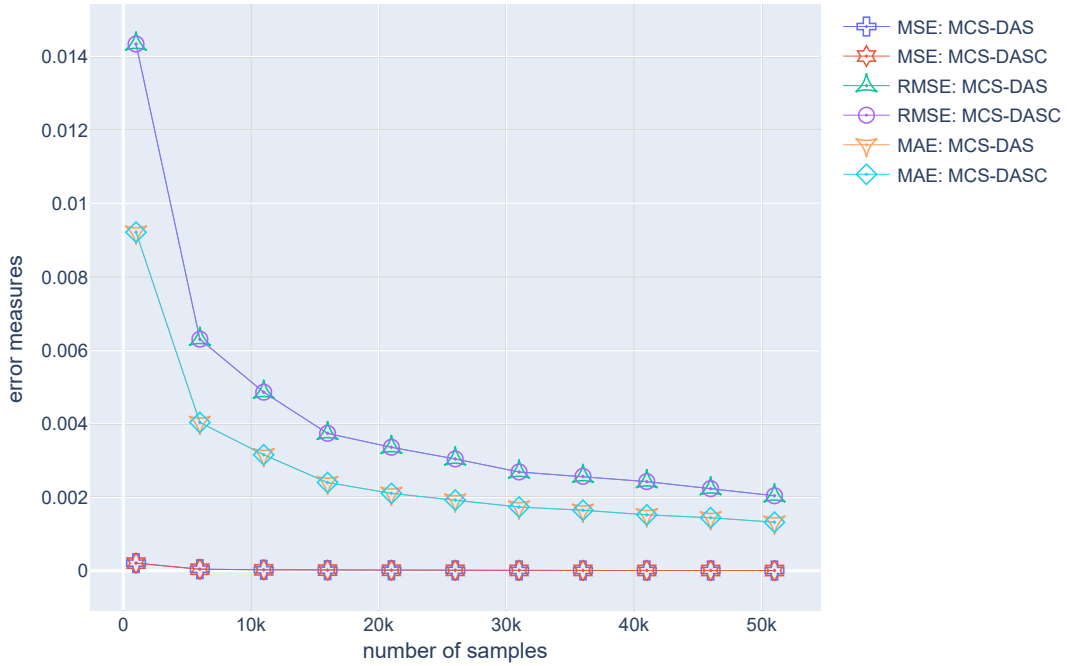
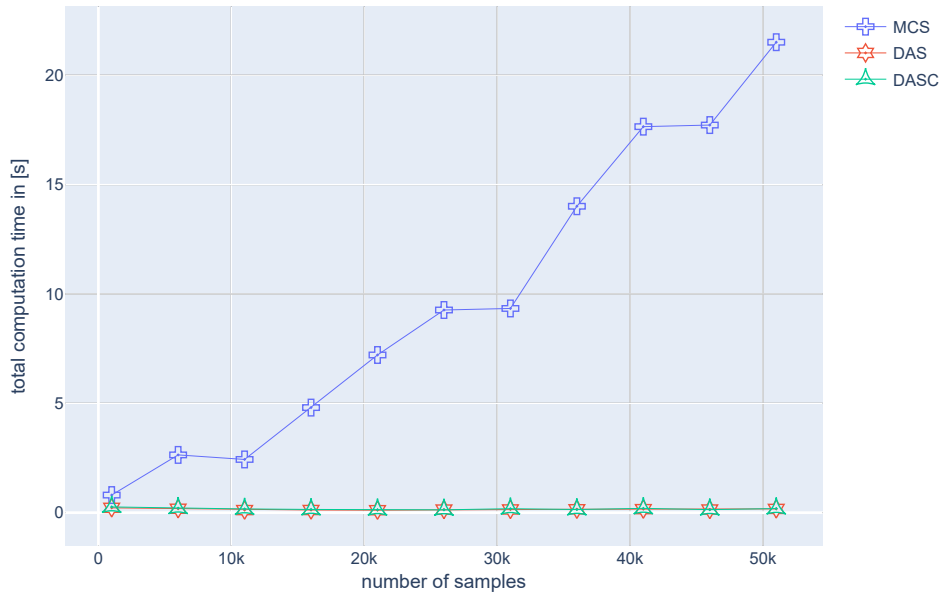


Figure 5.10: 2-component-min-system: convergence study of MCS true solution estimate vs. DAS approximation of the continuous-state survival function with MAE, MSE and RMSE as error measures in terms of sample size N_{MCS} , while $N_{DAS} = 100\,000$.

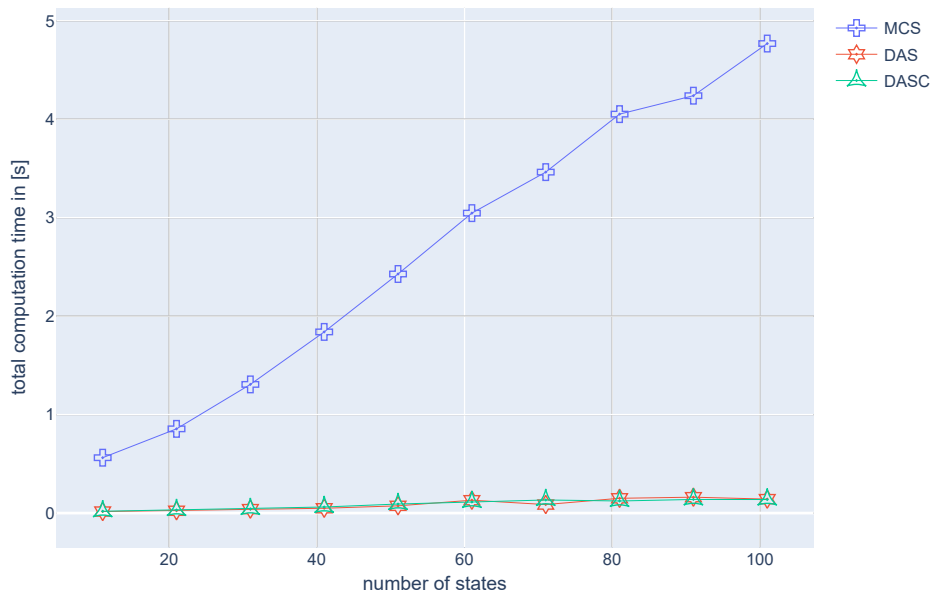
linear relation between the online computation time and the number of states. Both DAS and DASC are constant with respect to the sample size. A slight linear relation can be observed in the plot considering the number of states. In both plots the DAS and DASC exhibit computation time in the same magnitude around 0 that is lower than the one achieved by MCS already for $N = 1\,000$. This results from the fact that the sums over $n = 2$ and $\max(|\binom{n}{i_s}|) = 3$ for the DAS as well as $n = 2$ and $J = 2$ for the DASC are computationally not demanding compared to 1000 evaluations of the structure function.

2-component-max-system

Secondly, consider the computed results for the continuous-state survival function of the 2-Component-Max-System. Again, 5.12 shows the approximation of the continuous-state survival function by means of the DASC while 5.12b depicts the corresponding error. Considering 5.12a, the continuous-state survival function indicates higher reliability and robustness of the 2-Component-Max-System compared to the 2-Component-Min-System as expected. Not only is the domain for which $R(s, t) = 1$ larger but also the domain between the contour curves. In this example, the sample size $N = N_{MCS} = N_{DAS}$ equals 51 000. Similarly to the previous case study, slight variations occur along the contour curves. The error exhibits variations only due



(a) ...with respect to the number of samples N .

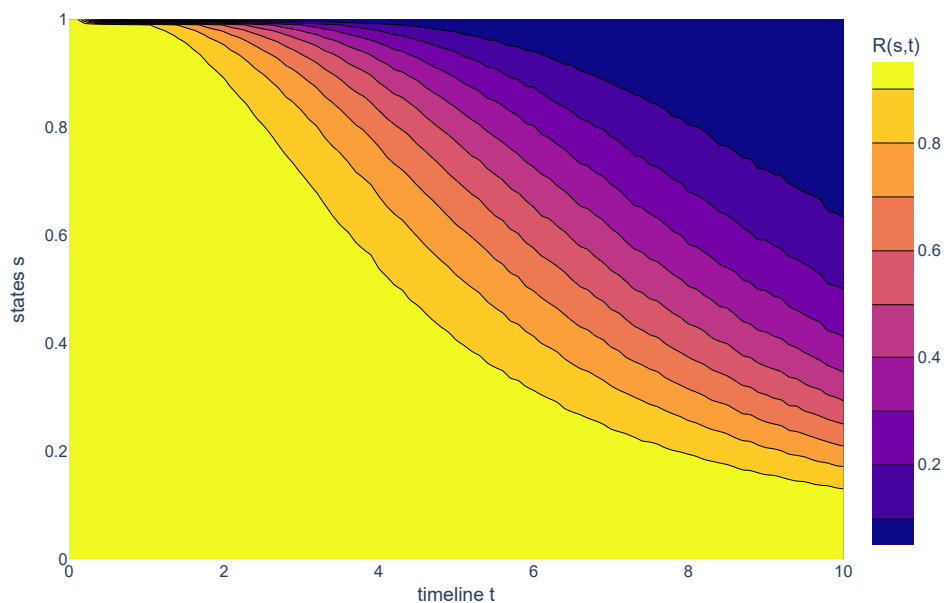


(b) ...with respect to the number of considered states.

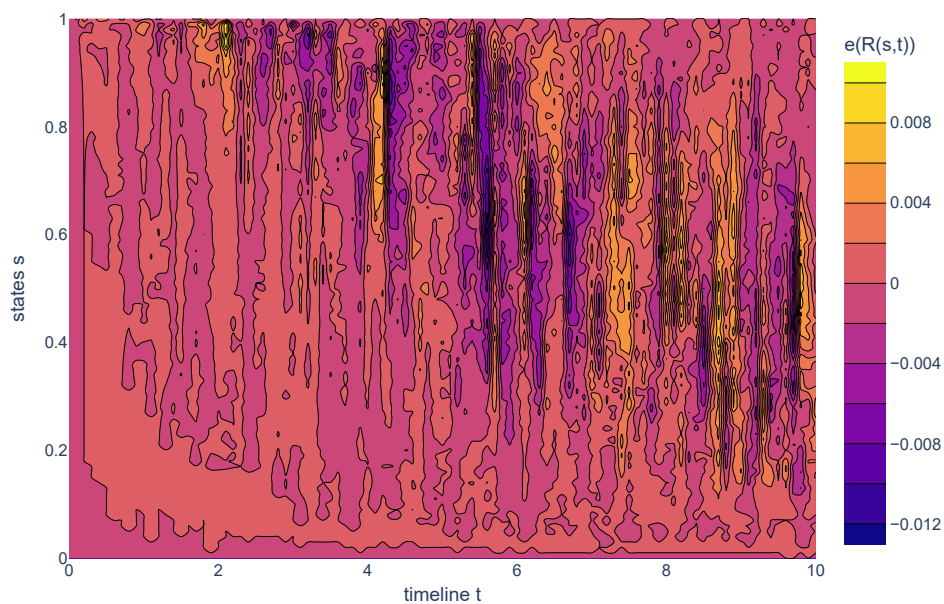
Figure 5.11: 2-component-min-system: study of computation time for MCS true solution estimate, DAS approximation, and DAS condensed approximation of the continuous-state survival function...

to the variance of the underlying sampling processes in the same magnitude of 0.012 as for the previous example.

Considering 5.13 it becomes evident that also for this case study $e(R(s, t)) \rightarrow 0$ if $N_{DAS} \rightarrow \infty$.



(a) Continuous-state survival function by means of DASC.



(b) Error between MCS estimate and DASC approximation.

Figure 5.12: 2-component-max-system: DAS condensed approximation of continuous-state survival function and the corresponding error.

The results, obtained for all error measures, are as expected and similar to the previous case study. With regard to 5.14, the sample sizes for both studies of computation time, compare 5.14a and 5.14b, are the same as in the previous example. Besides larger variations due to the in time

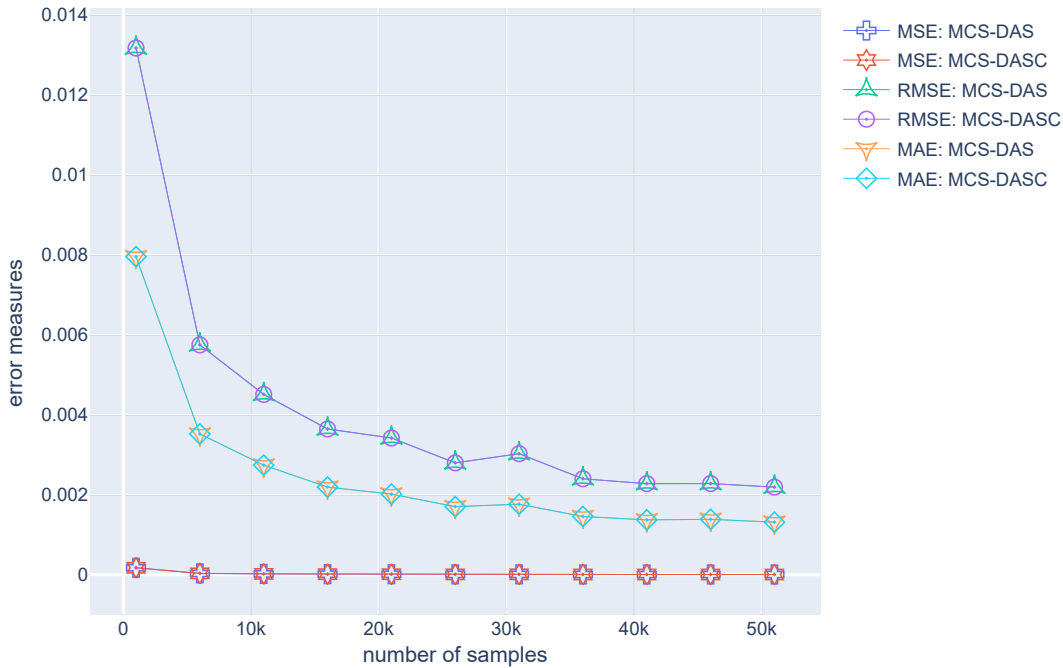


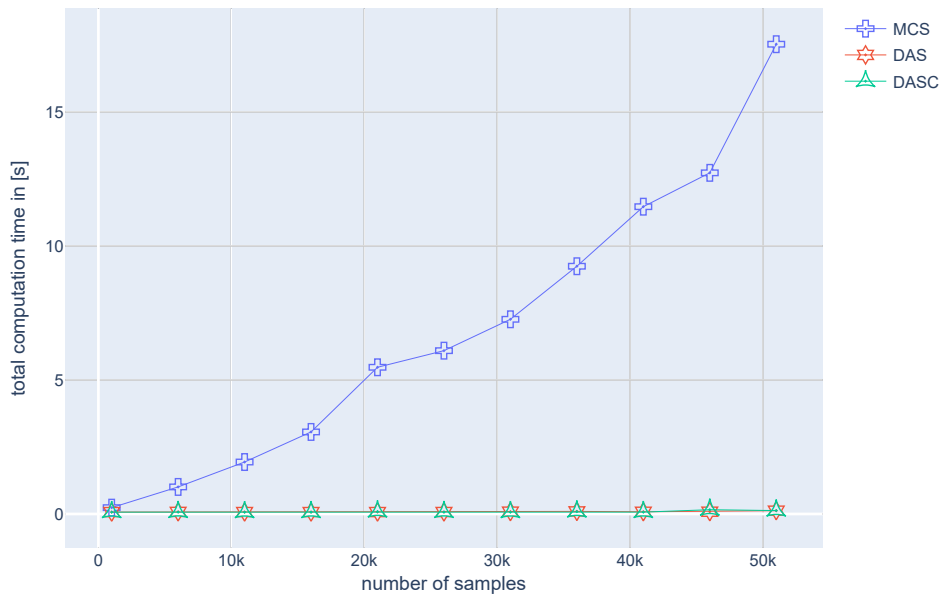
Figure 5.13: 2-component-max-system: convergence study of MCS true solution estimate vs. DAS approximation of the continuous-state survival function with MAE, MSE and RMSE as error measures in terms of sample size N_{MCS} , while $N_{DAS} = 100\,000$.

varying capacity of the local working memory, the computation time required in the online phase are similar to the previous example. The MCS exhibits a linear relation for both sample size and number of states. In contrast, the DAS and DASC shows a constant relation, see 5.14a. In terms of increasing states, a slight linear relation with significantly lower computation times can be observed, as illustrated in 5.14b.

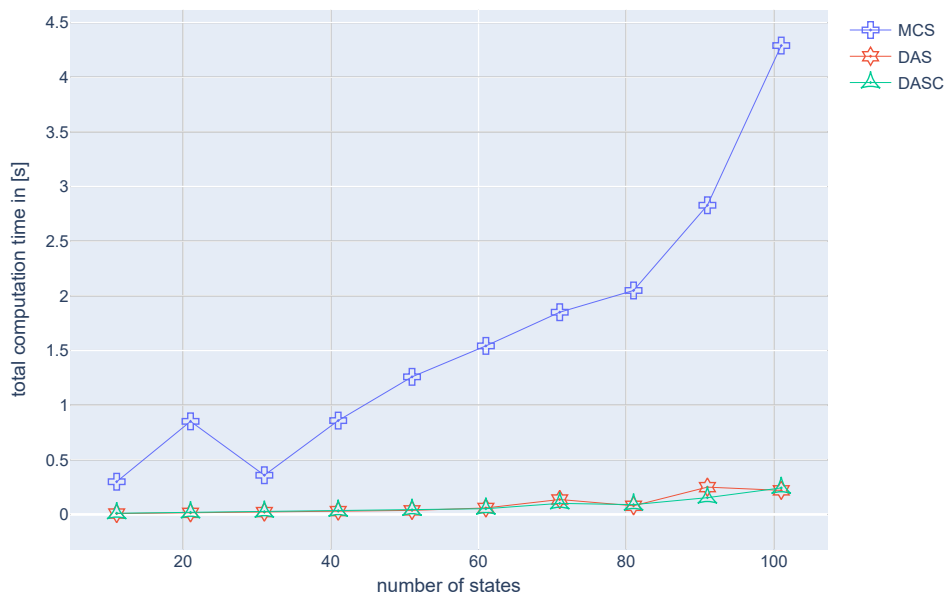
8-component-minmax-system

Again, 5.15 verifies the expected behavior of the DAS and the DASC. In this example, the sample size $N = N_{MCS} = N_{DAS}$ equals 51 000. The contour plot of the continuous-state survival function in 5.15a appears as a mixture of an 8-Component-System solely composed by min-operators as minimum and an 8-Component-System solely composed by max-operators. The error in 5.15a has the same maximum magnitude of 0.0012 as in the previous examples. The region with the largest errors lies between the contour curves with $R(s, t) < 1$ and $R(s, t) > 0$. Considering the previous contour plot of the error, this high magnitude region shifts to the bottom left for a Min-System and to the upper right for a Max-System.

When considering 5.16, the behavior of all three error measures appears similar to the previous examples. This is counterintuitive as one would expect an increasing error when sampling in



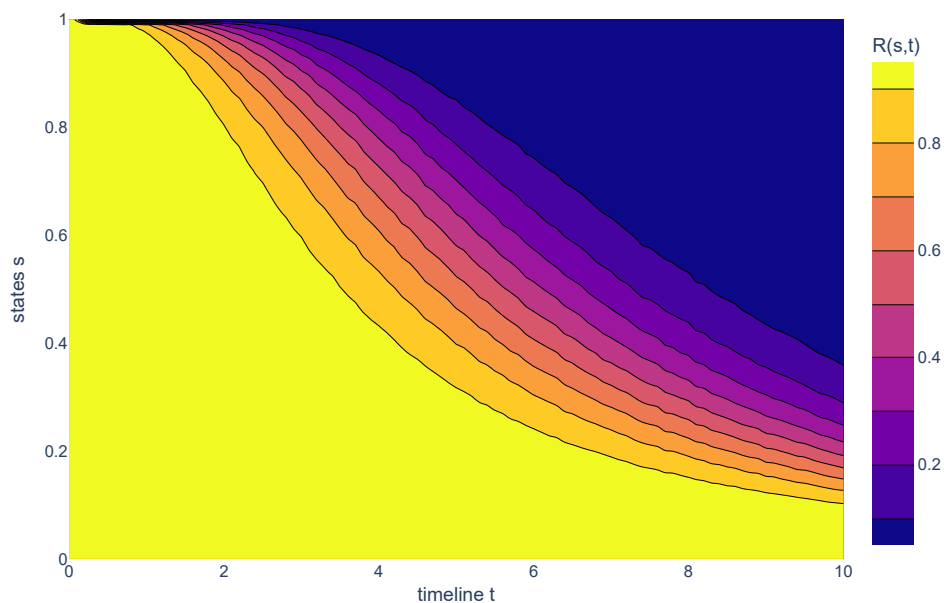
(a) ...with respect to the number of samples N .



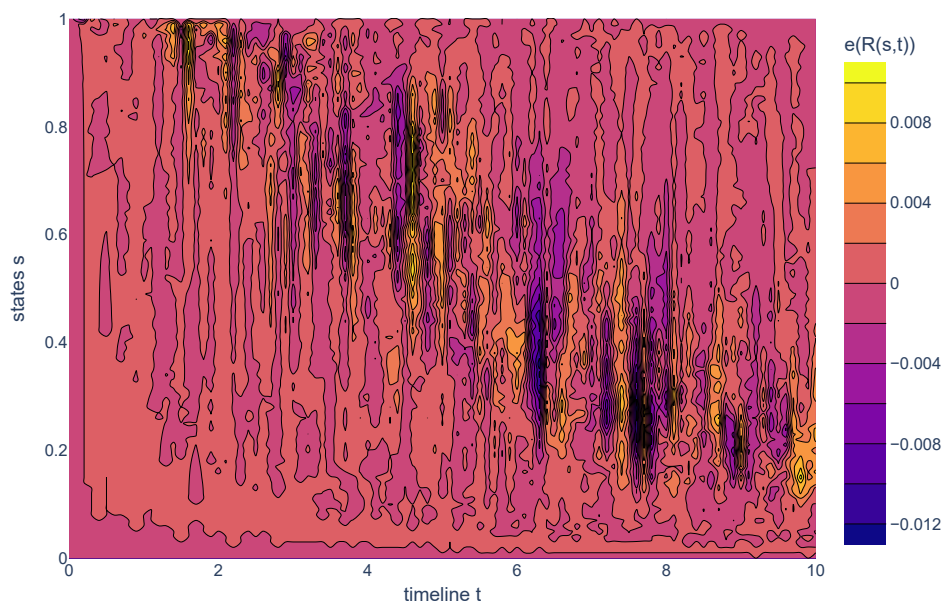
(b) ...with respect to the number of considered states.

Figure 5.14: 2-component-max-System: study of computation time for MCS true solution estimate, DAS approximation, and DAS condensed approximation of the continuous-state survival function...

higher dimensions, compare [317]. But this seems not to hold true for diagonally state invariant structure functions. The ranges of sample sizes for both studies of computation time shown in 5.17 are the same as in the previous example. Analogously to the previous examples, the



(a) Continuous-state survival function by means of DASC.



(b) Error between MCS estimate and DASC approximation.

Figure 5.15: 8-component-minmax-system: DAS condensed approximation of continuous-state survival function and the corresponding error.

computation times of the MCS are characterized by a similar linear relation with respect to both sample size and number of considered states. In contrast, DAS and DASC are constant in their relation with respect to the sample size. In terms of the number of considered state,

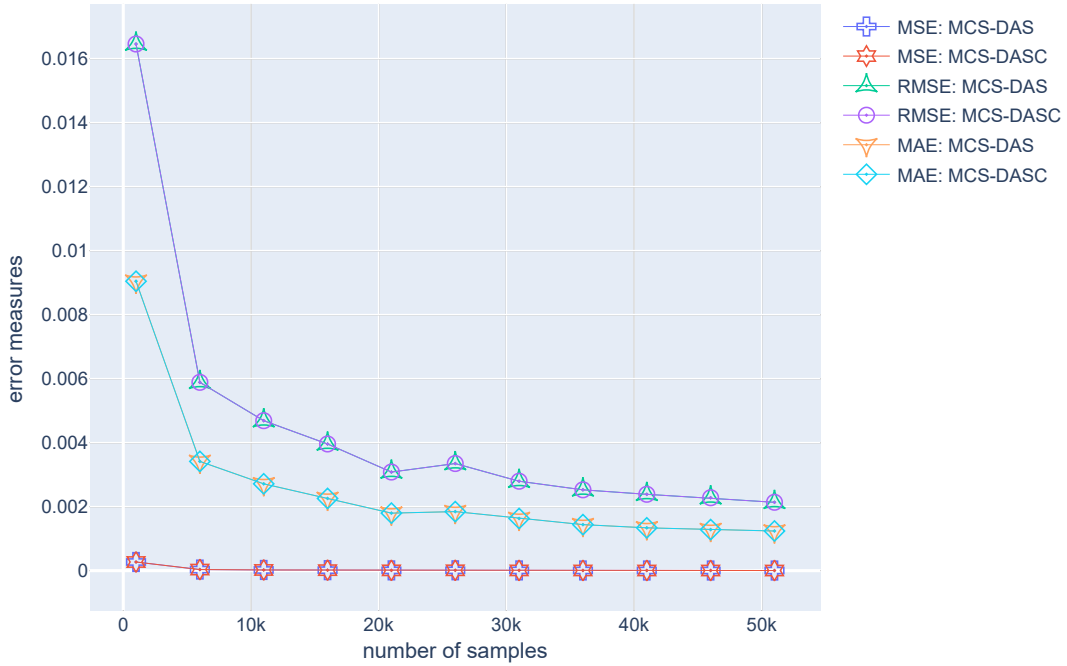
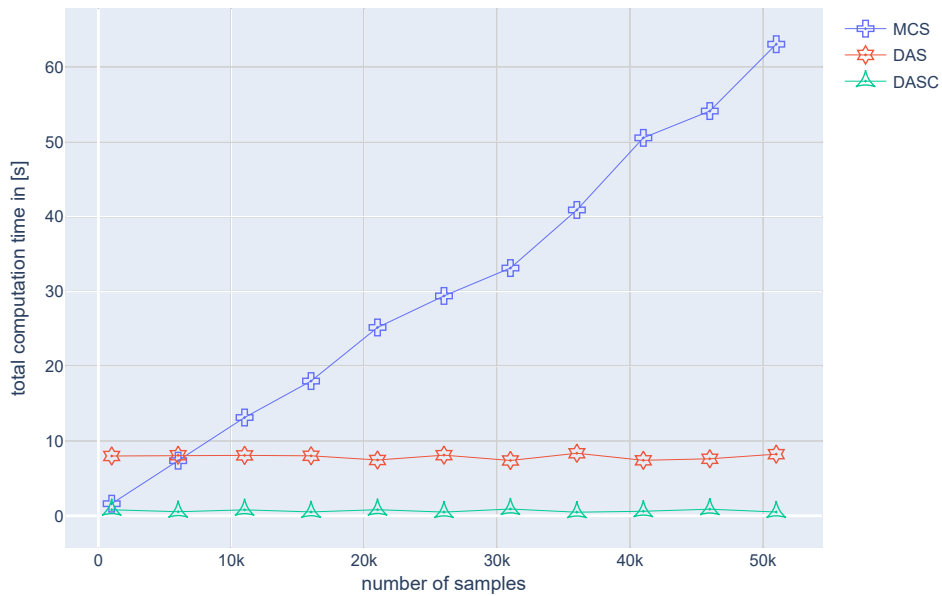


Figure 5.16: 8-component-minmax-system: convergence study of MCS true solution estimate vs. DAS approximation of the continuous-state survival function with MAE, MSE and RMSE as error measures in terms of sample size N_{MCS} , while $N_{DAS} = 100\,000$.

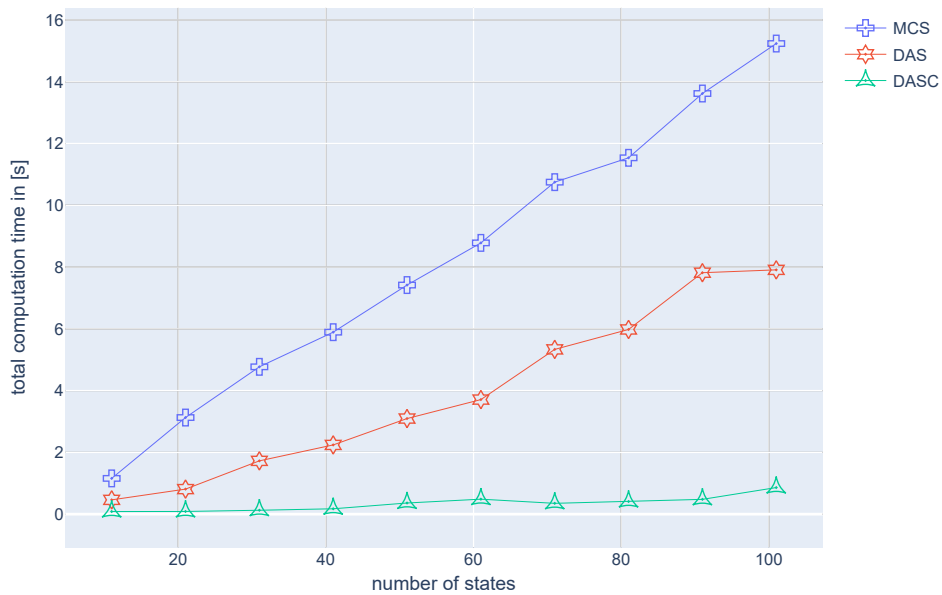
both DAS and DASC follow linear relations. It is noteworthy, that the factor of the linear relation of the DAS seems significantly larger than before. Also in terms of the sample size the computational time during the online phase significantly increased for the DAS. It can be observed that for $N = 1\,000$ the DAS is outperformed by the MCS approach. This result is reasonable as the number of permutations tremendously increase for higher dimensions corresponding to the binomial coefficient $\binom{n}{l_s}$, besides the already increasingly demanding sum over n leading to the slightly increased linear relation of the DASC. Nevertheless, the DASC still possesses a low factor in its linear relation while maintaining exact results.

21-component-minmax-system

For this case study, the fundamental concept of DAS was omitted due to the combinatorial complexity of $\binom{n}{l_s}$ becoming computationally too demanding, resulting in unreasonable computational time. Consequently, solely the condensed DAS is applied as surrogate modeling approach. Considering 5.18a and comparing it to the previous examples, the continuous-state survival function appears as a mixture of min- and max-operators as expected. It is observable that the domain in between of the contour curves are smaller than in the previous examples. In this example, the sample size $N = N_{MCS} = N_{DAS}$ equals 100 000. The sample size was increased to



(a) ...with respect to the number of samples N .

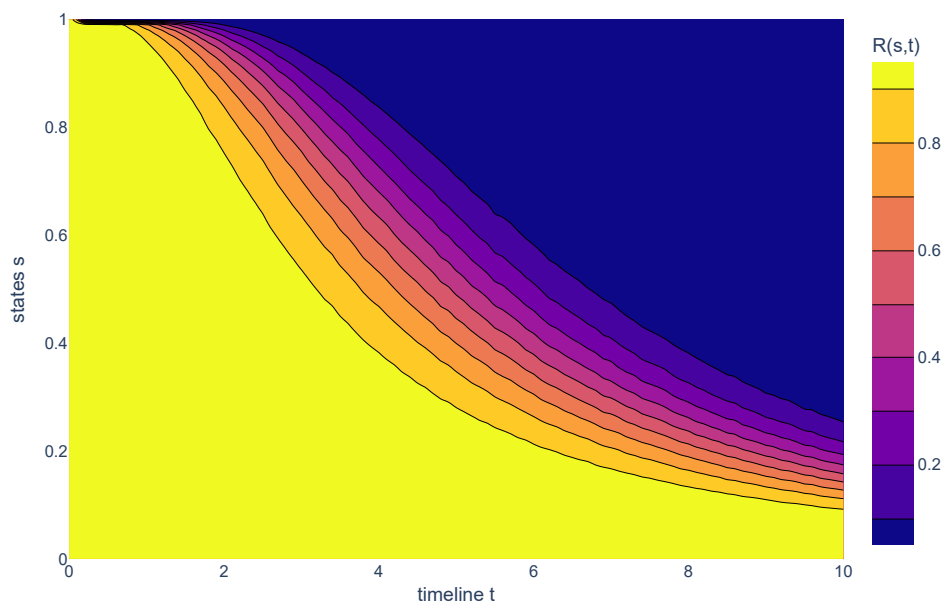


(b) ...with respect to the number of considered states.

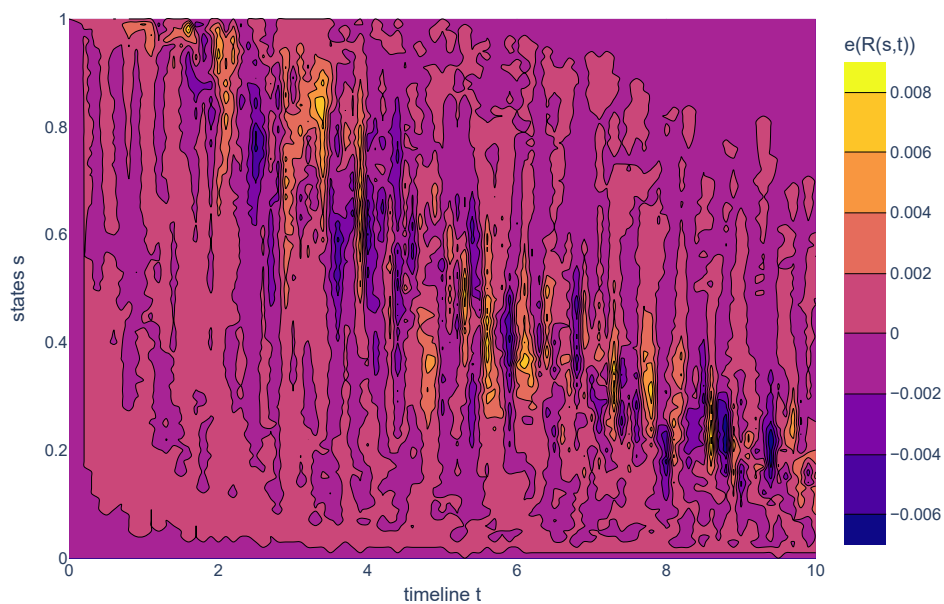
Figure 5.17: 8-component-minmax-system: study of computation time for MCS true solution estimate, DAS approximation, and DAS condensed approximation of the continuous-state survival function...

maintain a similar magnitude of errors as can be observed in 5.18b.

For the convergence study depicted in 5.19, the number of samples was increased for the entire range. The evaluated sample sizes lie in the interval $[20\,000, 200\,000]$ with a corresponding step



(a) Continuous-state survival function by means of DASC.



(b) Error between MCS estimate and DASC approximation.

Figure 5.18: 21-component-minmax-system: DAS condensed approximation of continuous-state survival function and the corresponding error.

size of 20 000. The DASC also converges to zero for this high-dimensional structure function that is diagonally state neutral and diagonally state extreme as composed by min- and max-operators. This coincides with the theory established in 5.3: The DAS and DASC yield the true solution

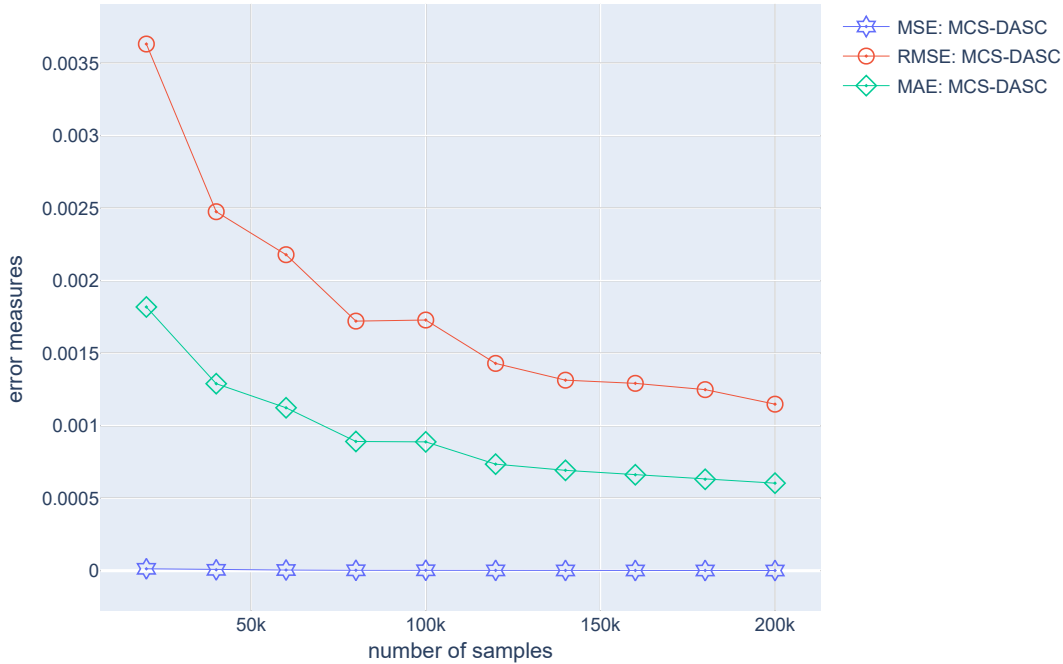


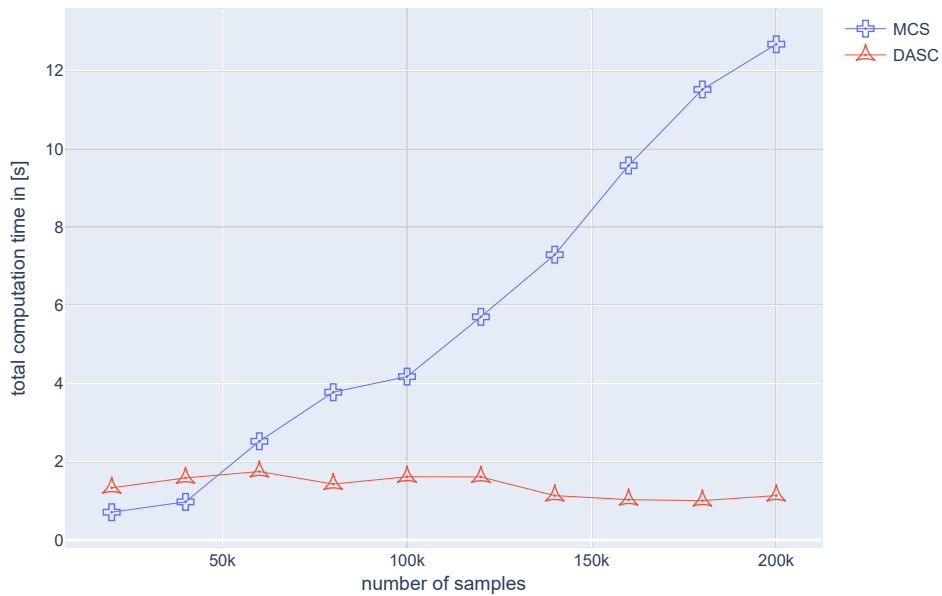
Figure 5.19: 21-component-minmax-system: convergence study of MCS true solution estimate vs. DAS approximation of the continuous-state survival function with MAE, MSE and RMSE as error measures in terms of sample size N_{MCS} , while $N_{DAS} = 100\,000$.

of such systems or at least an estimate only in dependence on the variance of the underlying estimator of the component probability structure. For the study of computation time regarding the number of considered states, the sample size N was set to 100 000. In terms of computation time, higher variance can be observed in 5.20 then in the previous examples. This relates to the variance in capacity of the deployed working memory. Again, a steep linear relation can be observed for the MCS in terms of an increasing sample size. The DASC exhibits a constant relation for N_{DAS} due to its independence. The expected linear relation of the DASC concerning the number of considered states significantly increased compared to the previous examples. Despite the tremendous increase of computational complexity, the DASC still outperforms the MCS globally. Only for smaller sample sizes where larger error magnitudes can be observed the MCS shows slightly shorter computation times compared to the constant.

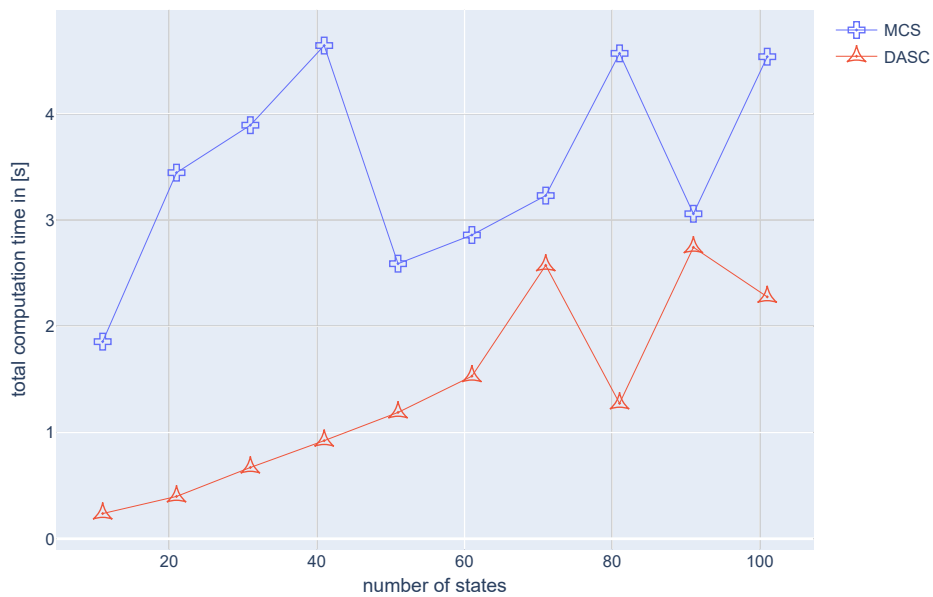
18-component-infrastructure-system

For this example, solely the DASC and the rounded DASC (referred to as DASC_R) were considered. To compute the underlying DAS for this example the maximum number of iteration steps h_{max} was set to 100.

The continuous-state survival function obtained by means of the DASC is depicted in 5.21a. The



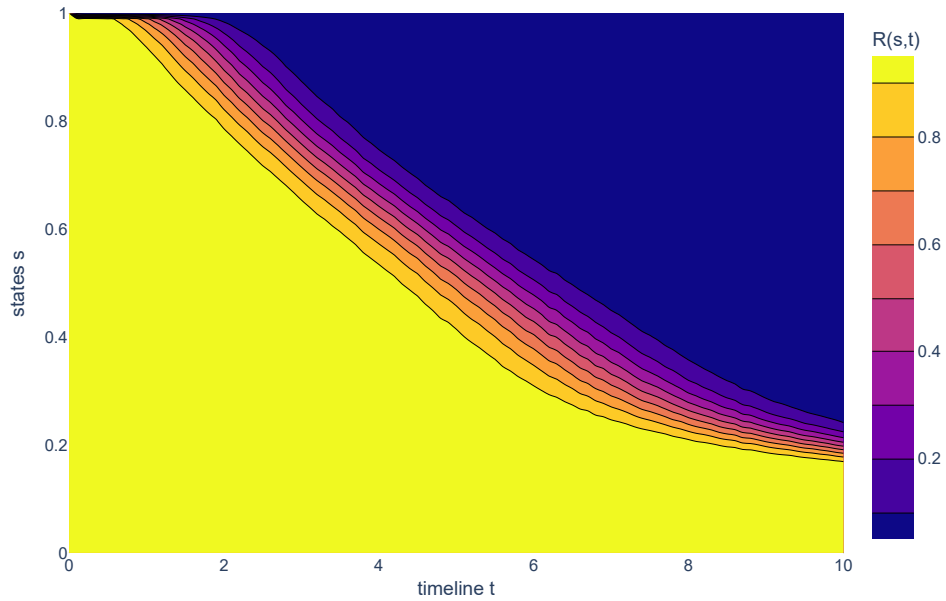
(a) ...with respect to the number of samples N .



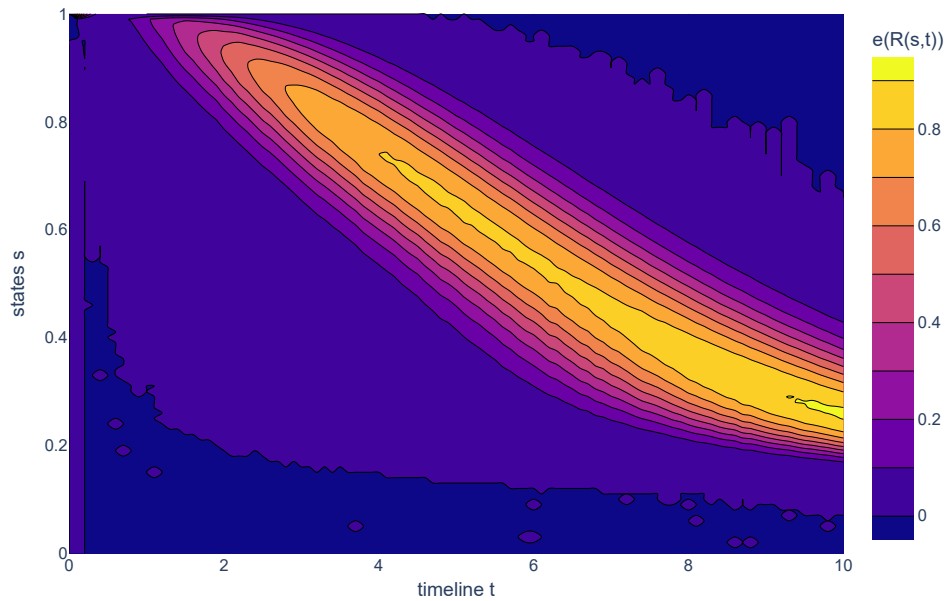
(b) ...with respect to the number of considered states.

Figure 5.20: 21-component-minmax-system: study of computation time for MCS true solution estimate, DAS approximation, and DAS condensed approximation of the continuous-state survival function...

contour plot appears reasonable. As expected, the DASC achieves an approximation that in the worst case underestimates the true solution but never overestimates it. The theoretical findings can be verified when considering 5.21b. The contour plot of the error between the MCS true



(a) Continuous-state survival function by means of DASC.



(b) Error between MCS estimate and DASC approximation.

Figure 5.21: 18-component-infrastructure-system: continuous-state survival functions computed by means of DASC and the corresponding error.

solution estimate and the approximation is positive over the entire domain. Dark blue indicates an error magnitude of zero while dark purple represents magnitudes in the scale of machine precision.

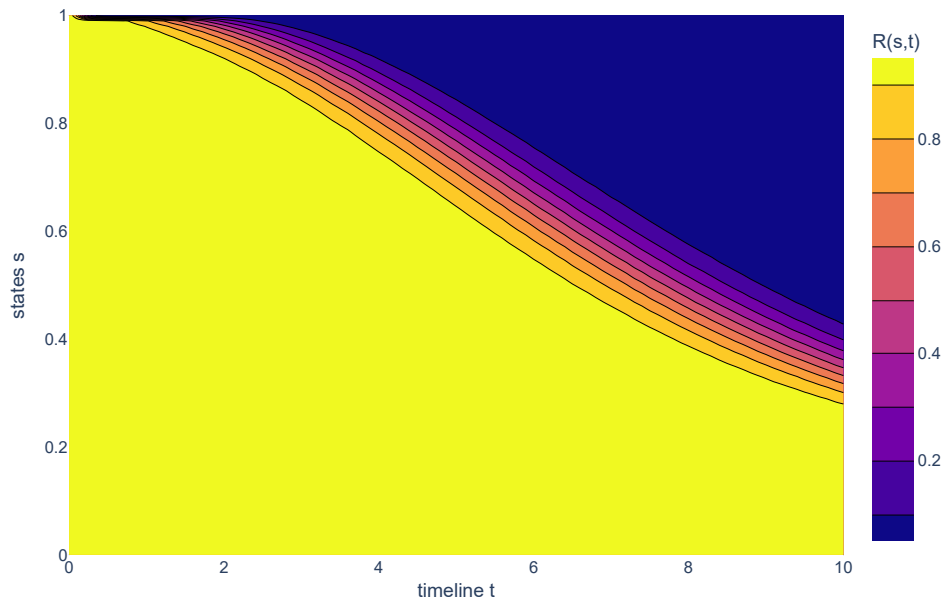
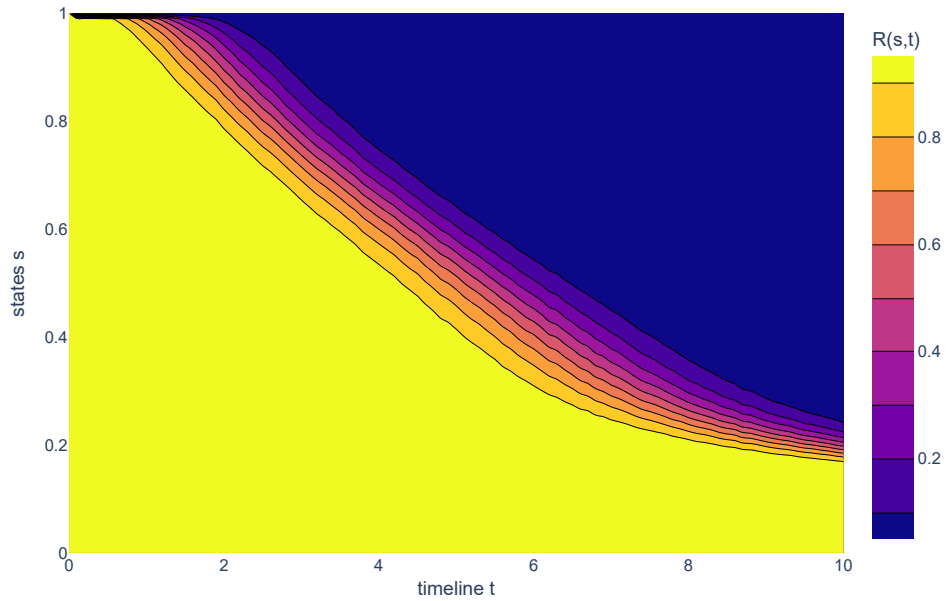


Figure 5.22: 18-component-infrastructure-system: MCS true solution estimate.

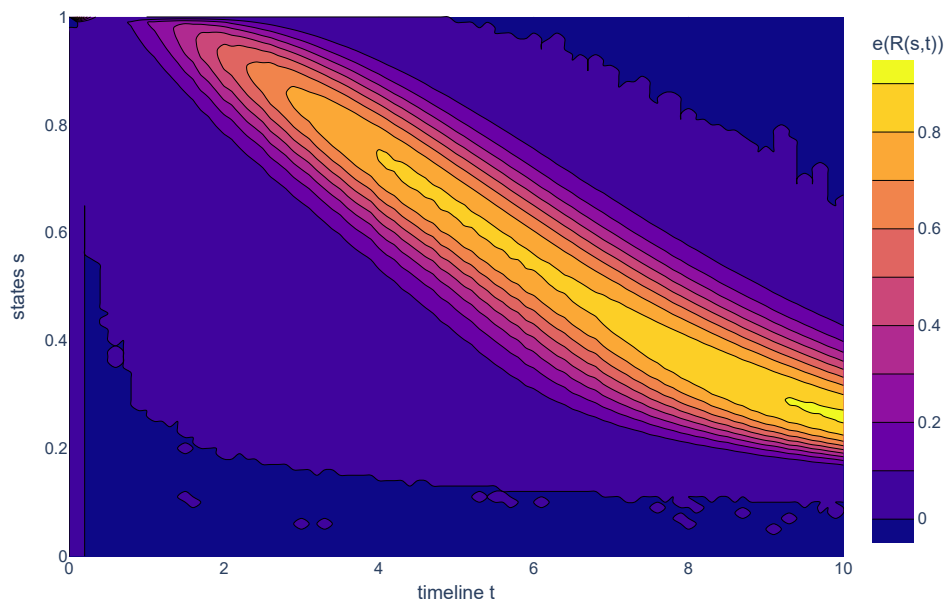
The applied scheme already yields satisfying results taking into account that it is only a first-order scheme for at least diagonally state neutral structure functions. However, a higher-order implementation could significantly decrease the error in the remaining domain. In general, the proposed methodology is also applicable to diagonally state negative structure functions when adjusting the corresponding formula. For this example, it was ensured that the structure function is at least diagonally state neutral by accordingly specifying the exponential transformation function mapping component degradation to travel time. 5.22 shows the true solution estimate of the continuous-state survival function obtained by means of MCS. The region of significant magnitudes of the error between the MCS and the DASC occurs as the underlying structure function is no longer diagonally state constant. As the structure function is still at least diagonally state neutral this is the only source for errors besides the natural variance of the stochastic degradation process.

The DASC was applied to further increase the computational efficiency. In the following, the potential decrease of accuracy is studied. The proposed methodology still ensures pure underestimation of the true solution. For $r = 5$, compare 5.21, the computation time already decreases significantly while the contour plots of the error appear similar, see 5.23b.

For $r = 3$, the computation time can be further reduced as J decreases significantly. Thereby, it can be observed that the accuracy increases as all regions of error contour curves decrease in terms of their area, see 5.24. The same observation can be made for $r = 2$: A tremendous reduction of computation time could be achieved as the DASC further condenses the information in



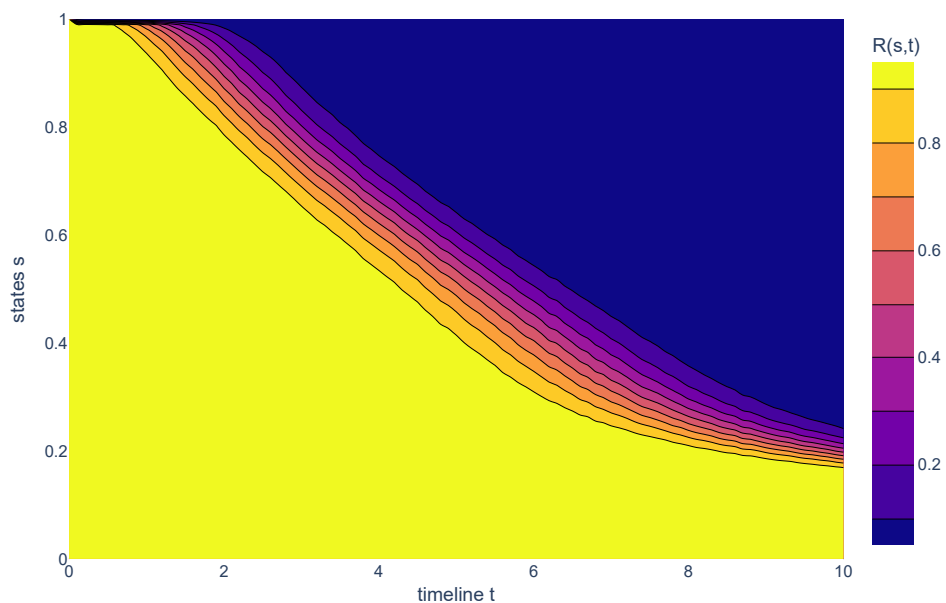
(a) Continuous-state survival function by means of DASC.



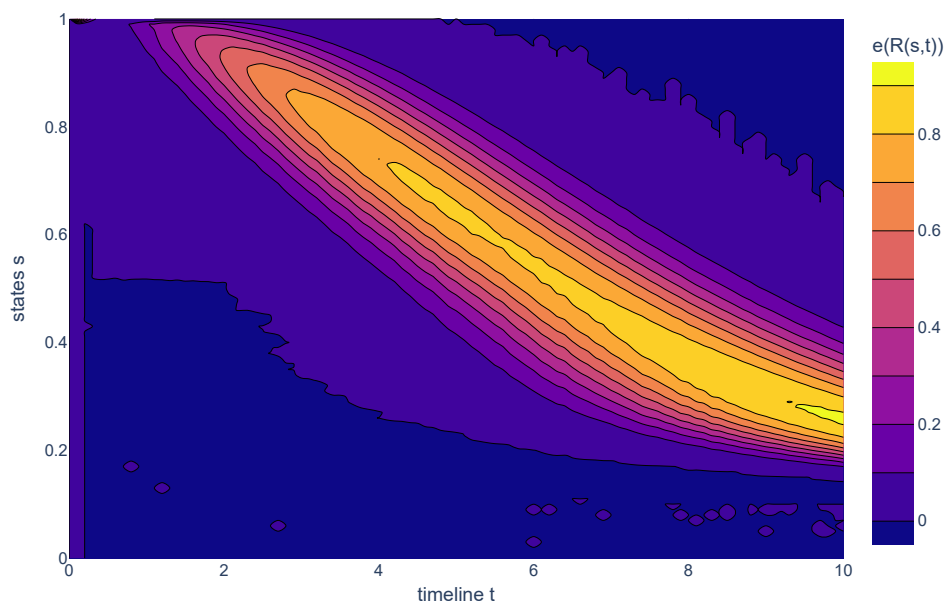
(b) Error between MCS estimate and DASC approximation.

Figure 5.23: 18-component-infrastructure-system: continuous-state survival functions computed by means of DASC with $r = 5$ and the corresponding error.

the DASC. By applying $r = 2$, J could be significantly decreased for all s along the diagonal of the state space and all l_s . In addition, it is noteworthy that the accuracy further increases, compare 5.25 with 5.24 and 5.23.

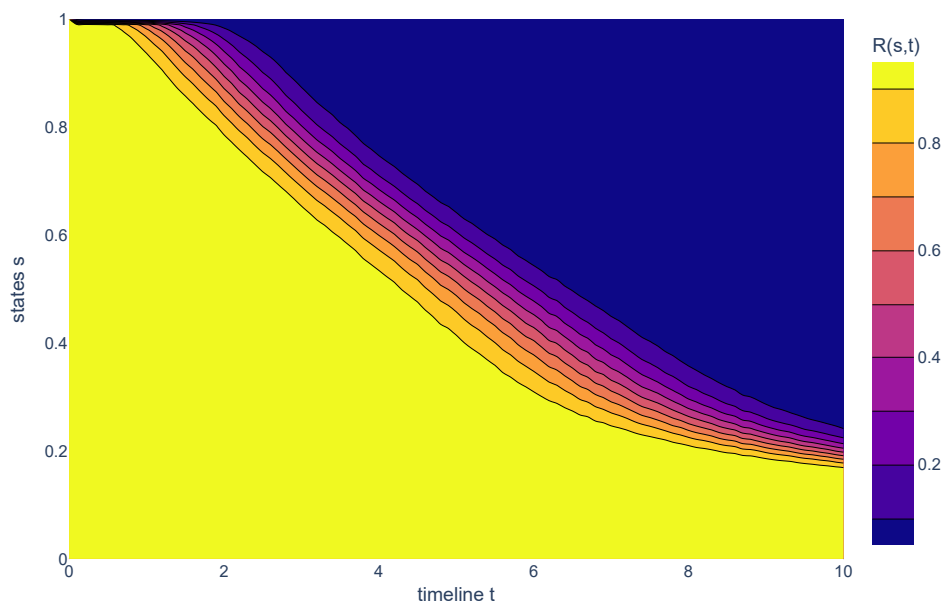


(a) Continuous-state survival function by means of DASCRC.

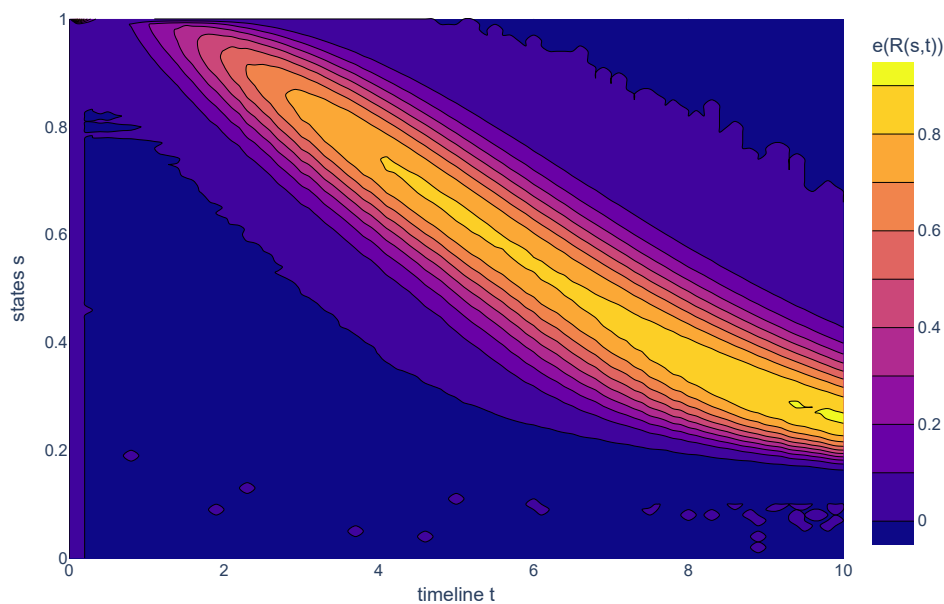


(b) Error between MCS estimate and DASCRC approximation.

Figure 5.24: 18-component-infrastructure-system: continuous-state survival functions computed by means of DASCRC with $r = 3$ and the corresponding error.



(a) Continuous-state survival function by means of DASCRC.



(b) Error between MCS estimate and DASCRC approximation.

Figure 5.25: 18-component-infrastructure-system: continuous-state survival functions computed by means of DASCRC with $r = 2$ and the corresponding error.

5.5 Discussion

5.5.1 Case studies

The case studies show that the DAS converges to the true solution of the continuous-state survival function for all MinMax-Systems regardless of their dimensionality. The global error vanishes for

$N \rightarrow \infty$ as can be seen in the convergence studies. As the sample size N_{DAS} for the establishment of $R_x(s, t)$ is assigned to be large, the convergence of the MCS solutions to the DAS solution can be observed for all case studies conducted for the proof of concept. Besides the theoretical prove these results underline the capability of the concept of DAS to achieve exact results for diagonally state constant systems. These findings verify in particular that the fundamental methodology introduced in 5.14 can be utilized as explicit formula when considering a diagonally state at least neutral, diagonal state extreme and coherent structure function. Further, the results show that the computation time is independent of the sample size when deploying the concept of DAS. For the DAS, the computation time in the online phase purely depends on the total number of components n and the number of considered components. Thereby, the DAS exhibits a linear relation between computation time and number of considered states, depending on the factor that is determined by n and correspondingly the binomial coefficient $\binom{n}{l_s}$. The observations coincide with the theory established in 5.3. The formula 5.14 is independent of the sample size N_{DAS} and clearly depending on the number of states that are considered and inserted as s . It can be observed that this basic approach becomes impractical for systems with $n \gg 10$ combined with a number of considered states that is $\gg 10$. For the first two case studies, the DAS still outperforms the MCS, although the evaluation of the corresponding structure function imposes minimal costs in the case of the MCS. For more complex structure function this difference in computational effort becomes even more evident.

The DASC was introduced and investigated as a naive solution to achieve increased computational efficiency also for larger systems that are characterized by an at least diagonally state constant and at least diagonally state neutral coherent structure function. The performance enhancement is achieved by condensing the DAS in terms of all possible permutations depending on l_s . In order to compute a DASC entry $\Psi(l_s, j) = (|C_j|, v_j)$, the number of occurrences of a value $\Phi(l_s, p)$ is determined and stored together with the value itself as a tuple. Thereby, the computational effort is reduced from a sum over $p = 1, 2, \dots, \binom{n}{l_s}$ to a sum over $j = 1, 2, \dots, J$, where J is the maximum number of different values for the DAS. The DASC shares the same convergence characteristics for diagonally state constant and extreme systems. Simultaneously, this approach exhibits significantly reduced numerical effort compared to its predecessor. The achieved reduction of J by means information condensation is optimal with $J = 2$ for diagonally state extreme structure functions as the number of tuples $\Psi(l_s, j)$ for a given number of components working in state s or above l_s . This can be explicitly expressed as $v_j \in \{0, s\}$ and their corresponding occurrences $|C_j(v_j)|$.

The application of the DASC is not required for diagonally state extreme structure functions. In contrast, it is particularly useful when this criterion is not fulfilled. In the case of a diagonally state constant or higher order structure function an iteration has to be performed in order to approximate the DAS for each combination of s , l_s and p . Values in the along the p -sum that are in the direct neighborhood in $[0, 1]$ are matched by means of a rounding procedure applied to $\Phi(l_s, p)$ and $\Psi(l_s, j)$ is further condensed to $\Psi_r(l_s, j)$. Thereby, for a naive approach a trade-

off has to be made in terms of computational cost and surrogate performance. Typically, it can be expected that $J_{r-1} \ll J_r$ but also that $|e_{r-1}(R(s, t))|_F \geq |e_r(R(s, t))|_F$, where $|e_r(R(s, t))|_F$ is the Frobenius norm of the error between the DASC approximation and the theoretically available true solution. However, a sophisticated rounding procedure should check the lower and upper digits and determine the more favorable choice. Consequently, applying a sophisticated rounding procedure can improve the results obtained by DASC and DASC with high r .

In the test of applicability for an arbitrary infrastructure system, the first-order DASC and DASC5,3,2 perform well and underestimate the true solution of the continuous-state survival function as expected. Depending on the parameter $r \in \{5, 3, 2\}$ significant efficiency improvements can be achieved. The largest errors occur in the central region. The concepts of DAS become particularly useful for demanding structure functions. The evaluation of the weighted network efficiency is computationally more demanding than a composition of min- and max-operators. At the same time, highly demanding structure functions are neither diagonally state neutral or positive nor diagonally extreme or constant. Consequently, the proposed approaches can be applied in these cases when higher-order schemes are integrated or schemes for the estimation of the error are established. In contrast, conventional approaches could not address such structure functions at all.

In its basic form, the DAS requires $\sum_s \sum_{l_s(n)} \sum_{p(l_s)}$ entries to be stored. The DASC already condenses the last sum that is the most critical for systems with a larger number of components up to a minimum of $J = 2$. Considering the storage requirement, the property of a structure function to be diagonally state invariant becomes important. However, note that for at least partly diagonally state invariant structure functions the entries of the $\Phi(l_s, p)$ and $\Psi(l_s, j)$ can be expressed in a linear relation for the range of s that is diagonally state invariant. The representation of the DAS and DASC by means of any type of function can enable to reduce the storage required among the first sum \sum_s , tremendously.

5.5.2 Comparison with related research

Subsequently, the developed concept of DAS is compared to approaches based on the concept of survival signature with regard to the properties of diagonal state sign, order, and variance and also based on the findings of the case studies. In [280], Eryilmaz & Tuncel introduced an explicit formula from a combinatorial perspective to compute a multi-state survival signature based on multiple path-wise binary-state structure functions to model the discrete multi-state perspective. The fundamental decomposition is based on the number of components in l_s . Thereby, the term path-wise corresponds to the terminology of a diagonally state extreme structure function. A classification in terms of the diagonal state sign is not reasonable in this case. The approach might consider diagonal state variance, as the structure functions can vary for each level. Theoretically, it is possible to define as many structure functions as states considered. In practice, however, this may prove infeasible when approaching a continuous view. However, these systems would still need to have some sort of path-wise measurability. The approach proposed in [165] by Qin &

Coolen exhibits similar properties to those of the concept developed by Eryilmaz & Tuncel. The authors investigate discrete multi-state systems with multi-state components based on rule-based structure functions. In comparison with [280], Qin & Coolen developed a refined notation. The researchers based the combinatorial decomposition on the number of components working in state s . The computation of the multi-state survival function describing the probability of a system to be in state s or above is then performed in a post-processing step. In [281], Yi et al. proposed a fundamentally different approach on how to establish the discrete multi-state survival signature values. The authors adopt an probabilistic and conditional interpretation of the survival signature and further establish transformation relations [318].

Recent developments show that the survival signature finds increased attention in the field of stress-strength reliability. The works [319, 320] investigate approaches for statistical inference based on the concept of survival signature for multi-state system with multi-state components in this context. In [216], Liu et al. proposed an approach to compute $R(s)$ for discrete and multi-state systems with discrete and continuous multi-state stress-strength components. The authors applied their approach to diagonally state neutral, state invariant and state extreme systems. Thereby, a single vector is sufficient to represent the continuous-state survival signature of the diagonally state invariant systems with a single component type.

In contrast to the approaches presented above, the DAS was developed to evaluate the continuous-state survival function $R(s, t)$, introduced in 5.3.1. Analogously, the concept of DAS and its variants can be utilized to compute $R(t)$ as well as $R(s)$. Recent literature in the context of survival signature addresses the computation of diagonally state extreme systems, i.e., path-wise measurable structure functions. In contrast, the methodology proposed in the current work enables surrogate modeling potentially for any kind of coherent structure function. Consequently, such structure functions might be diagonally state constant or of higher order. In the case of structure functions that are of higher order, the current concept of DAS yields an approximation error. It appears practical to reduce this error by developing higher order schemes and more sophisticated rounding procedures for the concept of DAS. Some of the reviewed approaches take into account diagonally state variance by establishing one corresponding survival signature for each considered state or level. For diagonally state invariant structure functions the DASC(R) comprises $\sum_{l_s}^n \sum_{p(l_s)}^J$ elements. The conventional concepts of survival signature are only applicable to diagonally state extreme structure functions. Considering systems with a single component type and let them be diagonally state invariant for the ease of notation, conventional approaches require the storage of n values for the representation and the computation of the sum $\sum_{l_s}^n$ to evaluate $R(t)$ or $R(s)$ for a single t or s . In the same case, the DASC includes $\sum_{l_s}^n \sum_{p(l_s)}^2$ elements to be stored and evaluated. In summary, the DAS concept enables a broader range of applications than similar and recently developed approaches, despite a slightly higher computational cost. The extent to which the range of applications can be broadened needs to be investigated in future work but the current findings appear promising.

5.5.3 Contextualization in terms of resilience

Three different approaches to determine $R(s, t)$ were outlined in 5.3. Regardless of the approach utilized to establish $R(s, t)$, the continuous-state survival function inherently captures the probability of occurrence of disruptive events and their effect on the performance of the considered entity. Thus, $R(s, t)$ strongly relates to two properties of a system, reliability and robustness, shown in 5.1 that govern its resilience when interpreted as in [268]. To show this theoretically, suppose that the performance deterioration over time being investigated empirically by exposing the entity to a certain environment in which potentially damaging effects or events occur in some frequency. Suppose the measurement only observes the state u_s at time t , where Δt between two time steps might be infinitesimal small. The occurrence of an event at t counts to the probability measure of the random variable to be less than s only if a deterioration in performance occurs as a consequence at the next time step under consideration. Thereby, the probability of the magnitude of the performance degradation of such a deteriorating event is intrinsically quantified as well. When established properly, both parts of information should also be captured when the continuous-state survival function is generated via stochastic processes modeling disruptive events either explicitly or implicitly. And similarly for the approach including a structure function, the disruptive events acting on components propagate their effects through the structure function $\phi(\mathbf{x})$ to the system state u_s and are captured by the continuous-state survival function. Eventually, despite not directly sampling a disruptive event from $R(s, t)$ but rather component performances, the occurrence of certain state sample is governed by the fundamental, measured or modeled disruptive events and the according response of the considered entity. Thereby, the structure function is critical for mitigating the effect of disruptive events acting on components. To conclude with regard to 5.1, it quantifies not only if and when a performance deterioration occurs (reliability) but also its magnitude (robustness). The continuous-state survival function incorporates both notions simultaneously simply by representing the time-dependent probability distribution of each state of functionality.

In the context of the multidimensional and sub-structured resilience framework established in [304], the fact that $R(s, t)$ models both reliability and robustness can be exploited to enhance the stochastic simulation of subsystem as well as components during the evaluation of the resilience metric. For basic components, $R(s, t)$ can be established empirically or based on a stochastic process. Then, the generated $R(s, t)$ characterizing the stochastic degradation behavior are propagated from bottom level to top level of the sub-structured system. The utilization of $R(s, t)$ allows for reduced computational effort in repeated evaluations of structure functions in subordinate levels during resilience optimization at $L \geq 1$ levels of subsystems. The concept of DAS enables a direct propagation of the $R(s, t)$ through each level by means of the explicit formulas provided in 5.3.2. On the top-level, the overall structure function is evaluated by means of performance samples in order to quantify the resilience metric. The corresponding performances can be retrieved by sampling the state from the individual $R_i(s, t_c)$, where t_c denotes the currently considered time step. The DASC approach developed in the current work

is immediately applicable to the case studies investigated in [304] after establishing a monotone sampling procedure based on $R(s, t)$ describing performance. Future work addresses the detailed investigation concerning the integration of the continuous-state survival function as reliability and robustness representation into the resilience framework for sub-structured systems.

5.6 Conclusions & outlook

In this work, the notion of the continuous-state survival function was presented and the concept of DAS was introduced as a corresponding surrogate modeling procedure. Thereby, the continuous-state survival function is defined as a time-dependent probability measure that characterizes the distribution of performance states of the considered system over time. This consideration gives engineers a new perspective when faced with the challenge of maintaining system performance in the face of disruptive events in a hostile environment. In light of the theoretical proof and the results in the case studies, the concept of DAS appears to be a solid foundation for more sophisticated surrogate modeling techniques. The relations to the phases characterized by reliability and robustness when quantifying system resilience were identified and discussed. The proposed methodology appears as an adequate approach to integrate a continuous-state consideration into a sub-structured resilience framework, as presented in [304].

In the course of this work, three different variants of the concept of DAS were established: At first, the fundamental statement 5.14 was introduced to provide a comprehensive proof that DAS yields exact results for diagonal extremal and constant structure functions. For systems with a small number of components the DAS outperforms the MCS in terms of both computational time and accuracy. Secondly, the DASC 5.20 was developed to overcome the limitations for larger systems. Moreover, DASC was defined in 5.21 to consider structure functions with a diagonal state order higher than constant. Thus, the current methodology extends the range of application of the separation property inherited by the concept of survival signature. It should be noted that the code can be further optimized, e.g., by integrating parallel computing. This leads to an additional increase in computational efficiency. In summary, the concepts of DAS developed in the current work show good results and open a rich and promising research topic. The following items can be listed as critical developments concerning the concept of DAS as an autonomous surrogate model but also in particular its integration into the resilience framework for complex and sub-structured systems [304].

- Integration into the resilience framework: The behavior of the DAS when integrated to the multidimensional and sub-structured resilience decision-making framework should be investigated in detail. The relationship between the endowment properties and the continuous-state survival function should also be explored.
- Broadening the range of application: Higher-order schemes should be addressed to reduce the approximation error for structure functions that are not diagonally state constant.

Further, the DAS formulas should be extended for diagonally state negative structure functions and multiple component types.

- Consideration of uncertainties: Extension of the DAS towards a consideration of uncertainties based on the proposed approach in [152] and integration into the multidimensional resilience decision-making framework for complex and sub-structured systems [304]. Approaches to reduce the storage requirements and to further condensate the developed formulas for enhanced efficiency during the online phase are of great interest.

Authors' contributions

Made substantial contributions to conception and design of the work: Winnewisser NR, Salomon J, Broggi M;

Performed data analysis and interpretation: Winnewisser NR;

Provided administrative and technical support: Broggi M, Beer M

Acknowledgments

This work was funded by the Deutsche Forschungsgemeinschaft (DFG, German Research Foundation) SPP 2388 501624329 and the "Reliability and Safety Engineering and Technology for large maritime engineering systems" (RESET) programme 730888.

6 | Resilience-based decision criteria for optimal regeneration

Resilience-based decision criteria for optimal regeneration

Julian Salomon^{a,*}, Matteo Broggi^a, Michael Beer^{a,b,c}

^aInstitute for Risk and Reliability, Leibniz Universität Hannover, Hannover, Germany

^bInstitute for Risk and Uncertainty, University of Liverpool, Liverpool, United Kingdom

^cInternational Joint Research Center for Resilient Infrastructure & International Joint Research Center for Engineering Reliability and Stochastic Mechanics, Tongji University, Shanghai, China

*Corresponding author

Accepted to *Regeneration of Complex Capital Goods*, Springer on July 2022

Abstract

Complex capital goods, such as jet engines, are critical to the functioning of modern societies. These systems are exposed to various threats that cannot be prevented entirely. Thus, the concept of resilience – encompassing reliability as well as robustness and recovery in the presence of a disruptive event – is combined with efficient reliability methods to support decision making for complex capital goods. As fundamental step, the current work addresses the generation of a functional model from a physical model based on sensitivity analyses. The developed resilience analysis framework is applied to this model in order to derive conclusions supporting decision maker while incorporating monetary and technical aspects. A combination with the concept of survival signature enables efficient reliability analysis in repeated model evaluations. A novel methodology is developed by amalgamating the non-intrusive stochastic simulation method and the concept of survival signature leading to a significant reduction of the computational effort when considering mixed uncertainties.

Keywords: Resilience optimization, Reliability analysis, Uncertainty quantification, Sensitivity analysis, Decision making.

6.1 Motivation

Modern societies are highly dependent on a broad variety of complex capital goods including aircraft engines, industrial plants, and infrastructure systems, [268]. Aircraft engines, for example, are of paramount importance for both private mobility and the industrial transportation sector of these societies. For economic and safety reasons, it is vital that such complex systems are as reliable as possible [152]. To ensure this efficiently and sustainably, the Collaborative Research Center “Regeneration of Complex Capital Goods” (CRC 871) investigates scientific fundamentals for the maintenance, repair and overhaul (MRO) of these complex capital goods, especially in the field of civil aviation, as proposed in [321]. In fact, these systems are exposed to various threats and it is extremely challenging to identify all possible critical impacts and prevent them accordingly. Therefore, recent developments focus not only on enhancing the reliability and robustness of these systems, but on increasing their recoverability as well. This has led to the concept of resilience that comprises all of these aspects, cf. [268].

Information required as basis in the design, maintenance, and repair of systems are commonly governed by uncertainties, [152]. Thus, it is critical for decision making in such processes to have tools capable of efficiently performing resilience and reliability analyses of complex systems,

taking into account precisely these uncertainties comprehensively. An additional major concern in MRO processes is not only the identification of direct influences of individual components, but more importantly of complex and elusive interaction effects among multiple components and their impact on the key performance measures of the capital good under investigation [322]. Global sensitivity analyses are a well-established tool in this specific context.

The current work addresses the development of a computationally efficient theoretical and algorithmic framework for evaluating the resilience and reliability of complex capital goods under consideration of uncertainty to support decision making in MRO processes. Correspondingly, the following guiding principles were defined as:

- guarantee of resilience before, during and after regeneration, and in particular on the functionality of the complex capital good;
- consideration of monetary and technical constraints;
- quantification of uncertainties during regeneration;
- identification of regeneration paths improving resilience such that technical and economic risks are minimized.

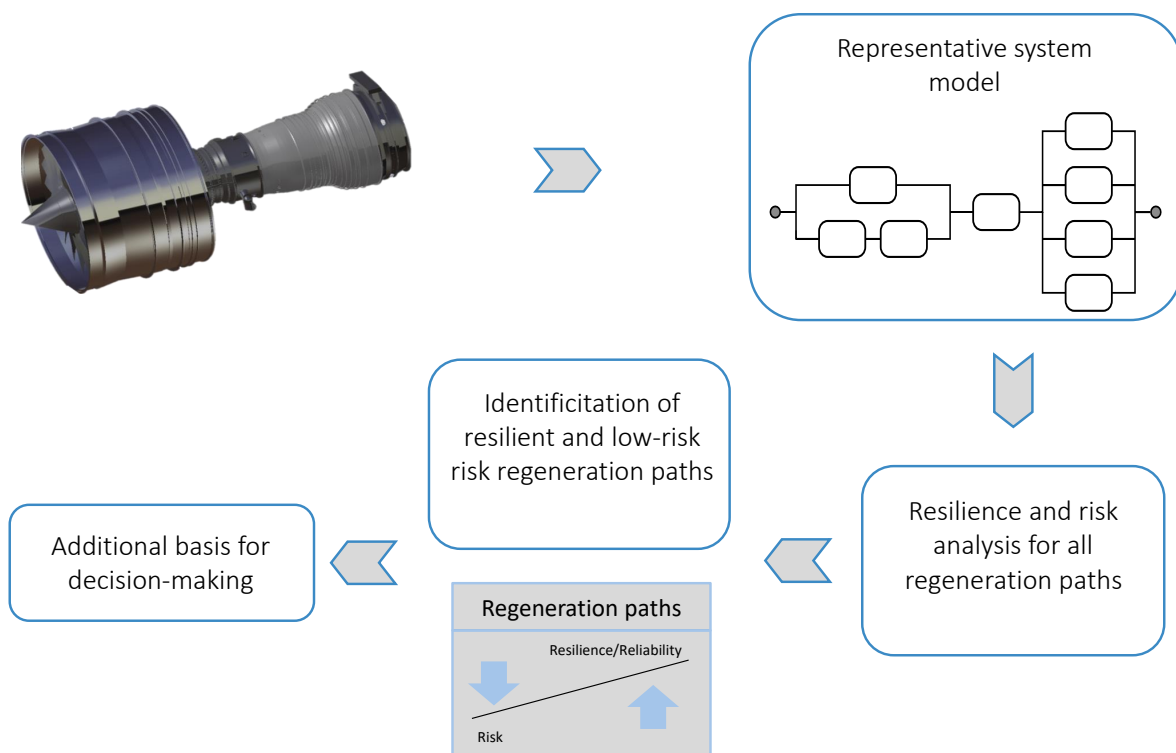


Figure 6.1: Objectives and corresponding work flow.

Typically, complex physical models are employed to derive conclusions in system engineering. A large number of model evaluations are required to analyze and optimize the performance of a system and its continuous guarantee. However, the utilization of a physical model for repeated evaluations with varying model parameters is often accompanied by an enormous computational burden. Thus, a derivation of a function-based model from the complex physical model, mapping the core properties of interest and thus reducing computational effort, is proposed in the current work, as illustrated in Fig. 6.1. After the generation of such a functional model, the developed resilience assessment framework is applied to derive additional information for the decision making process.

6.2 Scope of the paper

Given the principles above, four key objectives are formulated and addressed in the subproject *D5* “Resilience-based Decision Criteria for Optimal Regeneration” of the CRC 871:

1. the establishment of a comprehensive function-based modular system modeling approach of the overall engine for resilience and reliability assessment;
2. efficient dynamic system modeling in dependence of operating states due to the concept of survival signature for enhanced computational efficiency;
3. the development of models for mixed – aleatoric and epistemic – uncertainty and the utilization of simulation methods reducing computational effort for sampling;
4. the identification of resilient regeneration paths.

More precisely, this means that at first a representative system model is extracted from a physical simulation model, e.g., of an aircraft engine, by the utilization of a sensitivity analysis. The corresponding findings are presented in Sec. 6.3. As illustrated in Fig. 6.1, the resulting functional model is basis for further in-depth analysis and investigation.

Given the functional model of an arbitrary, complex capital good, the comprehensive resilience analysis includes the parts illustrated in Fig. 6.2. At the top level a resilience analysis forms the fundamental frame for the resilience assessment of complex capital goods, evaluating all possible regeneration paths. Subsequently, limiting technical and monetary constraints are taken into account and a reduced set of acceptable resilient and low-risk regeneration paths is identified.

The reliability analysis based on the concept survival signature, introduced in [149], for enhanced computational efficiency, especially in case of repeated model evaluations, is integrated into the resilience analysis for each regeneration path considered. This leads to a significantly reduced computational effort during resilience analyses of considered complex capital goods. The additional uncertainty analysis enables the consideration of diverse uncertainties utilizing novel developed, highly efficient algorithms, see [152], reduce the sample size tremendously.

The resilience analysis is introduced in Sec. 6.4 and the consideration of monetary constraints is demonstrated in Sec. 6.5. Further, an efficient approach for the integrated reliability analysis

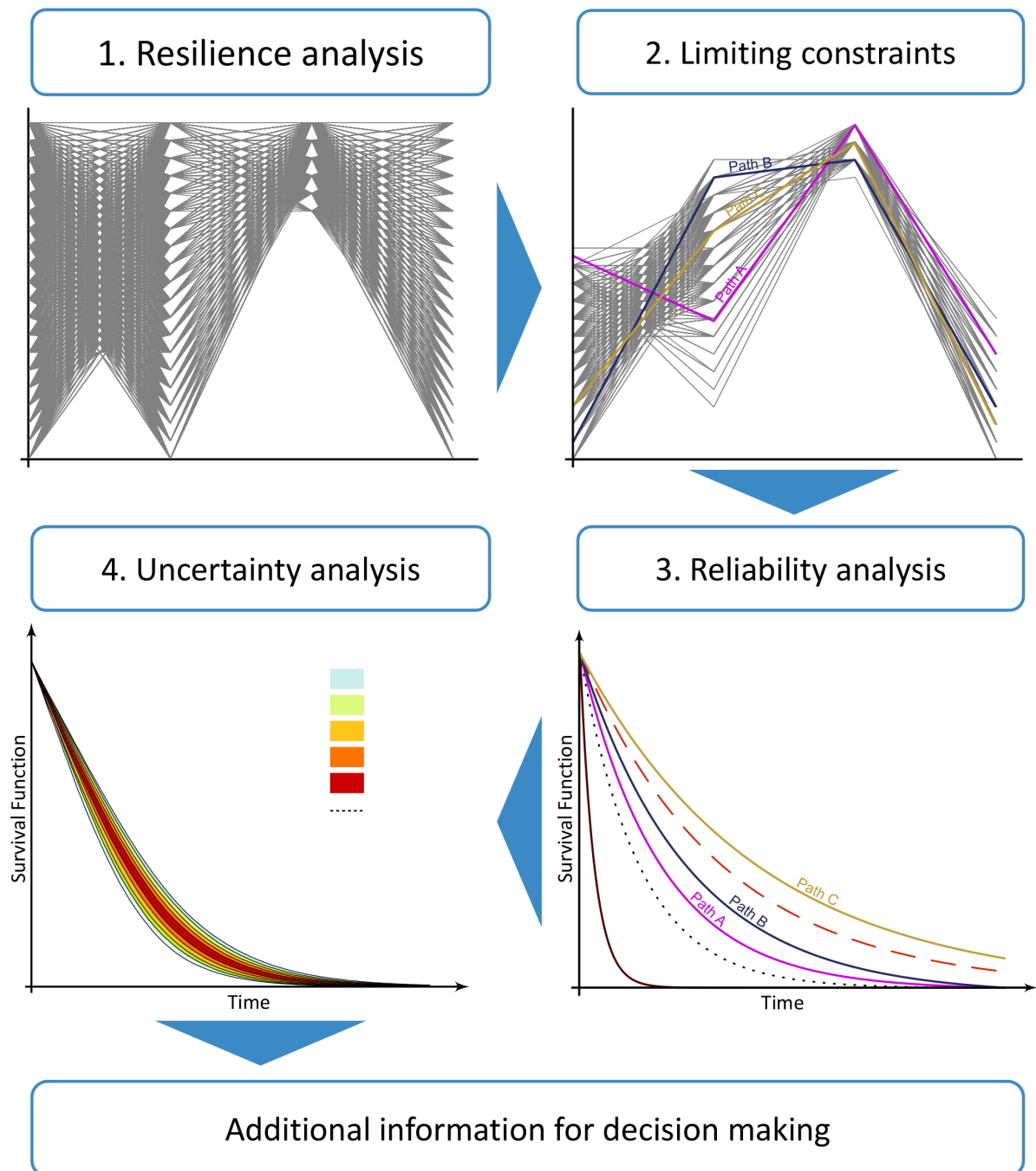


Figure 6.2: Work flow in the analysis framework.

is proposed in Sec. 6.6. The uncertainty analysis considered in Sec. 6.7 forms the last part and enables for a computationally efficient uncertainty quantification when it comes to mixed uncertainties. As a result, an additional basis for decision making in the virtual level of the regeneration process management is obtained taking into account systemic interactions and

uncertain data.

6.3 Functional modeling approach

In the current section, developments concerning various functional models and their generation, as illustrated in Fig. 6.1, are presented. In the context of the CRC 871, a fundamental procedure was established to generate a functional model based on sensitivity analysis utilizing Sobol indices, see [251]. However, these developments focused on binary-state systems. In the current work, the approach proposed in [251] is further developed for the consideration of multi-state systems. In addition, an alternative sensitivity measure is considered, allowing for the incorporation of interdependencies between various input parameters, enabling for a more comprehensive and realistic system modeling. Once derived from the physical model, the functional model is investigated in the analysis framework that was outlined in Sec. 6.2 and is presented in subsequent sections.

6.3.1 Extraction of structure functions based on sensitivity analyses

As fundamental step, the methodology to derive a functional model from a physical simulation is presented within the CRC 871, Miro et al. proposed in [251] a procedure to extract a functional model from a performance model of an multistage axial compressor. A multistage compressor combines multiple rotor and stator blade rows in an alternating series of connected stages. It was shown that various performance measures are dependent on the blade roughness. According to Miro et al., the blade surface roughness is considered as input variable for further analysis. The four-stage high-speed axial compressor of the Institute of Turbomachinery and Fluid Dynamics at Leibniz University Hannover is the baseline compressor of this study, consisting of four stator rows S1 - S4 and four rotor rows R1 - R4.

Miro et al. established a functional model based on results of a sensitivity analysis considering Sobol indices, see [323], of an one-dimensional aerodynamic simulation model of that axial compressor. They chose a variance threshold of 25% based on expert knowledge, see Fig. 6.3. Correspondingly, the system is considered to fail due to roughness related effects if a 25% total variation of the system performance measure, estimated via Monte Carlo Simulation (MCS), is reached.

The functional model developed by Miro et al. describes the dependence of the overall compressor performance, i.e., the total-to-total isentropic efficiency, on the roughness of the rotor and stator blades as binary-state structure function in the form of a Reliability Block Diagram (RBD), see Fig. 6.4. According to the concept of RBDs, the system functions if there exists a connection between start and end node and fails if this connection is interrupted, corresponding with a performance variation of at least 25%.

In the approach proposed by Miro et al., a certain row is specified as one of four component types c_i for $i \in \{1, \dots, 4\}$. Components of the same type are prone to identical distributions describing

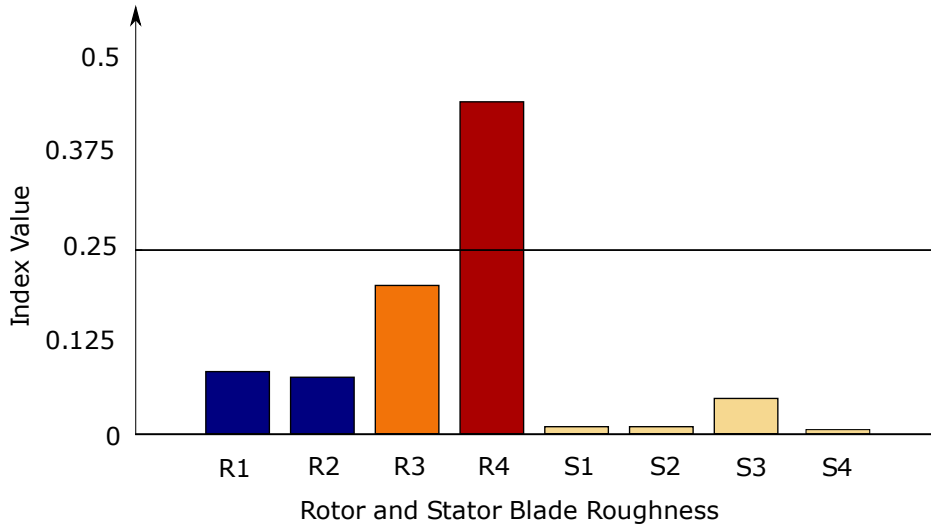


Figure 6.3: Component importance measure with threshold of 25%, adapted from [251].

degradation while being independent from each other. The classification of the component type and the arrangement of the components in the RBD is chosen based on the sensitivity of the component blade roughness affecting the total-to-total isentropic efficiency. Fig. 6.3 shows the sensitivity results that are based on Sobol indices. Components with similar sensitivity values are determined to be of one component type. In the current work, the component type allocation suggested by Miro et al. is adopted. Correspondingly, the stator and rotor rows are assigned as $(R1, c_1)$, $(R2, c_1)$, $(R3, c_2)$, $(R4, c_3)$, $(S1, c_4)$, $(S2, c_4)$, $(S3, c_4)$, $(S4, c_4)$.

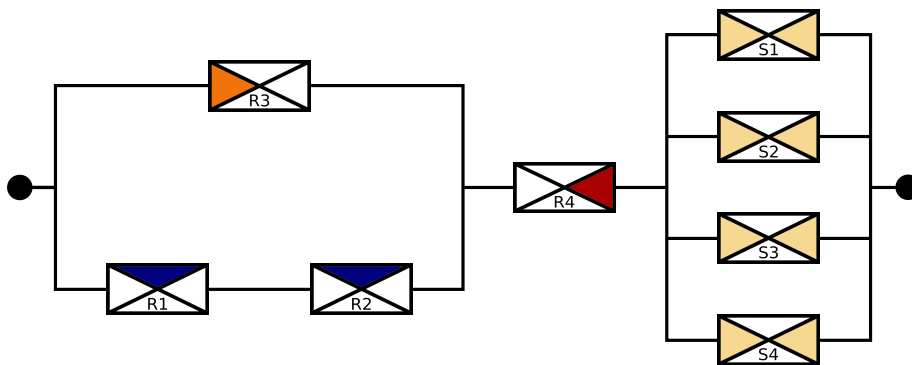


Figure 6.4: Functional model of the multistage high-speed axial compressor.

The arrangement of the components is established as follows: If the sensitivity value of a single component exceeds the threshold, it is set in series with other components going beyond the threshold due to significant importance to the overall system performance; if a sum of sensitivity values exceeds the threshold the corresponding components are set in parallel and then linked in series. For example, component R4 goes beyond the threshold alone and therefore is considered

as the most important component. Thus, the system should fail if component R4 fails, i.e., R4 exceeds a critical roughness and due to that the roughness-related performance variation of the system exceeds the threshold. Further, R1 or R2 only go beyond the threshold in sum with R3. Correspondingly, the functioning of this subsystem is described as $(R1 \vee R3) \wedge (R2 \vee R3) = (R1 \wedge R2) \vee R3$, as shown in Fig. 6.4, where $R1, R2, R3 \in \{0, 1\}$. Following this idea all stators should be arranged in parallel as each of them has rather a small impact. This parallel block $S = S1 \vee S2 \vee S3 \vee S4$ is again in series with the R1, R2, R3 block as well as with R4. Miro et al. argued that the parallel stator block should be allocated in series as shown in Fig. 6.4 based on expert knowledge, even though the sum of their sensitivity values doesn't reach the threshold. To summarize, the entire system and its functional state is described by $F = (R1 \wedge R2) \vee R3) \wedge R4 \wedge (S1 \vee S2 \vee S3 \vee S4)$ with $F \in \{0, 1\}$ and the system components $R1, R2, R3, R4, S1, S2, S3, S4 \in \{0, 1\}$

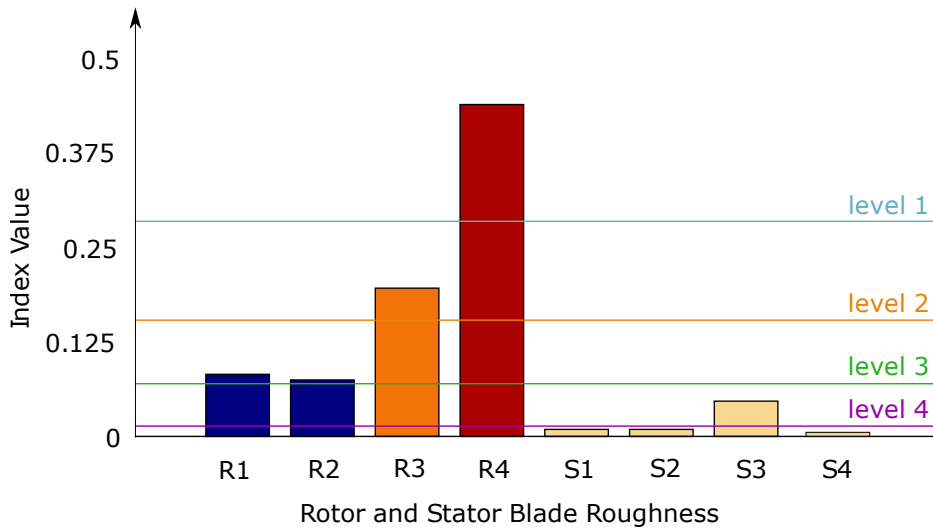


Figure 6.5: Component importance measure with thresholds of 2.5%, 7.5%, 15% and 30%.

In the current work, this approach is adapted for a multi-state system multi-state component consideration to prove the applicability of the functional modeling approach in the context of partial functionality. Thereby, suppose the system is functioning in the state j or above if the j -th rule is satisfied for components in state j or above with $j = 1, \dots, J$. For illustrative purposes, four rules are defined as structure functions represented by RBDs and thus $J = 4$. Correspondingly, four thresholds are determined as basis to generate four structure functions corresponding to four levels, see Fig. 6.5.

Fig. 6.6a shows the structure function via an RBD for the system state of perfect functioning $j = J = 4$. The corresponding threshold is set to 2.5%. The components R1, R2, R3, R4 and S3 exceed this threshold, while components S1, S2 and S4 only go beyond the threshold if summed up. Thus, R1, R2, R3, R4 and S3 are connected in series, while S1, S2 and S4 are connected in parallel and then set in series. This seems reasonable as the components S1, S2 and S4 do not

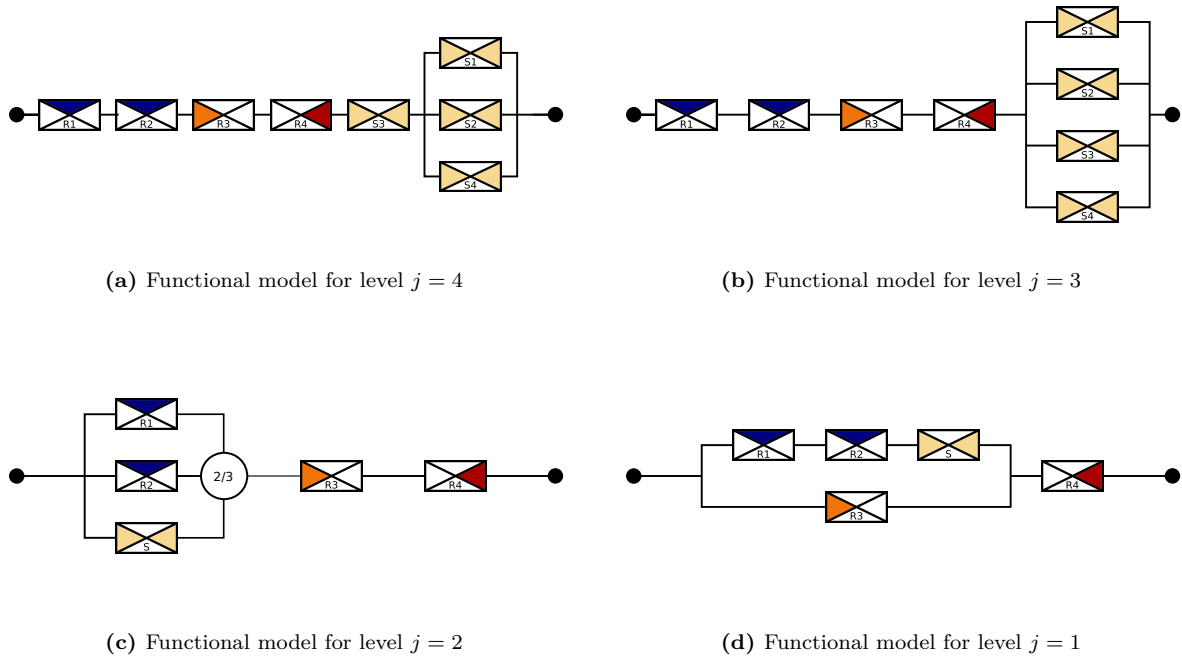


Figure 6.6: RBDs for different performance levels.

have a critical impact, while the components R1, R2, R3, R4 and S3 definitely harm the perfect state due to their significant influence on the system performance variation.

Fig. 6.6b shows the structure function via an RBD for the intermediate system state $j = 3$. The corresponding threshold is set to 7.5%. The components R1, R2, R3 and R4 exceed this threshold, while components S1, S2, S3 and S4 only go beyond the threshold if summed up. Thus, R1, R2, R3 and R4 are connected in series, while S1, S2, S3 and S4 are connected in parallel and then set in series.

Fig. 6.6c shows the structure function via an RBD for the intermediate system state $j = 2$. The corresponding threshold is set to 15%. The components R3 and R4 go beyond this threshold. Thus, R3 and R4 are connected in series. In contrast, the components R1, R2 as well as the parallel stator block S only exceed the threshold if at least two of those are summed up. Based on the series connection of R3 and R4, the system functions in state $j = 2$ if at least $R1 \vee R2$, $R1 \vee S$ and $S \vee R2$ take a value of 1, i.e., function in state $j = 2$ or above. As a consequence, the latter relationship is modeled via an at-least-2-out-of-3-connection.

Fig. 6.6d shows the structure function via an RBD for the last system state $j = 1$ before complete failure. The corresponding threshold is set to 30%. Note that all thresholds are set arbitrarily and only for illustrative purpose. The component R4 goes beyond this threshold and is connected in series. The components R1, R2 and S only exceed this threshold if summed up with R3. In case of functioning it holds that $(R1 \vee R3) \wedge (R2 \vee R3) \wedge (S \vee R3) = (R1 \wedge R2 \wedge S) \vee R3$.

The obtained binary-state structure functions represented in Fig. 6.4 and Fig. 6.6 are utilized for multi-state system reliability analysis. The corresponding findings are presented in Subsec. 6.6.3.

6.3.2 Kucherenko indices

Typically, Sobol indices are utilized for conducting sensitivity analysis as, e.g., proposed in [251]. These variance-based indices display effects of single input variables on output variables (first-order effect indices), and interaction effects between several input variables and their impact on the output variables (total-effect indices). The Sobol indices, as well as most other sensitivity analysis tools, are based on the assumption that all input variables are independent of each other. However, this assumption rarely applies in reality, and in various engineering fields, input variables are correlated, see e.g., [324, 325]. Therefore, in this work, a sensitivity analysis of the above mentioned steady-state performance model for an aircraft engine is conducted by applying a generalized form of the Sobol indices according to [326], hereinafter referred to as Kucherenko indices. These indices are capable of taking into account dependencies between input variables and are therefore more suitable for addressing real world problems.

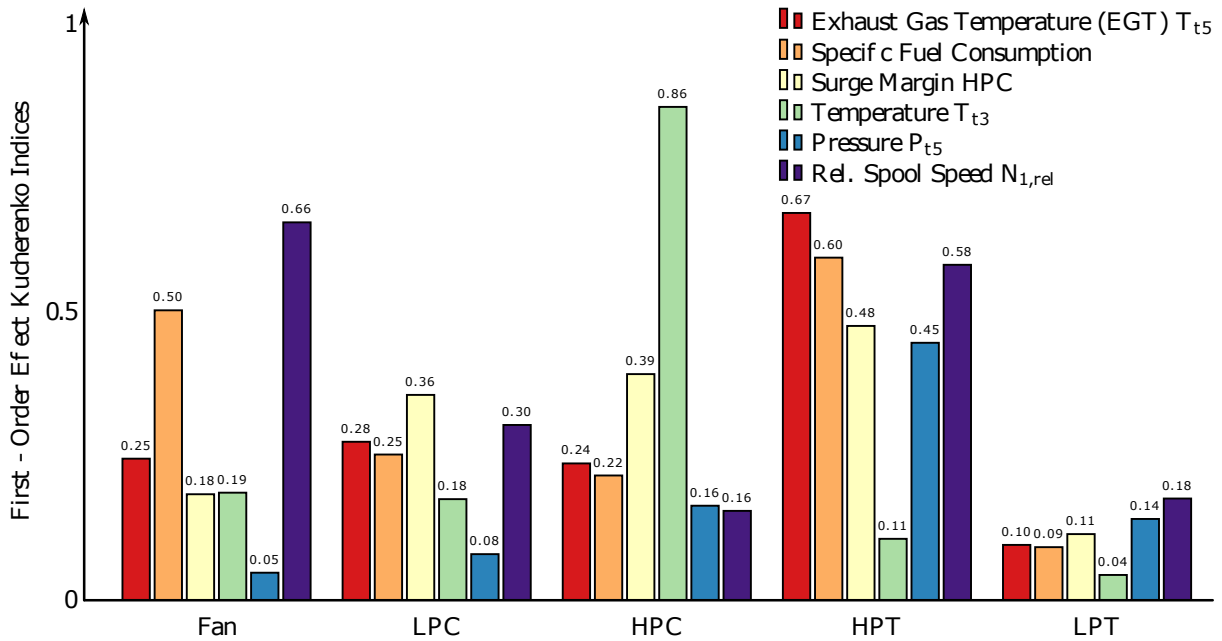


Figure 6.7: First-order effect Kucherenko indices; adapted from [322].

In practice, an analytical determination of the Kucherenko indices is often not feasible. Therefore, Kucherenko et al. presented Monte Carlo estimators for their indices in their work, [326]. Both estimators require a conditional sampling. Conditional sampling, however, might be tedious or even impossible for some models due to computational demand, such as for the jet engine iteration matching model, considered in this work. Therefore, in [327], Marelli et al. provide sample-based Monte Carlo estimators for both Kucherenko indices.

As an example, consider the V2500-A1 jet engine that is a two-spool turbofan with a fan, low-pressure compressor (LPC), high-pressure compressor (HPC), high-pressure turbine (HPT), low-pressure turbine (LPT) and a common thrust nozzle. This jet engine was considered in [322]

to show the applicability of a sophisticated sensitivity measure for an entire jet engine. In cooperation with the subproject D6 of the CRC 871 concerning module interactions and the overall system behavior, the first-order effects for the six considered output quantities with respect to the five varying input efficiencies of the main turbomachines, are determined by utilizing the sample-based Monte Carlo estimators. The corresponding results are shown in Fig. 6.7. It can be seen that among all of the direct effects on output variances, the variance of the HPT efficiency is the dominant factor for four to five out of all six output quantities. This is the fact as the HPT exhibits the highest index value and therefore constitutes the main influence on the system performance. In this manner the approach is applicable for the assessment of an entire jet engine under consideration of interdependencies between engine components.

In [322], Salomon et al. additionally compute the total-effect Kucherenko indices and both results are discussed in detail. To summarize, the study shows that simple correlations are not sufficient to explain the influence of combined module variances and find the causes of deterioration. Therefore, sensitivity analyses under consideration of dependent variables by means of Kucherenko indices and digital performance twins are powerful tools to determine the influence on a scientific basis. For an overall view, however, the change in capacity and work must also be examined at different operating points with an engine pressure ratio regulation. It shall be noted, that these results can be utilized as a basis for a detailed reliability analysis by developing a functional model according to [251] and [280] of the V2500-A1 aircraft engine performance model.

6.4 Resilience analysis

The resilience analysis, developed in [268], forms the first phase and basis of the analysis framework, illustrated in Fig. 6.2, and is presented in the current section. Therefore, a fundamental notion of resilience and a corresponding metric is suggested. Subsequently, a resilience decision making framework is developed consisting of two key ingredients, an adapted systemic risk measure and a sophisticated resilience metric, enabling for systematic computation of the resilience for various endowment configurations. These endowment configurations can be interpreted in a variety of ways, e.g., as different regeneration paths of the considered complex capital good. Finally, the grid search algorithm and its advantageous properties in terms of computational efficiency are presented. For illustrative purposes, the developed algorithmic framework is then applied to the functional model established in Sec. 6.3.1, whereby it is not limited to this particular use case, but can be utilized to a variety of system models. Illustrative results are presented in combination with the second phase of the analysis framework in Sec. 6.5.

6.4.1 Resilience metric

Given a system being exposed to a disruptive event and recovering its functionality afterwards, three essential phases can be defined classifying the system states, as illustrated in Fig. 6.8: (i)

The original stable state, whose duration relates to the reliability of the system, forms the first phase. (ii) The second phase is the loss of performance after the occurrence of a disruptive event. This loss depends on the vulnerability or robustness of the system; the robustness of the system is interpreted as the resistance to a loss of performance. (iii) The disrupted state of the system and its recovery to a new stable state is the last phase and governed by the recoverability. In general, the new stable state may differ from the original state and, accordingly, its performance may be higher or lower. The majority of resilience metrics available in the current literature is based on system performance, i.e., on the three states and their transitions shown in Fig. 6.8. Consequently, a quantitative measure of resilience depends on the specific choice and definition of system performance, see e.g., [10]. Performance-based approaches may be ratio-based, integral-based, or both.

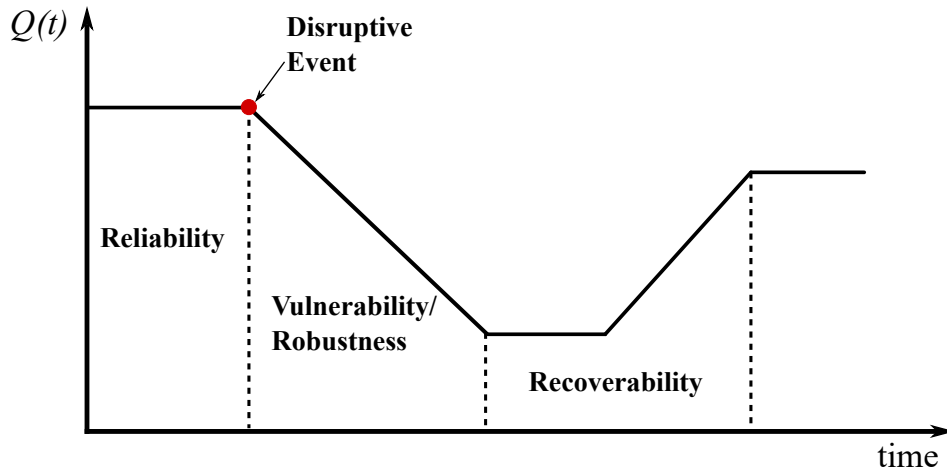


Figure 6.8: The three resilience phases before and after a disruptive event; adapted from [76].

In the current work, the probabilistic resilience metric by Ouyang et al. [86] is utilized. The metric is denoted by Res and defines the expected ratio of the integral of the system performance $Q(t)$ over the time interval $[0, T]$ and the integral of the target system performance $\mathcal{T}Q(t)$ over the same time interval:

$$Res = E[Y], \quad \text{where} \quad Y = \frac{\int_0^T Q(t)dt}{\int_0^T \mathcal{T}Q(t)dt}. \quad (6.1)$$

The system performance $Q(t)$ is described as a stochastic process. In general, $\mathcal{T}Q(t)$ might be considered as a stochastic process as well, but for expediency it is assumed to be a non-random constant $\mathcal{T}Q$ in this work. The resilience metric takes values between 0 and 1 when limiting the recovered performance at maximum equivalent to the original performance. The value $Res = 1$ indicates a system performance corresponding to the target performance, while $Res = 0$ captures that the system is not working during the considered time period at all.

6.4.2 Adapted systemic risk measure

As proposed in [268], the resilience metric presented in Subsec. 6.4.1 is integrated into an adapted systemic risk measure, enabling the systematic assessment of various system configurations, that might be, e.g., regeneration paths. In particular, technical systems for which a meaningful system performance $Q(t)$ can be determined are considered.

Assume that the system encompasses l system components. Each component is characterized by its type and n relevant properties that influence the overall system performance. For convenience, apply matrix notation. A component $i \in \{1, \dots, l\}$ can be characterized by a row vector

$$(a_i; j_i) = (\eta_{i1}, \eta_{i2}, \dots, \eta_{in}; j_i) \in \mathbb{R}^{(1 \times n)} \times \mathbb{N}, \quad (6.2)$$

where $(\eta_{i1}, \eta_{i2}, \dots, \eta_{in})$ represent the numerical values of the n properties and $j_i \in \{1, 2, \dots, b\} \subseteq \mathbb{N}$ defines its type. The system is described by a pair including the matrix $A \in \mathbb{R}^{(l \times n)}$ and the column vector $z \in \mathbb{N}^l$ that captures the types of the components:

$$(A; z) = \begin{pmatrix} \eta_{11} & \eta_{12} & \dots & \eta_{1n}; & z_1 \\ \eta_{21} & \eta_{22} & \dots & \eta_{2n}; & z_2 \\ \vdots & \vdots & & \vdots & \vdots \\ \eta_{l1} & \eta_{l2} & \dots & \eta_{ln}; & z_l \end{pmatrix} \quad (6.3)$$

The input-output model $Y = (Y_{(A;z)})$ is evaluated for these pairs. In the following, a corresponding adapted systemic risk measure is constructed as follows. As a specific example, choose the acceptance set

$$\mathbb{A} = \{X \in \mathbb{X} \mid E[X] \geq \alpha\} \quad \text{with} \quad \alpha \in [0, 1] \quad (6.4)$$

The risk measure is defined as

$$R(Y; K) = R(Y; (K; z)) = \{A \in \mathbb{R}^{l \times n} \mid Y_{(K+A;z)} \in \mathbb{A}\}, \quad (6.5)$$

that is the set of all allocations of modified system properties A that are added to the base properties K for which the altered system $(K + A; z)$ exhibits a resilience greater or equal to α . Without loss of generality but to keep the notation simple, set $K = 0$, and $R(Y; 0)$ is written as $R(Y)$.

Practical applications might require to impose restrictions for the structure of the matrix in Eq. 6.3. For instance, components of a specific type might require an equivalent configuration, i.e., the corresponding row vectors a_i must possess equal values. Following [245], such constraints can be captured by functions $g_z : \mathbb{R}^p \rightarrow \mathbb{R}^{(l \times n)}$ that are monotonously increasing with $a' \mapsto (A; z)$, where $z \in \mathbb{R}^l$ indicates the types of the components. Such a function maps a lower-dimensional set of parameters $a' \in \mathbb{R}^p$ to the system description.

6.4.3 Grid search algorithm

In accordance with [245], a set-valued systemic risk measures as presented in Subsec. 6.4.2 can be computed via a combination of the so-called grid search algorithm and stochastic simulation. In two dimensions, a box-shaped subset of endowment properties is subdivided by a grid of equidistant points.

The algorithm proceeds as follows. The search starts at the origin of the search space; assume that the origin is outside of $R(Y)$. In a successive manner, the acceptance criterion is evaluated for each adjacent grid point on the grid diagonal along the direction $(1, 1, \dots, 1)^\top$. Typically, in each evaluation stochastic simulation is performed. The search along the diagonal terminates as soon as a grid point that meets the acceptance criterion is identified. Given the monotonicity of the input-output model and the properties associated with the acceptance criterion (cf. [245]), all grid point configurations in the box-shaped subset with the first accepted one as the bottom left corner are acceptable as well and consequently belong to $R(Y)$. Analogously, all endowments in the box-shaped subset with the first accepted one as the top right corner are rejected. Thus, these points belong to $R(Y)^c$ that is the complement of the systemic risk measure. Precisely this monotonicity property makes the algorithm efficient.

Each neighboring pair of diagonally adjacent points with one of these points meeting the requirements and the other not, defines a sub-box. In the next step, the algorithm checks the remaining corners of this sub-box, assigning a status to dominating and dominated endowments, respectively. Subsequently, the next neighboring pairs of points can be determined. The algorithm terminates as soon as all points on the grid have an assigned acceptance status. Finally, risk measure $R(Y)$ is determined as a discrete grid-approximation. This algorithm, combined with the methods proposed in Subsec. 6.4.1 and Subsec. 6.4.2, allows decision-making to be made regarding the optimal trade-off between resilience-enhancing endowments for complex capital goods.

6.5 Constrained resilience analysis of an axial compressor

In the current section, the methodology presented in Section 6.4 is demonstrated for illustrative scenarios, while the procedure for considering monetary constraints is elaborated, see phase one and two in Fig. 6.2. The method can be applied to assess a variety of complex capital goods. In [328] and [268], Salomon et al. proved the applicability of the proposed approach for a wide range of complex systems, e.g., flow networks, an axial compressor and the Berlin metro network.

6.5.1 Resilience analysis setting

In the context of the CRC 871, consider the functional model illustrated in Fig. 6.4 of the axial compressor developed in [251] presented in Subsec. 6.3.1. Again, an interruption between start and end represents system failure, i.e., a roughness-related performance variation of the physical system of at least 25%. The system functionality is utilized as meaningful system performance

$Q(t)$ that was claimed in Subsec. 6.4.2 for the subsequent application of the resilience decision making procedure. The system performance is evaluated at each point in time t_h and equals 1 if there is a connection from start to end and is 0 if the connection is interrupted.

Components $i \in \{1, \dots, 8\}$ of the functional model represent stator blade rows and rotor blade rows. In this example, each of them is assumed to have the same component type, i.e., it holds that $j_i = 1 \forall i \in \{1, \dots, 8\}$. For simplicity, denote $(a_i; j_i) = (a_i; 1) = a_i \forall i \in \{1, \dots, 8\}$. Suppose that each row, i.e., each component, is characterized by two endowment properties, namely, a roughness resistance re and a recovery improvement r^* . Then, the component is described by $a_i = (re_i, r_i^*)$. It holds true that $re_i = re_{i'}$, $r_i^* = r_{i'}^*$ if $j_i = j_{i'}$, consequently, the endowment pair (re_i, r_i^*) has equal numerical values for all components. Each of these configuration pairs might represent a particular regeneration path.

After evaluating the system performance in a previous time step t_h , each component can fail randomly. A failed component is removed from the model and no longer contributes to the system performance at time t_{h+1} . The component remains in the failed state until its full recovery. Assume that the failure probability of the component i is assumed to be constant in the time interval (t_h, t_{h+1}) . For illustrative purposes, it is given by

$$P \{\text{Component } i \text{ fails during } (t_h, t_{h+1})\} = \Delta t \cdot \lambda_i \quad (6.6)$$

with

$$\lambda_i = 0.8 - 0.03 \cdot re_i, \quad (6.7)$$

where λ_i is the time-independent failure rate. This single-step failure model corresponds to a simple approach for considering reliability and robustness. A consideration of system reliability in multiple states, where the system passes through several intermediate states before failure, as presented in a subsequent section, is one possibility for a more comprehensive modeling approach. Suppose that a failed component instantly recovers to the original performance level after a certain number of time steps passed. Then, the component recovery is described by

$$r_i = r_{max} - r_i^* \quad \text{with} \quad r_i^* < r_{max}, \quad (6.8)$$

where r_{max} denotes the maximum number of time steps required for recovery and r_i^* is a reduction depending on the current endowment of the component i . Since each time step is of the length $\Delta t = \frac{T}{u}$, with T denoting the investigated duration and u the amount of considered time steps, the duration of the recovery process is $r_i \cdot \frac{T}{u}$. In accordance with [6] and [10], this simple recovery model corresponds to a one step recovery profile; however, various other characteristic profiles of recovery in time are conceivable.

Note that in this setting increasing the roughness resistance of a blade row, i.e., a component i , mitigates the degradation of the surface, i.e., counteracts the roughening process, and correspondingly reduces the failure rate λ_i . If the component i fails, its functionality is fully recovered after r_i time steps specified via Eq. 6.8.

6.5.2 Costs of endowment properties

A certain endowment relates to the property quality of one or more components. In general, a higher quality of components results in a more resilient system. However, an increase in quality is typically associated with an increase in costs. Consequently, it is essential to take into account monetary aspects for an expedient decision making procedure. In accordance to [256], assume that increasing the reliability of components in complex systems corresponds to an exponential increase in their costs.

Assume that the cost associated with improving the endowment property roughness resistance is given by

$$cost^{re} = \sum_{i=1}^8 price^{re} \cdot 1.2^{(re_i-1)}, \quad (6.9)$$

where re_i is the roughness resistance value of component i . Further, $price^{re}$ is a common basic price independent of i in the current case study. Analogously, assume an exponential relationship for the costs associated with the recovery improvement r_i^* :

$$cost^{r^*} = \sum_{i=1}^8 price^* \cdot 1.2^{(r_i^*-1)}. \quad (6.10)$$

The total cost of an endowment results from the sum of these costs:

$$cost = cost^{re} + cost^{r^*}. \quad (6.11)$$

This cost function shown is subsequently utilized to determine the cost of a certain endowment. Consequently, the endowment pair with minimum cost can be identified. The combination of the adapted systemic risk measure developed in Subsec. 6.4.2, including the corresponding acceptance set, with the cost function enables the evaluation of optimal endowment pairs regarding resilience and monetary constraints.

6.5.3 Scenario and numerical results in a two-dimensional setting

In the following, the decision making method for identifying resilience-enhancing endowments under consideration of monetary constraints is demonstrated for the multi-stage high-speed axial compressor presented in Fig. 6.4 in Subsec. 6.3. For illustrative purposes, the model parameters and simulation parameter values, shown in Tab. 6.1, are considered.

Assume an resilience acceptance threshold of $\alpha = 0.8$, an arbitrarily selected number of $u = 200$ time steps, a constant failure rate of $\lambda = 0.8$ as well as an arbitrarily selected time step length of $\Delta t = 0.05$. The first step in the analysis is to determine the set of all acceptable endowments that correspond to a resilience value of at least $Res = 0.8$ over the time period under consideration. In practice, any improvement of the axial compressor blades is associated with costs. Consequently, the second step is to identify the least expensive acceptable endowment, denoted by \hat{A} . The grid

Table 6.1: Parameter values for the resilience decision making method for the functional model of the multi-stage high-speed axial compressor.

Parameter	Index	Value in Scenario
Number of Rotor/Stator blade rows	l	8
Acceptance threshold	α	0.8
Number of time steps	u	200
Length of a time step	Δt	0.05
Failure rate	λ	0.8
Maximum recovery time	r_{max}	21
Recovery improvement	r^*	$r_i^* \in \{1, \dots, 20\}$
Roughness resistance	re	$re_i \in \{1, \dots, 20\}$
Recovery improvement price	$price^{r^*}$	600€
Roughness resistance price	$price^{re}$	500€

search algorithm described in Subsec. 6.4.3 explores the roughness resistance re and the recovery improvement r^* over $re_i \in \{1, \dots, 20\}$, $r_i^* \in \{1, \dots, 20\} \forall i \in \{1, \dots, l\}$. Increasing a value of the properties of a component i is interpreted as increasing its the quality level. The roughness resistance values are interpreted as various quality levels of coatings applied to the blades. In terms of recovery, the quality increasing leads to a reduced recovery time for the components taking values from a maximum of 20 time steps (for $r_i^* = 1$) to a minimum of one time step (for $r_i^* = 20$) given $r_{max} = 21$.

Figure 6.9 shows the results of the grid search algorithm. The acceptable pairs of component properties, i.e., roughness resistance and recovery improvement, are depicted as blue, filled dots. Clearly, the quality of recovery improvement and the quality of the blade coatings can be compared regarding their impact on the system resilience. For instance, given recovery improvement values with $r_i^* \geq 15$, the minimum roughness resistance value of $re_i = 1$ is already sufficient to achieve the desired level of resilience.

For the determination of $R(Y)$ only about 10% of all possible endowment pairs had to be evaluated due to the grid search algorithm presented in Subsec. 6.4.3. More precisely, the number of endowment pairs on the diagonal plus the number of pairs equivalent to the size of the set of pairs with minimum acceptable resilience, i.e., the boundary or pareto front of $R(Y)$, had to be evaluated. Taking into account the base prices in Tab. 6.1, the most cost-efficient endowment i among the boundary set is characterized by a roughness resistance of $re_i = 8$ and a recovery improvement of $r_i^* = 13$ for each of the eight components. In Fig. 6.9 the corresponding pair is highlighted by a green circle. According to Eq. 6.11 the total cost equals 136 930€. Based on these results, the decision maker is advised to realize $re_i = 8$ and $r_i^* = 13$.

Note that in case of analyzing regeneration paths, resilience applies to the regeneration paths in two ways: 1. as a part of the overall performance over the entire life cycle of the complex capital good, and 2. as a resilient regeneration path in itself. Clusters are formed or identified of similar,

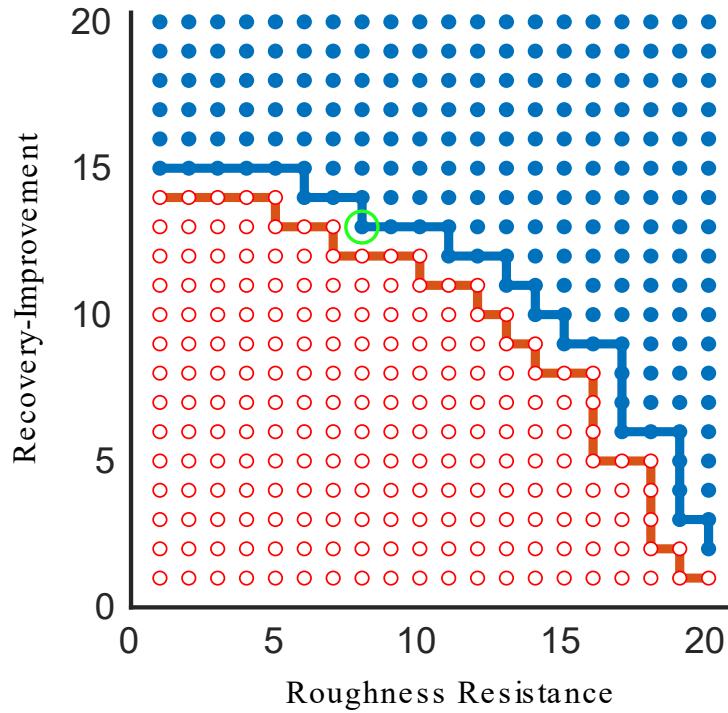


Figure 6.9: Numerical results of the grid search algorithm for the functional model of the axial compressor with explored roughness resistance/recovery improvement values; adapted from [268].

equally acceptable regeneration paths to which, in the event of a problem, it is possible to switch without great effort.

6.5.4 Scenario and numerical results in multiple dimensions

As shown in [328], the methodology developed in [268] can be utilized in the multi-dimensional case as well. The current subsection shall prove the applicability in a four dimensional setting given the model of the multistage high-speed axial compressor. The model parameter and simulation parameter values shown in Tab. 6.2 are considered. Assume the recovery improvement r^* to be fixed for all components, regardless of their type, $r_i^* = 11 \forall i \in \{1, \dots, l\}$, while the roughness resistance re is explored over $re_i \in \{1, \dots, 20\} \forall i \in \{1, \dots, l\}$. Again, the roughness resistance values can be interpreted as increasing quality levels of coatings. In this scenario, the four component types suggested in Subsec. 6.3.1 are adopted. Correspondingly, the first and second rotor blade rows are assigned as c_1 , the third and fourth as c_2 and c_3 , respectively, while all stator blade rows are assigned as c_4 . The set of all acceptable endowments leading to a system resilience value of at least $Res = 0.85$ over the time period under consideration is determined via the grid search algorithm. Then, the most cost-efficient endowment denoted by \hat{A} is identified. Figure 6.10 shows the corresponding results. In Fig. 6.10a, all combinations with a satisfactory system resilience of at least $Res = 0.85$ are depicted, corresponding to phase one in the analysis framework, see Fig. 6.2. This is the set of roughness resistance endowment pairs contained in $R(Y)$. In fact, the roughness resistance of the fourth rotor blade row (c_3) has the highest impact

Table 6.2: Parameter values for the resilience decision making method for the functional model of the multistage high-speed axial compressor.

Parameter	Index	Value in Scenario
Number of blade rows	l	8
Acceptance threshold	α	0.85
Number of time steps	u	200
Length of a time step	Δt	0.05
Failure rate	λ	0.8
Maximum recovery time	r_{max}	21
Recovery improvement	r^*	11
Roughness resistance	re	$re_i \in \{1, \dots, 20\}$
Recovery improvement price	$price_{(r^*, j_i)}^*$	600€
Roughness resistance price	$price_{(re_i, j_i)}^{re}$	800€ $\forall j_i \in \{1, 2, 3\}$ 500€ $\forall j_i = 4$

on the system resilience compared to other rows. This can be concluded as only pairs with a high roughness resistance quality for this type are acceptable. Regardless of the endowment property values of all other component types $c_i \in \{1, \dots, 4\}$, the endowment pairs with coating qualities of $re_i \leq 15$ for c_3 are not sufficient to provide an acceptable level of system resilience. In contrast, the roughness resistance of the four stators (c_4) has minor influence on the system resilience compared to all other types. Even endowments with $(re_i, 4) = 1$, i.e., a minimum coating quality level, are sufficient to achieve acceptable resilience values. The same holds true for the rotors of type c_1 and c_2 . Although, in comparison to the stators, components of types c_1 and c_2 require significantly higher level of coating quality to compensate small, i.e., values other than maximum values of roughness resistance for c_3 .

For decision making, it is crucial to be able to take into account monetary constraints. Therefore, Fig. 6.10b shows the endowment pairs contained in $R(Y)$ that lead to a satisfying system resilience of $Res = 0.85$ considering a budget threshold that is set to $cost_{max}^{re} = 50\,000\text{€}$ for illustrative purposes, corresponding to phase two in the analysis framework, see Fig. 6.2.

The results illustrated in Fig. 6.10b show that only configurations with low coating quality levels for all stators (c_4) are below the cost limit. Firstly, this is the case due to their low influence on system resilience, and secondly, to the high costs for increasing the quality levels for the stators caused by their amount and exponential cost-quality behavior. In contrast, only configurations that provide the highest quality levels of $(re_i, 3) \geq 17$ for the rotor of type 3 are acceptable and below the price limit simultaneously. The roughness resistance of the rotor of type c_3 has a critical influence on the system resilience. Consequently, the compensation of lower quality levels for c_3 by higher quality levels of the remaining blade rows exceed the given budget threshold. Even though the roughness resistance of the rotor of c_2 has a lower influence on the system resilience than that of c_3 , minimum quality levels for c_2 cannot be compensated by high qualities

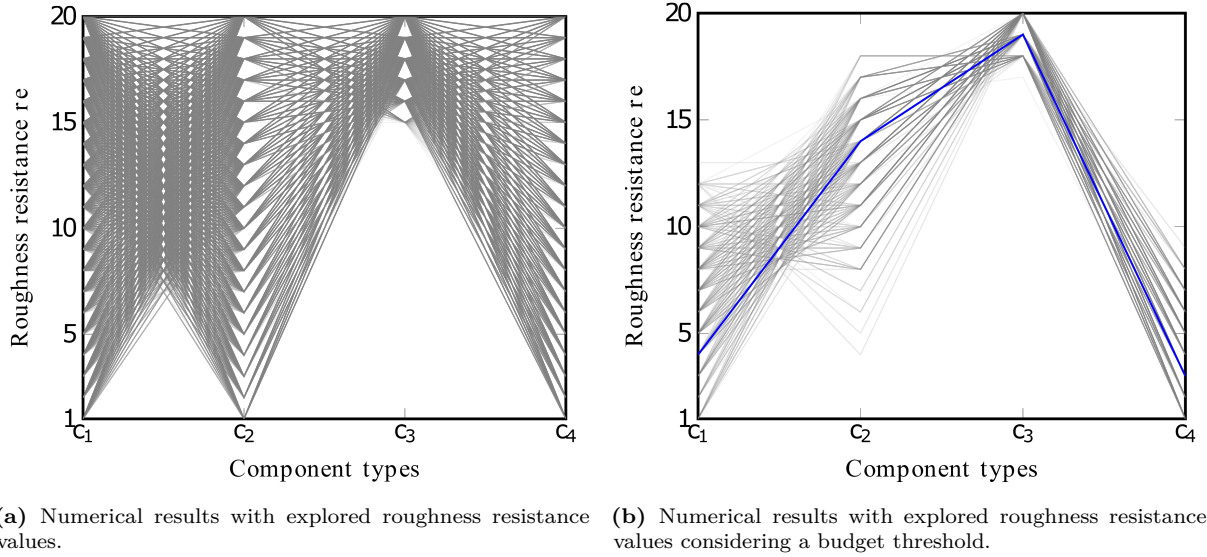


Figure 6.10: Numerical results for multi-dimensional setting; adapted from [328].

of the other components either. Correspondingly, at least $(re_i, 2) = 4$ is required to meet the acceptance criterion.

Considering the base prices in Tab. 6.2, the most cost-efficient endowment is characterized by the pair with roughness resistances of $(re_i, 1) = 4$, $(re_i, 2) = 14$, $(re_i, 3) = 19$ and $(re_i, 4) = 3$. The corresponding configuration is highlighted in blue in Fig. 6.10b. Via Eq. 6.11 the total cost is obtained as $cost_{(\hat{A};z)} = cost^{re} + cost^* = 42\,604\text{€} + 35\,664\text{€} = 78\,268\text{€}$.

The numerical effort for the computation of $R(Y)$ was reduced by about 98% due to the grid search algorithm compared to a naive evaluation of the search space. Correspondingly, only 2% of all possible combinations of roughness resistance values had to be evaluated. Note that the application of this methodology to higher-dimensional problems is only limited by constraints of computational memory and time.

6.6 Reliability analysis

The reliability analysis follows the resilience analysis and the reduction of all, in terms of system resilience, acceptable system configurations respectively regeneration paths due to technical and monetary restrictions. It thus forms the third phase in the analysis framework, see Fig. 6.2.

6.6.1 Repeated evaluation of the survival function

For all remaining endowment pairs of interest for decision makers, a system reliability analysis is conducted to evaluate the system failure probability at given time t . The system reliability is evaluated based on the stochastic properties of the system components represented as probability distribution functions that describe the event probability of failure due to degradation or a

disruptive event. Each model evaluation leads to the so-called survival function, i.e., the probability that the system is still functioning at time point t , performing its predefined task. In Fig. 6.11 three different survival functions are shown as Path A, B and C for illustrative purposes.

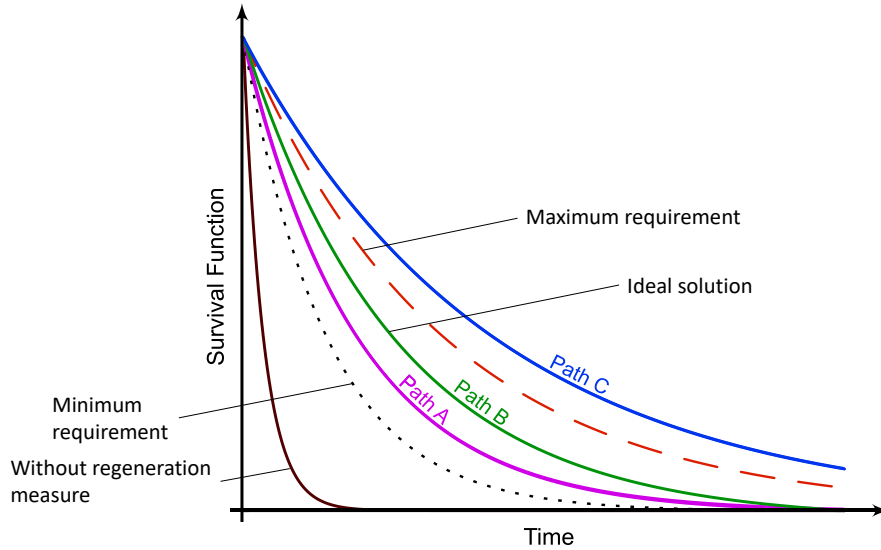


Figure 6.11: Reliability analysis based on the concept of survival signature considering multiple regeneration paths.

Different endowment pairs evaluated in the grid search algorithm correspond to various component properties due to different regeneration paths and lead to different survival functions. The three survival functions in Fig. 6.11 correspond to three different regeneration paths, i.e., endowment pairs. In addition, there might exist minimum and maximum requirements of system reliability due to practical experiences, customer requirements, e.g., budget limitations, or other circumstances. An efficient procedure is required to realize the large number of repeated model evaluations, i.e., computations of survival functions, with changing component properties.

6.6.2 Concept of binary-state survival signature

Fig. 6.12 illustrates the concept of survival signature introduced in [149]. The most beneficial attribute of this approach is its separation property. That means that the system structure is separated from the probability structure of the system describing the component failure behavior. This leads to a significant reduction of the computational effort, since once the typical costly to determine system structure has been computed, any possible characterization of the probabilistic part can be tested with no need to recompute the structure. This means that any number of system configurations, i.e. regeneration paths, can be simulated and analyzed, since these only affect the probability structure and usually not the system structure. At the same time, the survival signature radically condenses information on the topological reliability for systems with

multiple component types with K being the maximum number of component types. The failure times of components of one type are claimed to be independent and identically distributed (*iid*) or exchangeable. For more information on claimed exchangeability in practice, see [153] and [152].

$$P(T_S > t) = \sum_{l_1=0}^{m_1} \cdots \sum_{l_k=0}^{m_k} \Phi(l_1, \dots, l_k) \cdot P\left(\bigcap_{k=1}^K \{C_k(t) = l_k\}\right)$$

Figure 6.12: Illustration of the advantageous properties of the concept of survival signature.

For a deeper understanding of this concept, consider a coherent system with a given binary-state structure function defining the system state to be either 0 or 1 for a binary-state vector out of the set of all possible state vectors. The binary-state vector specifies the state of $n = \sum_{k=1}^K n_k$ components in total, there are $\binom{n}{l}$ state vectors \mathbf{x} with exactly l components with $x_i = 1$, i.e., $\sum_{i=1}^n x_i = l$. Let the set of these state vectors with l functioning components refer to as S_l . In the case of $k \geq 2$, the survival signature summarizes the probability that a system is working as a function depending on the number of working components l_k for each type $k = 1, \dots, K$. Assume the failure times within a component type to be *iid* or exchangeable. Consequently, all possible state vectors are equally likely to occur. Then, the survival signature is defined as

$$\Phi(l_1, l_2, \dots, l_K) = \left[\prod_{k=1}^K \binom{n_k}{l_k}^{-1} \right] \sum_{\mathbf{x} \in S_{l_1, l_2, \dots, l_K}} \phi(\mathbf{x}), \quad (6.12)$$

where $\binom{n_k}{l_k}$ corresponds to the total number of state vectors \mathbf{x}_k of type k and S_{l_1, l_2, \dots, l_K} denotes the set of all state vectors of the entire system for which $l_k = \sum_{i=1}^{n_k} x_{k,i}$. Then, the survival signature $\Phi(l_1, l_2, \dots, l_K)$ characterizes the probability that a system is working given that exactly l of its components working for $l = 1, \dots, n$. Note that the survival signature depends only on the topological reliability of the system, independent of the time-dependent failure behavior of its components, namely, the probability structure. Note that it is differentiated between the concept of survival signature with its separation property shown in Fig. 6.12 and the mathematical object survival signature itself shown in Eq. 6.12.

Further, assume the probability distribution for the failure times of type k to be known with $F_k(t)$, denoting the corresponding cumulative distribution function. Then,

$$\begin{aligned} P\left(\bigcap_{k=1}^K \{C_k(t) = l_k\}\right) &= \prod_{k=1}^K P(C_k(t) = l_k) \\ &= \prod_{k=1}^K \binom{n_k}{l_k} [F_k(t)]^{n_k - l_k} [1 - F_k(t)]^{l_k} \end{aligned} \quad (6.13)$$

describes the probability structure of the system, regardless of its topology. $C_k(t) \in \{0, 1, \dots, n_k\}$ represents the number of components of type k in a working state at time t .

Both Eq. 6.12 and Eq. 6.13 form together the concept of survival signature illustrated in Fig. 6.12. The concept is integrated into the proposed framework, see phase three in Fig. 6.2, to leverage its salient beneficial properties for repeated model evaluations that are required for comprehensive MRO decision making.

6.6.3 Concept of multi-state survival signature

While a binary-state consideration of systems and their components is state-of-the-art, further research on multi-state systems with multi-state components is inevitable for a more realistic and comprehensive assessment of system reliability. In [280], Eryilmaz & Tuncel proposed a generalized concept of survival signature in the context of unrepairable homogeneous multi-state systems. In accordance with the approach presented in [149], the survival function for multiple types with type $k = 1, \dots, K$ can be derived as:

$$P\{T^{\geq J} > t\} = \sum_{i^1 \geq \dots \geq i^J} \Phi^{\geq J}(i_1^1, \dots, i_k^j, \dots, i_K^J) \times P\{C_1^1(t) = i_1^1, \dots, C_k^j(t) = i_k^j, \dots, C_K^J(t) = i_K^J\}. \quad (6.14)$$

with maximum system and component level J and $T^{\geq J}$ that is the system failure time in state J . Thereby, $\Phi^{\geq J}(i_1^1, \dots, i_k^j, \dots, i_K^J)$ represents the j -th level survival signature for level J , i.e., the probability that the system is working in state J or above if i_k^j components are working for types $k = 1, \dots, K$ and states $j = 1, \dots, J$ with $i_k^{j-1} \geq i_k^j$. The total number of state vectors given i_k^j components of type k functioning in state j or above is

$$v_{n_1, \dots, n_K}(i_1^1, \dots, i_k^j, \dots, i_K^J) = \prod_{j=1}^J \binom{n_1 - i_1^{j+1}}{i_1^j - i_1^{j+1}} \dots \binom{n_K - i_K^{j+1}}{i_K^j - i_K^{j+1}}, \quad (6.15)$$

where $i_1^{J+1} = \dots = i_K^{J+1} = 0$ and n_k denotes the total number of components of type k . The j -th level survival signature for level J for multiple types is given as

$$\Phi^{\geq J}(i_1^1, \dots, i_k^j, \dots, i_K^J) = \frac{\sum_{\mathbf{x} \in S_{i_1^1, \dots, i_k^j, \dots, i_K^J}} \phi(\mathbf{x})}{v_{n_1, \dots, n_K}(i_1^1, \dots, i_k^j, \dots, i_K^J)}. \quad (6.16)$$

Again the j -th level survival signature and the survival function with multiple components are derived similarly to Eq. 6.16 and Eq. 6.14, respectively.

The approach proposed in [280] enables to compute the reliability of multi-state systems for J binary-state structure functions with components following a Markov degradation process with minor failures. Given the four binary-state structure functions established in Subsec. 6.3.1 and the probability structure describing component degradation from state to state, the reliability of

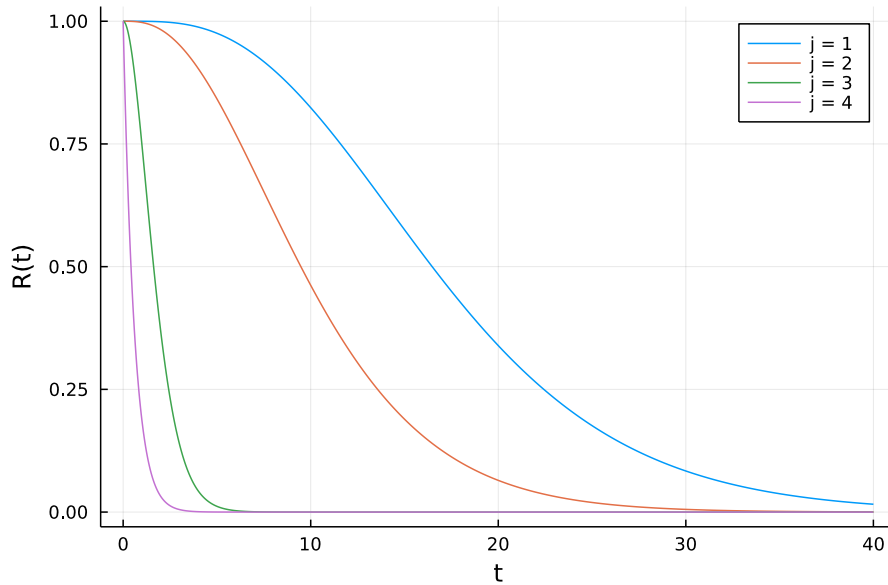


Figure 6.13: j -th level survival functions for $j \in \{1, \dots, 4\}$.

the multi-state axial compressor to be in one of four states can be evaluated. For illustrative purposes, the component degradation model was established as suggested in [280] with arbitrarily selected instantaneous degradation rates. Fig. 6.13 shows the survival functions of the levels $j = 1, \dots, 4$ of the multi-state axial compressor previously introduced. The combination of this multi-state system consideration with the developed analysis framework enables the assessment of the resilience of multi-state systems with multi-state components.

6.7 Uncertainty analysis

In reality, the information on a complex capital good and its behavior is subject to aleatoric or so-called irreducible uncertainties but typically also epistemic uncertainties or so-called imprecision. For instance, this is the case due to estimates of distribution parameters based on expert knowledge, measurement errors or a simple lack of data. In the context of the CRC 871, the influence of a regeneration measure on the survival behavior of a complex capital good might not be precisely known, i.e., the distribution parameters describing the failure behavior can only be estimated. Thus, the models and corresponding simulations are also governed by these uncertainties. However, for comprehensive decision making existing uncertainties need to be considered in analysis and therefore beneficial approaches to implement these are an important research topic, see [227] and [194]. Consequently, the novel uncertainty analysis developed in this work constitutes the fourth and final phase of the analysis framework, see Fig. 6.2.

6.7.1 Imprecision and its implementation via fuzzy probability

Fig. 6.14 shows the concept of survival signature with an adaption of the probability structure via fuzzy probabilities, cf. [152]. Thus, the imprecision is propagated through the model. This enables the advantageous properties of this concept to be exploited while accounting for imprecision.

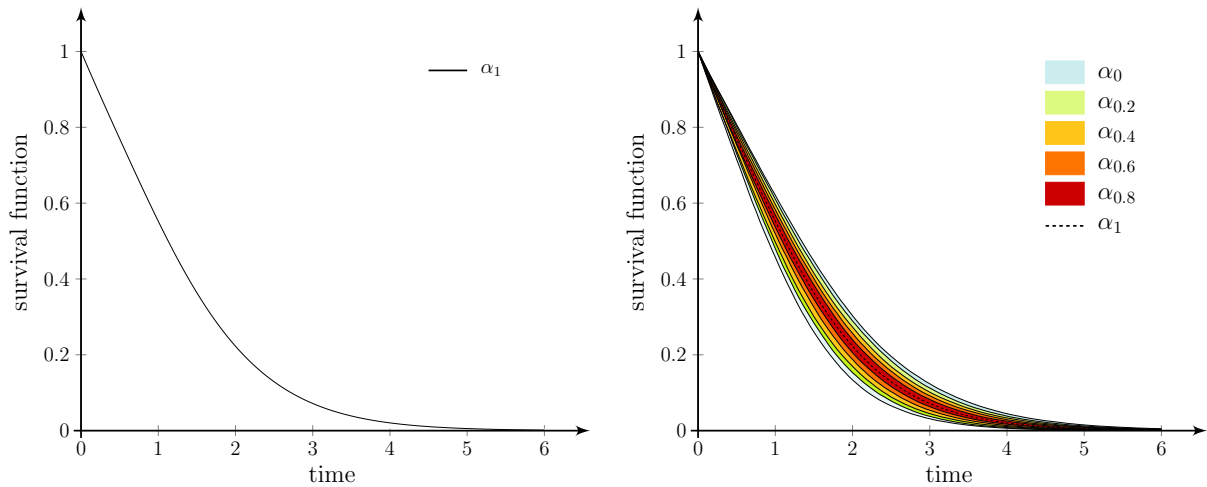
$$P(T_S > t) = \sum_{l_1=0}^{m_1} \dots \sum_{l_k=0}^{m_k} \Phi(l_1, \dots, l_k) \cdot P\left(\bigcap_{k=1}^K \{C_k(t) = l_k\}\right)$$

← Fuzzy probabilities

Probability Structure

Figure 6.14: Fuzzy probabilities included in the concept of survival signature.

The result is not a sharp survival function, as seen in Fig. 6.15a, but an imprecise survival function with regions, as seen in Fig. 6.15b. The imprecise survival functions are computed on basis of stochastic input variables described via fuzzy probabilities. The reliability analysis under consideration of imprecision can be simplified by considering various discrete alpha-cuts with $\alpha \in [0, 1]$ as illustrated in Fig. 6.15b for $\alpha \in \{0, 0.2, 0.4, 0.6, 0.8\}$.



(a) Precise survival function that is equivalent to an alpha-cut $\alpha = 1$ of the fuzzy probability. **(b)** Imprecise survival function described via fuzzy probability with five alpha-cuts $\alpha \in \{0, 0.2, 0.4, 0.6, 0.8, 1\}$.

Figure 6.15: Precise and imprecise survival functions; adapted from [152].

The survival function generated with $\alpha = 0$ represents the maximum level of uncertainty. For example, an expert specifies the parameter interval corresponding to an alpha level $\alpha = 0$ of the fuzzy probability as the maximum degree of uncertainty, i.e. the parameters will certainly not violate the interval limits. This might be the case in design and maintenance, if, e.g., only insufficient information on the installed components has been collected so far and only an educated guess of an expert is available. In contrast, an alpha-level of $\alpha = 1$ corresponds

to a precise survival function that is typically not known. Note that this is only the case for triangular fuzzy probabilities as presented in [152]. However, there exist fuzzy probabilities that describe an interval of parameters for $\alpha = 1$ as well. Depending on the budget, gathering precise information for each component type, e.g., via experimental campaigns, might not be feasible, impeding proper reliability analyses. In fact, a complete elimination of imprecision is in most cases neither necessary nor cost-efficient. Therefore, a method for determining a critical level of imprecision is crucial for cost-effective decision making that balances imprecision against the cost associated with reducing it. In [152], Salomon et al. developed a comprehensive decision making procedure for uncertainty reduction. Integral parts are target values for the system reliability at certain points in time. If the current setting of parameters modeled via fuzzy probabilities fail to ensure these target reliabilites the imprecision in the fundamental data should be reduced. The procedure is cost-efficient, since it proceeds successively from $\alpha = 0$ up to $\alpha = 1$ until the reliability requirements are met.

6.7.2 Efficient simulation algorithm under consideration of imprecision

The consideration of both irreducible uncertainty and imprecision requires adequate treatment in systems analysis. A frequently implemented approach is a two-stage simulation, commonly known as a “double-loop” approach. Correspondingly, variables describing imprecision on parameters are sampled in an “outer loop” and variables representing irreducible uncertainty and depending on the imprecise parameters, as, e.g., failure time of components, are sampled in an “inner loop,” cf. [203], or vice versa, in an “outer loop” aleatory variables are sampled and epistemic uncertainty is treated in the “inner loop”, cf. [204]. Clearly, for complex systems, this naive sampling approach leads to an extremely large sample size and consequently a high computational cost, see, e.g. [294]. Consequently, simulation approaches that increase computational efficiency and yield high accuracy at minimal sample size are desirable. Recently, the Non-Intrusive Stochastic Simulation (NISS), a promising approach to efficiently compute imprecise structural models with significantly reduced sample size was introduced in [220]. The method is divided into two basic approaches, Local Extended Monte Carlo Simulation (LEMCS) and Global Extended Monte Carlo Simulation (GEMCS), which provide different advantages in terms of accuracy and variation.

In [152], a novel methodology was developed in the context of imprecise system reliability analysis by adapting the LEMCS and the GEMCS and combining them with the concept of survival signature. The imprecision of parameters is modeled via fuzzy probabilities. This imprecision is then propagated efficiently through the analysis framework by means of the new method as illustrated in Fig. 6.16. The complex amalgamation brings together the advantages of both the concept of survival signature and NISS concepts: a significant memory reduction of topological information and large efficiency benefits in repeated model evaluations, combined with a comprehensive consideration of uncertainties with only one required stochastic simulation, thus drastically reducing the sample size. This combination leads to beneficial synergy effects, increasing the efficiency even more. The savings due to the new methodology regarding sampling

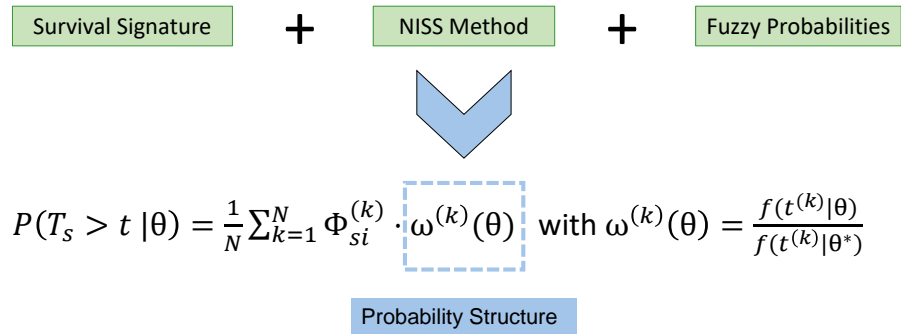
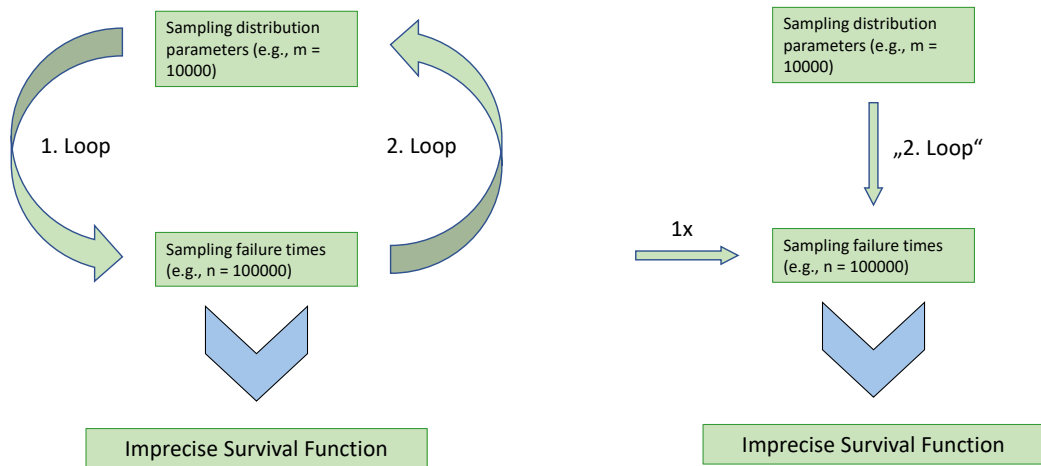


Figure 6.16: NISS method and the LEMCS estimator.

effort compared with the naive double loop approach are illustrated in Fig. 6.17. Fig 6.17a and Fig. 6.17b The most attractive aspect of both the LEMCS and GEMCS algorithms is the fact



(a) Sampling procedure via the traditional “double loop” approach. (b) Sampling procedure via novel developed uncertainty analysis.

Figure 6.17: Sampling via the “double loop” approach and the novel uncertainty analysis developed in this work.

that only a single stochastic simulation is necessary to account for the imprecisions. Therefore, the traditionally employed “double loop” simulation can be circumvented. In both LEMCS and GEMCS, the interval analysis and the stochastic analysis have been decoupled successfully, and the computational expense is mainly driven by the single stochastic simulation performed. Moreover, the stochastic analysis has been separated from the system topology by merging it with the survival signature, so that only one reliability analysis in terms of topology is required to generate the survival signature. In addition to these beneficial features of the survival signature, it is exactly the single stochastic simulation required that gives the proposed methodology its efficiency and differentiates it clearly from traditional approaches. Thanks to this approach the

imprecise stochastic analysis used to estimate the bounds on the system survival function has been greatly simplified.

In [152], the new methodology was demonstrated, among others, on the functional model of the axial compressor presented in Subsec. 6.3 and shown in Fig. 6.4. The “double loop” approach is conducted with 5 000 samples (failure times) on the inner loop and 1 000 samples (model parameters) on the outer loop, i.e., a total of 5 000 000 samples. While even improving the quality in results, for both LEMCS and GEMCS, only one simulation was required with 100 000 generated samples (failure times for 100 000 different model parameters). Correspondingly, only 1/50th of the sample size compared to the “double loop” approach was required.

6.8 Conclusions

A decision making process has been developed that enables the identification of optimal trade-offs among numerous resilience-enhancing features/measures for complex capital goods of various types. During the period of the CRC 871 the approach as been applied to models of an axial compressor, of a flow network, of an arbitrary complex system, and of the Berlin metro network. The consideration of monetary and technical constraints into the decision making process is realized. The broad applicability of all developed methods is ensured, i.e., there are no limitations to a specific system type. A reduction in computational effort has been achieved, mainly due to the separation property of the survival signature, i.e., once the system structure has been computed, any possible characterization of the probabilistic part can be evaluated without the need to recompute the structure. The integration of uncertainties in the reliability analysis is enabled and the sample size is drastically reduced due to the adapted NISS methods requiring only a single stochastic simulation, avoiding the tedious “double loop” simulation traditionally applied.

It could be shown that functional models are a good and effective approach to represent physically complex systems. This approach was further developed to not only consider dependencies in the input parameters but also to include a time dependency of the sensitivities by means of importance indices. Still challenging is the merging of the several developed functional models of subsystems within the overall jet engine into an encompassing representative overall model. It is very computationally expensive due to the costly sensitivity analysis for complex systems with numerous input and output parameters. Further in-depth research on this topic is required to enable the generation of such an extensive model.

The comprehensive and encompassing analysis framework developed in this work, consisting of resilience analysis, consideration of technical and monetary constraints, reliability analysis, and uncertainty analysis, provides decision makers with an additional basis for decision making in MRO processes, enabling sophisticated decisions on an efficient background. Thereby, resilience applies to regeneration paths not exclusively as a part of the overall life cycle performance of the complex capital good, but as an important property for the regeneration path in itself. Clusters are identified of similar, equally acceptable regeneration paths to which, in the event

of a problem, effortlessly can be switched, leading to a variety of resilient regeneration paths. Furthermore, strict attention was given that all developed phases within the analysis framework are applicable to complex capital goods of any kind and in every field of application, e.g., design process, optimization process etc.

The outlook that goes beyond the scope of this project is the combination of all presented approaches into a single encompassing methodology in order to be able to take even greater advantage of the excellent synergy effects between them.

Acknowledgments

Funded by the Deutsche Forschungsgemeinschaft (DFG, German Research Foundation) – CRC 871/3 – 119193472.

7 | Conclusions and outlook

In this concluding chapter, the main developments of the dissertation are summarized, and meaningful extensions and potential improvements are suggested for future works.

7.1 Conclusions

The five publications in the dissertation focus on developing comprehensive methodologies for decision-making for complex engineering systems with the aim of optimizing resource allocation for resilience enhancement. The overall framework allows for the comparison of heterogeneous controls on system resilience and the consideration of monetary aspects in the decision-making process. The controls range from failure prevention to recovery improvement measures, at any stage of the system's life cycle. Furthermore, two methodologies in the domain of system reliability are developed. Each represents a novelty in its own right but also serves as a powerful extension to the resilience framework. The proposed work, in particular, the resilience decision-making framework with its extensions, contributes significantly to the resilience analysis of complex engineering systems and closes important scientific gaps in this field.

A core innovation of this dissertation is given in the first publication by the universally applicable resilience decision-making framework. It consists of an adapted systemic risk measure and a sophisticated probabilistic, and time-dependent resilience metric, enabling decision-makers to optimally balance resilience-enhancing measures of any kind. The system behavior may depend on a variety of stochastic variables that influence its performance. In a first step, the provided methodology characterizes all acceptable configurations of system components that lead to a desired level of system resilience. In a second step, the approach incorporates monetary aspects into the decision-making process and allows for the identification of the most cost-efficient allocation. The framework is capable of considering all types of system performance quantities, offering a high degree of flexibility in its application. Furthermore, the utilization of a grid search algorithm for systemic risk measures, significantly reduces the required computational effort.

In the second publication, the resilience decision-making method from the first publication is extended for application to multidimensional search spaces. Then, an efficient and novel methodology is developed by merging this extension with the concept of survival signature. The approach continues to enable direct comparison of heterogeneous resilience-enhancing measures on system resilience. Compared to the origin approach, the novel methodology is characterized by high numerical efficiency, especially for large, substructured, complex systems. The majority of

endowment properties under investigation affect the probability structure of system components. The numerous changes in the probability structure caused by constantly changing endowment properties during resilience analysis are typically costly to simulate and can be ideally accounted for with minimal effort due to the separation property of the survival signature. The novel approach incorporates a substructuring approach for large, complex systems. This and the integration of the survival signature allow the propagation of subsystem reliabilities through any number of system levels up to the top level and lead to a significant reduction in computational effort. In this way, and with the extension of the adapted systemic risk measure, it is now possible to analyze systems with a large number of components for their resilience.

The third publication of the dissertation presents an innovative methodology for system reliability analysis, accounting for imprecision through fuzzy probabilities and nested p-box analysis. It utilizes two adapted extended Monte Carlo simulation methods, which only require a single stochastic simulation per considered uncertainty level. This approach is efficient, widely applicable, and provides decision-makers with the ability to identify a bearable level of imprecision that still ensures acceptable system reliability. Further, the provided novel methodology is developed such that an embedding into the resilience decision-making framework established in the second publication of this dissertation is straightforward.

The advancements made in the fourth publication, like those made in the third publication, serve both as an extension of the encompassing resilience decision-making framework and, in themselves, represent a novelty in the field of reliability analysis. The cornerstone of these innovative contributions lies in tackling the constraints imposed by a binary consideration of component and system states at the subsystem level for substructured complex systems within the resilience framework. This objective is fulfilled through the newly introduced continuous-state survival function and the introduction of the DAS as a corresponding surrogate model, based on combinatorial decomposition adopted from the survival signature concept, allowing for the separation of topological and probabilistic information. The results offer a more comprehensive perspective for resilience analyses of practical systems.

The fifth publication provides a significant contribution by introducing a comprehensive decision-making approach for the regeneration of complex capital goods. The publication demonstrates the versatility and transferability of numerous methodologies previously developed in the dissertation, which can be applied to any type of system and integrated into different application domains and frameworks. The developed approach addresses two challenges: it analyzes the resilience of a regeneration pathway itself and provides decision-makers with solid information for selecting from a variety of (resilient) regeneration paths. This synergistic approach combines resilience, reliability, and lifetime analyses, as well as consideration of uncertainties, to provide effective resilience-based decision criteria for the optimal regeneration of complex capital goods. In addition, the publication demonstrates the value of functional models in representing physically complex systems, accounting for input parameter dependencies via time-dependent sensitivity analyses and importance indices. In summary, this framework provides an improved foundation

for decision-making and enhances the understanding and implementation of resilience in MRO processes.

7.2 Outlook

The novel methodologies presented in this dissertation have proven to be capable of addressing an efficient resilience analysis and decision-making of complex engineering systems. In the following, some suggestions for extensions and future challenges in the context of these methods are presented.

From a conceptual perspective, real-world problems often involve multiple objectives and are not limited to a finite time horizon. Therefore, future work should focus not only on system resilience and the cost of resilience-enhancing controls alone, but also on long-term impacts, such as differential expected gains from modified system resilience. Comprehensive decisions require a deep understanding of the trade-off between the costs and gains of resilience. Further work will therefore need to address balancing monetary and other criteria, such as safety, social, moral, and environmental considerations for decision-making, to name only a few.

In order to be capable of analyzing the increasingly growing and converging systems that characterize our modern societies in the future, the efficiency of the developed methods must be continuously improved under the aspect of the so-called “curse of dimensionality”. Although the presented methods in this dissertation show high efficiency in terms of computational effort, an efficient handling of interconnected systems (systems-of-systems), consisting of possibly billions of components, has to be explored.

In view of the two aforementioned challenges of future research, the comprehensive integration of uncertainties, which has already been addressed in this dissertation, must be pursued even further in future research. Uncertainties are real and ubiquitous. However, their consideration exacerbates and potentiates the aspect of increasing computational costs and complexity of comprehensive resilience analyses.

The last and possibly most important aspect is the time pressure under which these developments have to be carried out. Global challenges, first and foremost the accelerating climate crisis, make it imperative to identify and implement solutions on an unprecedented scale to limit the impacts and to build our societies more robust, more adaptable, more reliable, or in short, more resilient.

8 | List of publications

Journal articles:

- Jan Goeing, Hendrik Seehausen, Lennart Stania, Nicolas Nuebel, Julian Salomon, Panagiotis Ignatidis, Friedrich Dinkelacker, Michael Beer, Berend Denkena, Joerg Seume, and Jens Friedrichs. *Virtual process for evaluating the influence of real combined module variations on the overall performance of an aircraft engine*. In: Journal of the Global Power and Propulsion Society 7 (2023), pages 95-112.
- Niklas Winnewisser, Julian Salomon, Matteo Broggi, and Michael Beer. *The concept of diagonal approximated signature: new surrogate modeling approach for continuous-state systems in the context of resilience optimization*. In: Disaster Prevention and Resilience 2.2 (2023), pages 4. DOI: 10.20517/dpr.2023.03.
- Julian Salomon, Jasper Behrendorf, Niklas Winnewisser, Matteo Broggi, and Michael Beer. *Multidimensional resilience decision-making for complex and substructured systems*. In: Resilient Cities and Structures 1.3 (2022), pages 61–78. DOI: 10.1016/j.rcns.2022.10.005.
- Julian Salomon, Niklas Winnewisser, Pengfei Wei, Matteo Broggi, and Michael Beer. *Efficient reliability analysis of complex systems in consideration of imprecision*. In: Reliability Engineering & System Safety 216 (2021), page 107972. DOI: 10.1016/j.ress.2021.107972.
- Julian Salomon, Matteo Broggi, Sebastian Kruse, Stefan Weber, and Michael Beer. *Resilience decision-making for complex systems*. In: ASCE-ASME Journal of Risk and Uncertainty in Engineering Systems, Part B: Mechanical Engineering, 6.2 (2020), Article 020901. DOI: 10.1115/1.4044907.

Book contributions:

- Julian Salomon, Matteo Broggi, and Michael Beer. *Resilience-based decision criteria for optimal regeneration*. In: Regeneration of Complex Capital Goods, Springer (2023), accepted in 2022.
- Julian Salomon, Jasper Behrendorf, and Michael Beer. *Resilienz baulicher Infrastruktur*. In: 26. Dresdner Baustatik-Seminar, Realität – Modellierung – Tragwerksplanung. Institute for Statics and Dynamics of Structures (2022), TU Dresden.

Conference papers:

- Niklas Winnewisser, Julian Salomon, Matteo Broggi, and Michael Beer. *The concept of diagonal approximated signature: new surrogate modeling approach for continuous-state systems.*, Infrastructure Innovation & Adaptation for a Sustainable & Resilient World (INSPIRE) (2023), Virginia, USA. Accepted in 2023.
- Julian Salomon, Sebastian Kruse, Matteo Broggi, Stefan Weber, and Michael Beer. *Resilience decision-making for complex and Substructured systems*, 8th International Symposium on Reliability Engineering and Risk Management (ISRERM) (2022), Hannover, Germany.
- Jan Goeing, Hendrik Seehausen, Lennart Stania, Nicolas Nuebel, Julian Salomon, Panagiotis Ignatidis, Friedrich Dinkelacker, Michael Beer, Berend Denkena, Joerg Seume, and Jens Friedrichs. *Virtual process for evaluating the influence of real combined module variations on the overall performance of an aircraft engine*, Proceedings of Global Power and Propulsion Society (GPPS) (2022), Chania, Greece.
- Julian Salomon, Jan Göing, Sebastian Lück, Matteo Broggi, Jens Friedrichs, and Michael Beer. *Sensitivity analysis of an aircraft engine model under consideration of dependent variables*, ASME TURBOEXPO: Turbomachinery Technical Conference & Exposition (2021), Pittsburg, USA.
- Julian Salomon, Niklas Winnewisser, Pengfei Wei, Matteo Broggi, and Michael Beer. *Efficient reliability of an axial compressor in consideration of epistemic uncertainty*, e-proceedings of the 30th European Safety and Reliability Conference (ESREL) and 15th Probabilistic Safety Assessment and Management Conference (PSAM) (2020), Venice, Italy.
- Julian Salomon, Jasper Behrendorf, Stefan Weber, Matteo Broggi, and Michael Beer. *Multidimensional resilience decision-making on a multistage high-speed axial compressor*, 29th International European Safety and Reliability Conference (ESREL) (2019), Hannover, Germany.
- Julian Salomon, Sebastian Kruse, Matteo Broggi, Stefan Weber, and Michael Beer. *Decision-making for resilience-enhancing endowments in complex systems using principles of risk measures*, 6th International Symposium on Reliability Engineering and Risk Management (ISRERM) (2018), Singapore, Singapore.

Bibliography

- [1] Igor Linkov, Todd Bridges, Felix Creutzig, Jennifer Decker, Cate Fox-Lent, Wolfgang Kröger, James H Lambert, Anders Levermann, et al. “Changing the resilience paradigm”. In: *Nature Climate Change* 4.6 (2014), pages 407–409.
- [2] Yi-Ping Fang, Nicola Pedroni, and Enrico Zio. “Resilience-based component importance measures for critical infrastructure network systems”. In: *IEEE Transactions on Reliability* 65.2 (2016), pages 502–512.
- [3] William Hynes, Benjamin Trump, Patrick Love, and Igor Linkov. “Bouncing forward: a resilience approach to dealing with COVID-19 and future systemic shocks”. In: *Environment Systems and Decisions* 40 (2020), pages 174–184.
- [4] Sara Meerow, Joshua P Newell, and Melissa Stults. “Defining urban resilience: A review”. In: *Landscape and urban planning* 147 (2016), pages 38–49.
- [5] Gian Paolo Cimellaro, Andrei M. Reinhorn, and Michel Bruneau. “Framework for analytical quantification of disaster resilience”. In: *Engineering Structures* 32.11 (2010), pages 3639–3649. DOI: 10.1016/j.engstruct.2010.08.008.
- [6] Bilal M. Ayyub. “Systems resilience for multihazard environments: Definition, metrics, and valuation for decision making”. In: *Risk Analysis* 34.2 (2014), pages 340–355. DOI: 10.1111/risa.12093.
- [7] Yiping Fang, Nicola Pedroni, and Enrico Zio. “Optimization of Cascade-Resilient Electrical Infrastructures and its Validation by Power Flow Modeling”. In: *Risk Analysis* 35.4 (2015), pages 594–607. DOI: 10.1111/risa.12396.
- [8] C. S. Holling. “Resilience and Stability of Ecological Systems”. In: *Annu.Rev.Ecol.Syst.* 4 (1973), pages 1–23. DOI: 10.1146/annurev.es.04.110173.000245. arXiv: arXiv:1011.1669v3.
- [9] Norman Garnezy. “Vulnerability research and the issue of primary prevention.” In: *American Journal of orthopsychiatry* 41.1 (1971), page 101.
- [10] Bilal M. Ayyub. “Practical Resilience Metrics for Planning, Design, and Decision Making”. In: *ASCE-ASME Journal of Risk and Uncertainty in Engineering Systems, Part A: Civil Engineering* 1.3 (2015), page 04015008. DOI: 10.1061/ajrua6.0000826.
- [11] Gian Paolo Cimellaro. “Urban resilience for emergency response and recovery”. In: *Fundamental Concepts and Applications* (2016).

- [12] Seyedmohsen Hosseini, Kash Barker, and Jose E. Ramirez-Marquez. “A review of definitions and measures of system resilience”. In: *Reliability Engineering & System Safety* 145 (2016), pages 47–61. DOI: 10.1016/j.ress.2015.08.006.
- [13] Ayyoob Sharifi. “Urban resilience assessment: Mapping knowledge structure and trends”. In: *Sustainability* 12.15 (2020), page 5918.
- [14] Yeowon Kim, Daniel A Eisenberg, Emily N Bondank, Mikhail V Chester, Giuseppe Mascaro, and B Shane Underwood. “Fail-safe and safe-to-fail adaptation: decision-making for urban flooding under climate change”. In: *Climatic Change* 145 (2017), pages 397–412.
- [15] David Butler, Sarah Ward, Chris Sweetapple, Maryam Astaraie-Imani, Kegong Diao, Raziyyeh Farmani, and Guangtao Fu. “Reliable, resilient and sustainable water management: the Safe & SuRe approach”. In: *Global Challenges* 1.1 (2017), pages 63–77.
- [16] Kash Barker, James H Lambert, Christopher W Zobel, Andrea H Tapia, Jose E Ramirez-Marquez, Laura Albert, Charles D Nicholson, and Cornelia Caragea. “Defining resilience analytics for interdependent cyber-physical-social networks”. In: *Sustainable and Resilient Infrastructure* 2.2 (2017), pages 59–67.
- [17] Giuliano Punzo, Anurag Tewari, Eugene Butans, Massimiliano Vasile, Alan Purvis, Martin Mayfield, and Liz Varga. “Engineering resilient complex systems: the necessary shift toward complexity science”. In: *IEEE Systems Journal* 14.3 (2020), pages 3865–3874.
- [18] Victoria Haldane, Chuan De Foo, Salma M Abdalla, Anne-Sophie Jung, Melisa Tan, Shishi Wu, Alvin Chua, Monica Verma, et al. “Health systems resilience in managing the COVID-19 pandemic: lessons from 28 countries”. In: *Nature Medicine* 27.6 (2021), pages 964–980.
- [19] Shenggen Fan, Paul Teng, Ping Chew, Geoffry Smith, and Les Copeland. “Food system resilience and COVID-19—Lessons from the Asian experience”. In: *Global Food Security* 28 (2021), page 100501.
- [20] Som Naidu. *Building resilience in education systems post-COVID-19*. 2021.
- [21] Maureen S Golan, Laura H Jernegan, and Igor Linkov. “Trends and applications of resilience analytics in supply chain modeling: systematic literature review in the context of the COVID-19 pandemic”. In: *Environment Systems and Decisions* 40.2 (2020), pages 222–243.
- [22] Beata Javorcik. “Global supply chains will not be the same in the post-COVID-19 world”. In: *COVID-19 and trade policy: Why turning inward won’t work* 111 (2020).
- [23] Johan Bergström, Roel Van Winsen, and Eder Henriqson. “On the rationale of resilience in the domain of safety: A literature review”. In: *Reliability Engineering and System Safety* 141 (2015), pages 131–141. DOI: 10.1016/j.ress.2015.03.008.

- [24] Riccardo Patriarca, Johan Bergström, Giulio Di Gravio, and Francesco Costantino. “Resilience engineering: Current status of the research and future challenges”. In: *Safety Science* 102 (2018), pages 79–100. ISSN: 18791042. DOI: 10.1016/j.ssci.2017.10.005.
- [25] Ann S Masten and Abigail H Gewirtz. “Resilience in development: The importance of early childhood”. In: (2006).
- [26] Patrick Martin-Breen and J Marty Anderies. “Resilience: A literature review”. In: (2011).
- [27] Ann S Masten. “Global perspectives on resilience in children and youth”. In: *Child development* 85.1 (2014), pages 6–20.
- [28] Lois B Murphy and Alice E Moriarty. “Vulnerability, coping and growth from infancy to adolescence.” In: (1976).
- [29] Ludwig von Bertalanffy. *General system theory: Foundations, development, applications*. G. Braziller, 1968.
- [30] Ann S Masten. “Ordinary magic: Resilience processes in development.” In: *American psychologist* 56.3 (2001), page 227.
- [31] Ann S Masten. *Ordinary magic: Resilience in development*. Guilford Publications, 2015.
- [32] Michael Rutter. “Psychosocial resilience and protective mechanisms”. In: *American journal of orthopsychiatry* 57.3 (1987), pages 316–331.
- [33] Charles Richard Snyder and Shane J Lopez. *Handbook of positive psychology*. Oxford university press, 2001.
- [34] Helen Herrman, Donna E Stewart, Natalia Diaz-Granados, Elena L Berger, Beth Jackson, and Tracy Yuen. “What is resilience?” In: *The Canadian Journal of Psychiatry* 56.5 (2011), pages 258–265.
- [35] David Fletcher and Mustafa Sarkar. “Psychological resilience”. In: *European psychologist* (2013).
- [36] Ron Martin. “Regional economic resilience, hysteresis and recessionary shocks”. In: *Journal of economic geography* 12.1 (2012), pages 1–32.
- [37] Charles Perrings. “Resilience and sustainable development”. In: *Environment and Development economics* 11.4 (2006), pages 417–427.
- [38] Marco Modica and Aura Reggiani. “Spatial economic resilience: overview and perspectives”. In: *Networks and Spatial Economics* 15 (2015), pages 211–233.
- [39] William Hynes, Benjamin D Trump, Alan Kirman, Andrew Haldane, and Igor Linkov. “Systemic resilience in economics”. In: *Nature Physics* 18.4 (2022), pages 381–384.
- [40] Marina Alberti, John M Marzluff, Eric Shulenberger, Gordon Bradley, Clare Ryan, and Craig Zumbrunnen. “Integrating humans into ecology: opportunities and challenges for studying urban ecosystems”. In: *BioScience* 53.12 (2003), pages 1169–1179.

- [41] Crawford S Holling. “Understanding the complexity of economic, ecological, and social systems”. In: *Ecosystems* 4 (2001), pages 390–405.
- [42] Ran Bhamra, Samir Dani, and Kevin Burnard. “Resilience: the concept, a literature review and future directions”. In: *International journal of production research* 49.18 (2011), pages 5375–5393.
- [43] Royce Francis and Behailu Bekera. “A metric and frameworks for resilience analysis of engineered and infrastructure systems”. In: *Reliability Engineering and System Safety* 121 (2014), pages 90–103. ISSN: 09518320. DOI: 10.1016/j.ress.2013.07.004. arXiv: arXiv:1011.1669v3.
- [44] Steven M Southwick, George A Bonanno, Ann S Masten, Catherine Panter-Brick, and Rachel Yehuda. “Resilience definitions, theory, and challenges: interdisciplinary perspectives”. In: *European journal of psychotraumatology* 5.1 (2014), page 25338.
- [45] Igor Linkov and José Manuel Palma-Oliveira. *Resilience and Risk*. Springer, Dordrecht, 2017. ISBN: 978-94-024-1122-5. DOI: 10.1007/978-94-024-1123-2. URL: <http://link.springer.com/10.1007/978-94-024-1123-2>.
- [46] Joseph S Mayunga. “Understanding and applying the concept of community disaster resilience: a capital-based approach”. In: *Summer academy for social vulnerability and resilience building* 1.1 (2007), pages 1–16.
- [47] Siambabala Bernard Manyena. “The concept of resilience revisited”. In: *Disasters* 30.4 (2006), pages 434–450.
- [48] Michel Bruneau, Stephanie E. Chang, Ronald T. Eguchi, George C. Lee, Thomas D. O’Rourke, Andrei M. Reinhorn, Masanobu Shinozuka, Kathleen Tierney, et al. “A Framework to Quantitatively Assess and Enhance the Seismic Resilience of Communities”. In: *Earthquake Spectra* 19.4 (2003), pages 733–752. DOI: 10.1193/1.1623497.
- [49] Stephanie E Chang and Masanobu Shinozuka. “Measuring improvements in the disaster resilience of communities”. In: *Earthquake spectra* 20.3 (2004), pages 739–755.
- [50] Sabarethinam Kameshwar, Daniel T Cox, Andre R Barbosa, Karim Farokhnia, Hyounghu Park, Mohammad S Alam, and John W van de Lindt. “Probabilistic decision-support framework for community resilience: Incorporating multi-hazards, infrastructure interdependencies, and resilience goals in a Bayesian network”. In: *Reliability Engineering & System Safety* 191 (2019), page 106568.
- [51] Kathleen Tierney and Michel Bruneau. “Conceptualizing and measuring resilience: A key to disaster loss reduction”. In: *TR news* 250 (2007).
- [52] Reza Faturechi and Elise Miller-Hooks. “Measuring the performance of transportation infrastructure systems in disasters: A comprehensive review”. In: *Journal of infrastructure systems* 21.1 (2015), page 04014025.

- [53] Joseph Fiksel. “Designing Resilient, Sustainable Systems”. In: *Environmental Science and Technology* 37.23 (2003), pages 5330–5339. DOI: 10.1021/es0344819.
- [54] R. G. Little. “Toward more robust infrastructure: Observations on improving the resilience and reliability of critical systems”. In: *Proceedings of the 36th Annual Hawaii International Conference on System Sciences, HICSS 2003* (2003). ISSN: 0769518745. DOI: 10.1109/HICSS.2003.1173880.
- [55] E. Hollnagel, D. E. Woods, and N. Levensen. *Resilience Engineering: Concepts and Precepts*. Aldershot, UK: Ashgate Publishing, 2006.
- [56] Michel Bruneau and Andrei Reinhorn. “Exploring the concept of seismic resilience for acute care facilities”. In: *Earthquake Spectra* 23.1 (2007), pages 41–62. DOI: 10.1193/1.2431396.
- [57] Byeng D. Youn, Chao Hu, and Pingfeng Wang. “Resilience-Driven System Design of Complex Engineered Systems”. In: *Journal of Mechanical Design* 133.10 (2011), page 101011. ISSN: 10500472. DOI: 10.1115/1.4004981.
- [58] Jeryang Park, Thomas P Seager, Palakurth Suresh Chandra Rao, Matteo Convertino, and Igor Linkov. “Integrating risk and resilience approaches to catastrophe management in engineering systems”. In: *Risk analysis* 33.3 (2013), pages 356–367.
- [59] Crawford Stanley Holling. “Engineering resilience versus ecological resilience”. In: *Engineering within ecological constraints* 31.1996 (1996), page 32.
- [60] David D Woods. “Four concepts for resilience and the implications for the future of resilience engineering”. In: *Reliability Engineering & System Safety* 141 (2015), pages 5–9.
- [61] Yaoming Zhou, Junwei Wang, and Hai Yang. “Resilience of transportation systems: concepts and comprehensive review”. In: *IEEE Transactions on Intelligent Transportation Systems* 20.12 (2019), pages 4262–4276.
- [62] Presidential Policy Directive (PPD). *Critical infrastructure security and resilience*. PPD-21. Released Feb. 12, 2013. Accessed Nov. 9, 2018. 2013. URL: <https://obamawhitehouse.archives.gov/the-press-office/2013/02/12/presidential-policy-directive-critical-infrastructure-security-and-resil>.
- [63] National Research Council (NRC). *Disaster Resilience: A National Imperative*. Washington, DC: National Academies Press, 2013.
- [64] ASCE Policy Statement 518. *Unified definitions for critical infrastructure resilience*. Approved Apr. 30, 2021. Accessed Apr. 20, 2023. URL: <https://www.asce.org/advocacy/policy-statements/ps518---unified-definitions-for-critical-infrastructure-resilience>.
- [65] Civil Contingencies Secretariat of the Cabinet Office, London, UK. 2003. Accessed Apr. 20, 2023. URL: www.cabinetoffice.gov.uk.

- [66] Presidential Policy Directive (PPD). *National preparedness*. PPD-8. Released Mar. 30, 2011. Accessed Apr. 20, 2023. 2011. URL: <https://www.dhs.gov/presidential-policy-directive-8-national-preparedness>.
- [67] SW Gilbert. “Disaster resilience: A guide to the literature (NIST Special Publication 1117)”. In: (2010).
- [68] Chris S Renschler, Amy E Frazier, Lucy A Arendt, Gian Paolo Cimellaro, Andrei M Reinhorn, and Michel Bruneau. *A framework for defining and measuring resilience at the community scale: The PEOPLES resilience framework*. MCEER Buffalo, 2010.
- [69] Michael Ungar. “Qualitative contributions to resilience research”. In: *Qualitative social work* 2.1 (2003), pages 85–102.
- [70] Igor Linkov, Daniel A Eisenberg, Kenton Plourde, Thomas P Seager, Julia Allen, and Alex Kott. “Resilience metrics for cyber systems”. In: *Environment Systems and Decisions* 33 (2013), pages 471–476.
- [71] Sophie Sarre, Cara Redlich, Anthea Tinker, Euan Sadler, Ajay Bhalla, and Christopher McKeivitt. “A systematic review of qualitative studies on adjusting after stroke: lessons for the study of resilience”. In: *Disability and rehabilitation* 36.9 (2014), pages 716–726.
- [72] Habibollah Raoufi, Vahid Vahidinasab, and Kamyar Mehran. “Power systems resilience metrics: A comprehensive review of challenges and outlook”. In: *Sustainability* 12.22 (2020), page 9698.
- [73] Wenjuan Sun, Paolo Bocchini, and Brian D Davison. “Resilience metrics and measurement methods for transportation infrastructure: the state of the art”. In: *Sustainable and Resilient Infrastructure* 5.3 (2020), pages 168–199.
- [74] Yao Cheng, Elsayed A Elsayed, and Zhiyi Huang. “Systems resilience assessments: a review, framework and metrics”. In: *International Journal of Production Research* 60.2 (2022), pages 595–622.
- [75] Masanubu Shinozuka, Stepahanie E Chang, Tsen-Chung Cheng, Maria Feng, Thomas D O’Rourke, M Ala Saadeghvaziri, Xuejiang Dong, Xianhe Jin, et al. *Resilience of integrated power and water systems*. Citeseer, 2004.
- [76] Devanandham Henry and Jose Emmanuel Ramirez-Marquez. “Generic metrics and quantitative approaches for system resilience as a function of time”. In: *Reliability Engineering and System Safety* 99 (2012), pages 114–122. ISSN: 0951-8320. DOI: 10.1016/j.res.2011.09.002.
- [77] Hiba Baroud, Kash Barker, Jose E Ramirez-Marquez, et al. “Importance measures for inland waterway network resilience”. In: *Transportation research part E: logistics and transportation review* 62 (2014), pages 55–67.

- [78] Raghav Pant, Kash Barker, Jose Emmanuel Ramirez-Marquez, and Claudio M Rocco. “Stochastic measures of resilience and their application to container terminals”. In: *Computers & Industrial Engineering* 70 (2014), pages 183–194. ISSN: 0360-8352. DOI: 10.1016/j.cie.2014.01.017. URL: <http://dx.doi.org/10.1016/j.cie.2014.01.017>.
- [79] SE Galaitsi, Jeffrey M Keisler, Benjamin D Trump, and Igor Linkov. “The need to reconcile concepts that characterize systems facing threats”. In: *Risk Analysis* 41.1 (2021), pages 3–15.
- [80] Azad M Madni and Scott Jackson. “Towards a conceptual framework for resilience engineering”. In: *IEEE Systems Journal* 3.2 (2009), pages 181–191.
- [81] Leslie Gillespie-Marthaler, Katherine S Nelson, Hiba Baroud, David S Kosson, and Mark Abkowitz. “An integrative approach to conceptualizing sustainable resilience”. In: *Sustainable and Resilient Infrastructure* 4.2 (2019), pages 66–81.
- [82] Salim Moslehi and T Agami Reddy. “Sustainability of integrated energy systems: A performance-based resilience assessment methodology”. In: *Applied energy* 228 (2018), pages 487–498.
- [83] Baoping Cai, Min Xie, Yonghong Liu, Yiliu Liu, and Qiang Feng. “Availability-based engineering resilience metric and its corresponding evaluation methodology”. In: *Reliability Engineering & System Safety* 172 (2018), pages 216–224.
- [84] Rohit Ranjan Singh, Michel Bruneau, Andreas Stavridis, and Kallol Sett. “Resilience deficit index for quantification of resilience”. In: *Resilient Cities and Structures* 1.2 (2022), pages 1–9. ISSN: 2772-7416. DOI: <https://doi.org/10.1016/j.rcns.2022.06.001>.
- [85] Max Didier, Marco Broccardo, Simona Esposito, and Bozidar Stojadinovic. “A compositional demand/supply framework to quantify the resilience of civil infrastructure systems (Re-CoDeS)”. In: *Sustainable and Resilient Infrastructure* 3.2 (2018), pages 86–102.
- [86] Min Ouyang, Leonardo Dueñas-Osorio, and Xing Min. “A three-stage resilience analysis framework for urban infrastructure systems”. In: *Structural Safety* 36-37 (2012), pages 23–31. DOI: 10.1016/j.strusafe.2011.12.004.
- [87] Chloe Johansen, Jennifer Horney, and Iris Tien. “Metrics for evaluating and improving community resilience”. In: *Journal of Infrastructure Systems* 23.2 (2017), page 04016032.
- [88] Mayada Omer, Ali Mostashari, and Udo Lindeman. “Resilience analysis of soft infrastructure systems.” In: *Procedia Computer Science* 28 (2014), pages 873–882. DOI: 10.1016/j.procs.2014.03.104. URL: <http://dx.doi.org/10.1016/j.procs.2014.03.069>.
- [89] Andrew Cox, Fynnwin Prager, and Adam Rose. “Transportation security and the role of resilience: A foundation for operational metrics”. In: *Transport Policy* 18.2 (2011), pages 307–317. DOI: 10.1016/j.tranpol.2010.09.004. URL: <http://dx.doi.org/10.1016/j.tranpol.2010.09.004>.

- [90] Simon Enjalbert, Frédéric Vanderhaegen, Marianne Pichon, Kiswendsida Abel Ouedraogo, and Patrick Millot. “Assessment of transportation system resilience”. In: *Human modelling in assisted transportation: Models, tools and risk methods*. Springer. 2011, pages 335–341.
- [91] Lichun Chen and Elise Miller-Hooks. “Resilience: an indicator of recovery capability in intermodal freight transport”. In: *Transportation Science* 46.1 (2012), pages 109–123.
- [92] Kiswendsida Abel Ouedraogo, Simon Enjalbert, and Frédéric Vanderhaegen. “How to learn from the resilience of Human-Machine Systems?” In: *Engineering Applications of Artificial Intelligence* 26.1 (2013), pages 24–34. ISSN: 09521976. DOI: 10.1016/j.engappa.2012.03.007.
- [93] Qiling Zou and Suren Chen. “Resilience modeling of interdependent traffic-electric power system subject to hurricanes”. In: *Journal of Infrastructure Systems* 26.1 (2020), page 04019034.
- [94] Christopher W. Zobel. “Representing perceived tradeoffs in defining disaster resilience”. In: *Decision Support Systems* 50.2 (2011), pages 394–403. DOI: 10.1016/j.dss.2010.10.001. URL: <http://dx.doi.org/10.1016/j.dss.2010.10.001>.
- [95] Teresa M. Adams, Kaushik R. Bekkem, and Edwin J. Toledo-Durán. “Freight Resilience Measures”. In: *Journal of Transportation Engineering* 138.11 (2012), pages 1403–1409. DOI: 10.1061/(ASCE)TE.1943-5436.0000415. URL: <http://ascelibrary.org/doi/10.1061/%7B%5C%7D28ASCE%7B%5C%7D29TE.1943-5436.0000415>.
- [96] N. Sahebjamnia, S. A. Torabi, and S. A. Mansouri. “Integrated business continuity and disaster recovery planning: Towards organizational resilience”. In: *European Journal of Operational Research* 242.1 (2015), pages 261–273. ISSN: 03772217. DOI: 10.1016/j.ejor.2014.09.055. eprint: 1105.0149. URL: <http://dx.doi.org/10.1016/j.ejor.2014.09.055>.
- [97] Adam Rose. “Economic resilience to natural and man-made disasters: Multidisciplinary origins and contextual dimensions”. In: *Environmental Hazards* 7.4 (2007), pages 383–398.
- [98] Paolo Franchin and Francesco Cavalieri. “Probabilistic assessment of civil infrastructure resilience to earthquakes”. In: *Computer-Aided Civil and Infrastructure Engineering* 30.7 (2015), pages 583–600. DOI: 10.1111/mice.12092.
- [99] Nii O. Attoh-Okine, Adrienne T. Cooper, and Stephen A. Mensah. “Formulation of resilience index of urban infrastructure using belief functions”. In: *IEEE Systems Journal* 3.2 (2009), pages 147–153. DOI: 10.1109/JSYST.2009.2019148.
- [100] Roberto Guidotti, Paolo Gardoni, and Nathanael Rosenheim. “Integration of physical infrastructure and social systems in communities’ reliability and resilience analysis”. In: *Reliability Engineering & System Safety* 185 (2019), pages 476–492.

- [101] Tsuyoshi Hashimoto, Jerry R Stedinger, and Daniel P Loucks. “Reliability, resiliency, and vulnerability criteria for water resource system performance evaluation”. In: *Water resources research* 18.1 (1982), pages 14–20.
- [102] Kash Barker, Jose Emmanuel Ramirez-Marquez, and Claudio M. Rocco. “Resilience-based network component importance measures”. In: *Reliability Engineering and System Safety* 117 (2013), pages 89–97. DOI: 10.1016/j.ress.2013.03.012.
- [103] Zhiguo Zeng, Yi-Ping Fang, Qingqing Zhai, and Shijia Du. “A Markov reward process-based framework for resilience analysis of multistate energy systems under the threat of extreme events”. In: *Reliability Engineering & System Safety* 209 (2021), page 107443.
- [104] Zhaoping Xu, Jose Emmanuel Ramirez-Marquez, Yu Liu, and Tangfan Xiahou. “A new resilience-based component importance measure for multi-state networks”. In: *Reliability Engineering & System Safety* 193 (2020), page 106591.
- [105] Bruce R Ellingwood and Yasuhiro Mori. “Probabilistic methods for condition assessment and life prediction of concrete structures in nuclear power plants”. In: *Nuclear engineering and design* 142.2-3 (1993), pages 155–166.
- [106] Sheng-Hsien Gary Teng and Shin-Yann Michael Ho. “Failure mode and effects analysis: An integrated approach for product design and process control”. In: *International journal of quality & reliability management* 13.5 (1996), pages 8–26. DOI: 10.1108/02656719610118151.
- [107] Diomidis H Stamatis. *Failure mode and effect analysis: FMEA from theory to execution*. 2nd edition. ASQ Quality Press, 2003.
- [108] Mohammad Modarres. *What every engineer should know about reliability and risk analysis*. Volume 30. CRC Press, 1992.
- [109] Marko Čepin and Borut Mavko. “A dynamic fault tree”. In: *Reliability Engineering & System Safety* 75.1 (2002), pages 83–91. DOI: 10.1016/S0951-8320(01)00121-1.
- [110] Hananeh Aliche, Michael Glaß, Felix Reimann, and Jürgen Teich. “Automatic success tree-based reliability analysis for the consideration of transient and permanent faults”. In: *2013 Design, Automation & Test in Europe Conference & Exhibition (DATE)*. IEEE, 2013, pages 1621–1626. DOI: 10.7873/DATE.2013.329.
- [111] Balaram Jakkula, Govinda Raj Mandela, and Murthy Ch SN. “Reliability block diagram (RBD) and fault tree analysis (FTA) approaches for estimation of system reliability and availability—a case study”. In: *International Journal of Quality & Reliability Management* 38.3 (2020), pages 682–703.
- [112] Yu-Shu Hu and Mohammad Modarres. “Evaluating system behavior through dynamic master logic diagram (DMLD) modeling”. In: *Reliability Engineering & System Safety* 64.2 (1999), pages 241–269.

- [113] Elisa Ferrario and Enrico Zio. “Goal Tree Success Tree–Dynamic Master Logic Diagram and Monte Carlo simulation for the safety and resilience assessment of a multistate system of systems”. In: *Engineering Structures* 59 (2014), pages 411–433.
- [114] Edoardo Patelli, Geng Feng, Frank PA Coolen, and Tahani Coolen-Maturi. “Simulation methods for system reliability using the survival signature”. In: *Reliability Engineering & System Safety* 167 (2017), pages 327–337.
- [115] Joanne Bechta Dugan, Salvatore J Bavuso, and Mark A Boyd. “Fault trees and Markov models for reliability analysis of fault-tolerant digital systems”. In: *Reliability Engineering & System Safety* 39.3 (1993), pages 291–307. DOI: 10.1016/0951-8320(93)90005-J.
- [116] Daniel Straub. “Value of information analysis with structural reliability methods”. In: *Structural Safety* 49 (2014), pages 75–85.
- [117] Sankaran Mahadevan, Ruoxue Zhang, and Natasha Smith. “Bayesian networks for system reliability reassessment”. In: *Structural Safety* 23.3 (2001), pages 231–251.
- [118] Ozge Doguc and Jose Emmanuel Ramirez-Marquez. “A generic method for estimating system reliability using Bayesian networks”. In: *Reliability Engineering & System Safety* 94.2 (2009), pages 542–550.
- [119] Michelle Bensi, Armen Der Kiureghian, and Daniel Straub. “Efficient Bayesian network modeling of systems”. In: *Reliability Engineering & System Safety* 112 (2013), pages 200–213.
- [120] Nabil Sadou and Hamid Demmou. “Reliability analysis of discrete event dynamic systems with Petri nets”. In: *Reliability Engineering & System Safety* 94.11 (2009), pages 1848–1861. DOI: 10.1016/j.ress.2009.06.006.
- [121] Sohag Kabir and Yiannis Papadopoulos. “Applications of Bayesian networks and Petri nets in safety, reliability, and risk assessments: A review”. In: *Safety science* 115 (2019), pages 154–175.
- [122] Jinhua Mi, Yan-Feng Li, Weiwen Peng, and Hong-Zhong Huang. “Reliability analysis of complex multi-state system with common cause failure based on evidential networks”. In: *Reliability Engineering & System Safety* 174 (2018), pages 71–81.
- [123] Ping-Chen Chang, Yi-Kuei Lin, and Yu-Min Chiang. “System reliability estimation and sensitivity analysis for multi-state manufacturing network with joint buffers—A simulation approach”. In: *Reliability Engineering & System Safety* 188 (2019), pages 103–109.
- [124] Yan-Feng Li, Hong-Zhong Huang, Jinhua Mi, Weiwen Peng, and Xiaomeng Han. “Reliability analysis of multi-state systems with common cause failures based on Bayesian network and fuzzy probability”. In: *Annals of Operations Research* (2022), pages 1–15.
- [125] Jian Guo, Zhaojun Steven Li, and Jionghua Judy Jin. “System reliability assessment with multilevel information using the Bayesian melding method”. In: *Reliability Engineering & System Safety* 170 (2018), pages 146–158.

- [126] Xufeng Yang, Yongshou Liu, Caiying Mi, and Chenghu Tang. “System reliability analysis through active learning Kriging model with truncated candidate region”. In: *Reliability Engineering & System Safety* 169 (2018), pages 235–241.
- [127] Mi Xiao, Jinhao Zhang, and Liang Gao. “A system active learning Kriging method for system reliability-based design optimization with a multiple response model”. In: *Reliability Engineering & System Safety* 199 (2020), page 106935.
- [128] Ning-Cong Xiao, Kai Yuan, and Hongyou Zhan. “System reliability analysis based on dependent Kriging predictions and parallel learning strategy”. In: *Reliability Engineering & System Safety* 218 (2022), page 108083.
- [129] Xiang-Yu Li, Hong-Zhong Huang, and Yan-Feng Li. “Reliability analysis of phased mission system with non-exponential and partially repairable components”. In: *Reliability Engineering & System Safety* 175 (2018), pages 119–127.
- [130] Chunling Luo, Lijuan Shen, and Ancha Xu. “Modelling and estimation of system reliability under dynamic operating environments and lifetime ordering constraints”. In: *Reliability Engineering & System Safety* 218 (2022), page 108136.
- [131] Mohamed Arezki Mellal and Enrico Zio. “System reliability-redundancy optimization with cold-standby strategy by an enhanced nest cuckoo optimization algorithm”. In: *Reliability Engineering & System Safety* 201 (2020), page 106973.
- [132] Enrico Zio. “Reliability engineering: Old problems and new challenges”. In: *Reliability engineering & system safety* 94.2 (2009), pages 125–141. DOI: 10.1016/j.ress.2008.06.002.
- [133] Ajit Kumar Verma, Srividya Ajit, Durga Rao Karanki, et al. *Reliability and Safety Engineering*. Volume 43. Springer, 2010. DOI: 10.1007/978-1-84996-232-2.
- [134] Patrick O’Connor and Andre Kleyner. *Practical reliability engineering*. John Wiley & Sons, 2012.
- [135] Claudia Klüppelberg, Daniel Straub, and Isabell M Welpel. *Risk-A multidisciplinary introduction*. Springer, 2014.
- [136] Mohammad Modarres, Mark P Kaminskiy, and Vasiliy Krivtsov. *Reliability engineering and risk analysis: a practical guide*. CRC press, 2016.
- [137] David W Coit and Enrico Zio. “The evolution of system reliability optimization”. In: *Reliability Engineering & System Safety* 192 (2019), page 106259.
- [138] Junho Song and Won-Hee Kang. “System reliability and sensitivity under statistical dependence by matrix-based system reliability method”. In: *Structural Safety* 31.2 (2009), pages 148–156.

- [139] S Eryilmaz. “Review of recent advances in reliability of consecutive k-out-of-n and related systems”. In: *Proceedings of the Institution of Mechanical Engineers, Part O: Journal of Risk and Reliability* 224.3 (2010), pages 225–237.
- [140] Gregory Levitin, Liudong Xing, Hanoch Ben-Haim, and Yuanshun Dai. “Multi-state systems with selective propagated failures and imperfect individual and group protections”. In: *Reliability Engineering & System Safety* 96.12 (2011), pages 1657–1666. DOI: 10.1016/j.ress.2011.08.002.
- [141] Hindolo George-Williams and Edoardo Patelli. “A hybrid load flow and event driven simulation approach to multi-state system reliability evaluation”. In: *Reliability Engineering & System Safety* 152 (2016), pages 351–367.
- [142] Elena Zaitseva and Vitaly Levashenko. “Construction of a reliability structure function based on uncertain data”. In: *IEEE Transactions on Reliability* 65.4 (2016), pages 1710–1723. DOI: 10.1109/TR.2016.2578948.
- [143] Kai Yuan, Ning-Cong Xiao, Zhonglai Wang, and Kun Shang. “System reliability analysis by combining structure function and active learning kriging model”. In: *Reliability Engineering & System Safety* 195 (2020), page 106734.
- [144] Philip J Boland and Francisco J Samaniego. “The signature of a coherent system and its applications in reliability”. In: *Mathematical Reliability: An Expository Perspective*. Springer, 2004, pages 3–30. DOI: 10.1007/978-1-4419-9021-1_1.
- [145] Frank PA Coolen, Tahani Coolen-Maturi, Louis JM Aslett, and Gero Walter. “Imprecise system reliability using the survival signature”. In: *ICAMER’16 : Proceedings of the 1st International Conference on Applied Mathematics in Engineering and Reliability* (2016), pages 207–214.
- [146] Enrico Zio, Piero Baraldi, and Edoardo Patelli. “Assessment of the availability of an offshore installation by Monte Carlo simulation”. In: *International Journal of Pressure Vessels and Piping* 83.4 (2006), pages 312–320.
- [147] Alessandro Birolini. *Reliability engineering*. Volume 5. Springer, 2007.
- [148] Francisco J Samaniego. *System Signatures and their Applications in Engineering Reliability*. Volume 110. Springer Science & Business Media, 2007. DOI: 10.1007/978-0-387-71797-5.
- [149] Frank PA Coolen and Tahani Coolen-Maturi. “Generalizing the signature to systems with multiple types of components”. In: *Complex Systems and Dependability*. Springer, 2013, pages 115–130. DOI: 10.1007/978-3-642-30662-4_8.
- [150] Yao Li, Frank PA Coolen, Caichao Zhu, and Jianjun Tan. “Reliability assessment of the hydraulic system of wind turbines based on load-sharing using survival signature”. In: *Renewable Energy* 153 (2020), pages 766–776. DOI: 10.1016/j.renene.2020.02.017.

- [151] Frank PA Coolen and Tahani Coolen-Maturi. “The survival signature for quantifying system reliability: an introductory overview from practical perspective”. In: *Reliability Engineering and Computational Intelligence* (2021), pages 23–37.
- [152] Julian Salomon, Niklas Winnewisser, Pengfei Wei, Matteo Broggi, and Michael Beer. “Efficient reliability analysis of complex systems in consideration of imprecision”. In: *Reliability Engineering & System Safety* 216 (2021), page 107972.
- [153] Frank PA Coolen and Tahani Coolen-Maturi. “The structure function for system reliability as predictive (imprecise) probability”. In: *Reliability Engineering & System Safety* 154 (2016), pages 180–187. DOI: 10.1016/j.ress.2016.06.008.
- [154] Geng Feng, Edoardo Patelli, Michael Beer, and Frank PA Coolen. “Imprecise system reliability and component importance based on survival signature”. In: *Reliability Engineering & System Safety* 150 (2016), pages 116–125. DOI: 10.1016/j.ress.2016.01.019.
- [155] Jasper Behrens Dorf, Tobias-Emanuel Regenhardt, Matteo Broggi, and Michael Beer. “Numerically efficient computation of the survival signature for the reliability analysis of large networks”. In: *Reliability Engineering & System Safety* 216 (2021), page 107935.
- [156] Sean Reed. “An efficient algorithm for exact computation of system and survival signatures using binary decision diagrams”. In: *Reliability Engineering & System Safety* 165 (2017), pages 257–267.
- [157] Frank PA Coolen, Tahani Coolen-Maturi, and Abdullah H Al-Nefaiee. “Nonparametric predictive inference for system reliability using the survival signature”. In: *Proceedings of the Institution of Mechanical Engineers, Part O: Journal of Risk and Reliability* 228.5 (2014), pages 437–448.
- [158] Hindolo George-Williams, Geng Feng, Frank PA Coolen, Michael Beer, and Edoardo Patelli. “Extending the survival signature paradigm to complex systems with non-repairable dependent failures”. In: *Proceedings of the Institution of Mechanical Engineers, part O: journal of risk and reliability* 233.4 (2019), pages 505–519.
- [159] G Feng, H George-Williams, E Patelli, FPA Coolen, and M Beer. “An efficient reliability analysis on complex non-repairable systems with common-cause failures”. In: *Safety and Reliability—Safe Societies in a Changing World*. CRC Press, 2018, pages 2531–2537.
- [160] Jasper Behrens Dorf, Matteo Broggi, and Michael Beer. “Reliability analysis of networks interconnected with copulas”. In: *ASCE-ASME Journal of Risk and Uncertainty in Engineering Systems, Part B: Mechanical Engineering* 5.4 (2019), pages 041006-1 –041006-9. DOI: 10.1115/1.4044043.
- [161] Tahani Coolen-Maturi, Frank PA Coolen, and Narayanaswamy Balakrishnan. “The joint survival signature of coherent systems with shared components”. In: *Reliability Engineering & System Safety* 207 (2021), page 107350.

- [162] Xianzhen Huang, Sujun Jin, Xuefeng He, and David He. “Reliability analysis of coherent systems subject to internal failures and external shocks”. In: *Reliability Engineering & System Safety* 181 (2019), pages 75–83.
- [163] Patrik Rusnak, Elena Zaitseva, Frank PA Coolen, Miroslav Kvassay, and Vitaly Levashenko. “Logic differential calculus for reliability analysis based on survival signature”. In: *IEEE Transactions on Dependable and Secure Computing* 20.2 (2022), pages 1529–1540.
- [164] Xianzhen Huang, Frank PA Coolen, and Tahani Coolen-Maturi. “A heuristic survival signature based approach for reliability-redundancy allocation”. In: *Reliability Engineering & System Safety* 185 (2019), pages 511–517.
- [165] Jinlei Qin and Frank PA Coolen. “Survival signature for reliability evaluation of a multi-state system with multi-state components”. In: *Reliability Engineering & System Safety* 218 (2022), page 108129.
- [166] Niklas R Winnewisser, Julian Salomon, Matteo Broggi, and Michael Beer. “The concept of diagonal approximated signature: new surrogate modeling approach for continuous-state systems in the context of resilience optimization”. In: *Disaster Prevention and Resilience* 2.2 (2023), page 4.
- [167] José M Bernardo. “The concept of exchangeability and its applications”. In: *Far East Journal of Mathematical Sciences* 4 (1996), pages 111–122.
- [168] Jason Matthew Aughenbaugh and Christiaan J. J. Paredis. “The Value of Using Imprecise Probabilities in Engineering Design”. In: *Journal of Mechanical Design* 128.4 (2005), pages 969–979. DOI: 10.1115/1.2204976.
- [169] Armen Der Kiureghian and Ove Ditlevsen. “Aleatory or epistemic? Does it matter?” In: *Structural Safety* 31.2 (2009), pages 105–112. DOI: 10.1016/j.strusafe.2008.06.020.
- [170] Scott Ferson, Cliff A Joslyn, Jon C Helton, William L Oberkampf, and Kari Sentz. “Summary from the epistemic uncertainty workshop: consensus amid diversity”. In: *Reliability Engineering & System Safety* 85.1-3 (2004), pages 355–369. DOI: 10.1016/j.ress.2004.03.023.
- [171] Jon C Helton and William L Oberkampf. “Alternative representations of epistemic uncertainty”. In: *Reliability Engineering & System Safety* 85.1-3 (2004), pages 1–10. DOI: 10.1016/j.ress.2004.03.001.
- [172] Efstratios Nikolaidis. “Types of uncertainty in design decision making”. In: *Engineering Design Reliability Handbook*. Edited by Dan M. Ghiocel Efstratios Nikolaidis and Suren Singhal. CRC Press, 2004. Chapter 2, pages 137–156. DOI: 10.1201/9780203483930.
- [173] Scott Ferson and Lev R Ginzburg. “Different methods are needed to propagate ignorance and variability”. In: *Reliability Engineering & System Safety* 54.2-3 (1996), pages 133–144. DOI: 10.1016/S0951-8320(96)00071-3.

- [174] William L Oberkampf, Jon C Helton, Cliff A Joslyn, Steven F Wojtkiewicz, and Scott Ferson. “Challenge problems: uncertainty in system response given uncertain parameters”. In: *Reliability Engineering & System Safety* 85.1-3 (2004), pages 11–19. DOI: 10.1016/j.res.2004.03.002.
- [175] Eduard Hofer. “When to separate uncertainties and when not to separate”. In: *Reliability Engineering & System Safety* 54.2-3 (1996), pages 113–118. DOI: 10.1016/S0951-8320(96)00068-3.
- [176] Piero Baraldi and Enrico Zio. “A combined Monte Carlo and possibilistic approach to uncertainty propagation in event tree analysis”. In: *Risk Analysis: An International Journal* 28.5 (2008), pages 1309–1326. DOI: 10.1111/j.1539-6924.2008.01085.x.
- [177] Christopher J Roy and William L Oberkampf. “A comprehensive framework for verification, validation, and uncertainty quantification in scientific computing”. In: *Computer Methods in Applied Mechanics and Engineering* 200.25-28 (2011), pages 2131–2144. DOI: 10.1016/j.cma.2011.03.016.
- [178] Ali Azadeh, N Atrchin, Vahid Salehi, and Hasan Shojaei. “Modelling and improvement of supply chain with imprecise transportation delays and resilience factors”. In: *International Journal of Logistics Research and Applications* 17.4 (2014), pages 269–282.
- [179] Roberto Rocchetta, Enrico Zio, and Edoardo Patelli. “A power-flow emulator approach for resilience assessment of repairable power grids subject to weather-induced failures and data deficiency”. In: *Applied energy* 210 (2018), pages 339–350.
- [180] Gianluca Filippi, Massimiliano Vasile, Daniel Krpelik, Peter Zeno Korondi, Mariapia Marchi, and Carlo Poloni. “Space systems resilience optimisation under epistemic uncertainty”. In: *Acta Astronautica* 165 (2019), pages 195–210.
- [181] Mohamed Sallak, Walter Schön, and Felipe Aguirre. “Reliability assessment for multi-state systems under uncertainties based on the Dempster–Shafer theory”. In: *IIE Transactions* 45.9 (2013), pages 995–1007.
- [182] Roberto Rocchetta, Matteo Broggi, and Edoardo Patelli. “Do we have enough data? Robust reliability via uncertainty quantification”. In: *Applied Mathematical Modelling* 54 (2018), pages 710–721. DOI: 10.1016/j.apm.2017.10.020.
- [183] Bingyi Kang, Pengdan Zhang, Zhenyu Gao, Gyan Chhipi-Shrestha, Kasun Hewage, and Rehan Sadiq. “Environmental assessment under uncertainty using Dempster–Shafer theory and Z-numbers”. In: *Journal of Ambient Intelligence and Humanized Computing* 11 (2020), pages 2041–2060.
- [184] Tosin Adedipe, Mahmood Shafiee, and Enrico Zio. “Bayesian network modelling for the wind energy industry: An overview”. In: *Reliability Engineering & System Safety* 202 (2020), page 107053.

- [185] Jinhua Mi, Yan-Feng Li, Michael Beer, Matteo Broggi, and Yuhua Cheng. “Importance measure of probabilistic common cause failures under system hybrid uncertainty based on bayesian network”. In: *Eksploatacja i Niezawodność* 22.1 (2020).
- [186] Yakov Ben-Haim. “Uncertainty, probability and information-gaps”. In: *Reliability Engineering & System Safety* 85.1 (2004), pages 249–266. DOI: 10.1016/j.ress.2004.03.015.
- [187] Durga Rao Karanki, Hari Shankar Kushwaha, Ajit Kumar Verma, and Srividya Ajit. “Uncertainty analysis based on probability bounds (p-box) approach in probabilistic safety assessment”. In: *Risk Analysis: An International Journal* 29.5 (2009), pages 662–675.
- [188] Christophe Simon and Frédérique Bicking. “Hybrid computation of uncertainty in reliability analysis with p-box and evidential networks”. In: *Reliability Engineering & System Safety* 167 (2017), pages 629–638. DOI: 10.1016/j.ress.2017.04.015.
- [189] Matthias GR Faes, Marco Daub, Stefano Marelli, Edoardo Patelli, and Michael Beer. “Engineering analysis with probability boxes: a review on computational methods”. In: *Structural Safety* 93 (2021), page 102092.
- [190] Sohag Kabir and Yiannis Papadopoulos. “A review of applications of fuzzy sets to safety and reliability engineering”. In: *International Journal of Approximate Reasoning* 100 (2018), pages 29–55. DOI: 10.1016/j.ijar.2018.05.005.
- [191] Marzio Marseguerra, Enrico Zio, Luca Podofillini, and David W Coit. “Optimal design of reliable network systems in presence of uncertainty”. In: *IEEE Transactions on Reliability* 54.2 (2005), pages 243–253.
- [192] Terje Aven and Enrico Zio. “Some considerations on the treatment of uncertainties in risk assessment for practical decision making”. In: *Reliability Engineering & System Safety* 96.1 (2011), pages 64–74.
- [193] Terje Aven, Enrico Zio, Piero Baraldi, and Roger Flage. *Uncertainty in risk assessment: the representation and treatment of uncertainties by probabilistic and non-probabilistic methods*. John Wiley & Sons, 2013.
- [194] Michael Beer, Scott Ferson, and Vladik Kreinovich. “Imprecise probabilities in engineering analyses”. In: *Mechanical Systems and Signal Processing* 37.1-2 (2013), pages 4–29. DOI: 10.1016/j.ymssp.2013.01.024.
- [195] Thomas Augustin, Frank PA Coolen, Gert De Cooman, and Matthias CM Troffaes. *Introduction to imprecise probabilities*. John Wiley & Sons, 2014.
- [196] Roger Flage, Terje Aven, Enrico Zio, and Piero Baraldi. “Concerns, challenges, and directions of development for the issue of representing uncertainty in risk assessment”. In: *Risk analysis* 34.7 (2014), pages 1196–1207.
- [197] Morteza Aien, Ali Hajebrahimi, and Mahmud Fotuhi-Firuzabad. “A comprehensive review on uncertainty modeling techniques in power system studies”. In: *Renewable and Sustainable Energy Reviews* 57 (2016), pages 1077–1089.

- [198] Rui Kang, Qingyuan Zhang, Zhiguo Zeng, Enrico Zio, and Xiaoyang Li. “Measuring reliability under epistemic uncertainty: Review on non-probabilistic reliability metrics”. In: *Chinese Journal of Aeronautics* 29.3 (2016), pages 571–579.
- [199] Ali Ehsan and Qiang Yang. “State-of-the-art techniques for modelling of uncertainties in active distribution network planning: A review”. In: *Applied energy* 239 (2019), pages 1509–1523.
- [200] Geng Feng. “Survival Signature-based Reliability Approach for Complex Systems Susceptible to Common Cause Failures”. In: *International Journal of Reliability, Quality and Safety Engineering* 26.03 (2019), page 1950013.
- [201] Guodong Yang, Xianzhen Huang, Yuxiong Li, and Pengfei Ding. “System reliability assessment with imprecise probabilities”. In: *Applied Sciences* 9.24 (2019), page 5422.
- [202] Jinhua Mi, Michael Beer, Yan-Feng Li, Matteo Broggi, and Yuhua Cheng. “Reliability and importance analysis of uncertain system with common cause failures based on survival signature”. In: *Reliability Engineering & System Safety* 201 (2020), page 106988.
- [203] Eduard Hofer, Martina Kloos, Bernard Krzykacz-Hausmann, Jörg Peschke, and Martin Wolterreck. “An approximate epistemic uncertainty analysis approach in the presence of epistemic and aleatory uncertainties”. In: *Reliability Engineering & System Safety* 77.3 (2002), pages 229–238. DOI: 10.1016/S0951-8320(02)00056-X.
- [204] Diego A. Alvarez. “On the calculation of the bounds of probability of events using infinite random sets”. In: *International Journal of Approximate Reasoning* 43.3 (2006), pages 241–267. DOI: <https://doi.org/10.1016/j.ijar.2006.04.005>.
- [205] Saideep Nannapaneni and Sankaran Mahadevan. “Reliability analysis under epistemic uncertainty”. In: *Reliability Engineering & System Safety* 155 (2016), pages 9–20.
- [206] Matthias GR Faes, Marcos A Valdebenito, David Moens, and Michael Beer. “Operator norm theory as an efficient tool to propagate hybrid uncertainties and calculate imprecise probabilities”. In: *Mechanical Systems and Signal Processing* 152 (2021), page 107482.
- [207] Hao Zhang, Robert L Mullen, and Rafi L Muhanna. “Interval Monte Carlo methods for structural reliability”. In: *Structural Safety* 32.3 (2010), pages 183–190. DOI: 10.1016/j.strusafe.2010.01.001.
- [208] Hao Zhang. “Interval importance sampling method for finite element-based structural reliability assessment under parameter uncertainties”. In: *Structural Safety* 38 (2012), pages 1–10. DOI: 10.1016/j.strusafe.2012.01.003.
- [209] Zachary del Rosario, Richard W Fenrich, and Gianluca Iaccarino. “Cutting the double loop: Theory and algorithms for reliability-based design optimization with parametric uncertainty”. In: *International Journal for Numerical Methods in Engineering* 118.12 (2019), pages 718–740.

- [210] M.S. Eldred, L.P. Swiler, and G. Tang. “Mixed aleatory-epistemic uncertainty quantification with stochastic expansions and optimization-based interval estimation”. In: *Reliability Engineering & System Safety* 96.9 (2011), pages 1092–1113. DOI: 10.1016/j.ress.2010.11.010.
- [211] Xiaoping Du. “Saddlepoint approximation for sequential optimization and reliability analysis”. In: *Journal of Mechanical Design* 130.1 (2008).
- [212] Jinghong Liang, Zissimos P Mourelatos, and Efstratios Nikolaidis. “A single-loop approach for system reliability-based design optimization”. In: *Journal of Mechanical Design* 129.12 (2007), pages 1215–1224.
- [213] Zhen Hu and Sankaran Mahadevan. “A single-loop kriging surrogate modeling for time-dependent reliability analysis”. In: *Journal of Mechanical Design* 138.6 (2016).
- [214] Johannes O Royset, Armen Der Kiureghian, and Elijah Polak. “Reliability-based optimal structural design by the decoupling approach”. In: *Reliability Engineering & System Safety* 73.3 (2001), pages 213–221.
- [215] Harish Agarwal and John E Renaud. “New decoupled framework for reliability-based design optimization”. In: *AIAA journal* 44.7 (2006), pages 1524–1531.
- [216] Yiming Liu, Yimin Shi, Xuchao Bai, and Bin Liu. “Stress–strength reliability analysis of multi-state system based on generalized survival signature”. In: *Journal of Computational and Applied Mathematics* 342 (2018), pages 274–291.
- [217] Xiukai Yuan, Matthias G.R. Faes, Shaolong Liu, Marcos A. Valdebenito, and Michael Beer. “Efficient imprecise reliability analysis using the Augmented Space Integral”. In: *Reliability Engineering & System Safety* 210 (2021), page 107477. DOI: 10.1016/j.ress.2021.107477.
- [218] Roberto Rocchetta and Edoardo Patelli. “A post-contingency power flow emulator for generalized probabilistic risks assessment of power grids”. In: *Reliability Engineering & System Safety* 197 (2020), page 106817. DOI: 10.1016/j.ress.2020.106817.
- [219] Mingyang Li and Zequn Wang. “Surrogate model uncertainty quantification for reliability-based design optimization”. In: *Reliability Engineering & System Safety* 192 (2019), page 106432.
- [220] Pengfei Wei, Jingwen Song, Sifeng Bi, Matteo Broggi, Michael Beer, Zhenzhou Lu, and Zhufeng Yue. “Non-intrusive stochastic analysis with parameterized imprecise probability models: I. Performance estimation”. In: *Mechanical Systems and Signal Processing* 124 (2019), pages 349–368. DOI: 10.1016/j.ymsp.2019.01.058.
- [221] Seamus Bradley. “Imprecise probabilities”. In: *Computer Simulation Validation*. Springer, 2019, pages 525–540. DOI: 10.1007/978-3-319-70766-2_21.
- [222] William L Oberkampf and Christopher J Roy. *Verification and Validation in Scientific Computing*. Cambridge University Press, 2010. DOI: 10.1017/CB09780511760396.

- [223] Bernd Möller and Michael Beer. “Engineering computation under uncertainty – Capabilities of non-traditional models”. In: *Computers & Structures* 86.10 (2008), pages 1024–1041. DOI: 10.1016/j.compstruc.2007.05.041.
- [224] Bernd Möller, Wolfgang Graf, Michael Beer, and Jan-Uwe Sickert. “Fuzzy probabilistic method and its application for the safety assessment of structures”. In: *Proceedings of the European Conference on Computational Mechanics*. 2001.
- [225] James J Buckley. *Fuzzy Probabilities: New Approach and Applications*. Volume 115. Studies in Fuzziness and Soft Computing. Springer, 2005. DOI: 10.1007/3-540-32388-0.
- [226] Michael Beer. “Fuzzy Probability Theory”. In: *Encyclopedia of Complexity and Systems Science*. Edited by Robert A. Meyers. New York, NY: Springer New York, 2009, pages 4047–4059. ISBN: 978-0-387-30440-3. DOI: 10.1007/978-0-387-30440-3_237. URL: https://doi.org/10.1007/978-0-387-30440-3_237.
- [227] M Beer and S Ferson. “Fuzzy probability in engineering analyses”. In: *Vulnerability, Uncertainty, and Risk: Analysis, Modeling, and Management*. Edited by Bilal M Ayyub. American Society of Civil Engineers, 2012, pages 53–61. DOI: 10.1061/41170(400)7.
- [228] Xing Liu, Yi-Ping Fang, and Enrico Zio. “A hierarchical resilience enhancement framework for interdependent critical infrastructures”. In: *Reliability Engineering & System Safety* 215 (2021), page 107868.
- [229] David L Alderson, Gerald G Brown, and W Matthew Carlyle. “Operational models of infrastructure resilience”. In: *Risk Analysis* 35.4 (2015), pages 562–586.
- [230] Yiping Fang, Nicola Pedroni, and Enrico Zio. “Optimization of cascade-resilient electrical infrastructures and its validation by power flow modeling”. In: *Risk Analysis* 35.4 (2015), pages 594–607.
- [231] Min Ouyang and Yiping Fang. “A mathematical framework to optimize critical infrastructure resilience against intentional attacks”. In: *Computer-Aided Civil and Infrastructure Engineering* 32.11 (2017), pages 909–929.
- [232] Yasser Almoghathawi, Kash Barker, and Laura A Albert. “Resilience-driven restoration model for interdependent infrastructure networks”. In: *Reliability Engineering & System Safety* 185 (2019), pages 12–23.
- [233] Yi-Ping Fang and Giovanni Sansavini. “Optimum post-disruption restoration under uncertainty for enhancing critical infrastructure resilience”. In: *Reliability Engineering & System Safety* 185 (2019), pages 1–11.
- [234] Neetesh Sharma, Armin Tabandeh, and Paolo Gardoni. “Regional resilience analysis: A multiscale approach to optimize the resilience of interdependent infrastructure”. In: *Computer-Aided Civil and Infrastructure Engineering* 35.12 (2020), pages 1315–1330.

- [235] Amine Belhadi, Sachin Kamble, Samuel Fosso Wamba, and Maciel M Queiroz. “Building supply-chain resilience: an artificial intelligence-based technique and decision-making framework”. In: *International Journal of Production Research* 60.14 (2022), pages 4487–4507.
- [236] Yi-Ping Fang and Enrico Zio. “An adaptive robust framework for the optimization of the resilience of interdependent infrastructures under natural hazards”. In: *European Journal of Operational Research* 276.3 (2019), pages 1119–1136.
- [237] Nii O Attoh-Okine. *Resilience engineering: Models and analysis*. Cambridge University Press, 2016.
- [238] Sabrina Larkin, Cate Fox-Lent, Daniel A Eisenberg, Benjamin D Trump, Sean Wallace, Colin Chadderton, and Igor Linkov. “Benchmarking agency and organizational practices in resilience decision making”. In: *Environment Systems and Decisions* 35 (2015), pages 185–195.
- [239] Geoff A Wilson. “Community resilience, globalization, and transitional pathways of decision-making”. In: *Geoforum* 43.6 (2012), pages 1218–1231.
- [240] Stanley Gilbert and Bilal M. Ayyub. “Models for the Economics of Resilience”. In: *ASCE-ASME Journal of Risk and Uncertainty in Engineering Systems, Part A: Civil Engineering* 2 (2016). ISSN: 2376-7642.
- [241] Raghav Pant, Kash Barker, and Christopher W Zobel. “Static and dynamic metrics of economic resilience for interdependent infrastructure and industry sectors”. In: *Reliability Engineering & System Safety* 125 (2014), pages 92–102.
- [242] Maria Koliou, John W van de Lindt, Therese P McAllister, Bruce R Ellingwood, Maria Dillard, and Harvey Cutler. “State of the research in community resilience: Progress and challenges”. In: *Sustainable and resilient infrastructure* 5.3 (2020), pages 131–151.
- [243] Huy T. Tran, Michael Balchanos, Jean Charles Domercant, and Dimitri N. Mavris. “A framework for the quantitative assessment of performance-based system resilience”. In: *Reliability Engineering & System Safety* 158 (2017), pages 73–84. DOI: 10.1016/j.ress.2016.10.014.
- [244] Yiping Fang and Giovanni Sansavini. “Optimizing power system investments and resilience against attacks”. In: *Reliability Engineering and System Safety* 159 (2017), pages 161–173. ISSN: 09518320. DOI: 10.1016/j.ress.2016.10.028. URL: <http://dx.doi.org/10.1016/j.ress.2016.10.028>.
- [245] Zachary Feinstein, Birgit Rudloff, and Stefan Weber. “Measures of Systemic Risk”. In: *SIAM Journal on Financial Mathematics* 8.1 (2017), pages 672–708. ISSN: 1945-497X.
- [246] J. W. Wang, F. Gao, and W. H. Ip. “Measurement of resilience and its application to enterprise information systems”. In: *Enterprise Information Systems* 4.2 (2010), pages 215–223. DOI: 10.1080/17517571003754561.

- [247] Stefan Weber and Kerstin Weske. “The joint impact of bankruptcy costs, fire sales and cross-holdings on systemic risk in financial networks”. In: *Probability, Uncertainty and Quantitative Risk* 2.1 (2017). ISSN: 2367-0126. DOI: 10.1186/s41546-017-0020-9. URL: <https://doi.org/10.1186/s41546-017-0020-9>.
- [248] Alex Cassidy, Zachary Feinstein, and Arye Nehorai. “Risk measures for power failures in transmission systems”. In: *Chaos: An Interdisciplinary Journal of Nonlinear Science* 26.113110 (2016).
- [249] Hans Föllmer and Stefan Weber. “The Axiomatic Approach to Risk Measures for Capital Determination”. In: *Annual Review of Financial Economics* 7.1 (2015), pages 301–337. ISSN: 1941-1375. DOI: 10.1146/annurev-financial-111914-042031. eprint: <https://doi.org/10.1146/annurev-financial-111914-042031>. URL: <https://doi.org/10.1146/annurev-financial-111914-042031>.
- [250] Konstantin M. Zuev, Stephen Wu, and James L. Beck. “General network reliability problem and its efficient solution by Subset Simulation”. In: *Probabilistic Engineering Mechanics* 40 (2015), pages 25–35. ISSN: 02668920. DOI: 10.1016/j.probengmech.2015.02.002. URL: <http://dx.doi.org/10.1016/j.probengmech.2015.02.002>.
- [251] S. Miro, T. Willeke, M. Broggi, J.R. Seume, and M. Beer. “Reliability Analysis of an Axial Compressor Based on One-Dimensional Flow Modeling and Survival Signature”. In: *ASCE-ASME Journal of Risk and Uncertainty in Engineering Systems, Part B: Mechanical Engineering* 5 (2019), pages 031003-1–031003-9.
- [252] M. Braun and J.R. Seume. “Forward Sweep in a Four-Stage High-Speed Axial Compressor”. In: *ASME Turbo Expo 2006: Power for Land, Sea, and Air* Volume 6: Turbomachinery, Parts A and B (2006), pages 141–152.
- [253] Bernd Hellmich and Joerg Seume. “Causes of Acoustic Resonance in a High-Speed Axial Compressor”. In: *ASME. J. Turbomach.* 130.3 (2008), pages 031003–031003-9. ISSN: 0889504X. DOI: 10.1115/GT2006-90947.
- [254] Jan Siemann, Ingolf Krenz, and J.R. Seume. “Experimental Investigation of Aspiration in a Multi-Stage High-Speed Axial-Compressor”. In: *ASME. Turbo Expo: Power for Land, Sea, and Air* Volume 2A: Turbomachinery (2016).
- [255] S. Farokhi. *Aircraft Propulsion*. Aircraft propulsion Bd. 10. Wiley, 2009. ISBN: 9780470039069.
- [256] Adamantios Mettas. “Reliability allocation and optimization for complex systems”. In: *Reliability and Maintainability Symposium, 2000. Proceedings. Annual* (2000), pages 216–221. ISSN: 0149-144X. DOI: 10.1109/RAMS.2000.816310.
- [257] Berliner Verkehrsbetriebe. *Lagebericht und Jahresabschluss 2017*. (accessed Oct. 5, 2018). 2018. URL: <http://unternehmen.bvg.de/index.php?section=downloads%7B%5C%7Ddownload=3128>.

- [258] S-Bahn Berlin. <https://sbahn.berlin/das-unternehmen/unternehmensprofil/s-bahn-berlin-auf-einen-blick/>, (accessed Oct. 5, 2018). 2018. URL: <https://sbahn.berlin/das-unternehmen/unternehmensprofil/s-bahn-berlin-auf-einen-blick/>.
- [259] Jianhua Zhang, Mingwei Zhao, Haikuan Liu, and Xiaoming Xu. “Networked characteristics of the urban rail transit networks”. In: *Physica A: Statistical Mechanics and its Applications* 392.6 (2013), pages 1538–1546. DOI: 10.1016/j.physa.2012.11.036. URL: <http://dx.doi.org/10.1016/j.physa.2012.11.036>.
- [260] Dong-Ming Zhang, Fei Du, Hongwei Huang, Fan Zhang, Bilal M. Ayyub, and Michael Beer. “Resiliency assessment of urban rail transit networks: Shanghai metro as an example”. In: *Safety Science* 106 (2018), pages 230–243. ISSN: 18791042. DOI: 10.1016/j.ssci.2018.03.023. URL: <https://doi.org/10.1016/j.ssci.2018.03.023>.
- [261] Vito Latora and Massimo Marchiori. “Efficient behavior of small-world networks”. In: *Physical Review Letters* 87.19 (2001), pages 198701–1–198701–4. DOI: 10.1103/PhysRevLett.87.198701. arXiv: 0101396 [cond-mat].
- [262] F. B. Zhan and C. E. Noon. “Shortest Path Algorithms: An Evaluation Using Real Road Networks”. In: *Transportation Science* 32 (1998), pages 65–73. ISSN: 0041-1655. DOI: 10.1287/trsc.32.1.65.
- [263] Stuart E. Dreyfus. “An Appraisal of Some Shortest-Path Algorithms”. In: *Operations Research* 17.3 (1969), pages 395–412.
- [264] Albert-László Barabási and Réka Albert. “Emergence of Scaling in Random Networks”. In: *Science* 286 (1999), pages 509–512. ISSN: 00368075. DOI: 10.1126/science.286.5439.509.
- [265] Paolo Crucitti, Vito Latora, and Massimo Marchiori. “Model for cascading failures in complex networks”. In: *Physical Review E - Statistical Physics, Plasmas, Fluids, and Related Interdisciplinary Topics* 69.4 (2004), page 4. DOI: 10.1103/PhysRevE.69.045104. eprint: 0309141 (cond-mat).
- [266] Leonardo Dueñas-Osorio and Srivishnu Mohan Vemuru. “Cascading failures in complex infrastructure systems”. In: *Structural Safety* 31.2 (2009), pages 157–167. DOI: 10.1016/j.strusafe.2008.06.007. URL: <http://dx.doi.org/10.1016/j.strusafe.2008.06.007>.
- [267] Sergey V. Buldyrev, Roni Parshani, Gerald Paul, H. Eugene Stanley, and Shlomo Havlin. “Catastrophic cascade of failures in interdependent networks”. In: *Nature* 464.7291 (2010), pages 1025–1028. DOI: 10.1038/nature08932. URL: <http://dx.doi.org/10.1038/nature08932>.
- [268] Julian Salomon, Matteo Broggi, Sebastian Kruse, Stefan Weber, and Michael Beer. “Resilience decision-making for complex systems”. In: *ASCE-ASME J Risk and Uncert in Engrg Sys Part B Mech Engrg* 6.2 (2020).

- [269] Alice Alipour and Behrouz Shafei. “An overarching framework to assess the life-time resilience of deteriorating transportation networks in seismic-prone regions”. In: *Resilient Cities and Structures* 1.2 (2022), pages 87–96. ISSN: 2772-7416. DOI: <https://doi.org/10.1016/j.rcns.2022.07.002>.
- [270] Luca Capacci, Fabio Biondini, and Dan M. Frangopol. “Resilience of aging structures and infrastructure systems with emphasis on seismic resilience of bridges and road networks: Review”. In: *Resilient Cities and Structures* 1.2 (2022), pages 23–41. ISSN: 2772-7416. DOI: <https://doi.org/10.1016/j.rcns.2022.05.001>.
- [271] Sisi Duan and Bilal M Ayyub. “Assessment methods of network resilience for cyber-human-physical systems”. In: *ASCE-ASME Journal of Risk and Uncertainty in Engineering Systems, Part A: Civil Engineering* 6.1 (2020), page 03119001.
- [272] Roy Emanuel and Bilal Ayyub. “Assessing resilience model responsiveness in the context of stakeholder preferences in decision support systems”. In: *ASCE-ASME Journal of Risk and Uncertainty in Engineering Systems, Part A: Civil Engineering* 5.2 (2019), page 04019005.
- [273] Yalda Saadat, Bilal M. Ayyub, Yanjie Zhang, Dongming Zhang, and Hongwei Huang. “Resilience-Based Strategies for Topology Enhancement and Recovery of Metrorail Transit Networks”. In: *ASCE-ASME Journal of Risk and Uncertainty in Engineering Systems, Part A: Civil Engineering* 6.2 (2020), page 04020017. DOI: [10.1061/AJRUA6.0001057](https://doi.org/10.1061/AJRUA6.0001057).
- [274] Yating Zhang, Bilal M. Ayyub, and Juan F. Fung. “Projections of corrosion and deterioration of infrastructure in United States coasts under a changing climate”. In: *Resilient Cities and Structures* 1.1 (2022), pages 98–109. ISSN: 2772-7416. DOI: <https://doi.org/10.1016/j.rcns.2022.04.004>.
- [275] Claus Ballegaard Nielsen, Peter Gorm Larsen, John Fitzgerald, Jim Woodcock, and Jan Peleska. “Systems of systems engineering: basic concepts, model-based techniques, and research directions”. In: *ACM Computing Surveys (CSUR)* 48.2 (2015), pages 1–41.
- [276] Mo Jamshidi. *Systems of systems engineering: principles and applications*. CRC press, 2017.
- [277] Michael Batty. “Complexity in city systems: Understanding, evolution, and design”. In: *A planner’s encounter with complexity*. Routledge, 2016, pages 99–122.
- [278] Krzysztof Kolowrocki. *Reliability of large and complex systems*. Elsevier, 2014.
- [279] Seema Negi and SB Singh. “Reliability analysis of non-repairable complex system with weighted subsystems connected in series”. In: *Applied Mathematics and Computation* 262 (2015), pages 79–89.
- [280] Serkan Eryilmaz and Altan Tuncel. “Generalizing the survival signature to unrepairable homogeneous multi-state systems”. In: *Naval Research Logistics (NRL)* 63.8 (2016), pages 593–599.

- [281] He Yi, Lirong Cui, and Narayanaswamy Balakrishnan. “Computation of survival signatures for multi-state consecutive-k systems”. In: *Reliability Engineering & System Safety* 208 (2021), page 107429.
- [282] Jasper Behrendorf, Julian Salomon, and Niklas Winnewisser. *ResilienceDecisionMaking.jl*. 2022. DOI: 10.5281/zenodo.7034998.
- [283] Siu-Kui Au and Yu Wang. *Engineering risk assessment with subset simulation*. John Wiley & Sons, 2014.
- [284] Waguih ElMaraghy, Hoda ElMaraghy, Tetsuo Tomiyama, and Laszlo Monostori. “Complexity in engineering design and manufacturing”. In: *CIRP Annals* 61.2 (2012), pages 793–814. DOI: 10.1016/j.cirp.2012.05.001.
- [285] John Bongaarts. “Human population growth and the demographic transition”. In: *Philosophical Transactions of the Royal Society B: Biological Sciences* 364.1532 (2009), pages 2985–2990. DOI: 10.1098/rstb.2009.0137.
- [286] Anatoly Lisnianski and Gregory Levitin. *Multi-State System Reliability: Assessment, Optimization and Applications*. Volume 6. World Scientific, 2003. DOI: 10.1142/5221.
- [287] Marvin Rausand and Arnljot Høyland. *System Reliability Theory: Models, Statistical Methods, and Applications*. John Wiley & Sons, 2004. DOI: 10.1002/9780470316900.ch12.
- [288] Enrico Zio. *The Monte Carlo Simulation Method for System Reliability and Risk Analysis*. Springer, 2013. DOI: 10.1007/978-1-4471-4588-2.
- [289] Tao Jiang and Yu Liu. “Parameter inference for non-repairable multi-state system reliability models by multi-level observation sequences”. In: *Reliability Engineering & System Safety* 166 (2017), pages 3–15.
- [290] Louis JM Aslett, Frank PA Coolen, and Simon P Wilson. “Bayesian inference for reliability of systems and networks using the survival signature”. In: *Risk Analysis* 35.9 (2014), pages 1640–1651. DOI: 10.1111/risa.12228.
- [291] Jasper Behrendorf, Sebastian Brandt, Matteo Broggi, and Michael Beer. “Efficient Approximation of the Survival Signature for Large Networks”. In: *Proceedings of the 6th International Symposium on Reliability Engineering and Risk Management*. 2018. DOI: 10.3850/978-981-11-2726-7_CRR14.
- [292] Antonella Certa, Fabrizio Hopps, Roberta Inghilleri, and Concetta Manuela La Fata. “A Dempster-Shafer Theory-based approach to the Failure Mode, Effects and Criticality Analysis (FMECA) under epistemic uncertainty: application to the propulsion system of a fishing vessel”. In: *Reliability Engineering & System Safety* 159 (2017), pages 69–79. DOI: 10.1016/j.ress.2016.10.018.
- [293] Qimi Jiang and Chun-Hsien Chen. “A numerical algorithm of fuzzy reliability”. In: *Reliability Engineering & System Safety* 80.3 (2003), pages 299–307. DOI: 10.1016/S0951-8320(03)00055-3.

- [294] Atri Sarkar, Jianmei Guo, Norbert Siegmund, Sven Apel, and Krzysztof Czarnecki. “Cost-efficient sampling for performance prediction of configurable systems (T)”. In: *2015 30th IEEE/ACM International Conference on Automated Software Engineering (ASE)*. IEEE, 2015, pages 342–352. DOI: 10.1109/ASE.2015.45.
- [295] Ha-Rok Bae, Ramana V. Grandhi, and Robert A. Canfield. “An approximation approach for uncertainty quantification using evidence theory”. In: *Reliability Engineering & System Safety* 86.3 (2004), pages 215–225. DOI: 10.1016/j.ress.2004.01.011.
- [296] Pengfei Wei, Jingwen Song, Sifeng Bi, Matteo Broggi, Michael Beer, Zhenzhou Lu, and Zhufeng Yue. “Non-intrusive stochastic analysis with parameterized imprecise probability models: II. Reliability and rare events analysis”. In: *Mechanical Systems and Signal Processing* 126 (2019), pages 227–247. DOI: 10.1016/j.ymsp.2019.02.015.
- [297] Pengfei Wei, Zhenzhou Lu, and Jingwen Song. “Extended Monte Carlo simulation for parametric global sensitivity analysis and optimization”. In: *AIAA journal* 52.4 (2014), pages 867–878.
- [298] Jingwen Song, Marcos Valdebenito, Pengfei Wei, Michael Beer, and Zhenzhou Lu. “Non-intrusive imprecise stochastic simulation by line sampling”. In: *Structural Safety* 84 (2020), page 101936. DOI: 10.1016/j.strusafe.2020.101936.
- [299] Jingwen Song, Pengfei Wei, Marcos Valdebenito, and Michael Beer. “Adaptive reliability analysis for rare events evaluation with global imprecise line sampling”. In: *Computer Methods in Applied Mechanics and Engineering* 372 (2020), page 113344. DOI: 10.1016/j.cma.2020.113344.
- [300] Jingwen Song, Pengfei Wei, Marcos Valdebenito, Sifeng Bi, Matteo Broggi, Michael Beer, and Zuxiang Lei. “Generalization of non-intrusive imprecise stochastic simulation for mixed uncertain variables”. In: *Mechanical Systems and Signal Processing* 134 (2019), page 106316. DOI: 10.1016/j.ymsp.2019.106316.
- [301] Igor Linkov and Benjamin D Trump. *The science and practice of resilience*. Springer, 2019.
- [302] Terje Aven. “Improving the foundation and practice of reliability engineering”. In: *Proceedings of the Institution of Mechanical Engineers, Part O: Journal of Risk and Reliability* 231.3 (2017), pages 295–305.
- [303] Klaas B Klaassen and Jack CL Van Peppen. *System reliability*. VSSD, 2006.
- [304] Julian Salomon, Jasper Behrendorf, Niklas Winnewisser, Matteo Broggi, and Michael Beer. “Multidimensional resilience decision-making for complex and substructured systems”. In: *Resilient Cities and Structures* 1.3 (2022), pages 61–78.
- [305] Niketa Jain, Om Prakash Yadav, Ajay Pal Singh Rathore, and Rakesh Jain. “Reliability assessment framework for a multi-state multi-component system”. In: *Journal of Industrial and Production Engineering* 34.8 (2017), pages 580–589.

- [306] Kai Yang and Jianan Xue. “Continuous state reliability analysis”. In: *Proceedings of 1996 Annual Reliability and Maintainability Symposium*. IEEE. 1996, pages 251–257. DOI: 10.1109/rams.1996.500670.
- [307] Lars Skyttner. “General systems theory: origin and hallmarks”. In: *Kybernetes* (1996).
- [308] Joseph C Hudson and Kailash C Kapur. “Reliability bounds for multistate systems with multistate components”. In: *Operations Research* 33.1 (1985), pages 153–160.
- [309] Mariéa Luz Gámiz and MD Martíénez Miranda. “Regression analysis of the structure function for reliability evaluation of continuous-state system”. In: *Reliability Engineering & System Safety* 95.2 (2010), pages 134–142.
- [310] Joseph C Hudson and Kailash C Kapur. “Reliability analysis for multistate systems with multistate components”. In: *AIIE Transactions* 15.2 (1983), pages 127–135.
- [311] Charles E Ebeling. *An introduction to reliability and maintainability engineering*. Waveland Press, 2019.
- [312] Kowalska Beata, Kowalski Dariusz, and Mazurkiewicz Dariusz. “Survival function in the analysis of the factors influencing the reliability of water wells operation”. In: *Water Resources Management* 33 (2019), pages 4909–4921.
- [313] Vito Latora and Massimo Marchiori. “Economic small-world behavior in weighted networks”. In: *The European Physical Journal B-Condensed Matter and Complex Systems* 32.2 (2003), pages 249–263.
- [314] Zhi-Sheng Ye and Nan Chen. “The inverse Gaussian process as a degradation model”. In: *Technometrics* 56.3 (2014), pages 302–311.
- [315] Weiwen Peng, Yan-Feng Li, Yuan-Jian Yang, Jinhua Mi, and Hong-Zhong Huang. “Bayesian Degradation Analysis With Inverse Gaussian Process Models Under Time-Varying Degradation Rates”. In: *IEEE Transactions on Reliability* 66.1 (2017), pages 84–96. DOI: 10.1109/TR.2016.2635149.
- [316] Lorenzo Trippa, Peter Müller, and Wesley Johnson. “The multivariate beta process and an extension of the Polya tree model”. In: *Biometrika* 98.1 (2011), pages 17–34.
- [317] Fred Daum and Jim Huang. “Curse of dimensionality and particle filters”. In: *2003 IEEE aerospace conference proceedings (Cat. No. 03TH8652)*. Volume 4. IEEE. 2003, 4_1979–4_1993.
- [318] He Yi, Narayanaswamy Balakrishnan, and Xiang Li. “Multi-State Joint Survival Signature for Multi-State Systems with Shared Multi-State Components”. In: *Methodology and Computing in Applied Probability* 25.1 (2023), page 44.

- [319] Xuchao Bai, Xiangrong Li, Narayanaswamy Balakrishnan, and Mu He. “Statistical inference for dependent stress–strength reliability of multi-state system using generalized survival signature”. In: *Journal of Computational and Applied Mathematics* 390 (2021), page 113316. DOI: <https://doi.org/10.1016/j.cam.2020.113316>.
- [320] Xuchao Bai, Jieqiong Zhang, Mu He, and Narayanaswamy Balakrishnan. “Inference for stress–strength reliability of multi-state system with dependent stresses and strengths using improved generalized survival signature”. In: *Journal of Computational and Applied Mathematics* 420 (2023), page 114809. ISSN: 0377-0427. DOI: <https://doi.org/10.1016/j.cam.2022.114809>.
- [321] Berend Denkena, Peter Nyhuis, Benjamin Bergmann, Nicolas Nübel, and Torben Lucht. “Towards an autonomous maintenance, repair and overhaul process: Exemplary holistic data management approach for the regeneration of aero-engine blades”. In: *Procedia Manufacturing* 40 (2019), pages 77–82. DOI: [10.1016/j.promfg.2020.02.014](https://doi.org/10.1016/j.promfg.2020.02.014).
- [322] Julian Salomon, Jan Göing, Sebastian Lück, Matteo Broggi, Jens Friedrichs, and Michael Beer. “Sensitivity Analysis of an Aircraft Engine Model Under Consideration of Dependent Variables”. In: *Turbo Expo: Power for Land, Sea, and Air*. Volume 84898. American Society of Mechanical Engineers. 2021, V001T01A005. DOI: [10.1115/GT2021-58905](https://doi.org/10.1115/GT2021-58905).
- [323] Ilya M Sobol. “Global sensitivity indices for nonlinear mathematical models and their Monte Carlo estimates”. In: *Mathematics and computers in simulation* 55.1-3 (2001), pages 271–280.
- [324] Julien Jacques, Christian Lavergne, and Nicolas Devictor. “Sensitivity analysis in presence of model uncertainty and correlated inputs”. In: *Reliability Engineering & System Safety* 91.10-11 (2006), pages 1126–1134.
- [325] Holger Keitel and Andrea Dimmig-Osburg. “Uncertainty and sensitivity analysis of creep models for uncorrelated and correlated input parameters”. In: *Engineering Structures* 32.11 (2010), pages 3758–3767.
- [326] Sergei Kucherenko, Stefano Tarantola, and Paola Annoni. “Estimation of global sensitivity indices for models with dependent variables”. In: *Computer physics communications* 183.4 (2012), pages 937–946.
- [327] S. Marelli, C. Lamas, K. Konakli, C. Mylonas, P. Wiederkehr, and B. Sudret. *UQLab user manual – Sensitivity analysis*. Technical report. Report # UQLab-V1.3-106. Chair of Risk, Safety and Uncertainty Quantification, ETH Zurich, Switzerland, 2019.
- [328] Julian Salomon, Jasper Behrendorf, Matteo Broggi, Stefan Weber, and Michael Beer. “Multidimensional Resilience Decision-Making On A Multistage High-Speed Axial Compressor”. In: (2019). DOI: [10.3850/978-981-11-2724-30992-cd](https://doi.org/10.3850/978-981-11-2724-30992-cd).

Curriculum Vitae

Personal details

Name	Julian Salomon
Date of birth	27 December 1989
Place of birth	Hannover, Germany
Nationality	German

Education

since 04/2017	Doctoral student Institute for Risk and Reliability, Leibniz Universität Hannover
10/2013 – 09/2016	Master of Science, Computational Engineering Final grade: 1.3 (with distinction) Leibniz Universität Hannover
10/2009 – 09/2013	Bachelor of Science, Computational Engineering Leibniz Universität Hannover

Work experience

since 02/2017	Research associate Institute for Risk and Reliability, Leibniz Universität Hannover
10/2016 – 02/2017	Research assistant Institute for Risk and Reliability, Leibniz Universität Hannover
04/2015 – 10/2015	Intern Volkswagen AG, Innovation Management, Wolfsburg
04/2012 – 09/2016	Student assistant Institute of Continuum Mechanics, Institute of Dynamics and Vibration Research, Institute for Technical Combustion, Leibniz Universität Hannover

Awards

2017	Doctoral Summer School Scholarship Top Industrial Managers for Europe (T.I.M.E.) Association
2014	Deutschlandstipendium For gifted and high-achieving students, Federal Ministry of Education and Research